YGS Open File 2015-23

Provenance and depositional framework of braided and meandering gravel-bed river deposits and associated coal deposits in active intermontane piggyback basins: The Upper Jurassic to Lower Cretaceous Tantalus Formation, Yukon

Darrel G.F. Long

YUKON GEOLOGICAL SURVEY

Yukon
Energy, Mines and Resources

Open File 2015-23

Provenance and depositional framework of braided and meandering gravel-bed river deposits and associated coal deposits in active intermontane piggyback basins: The Upper Jurassic to Lower Cretaceous Tantalus Formation, Yukon

D.F.G. Long

Department of Earth Sciences, Laurentian University, Sudbury, Ontario, Canada. P3E 2C6
dlong@laurentian.ca

Published under the authority of the Department of Energy, Mines and Resources, Government of Yukon http://www.emr.gov.yk.ca.

Printed in Whitehorse, Yukon, 2015.

Publié avec l'autorisation du Ministères de l'Énergie, des Mines et des Ressources du gouvernement du Yukon, http://www.emr.gov.yk.ca.

Imprimé à Whitehorse (Yukon) en 2015.

A copy of this report can be obtained by download from www.geology.gov.yk.ca *or by emailing* geology@gov.yk.ca.

In referring to this publication, please use the following citation:

Long, D.G.F., 2015. Provenance and depositional framework of braided and meandering gravel-bed river deposits and associated coal deposits in active intermontane piggyback basins: The Upper Jurassic to Lower Cretaceous Tantalus Formation, Yukon. Yukon Geological Survey, Open File Report 2015-23., 80 p. plus appendices.

Cover photo: View of Tantalus Butte (1979), due north of the Trans-North Helicopter base. The Tantalus Formation starts at the conglomerate unit above the adit.

ABSTRACT

The Tantalus Formation developed within confined intermontane river valleys during the late stages of collision and amalgamation of Stikinia and associated arc systems with the North American plate in Upper Jurassic and early Lower Cretaceous times. While most of the extensive chert pebble conglomerate in the Tantalus Formation can be interpreted as shallow braided gravel-bed river deposits, some may represent the products of deposition from deeper, braided and meandering gravel-bed rivers. Floodplain and lake deposits are restricted to poorly exposed slope forming intervals. Coal deposits developed locally on abandoned segments of floodplains in confined river valleys, in places associated with high constructive river deposits. The age profiles of detrital zircons indicate major contributions from reworking of older strata, combined with continued unroofing of the Stikine terrane. In addition more distal sources were tapped in the Yukon-Tanana and adjacent terranes to the north and west of the Whitehorse trough. Much of the chert in the Tantalus Formation appears petrographically similar to chert in the Cache Creek terrane, now preserved only to the south of the Whitehorse trough. As both decrease in maximum grain size, and paleocurrents, are generally south to southwesterly trending, this source is considered unlikely. Chert may have been derived from now eroded supracrustal rocks that once formed the top of the Yukon-Tanana terrane, or more likely from an obducted block of Cache Creek terrane once present to the north and west of the Whitehorse trough. The latter may have been thrust over metamorphosed rocks of the Yukon-Tanana terrane beginning in the early Bajocian, and has subsequently been removed by erosion. A proximal North American cratonic source is excluded, as there are no Archean zircon grains in the Tantalus Formation. The possibility that strata of the Tantalus Formation may host significant conventional reserves of oil or gas is very low, due to lack of trapping mechanisms. There may be some undiscovered coal reserves, and limited potential for coal-bed methane production.

TABLE OF CONTENTS

INTRODUCTION

The primary objectives of this paper are to document the lithology, petrology and stratigraphy of chert-pebble conglomerate and associated minor sandstone, mudstone, and coal in the Upper Jurassic to Lower Cretaceous Tantalus Formation, and to use this information to evaluate fluvial style and basin development in terms of tectonic and paleogeographic framework. Clast petrography and age profiles of detrital zircon populations are used to evaluate the character and location of the provenance (catchment) area.

Preliminary results of this study have been presented by Long (1980, 1982a,b, 1983a,b, 1984, 1986; Long and Lowey, 2006). Location of new measured sections is indicated on Figure 1. Stratigraphy and hydrocarbon potential of the Yukon segment of the Whitehorse trough has been discussed by Beaton *et al.* (1992), National Energy Board (2001), Lowey (2004a,b, 2005, 2007a,b, 2008, 2011), Lowey and Long (2006), Lowey *et al.* (2009), Hayes (2012), Hayes and Archibald (2012) and White *et al.* (2006, 2012). Hannigan *et al.* (1995) and English *et al.* (2005) provide comparable data on the hydrocarbon potential from the southern part of the trough in British Columbia.

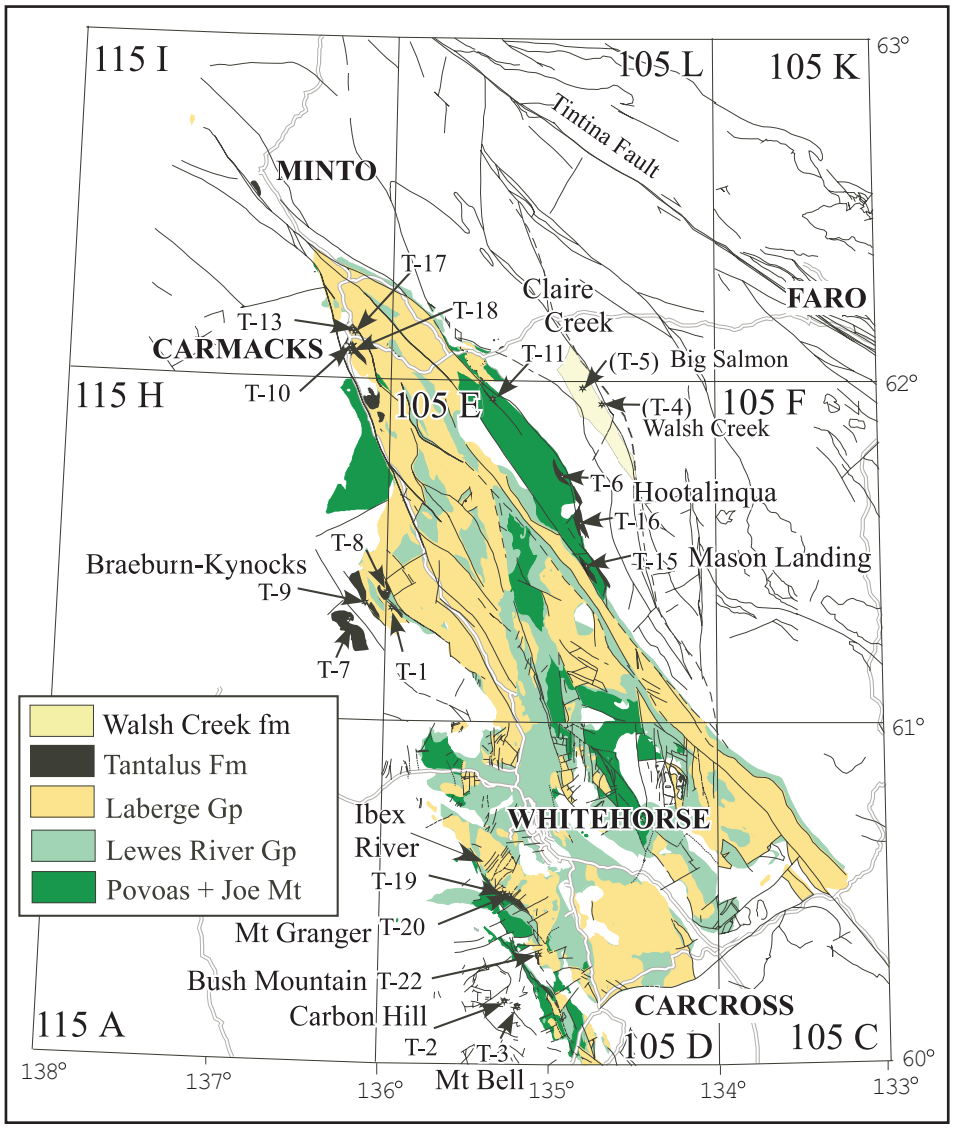

Figure 1. *Distribution of strata and major faults within the Whitehorse trough of southern Yukon. Tantalus Formation sub-basins (named) shown in black, with location of measured sections mentioned in text. The type section of the formation is located at T-17. Geology based on maps by Templeman-Kluit 1974, 1984; Gordey and Irwin 1987; Gordey and Stevens 1994b; Colpron et al. 2002, 2007a; Israel 2004; Gordey 2008 and Colpron 2011. Major roads are shown in light grey.*

GEOLOGICAL SETTING

Rocks of the Whitehorse trough, as originally delimited by Wheeler (1956, 1961), lie within the Intermontane belt of the Canadian Cordillera (Monger and Price, 1979; Tipper and Woodsworth, 1981; Monger *et al.*, 1982) and included strata of the Tantalus Formation along with underlying strata of the Laberge and Lewes River groups (Fig. 2). More recently White *et al.* (2012) have restricted the definition of the Whitehorse trough to the area underlain by strata of the Laberge Group. They suggest that the Laberge Group represents an overlap assemblage that straddles the Stikinia, Cache Creek and Quesnellia terranes (Fig. 3) that developed in a collapsing forearc basin that subsequently evolved into a piggyback basin (*cf.*, Mihalynuk *et al.*, 1994). The Whitehorse trough overlies, and is flanked to the west by rocks of the Lewes River-Stuhini arc (Stikinia), and is bound to the east by rocks of the Takla-Nicola arc (Quesnellia). These are bounded to the east, west and north by pericratonic rocks of the Yukon-Tanana terrane, which appear to wrap around the Whitehorse trough and the Cache Creek terrane (Fig. 3). Current models of the Cordillera suggest that it includes a large number of amalgamated peri-continental and exotic terranes, many of which accreted to the margin of western North America during the Mesozoic and Cenozoic (Monger and Price, 1979; Tempelman-Kluit, 1979; Monger *et al.*, 1982; Gehrels and Kapp 1997; English and Johnston 2005; Colpron *et al.*, 2006a, 2007a,b; Nelson and Colpron 2007; Colpron and Nelson 2009; Nelson *et al.*, 2013). The apparently anomalous position of the Cache Creek terrane, between terranes with North American peri-continental affinity is best explained by oroclinal enclosure. In this model (Mihalynuk *et al.*, 1994, 2004), the Lewes River-Stuhini and Takla-Nicola arcs were part of a single, continuous arc system that originally faced south, towards the Panthallasic ocean. Counterclockwise rotation of Stikinia in the Upper Triassic and Lower Jurassic around a flexural hinge a short distance north of the Whitehorse trough led to subduction and obduction (Gordey and Stevens, 1994b; Bickerton *et al.*, 2013) of

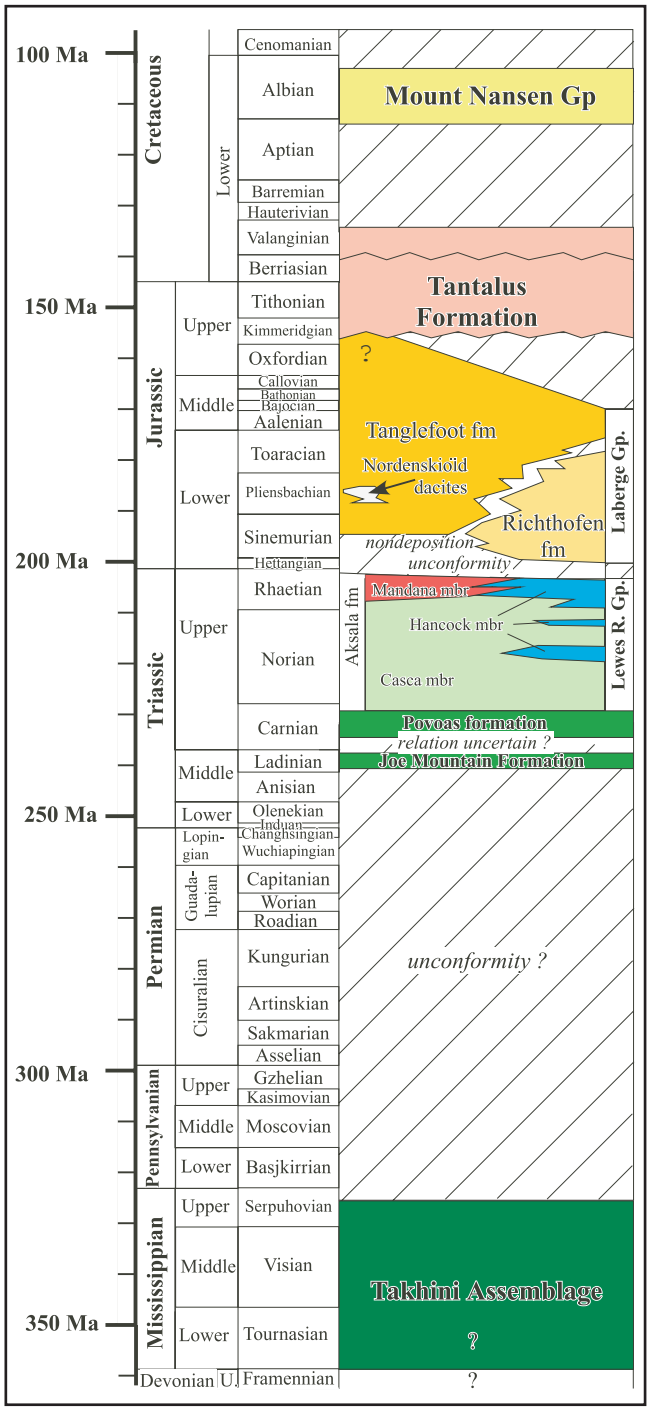

Figure 2. *Stratigraphy of Mississippian to Lower Cretaceous strata of Stikinia. Ages based on Cohen et al. (2013). Strata of the Whitehorse trough are restricted to rocks of the Laberge Group. If strata in the Ibex River area, dated as Kimmeridgian - Oxfordian by Hart and Radloff (1990), belong to the Tanglefoot formation as suggested in the text, then the break between the Laberge Group and Tantalus Formation may be short, at least along the central western margin of the basin.*

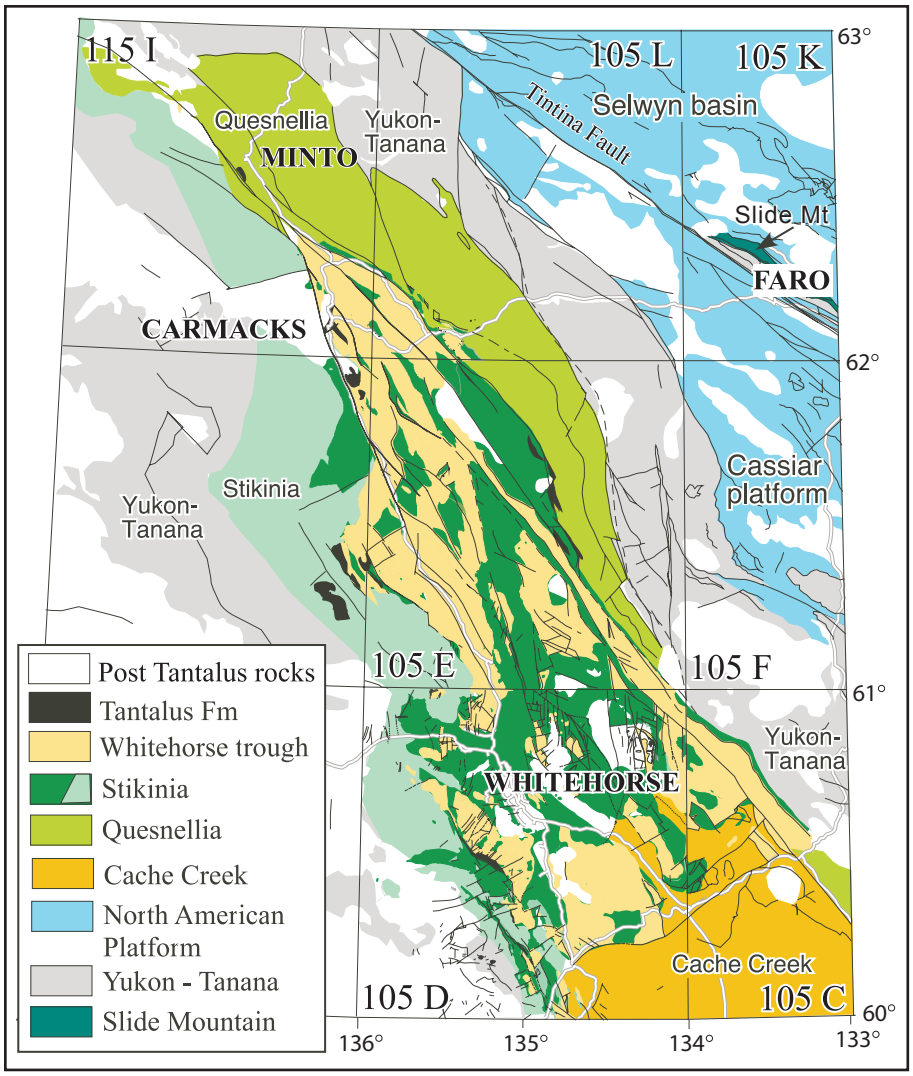

Figure 3. *Tectonic framework of the Whitehorse trough, based on Colpron (2011). The Whitehorse trough (Laberge Group) overlaps the Stikine arc (west), and Stikinia (east), and may onlap the Cache Creek terrane to the south.*

parts of the Cache Creek terrane, with subsequent enclosure of remnants of the Cache Creek accretionary complex. Rotational collision, with some northward translation, continued until closure with Quesnellia in the Middle Jurassic (Mihalynuk *et al.*, 2004). This allowed strata of the Laberge Group to accumulate in a piggyback basin (Whitehorse trough) at the north end of the embayment (White *et al.*, 2012) at the same time that arc related rocks of the Hazelton Group accumulated in northern British Columbia.

Stratigraphy of Stikinia and the Whitehorse trough

Stikinia contains a sequence of polydeformed Mississippian and older mafic volcanic rocks of the Takhini Assemblage (Hart, 1997), succeeded by (>2.5 km) Middle Triassic (Ladinian) mafic volcanic rocks of the Joe Mountain Formation, and (>3 km) of Upper Triassic strata of the Lewes River Group (Lees, 1934; Bostock, 1936; Bostock and Lees, 1938; Tozer, 1958; Wheeler, 1961; Fig. 2). The lower part of the Lewes River Group consists of fine-grained augite-phyric andesite to basaltic-andesite, with minor associated volcaniclastic and epiclastic rocks, assigned to the Povoas Formation (Tempelman-Kluit, 1984, 2009; Hart, 1997). The upper part of the group is represented by >1.5 km of strata belonging to the Aksala formation (Tempelman-Kluit, 1984; Reid, 1988; Hart,

1997; Long, 2005; Lowey, 2011). This includes a thick succession of turbiditic volcaniclastic and epiclastic sandstone and deep-water mudstone (Casca member), that are interbedded with shallow water carbonate (Hancock member), and shallow water (red) sandstone and mudstone (Mandana member).

The Lewes River Group is unconformably overlain by at least 2.9 km of sandstone, mudstone and conglomerate (with minor intrusive rocks) of the Jurassic (Sinemurian to ?Oxfordian) Laberge Group (Wheeler, 1961; Tozer, 1958; Lees, 1934; Bostock and Lees, 1938; Tempelman-Kluit, 1978; Reid, 1981; Reid and Ginsburg, 1986; Hart, 1997; Tempelman-Kluit, 2009; Lowey, 2007a,b, 2011) that collectively forms the fill of the Whitehorse trough (White *et al.*, 2012). Deeper water mudstone and minor sandstone are represented by the Richthofen formation (informal; Lowey, 2004b, 2005) and are predominantly volcaniclastic in nature, indicating incorporation of both contemporary arc-derived material and older strata of the Lewes River Group. Shallow water (marine and prodeltaic) and terrestrial strata are represented by predominantly arkosic and subarkosic sandstone and conglomerate of the Tanglefoot formation (informal). Minor facies include interbedded mudstone, minor volcaniclastic units, limestone and coal (Cairnes, 1910; Long, 1986; Allen, 2000; Cameron and Beaton, 2000; Lowey, 2004b, 2005). Upper Jurassic strata are more quartzo-feldspathic, reflecting unroofing of adjacent arc terranes. Units of massive dacite tuff at several horizons within the Tanglefoot (Lowey, 2004a) and Richthofen formations (Colpron *et al.*, 2007a) have been included in the Nordenskiöld formation (informal). Colpron and Friedman (2008) demonstrated that the formation represents multiple extrusive events when they obtained U-Pb zircon ages of 188.1 ± 0.4 Ma, 187.2 ± 0.4 Ma and 186.5 ± 0.3 Ma from a series of units ascribed to the Nordenskiöld formation, and an age of 187.1 ± 0.7 Ma for a tuff in the Tanglefoot formation. Fillmore (2006) used trace element geochemistry to link these to the Aishihik batholith (186.0 ± 1.0 Ma: Johnston *et al.*, 1996) west of the Whitehorse trough.

Late Upper Jurassic to early Lower Cretaceous Tantalus Formation

Up to 1.3 km of medium to large pebble conglomerate of the late Upper Jurassic to early Lower Cretaceous Tantalus Formation stratigraphically overlap strata of the Whitehorse trough, Stikinia, Quesnellia, and locally the Yukon-Tanana terrane (Fig. 3). The unit was originally named the "Tantalus Conglomerates" by Cairnes (1910), with a type area at Tantalus Butte, immediately north of the Yukon River at Carmacks (Fig. 1). This usage was continued by Lees (1934), but was later modified by Bostock (1936) who renamed it the Tantalus Formation. Minor rock types in the Tantalus Formation include feldspathic chert litharenite, mudstone and coal. Coal seams are confined to finer grained intervals within the Tantalus Formation, and are less well developed than those in underlying strata of the Tanglefoot formation.

Strata of the Tantalus Formation were deposited in a series of isolated terrestrial intermontane successor basins during collision-induced uplift and deformation of underlying strata (Wheeler, 1961; Long, 1986; Lowey and Hills, 1988; Lowey, 1984, 2007a,b). As such, they represent piggyback basins (Mihalynuk *et al.*, 1994, 2004; White *et al.*, 2012; Bickerton *et al.*, 2013). Paralellism of the preserved basins with major northwest oriented faults may imply limited strike slip activity within, and along, the basin margins (Tempelman-Kluit, 2009). Erosional remnants of the Tantalus Formation are confined to small, elongate basins, predominantly along the west side of the northern Whitehorse trough (Fig. 3). There is no evidence that these were ever part of a single, laterally extensive sheet that blanketed the Whitehorse trough. Basins on the eastern side of the trough straddle rocks of the Boswell terrane (Quesnellia) and those on the west straddle Stikinia and (at Carbon Hill, and Mt Bell, Localities T-2 and T-3 on Fig. 1) lie directly on strata of the Yukon-Tanana terrane, while strata at Malamute Mountain (61°17'N, 136°20'W) rest on quartz monzanite

belonging to plutons of the ~183 Ma Long Lake plutonic suite, that stitch together Stikinia and Yukon-Tanana (Tempelman-Kluit, 1974, 2009; Johnston *et al.*, 1996). Strata in the Big Salmon area, east of the Whitehorse trough, originally correlated with the Tantalus Formation (Tempelman-Kluit, 1984), are now placed in the (Pliocene?) Walsh Creek formation of Tempelman-Kluit (2009).

In northern British Columbia, Bultman (1979) identified strata that he considered to be equivalent to the Tantalus Formation in a fault bounded interval exposed along the northwest margin of Tutshi Lake (~59°55′17″N, 134°48′22″W), about 35 km southeast of section T-3 on Mount Bell (Fig. 1). These were later identified as questionable parts of the Laberge Group by Mihalynuk (1999). Petrographically similar strata in the Indian River area (200-235 km northwest of Carmacks), were assigned to the Tantalus Formation by Lowey and Hills (1988). As strata in the Indian River area contain terrestrial palynomorphs indicative of a late Lower Cretaceous (Albian) age (Lowey, 1984), these post-date volcanic strata in the Mount Nansen Group, and should be considered as a separate unit (Indian River Formation of Lowey, 1984, and Bond and Chapman, 2006), rather than part of the Tantalus Formation *sensu stricto*. Ash horizons in immature clastic sedimentary rocks, located along the Salmon River, adjacent to the Robert Campbell Highway, 46 km east of Carmacks, have been dated at ~92 Ma (Colpron, 2011). These strata, previously correlated with the Tantalus Formation, also post-date the Mount Nansen volcanic suite (Fig. 2), and hence may be equivalent to parts of the Indian River Formation.

Wheeler (1961) suggested that the Tantalus Formation was Upper Jurassic? to Lower Cretaceous, based on identification of plant remains from Mount Bush by Bell (1956), as of probable Neocomian (145.5±4 to 130±1.5 Ma) or Portlandian (146 to 142 Ma) age (*i.e.*, Tithonian to Hauterivian on Fig. 2). Lowey (1984) recovered a number of long ranging palynomorphs from drill core in the Tantalus Formation at Tantalus Butte, including some of probable middle to late Albian age. He suggested that the maximum age could have been late Upper Jurassic. A similar conclusion was made by Tempelman-Kluit (1974, 2009) based on plant remains from strata collected from roadside exposures 20 km south of Carmacks. Sandstone in this area contains abundant feldspar and minimal chert, hence these strata are now considered to be part of the Tanglefoot formation. Hart and Radloff (1990) recovered palynomorphs and dinocysts from the Ibex River area in strata here considered to be part of the Tanglefoot formation. These indicated the top of the Laberge Group to be as young as Kimmeridgian to Oxfordian (early to mid-Upper Jurassic), hence the maximum age of the Tantalus Formation may be Kimmeridgian. The minimum age of the formation is constrained by the (Albian) 109±0.7 Ma age of quartz-feldspar porphyries of the Mount Nansen Group (Appel, 1998). Andesitic strata of the Carbon Hill volcanic complex, considered to be part of the Mount Nansen Group by Hart and Radloff (1990) cut and cap the Tantalus Formation on the southwestern margin of the basin.

Previous authors have suggested that the bulk of the Tantalus Formation was deposited in a terrestrial fluvial setting (Tempelman-Kluit, 1974; Bultman, 1979; Bremner, 1988; Long, 1982a,b, 1983a,b, 1984, 1986, 2005; Lowey *et al.*, 2009). A beach origin was suggested by McConnell (1909): this was later supported by Hart and Pelletier (1989), and Hart and Radloff (1990), who suggested a beach or barrier island origin for the massive conglomerate, and a fluvial, or lagoonal setting for finer grained strata and coal deposits within the formation. Hart and Radloff (1990) supported their argument for a marine component using the presence of a diverse assemblage of dinoflagellate cysts in two samples of mudstone from the Ibex River area. As these strata (Section T-21, Appendix 1) are now considered as part of the Laberge Group (possibly part of the Tanglefoot formation, *see* Stratigraphy section), these dinocysts cannot be used to infer a marine or marginal marine origin for any part of the Tantalus Formation.

NEW OBSERVATIONS, METHODS

Fieldwork for this project took place in 1978, 1979, 1983, 2004 and 2005. New stratigraphic observations were made at several locations (Fig. 1 and Table 1). At each section observations on sedimentary structures, grain size (maximum and mean), and composition were made on a bed-by-bed basis. Samples were collected for petrographic analysis and detrital zircon analysis. Plots of measured stratigraphic sections are provided in Appendix 1. Terminology for bed thickness, stratification and cross-stratification follows McKee and Weir (1953). Petrographic terminology follows Folk (1974).

Table 1. *Locations of measured stratigraphic sections.*

SECTION	LOCATION	NTS	LATITUDE	LONGITUDE
T-1	Corduroy Mountain	105 E	61°19′31″N 61°19′45″N	125°55′42″W (base) 125°55′58″W (top)
T-2	Carbon Hill	105 D	60°11′21″N	135°14′12″W
T-3	Mount Bell	105 D	60°10′22″N	135°11′06″W
T-4	Walsh Creek	105 E	61°55′29″N	134°40′57″W
T-5	Big Salmon	105 E	61°58′30″N	134°48′25″W
T-6a	Hootalinqua	105 E	61°43′22″N	134°56′34″W
T-6b	Hootalinqua	105 E	61°43′28″N	134°57′07″W
T-7	Nordenskiöld River	115 H	61°15′38″N 61°16′00″N	136°16′11″W (base) 136°15′40″W (top)
T-8	Cub Mountain	115H/105E	61°23′07″N	135°59′26″W
T-9	Vowel Mountain	115 H	61°21′00″N	136°08′00″W
T-10	Tantalus Mine (old)	115 I	62°05′41″N	136°15′48″W
T-11	Claire Creek	105 E	61°56′53″N	135°22′23″W
T-12a	South of Carmacks	115 I	62°05′04″N	136°15′27″W
T-12b	South of Carmacks	115 I	62°04′59″N	136°15′21″W
T-12c	South of Carmacks	115 I	62°04′55″N	136°15′09″W
T-12d	South of Carmacks	115 I	62°04′51″N	136°15′12″W
T-12e	South of Carmacks	115 I	62°04′39″N	136°14′46″W
T-12f	South of Carmacks	115 I	62°04′36″N	136°14′37″W
T-13b	Tantalus Butte, Open Pit	115 I	62°08′14″N	136°15′51″W
T-13a	Tantalus Butte, Pit-east	115 I	62°08′23″N	136°15′50″W
T-14	Tantalus Butte, trench	115 I	62°08′20″N	136°15′33″W
T-15	Mason Landing	105 E	61°27′34″N	134°43′44″W
T-16	Hootalinqua, South	105 E	61°35′06″N	134°50′45″W
T-17	Tantalus Butte, Mine	115 I	62°07′34″N	136°15′44″W
T-18	Carmacks, Town Dump	115 I	62°04′42″N	136°15′57″W
T-19	Mount Granger	105 D	60°29′54″N	135°16′42″W
T-20	Mount Granger	105 D	60°29′29″N	135°15′33″W
T-21	Ibex River	105 D	60°37′13″N	135°26′34″W
T-22	Bush Mountain	105 D	60°18′55″N	135°04′34″W
T-23	Mount Granger	105 D	60°29′56″N 60°29′42″N	135°17′56″W (base) 135°17′16″W (top)
L-3	Division Mountain	115 H	61°20′36″N	136°04′49″W

An attempt was made to document the sedimentary architecture of two laterally extensive exposures near Mount Granger, where outcrops were relatively well exposed, moderately accessible, and not obscured by lichen or soil cover. The methodology used to develop this type of architectural model is described in detail in papers by Miall (1996) and Long (2006, 2011). The hierarchy of surfaces in fluvial settings is explained in Table 2.

Maximum observed thicknesses of the formation are shown on Figure 4. In the type area, at Tantalus Butte, immediately north of Carmacks (Figs. 1 and 4), the formation is at least 370 m thick (section T-17). The maximum preserved thickness is in the Braeburn-Kynocks area, at Vowel Mountain (section T-9 on Fig. 4) where the formation is at least 1273 m thick. The minimum preserved thickness is in the south, at Carbon Hill (T-2) and Mount Bell (T-3), where less than 100 m of strata are preserved. Outcrop patterns, combined with isolated dip measurements, indicate that as much as 850 m of the formation may be present in the subsurface between Hootalinqua south (T-16) and Mason Landing (T-15), but is very poorly exposed, and may include fault repetition. Exposure of the formation range from 100% at Claire Creek (T-11), to less than 10% between Hootalinqua and Mason Landing (T-15, T-16). Most measured sections had 50 to 70% exposure (Appendix 1).

Table 2. *Bedform Hierarchy (after Miall 1996).*

ORDER	TIME (YEARS)	PROCESS	EXAMPLE	MORE INFORMATION ON BOUNDING SURFACES
0	10^{-6}	Burst-sweep cycle	Lamina	
1	10^{-5} to 10^{-4} 10^{-2} to 10^{-1}	Bedform migration Bedform migration	Ripple-microform Diurnal dune increment, reactivation surface	Set boundary
2	10^{-2} to 10^{-1}	Bedform migration	Dune mesoform	Co-set boundary
3	10^{0} to 10^{1}	Seasonal events, 10a flood	Macroform growth increment, unit bars	Dips at 5–20°
4	10^{2} to 10^{3}	100 a flood, channel and bar migration	Macroform migration (point bar, levee, splay)	Convex up, macro-form top, minor channel scours
5	10^{3} to 10^{4}	Avulsion, long-term processes	Channel, delta lobe, mature paleosoils	Flat to concave up, channel base
6	10^{4} to 10^{5}	5th order Milankovich cycles and tectonic pulses	Channel belts, alluvial fan, minor sequence	Flat, regionally extensive
7	10^{5} to 10^{6}	106 4th order Milankovich cycles and tectonic pulses	Major deposystems, fan tract, sequence	Flat, regionally extensive or base of incised valley
8	10^{6} to 10^{7}	3rd order cycles, tectonic and eustatic	Basin-fill complex	Regional disconformity

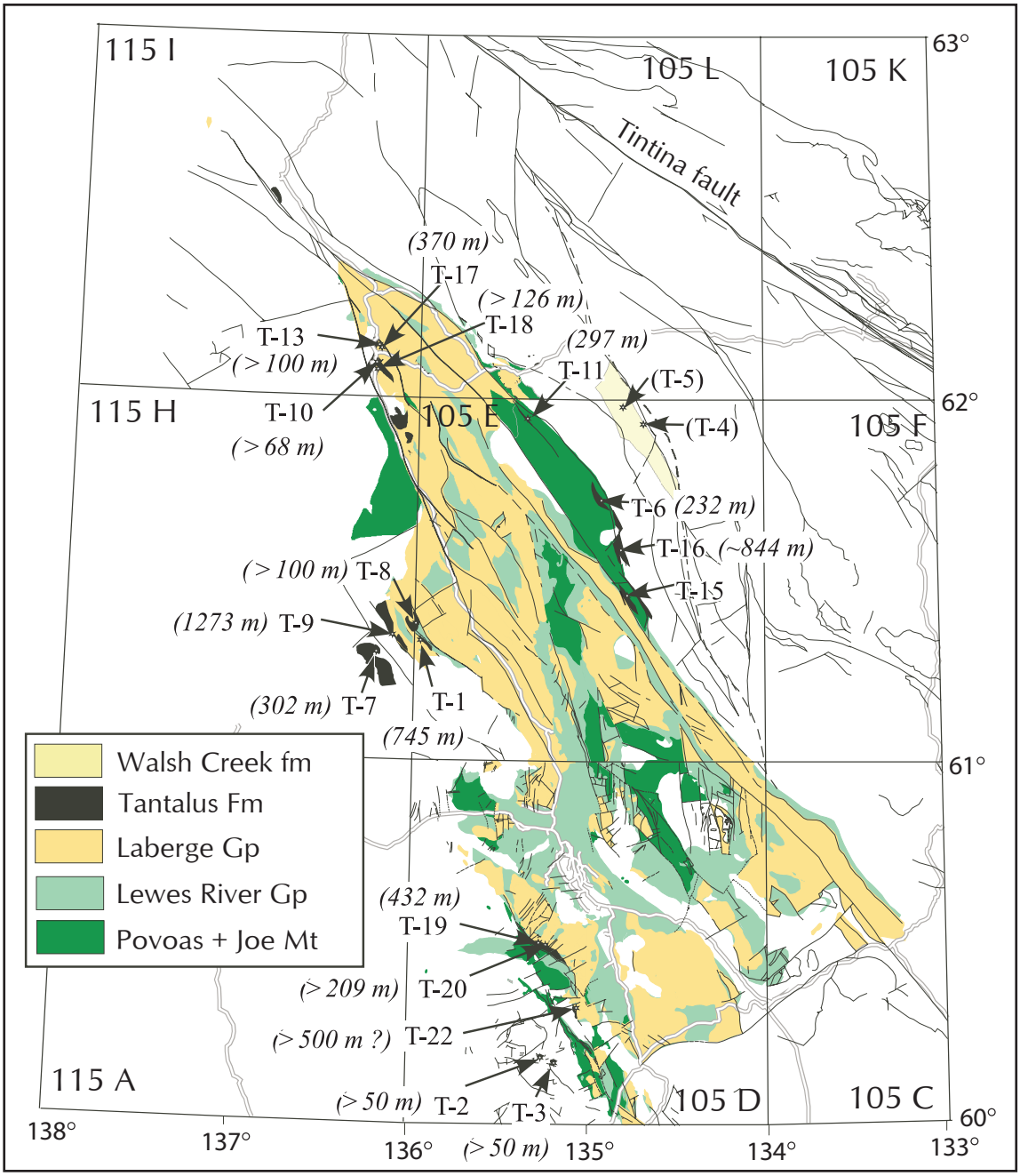

Figure 4. *Distribution and thickness of the Tantalus Formation. For location names see Figure 1. Measured and estimated thicknesses are indicated in brackets. Logs of individual sections are provided in Appendix 1.*

LITHOLOGY AND PETROLOGY

Conglomerate forms the bulk of exposed strata in the Tantalus Formation (86% of exposed strata in all measured sections), with sandstone forming about 10%, and mudstone about 4% (Fig. 5). Coal forms less than half a percent of the exposed parts of measured sections. The relative abundance of mudstone and coal may be slightly underestimated, as these are more readily obscured by slope debris in some sections.

Conglomerate

Lithology

Conglomerate units form 86% of all the exposed strata in the Tantalus Formation. They are dominated by well sorted to moderately well sorted, medium and large pebble conglomerate, with well-rounded sub-equant (*i.e.*, compact; Folk, 1974) clasts. Elongate and platy clasts are very rare. Individual units (beds and amalgamated bed-sets) are from 3 cm to 22.5 m thick (average 0.79 m; mode 0.5 m), and typically have moderate to high lateral continuity, at least at the outcrop scale (10-100 m). Composite storeys (packages of conglomerate bounded by erosion surfaces) can be traced laterally for several kilometres, and give rise to the characteristically striped appearance of outcrops at sites such as Vowel (T-9) and Corduroy (T-1) mountains (Figs. 1, 6 and 7).

The maximum grain size (measured as the intermediate clast diameter of the largest clast present) in conglomerate of the Tantalus Formation is 260 mm (large cobble grade) from section T-11, at Claire Creek (Fig. 8). Elsewhere maximum grain size is from 23-130 mm (medium pebble to small cobble grade). Most of the conglomerate is well sorted to moderately well sorted, and so plots close to the C=M line axis on logarithmic plots (Passega, 1964) of maximum (C), versus medium (M) grain size (Fig. 8).

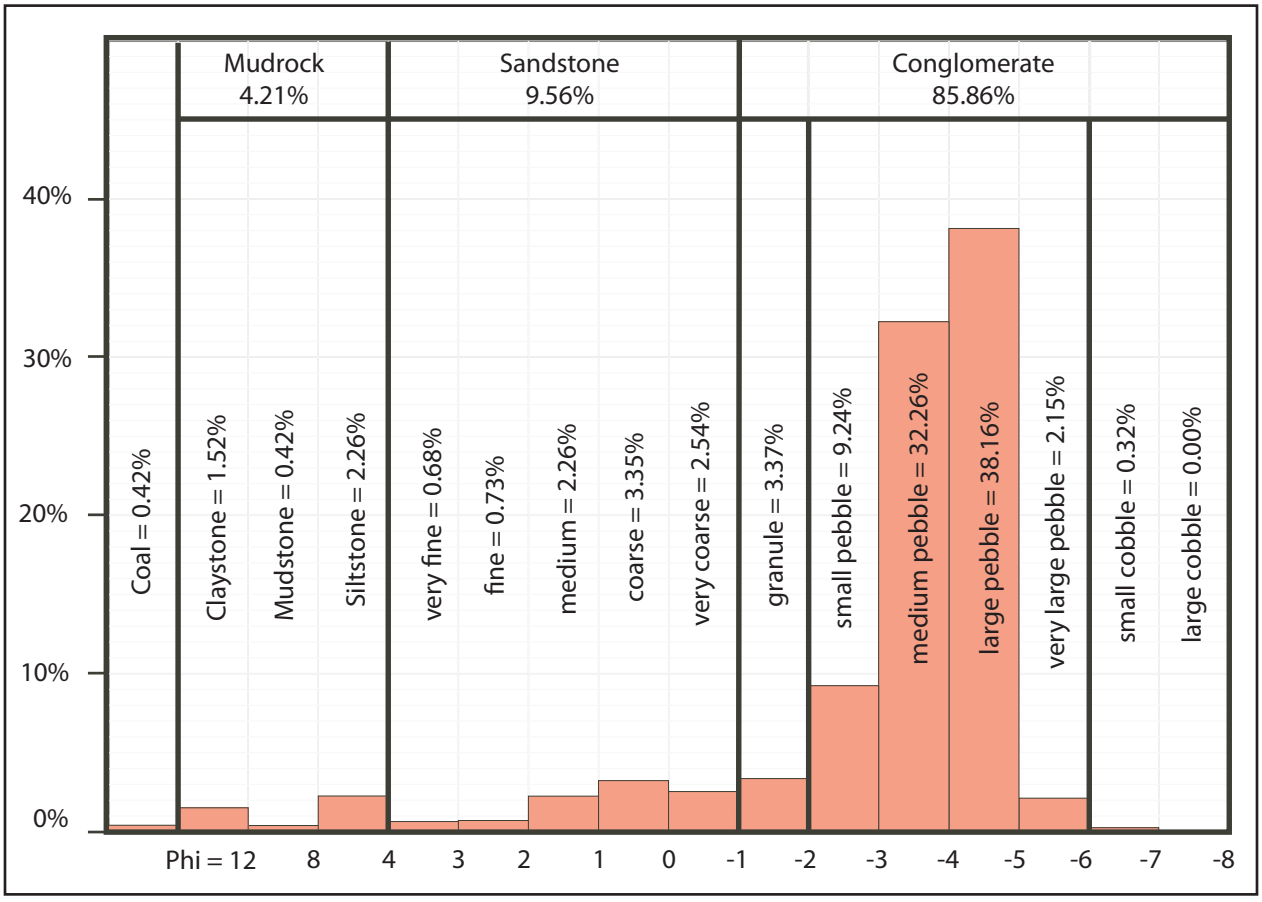

Figure 5. *Distribution of rock types in measured sections through the Tantalus Formation as volume percent (based on thickness and modal size observations of 2768 beds or bedsets).*

Most conglomerate in the Tantalus Formation is clast supported, and appears massive or weakly horizontally bedded (Fig. 9). Planar and trough cross-stratification is developed on a scale of 20 cm to >4 m (Fig. 10). Large-scale cross-stratification (4-17 m) is present locally. Corraision furrows (Massari, 1983; Long and Lowey, 2011) were found at the base one conglomerate unit, resting on finer grained strata in the Tantalus Open Pit (Fig. 10e).

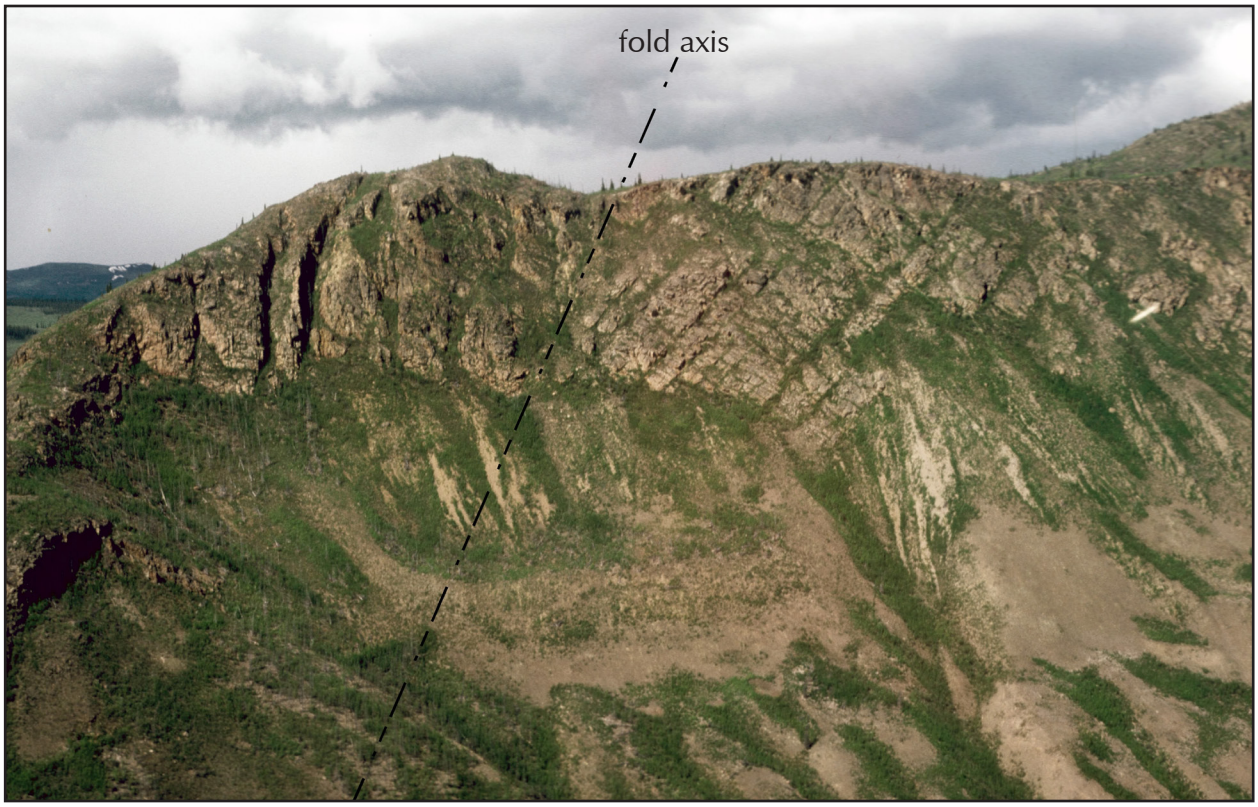

Figure 6. *Thick, multi-storey conglomerate units at Vowel Mountain at ~61°21′00″N, 136°07′27″W (Section T-9 in Appendix 1), a tight isoclinal syncline (chevron fold) with a gentle plunge to the south. View from south. Conglomerate storeys are separated by thin units of sandstone or granule to small pebble conglomerate.*

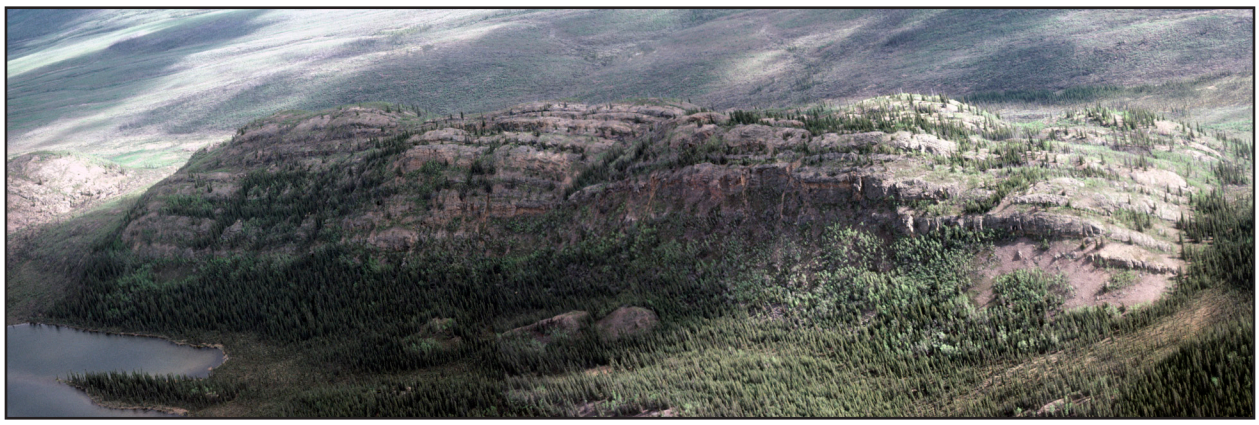

Figure 7. *Striped appearance of conglomeratic exposures in the Tantalus Formation at Corduroy Mountain (61°18′45″N, 135°54′52″W), as seen from the south. Field of view is about 1.6 km. Recessive intervals include sandstones and finer grained conglomerate. Contact with the Tanglefoot formation is close to the lake.*

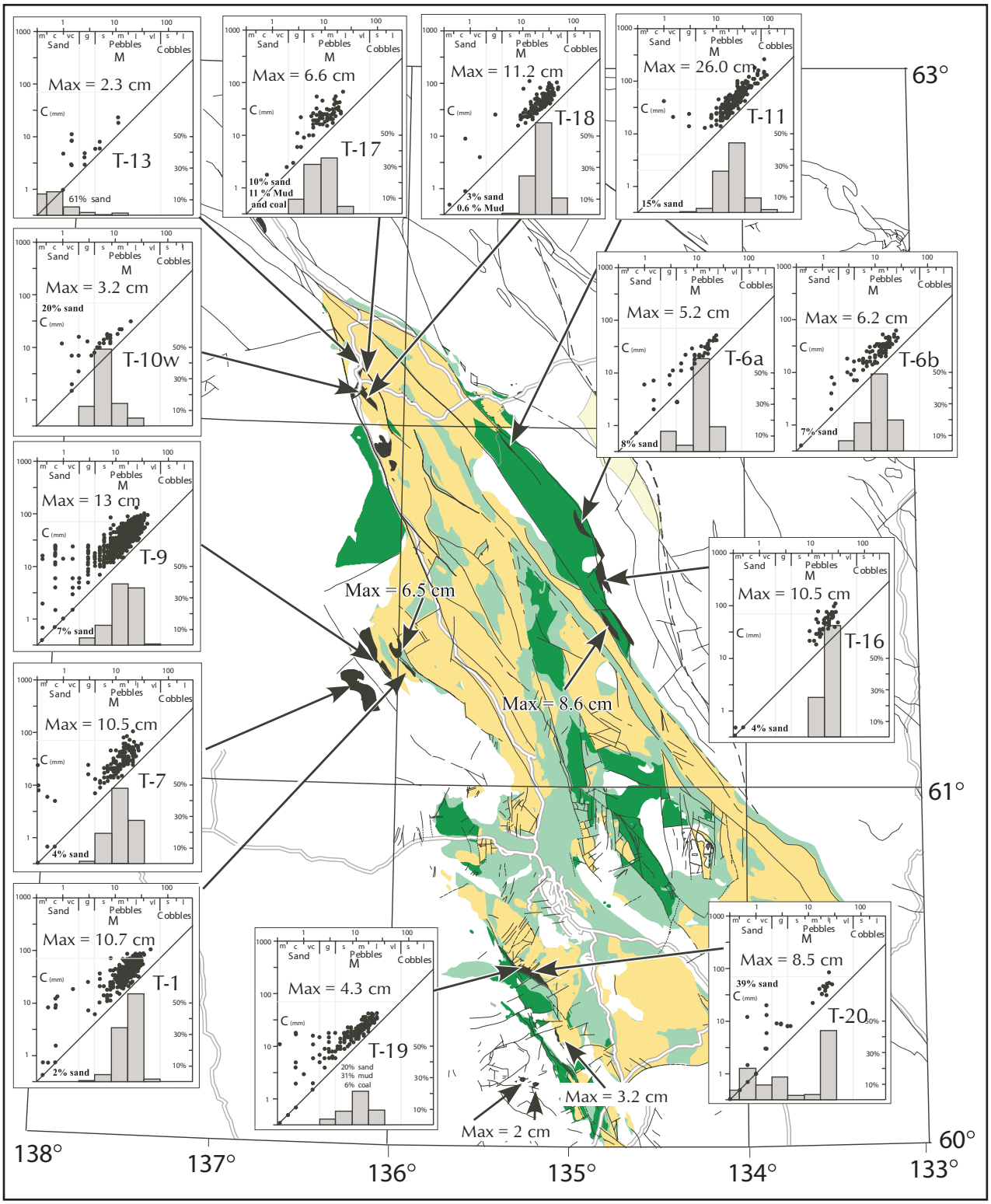

Figure 8. *Logarithmic plots of coarsest one percentile intermediate clast diameter (C) against median grain size (M) in millimetres for measured sections through the Tantalus Formation (CM plot method based on Passega, 1964). Lower histogram shows distribution of modal classes in one Phi intervals. Larger versions of CM plots are provided in Appendix 1.*

Figure 9. *Planar bedded conglomerates, Mount Granger. a) section T-20 and b) section T-19.*

Petrography

Conglomerate is dominated by well sorted to moderately well sorted, medium and large pebble grade clasts, with well-rounded clasts consisting predominantly of vari-coloured black, grey, white, and rare red and light green chert, with minor sandstone, igneous, and metamorphic clasts (Fig. 11). Point counts of cut slabs of 52 samples of conglomerate indicate that all samples are chert-lith-rudites (Fig. 12 and Appendix 2, table 1), with pebbles (>2 mm) consisting of 52-97% chert (average 83%), 1-29% quartz (average 12%), and 0-11 % felsic rock fragments and sandstone (average 3%). The maximum abundance of labile pebbles (felsic rock fragments and sandstone) is in the samples from Hootalinqua and Claire Creek on the northeastern side of the basin, with the minimum abundance in the Mount Granger area on the southwestern side of the basin. Chert clasts in the conglomerate are predominantly well rounded. Based on analysis of slabs, black chert forms between 7 and 67% (average 38%) of the total chert population, with grey chert forming 12-60% (average 34%), and grey-brown chert forming 4-71% (average 28%).
Red and green varieties typically form less than 2% of the total chert population (Appendix 2, table 1). Based on the analysis of slabs, there are no major differences in abundance of the three main chert types across the basin (Fig. 12).

Figure 10. *Conglomerates of the Tantalus Formation. a) Medium to large-scale trough cross-stratification in medium pebble conglomerate, old coal mine, south of the Yukon River at Carmacks (Section T-10, 62°05′39″N, 136°16′00″W). b) Large-scale planar-curved cross-stratification, Tantalus Butte Section (T-17, 62°07′34″N, 136°15′44″W). Photograph rotated to paleohorizontal. c) Four-metre thick planar cross-stratified medium pebble conglomerate, from Hootalinqua North (Section T-6, 61°43′22″N, 134°56′34″W). Dashed line represents upper contact with planar stratified conglomerate. d) Medium-scale planar cross-stratification, from ~10 m above the Whitehorse Coal pit (60°29′50″N, 135°17′13″W). e) Detail of base of conglomeratic strata above the main coal seam in the open-pit mine at Tantalus Butte. Arrows mark linear scours (corraision furrows of Massari, 1983) at base of conglomerate.*

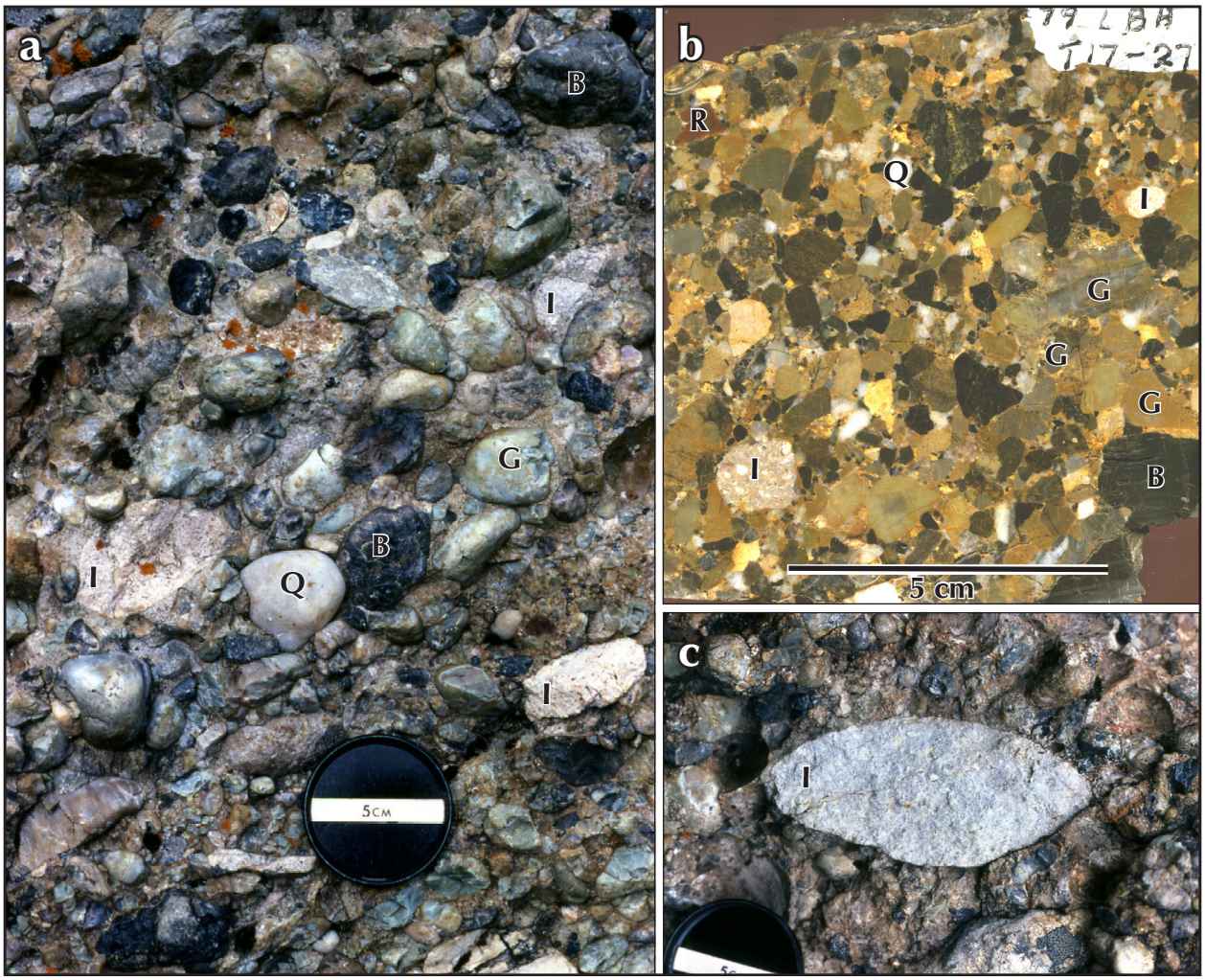

Figure 11. *Typical medium to large pebble conglomerate (chert-lithrudite) from the Tantalus Formation at Tantalus Butte (Section T-17), containing pebbles of black (B), white (W), and grey (G) chert, minor vein quartz (Q) and plutonic rocks (I). a) Large pebble conglomerate (chert-lithrudite) from Vowel Mountain (Section T-9: R=red chert). Minor igneous clasts (I) are a pink quartz monzonite. b) Cut slab of medium pebble conglomerate (chert-lithrudite) from Tantalus Butte (Section T-17). Minor igneous clasts are granodiorite (top right) and porphyritic quartz monzonite (bottom left). c) Detail of very large pebble of quartz monzonite in a large pebble conglomerate from Vowel Mountain.*

Petrographic analysis of 79 thin sections from across the basin show similar trends, with an average composition of 13.4% quartz, 2.4% feldspar and 84.2% lithic fragments (Fig. 13 and Appendix 2, tables 6 and 7). The quartz is predominantly strained (72.7%), with almost equal abundance of monocrystalline (13.3%) and polycrystalline (12.7%) varieties. The lithic component is dominated by chert (91.3%), with minor igneous (4.6%), sedimentary (3.4%) and metamorphic rock fragments (<1%). In thin section 48.5% (average) of the chert is white (range 10-100%), 35.5% is yellow (grey-brown: range 0-79%), 10.4% is black (range 0-61%) and 5.6% is grey (range 0-39%; Fig. 13). Differences between proportions of each type between the slabs and thin sections reflect the translucent nature of many of the chert grains. In terms of textural varieties, the thin sections average 37% of chert with spheres (range 0-87%), 35.7% with massive textures (range 5-88%) and 28.1% with brecciated textures (range 2-95%). Some of the varieties of chert encountered

are illustrated in Appendix 3. Regional variations will be discussed below. Unfilled pore-space (voids) forms an average of 1.1% of the 80 samples examined. Cement filled pore-space forms an average of 3.6% of the samples examined. Of this 2.7% is ferrugenous cement (hematite and iron-sesquioxide), 0.7% calcite, and 0.2% quartz. Clay cement was observed in only one sample (average = 0.01%). Comparative data from the underlying Tanglefoot formation are shown in Figure 14 (data in Appendix 2, table 2).

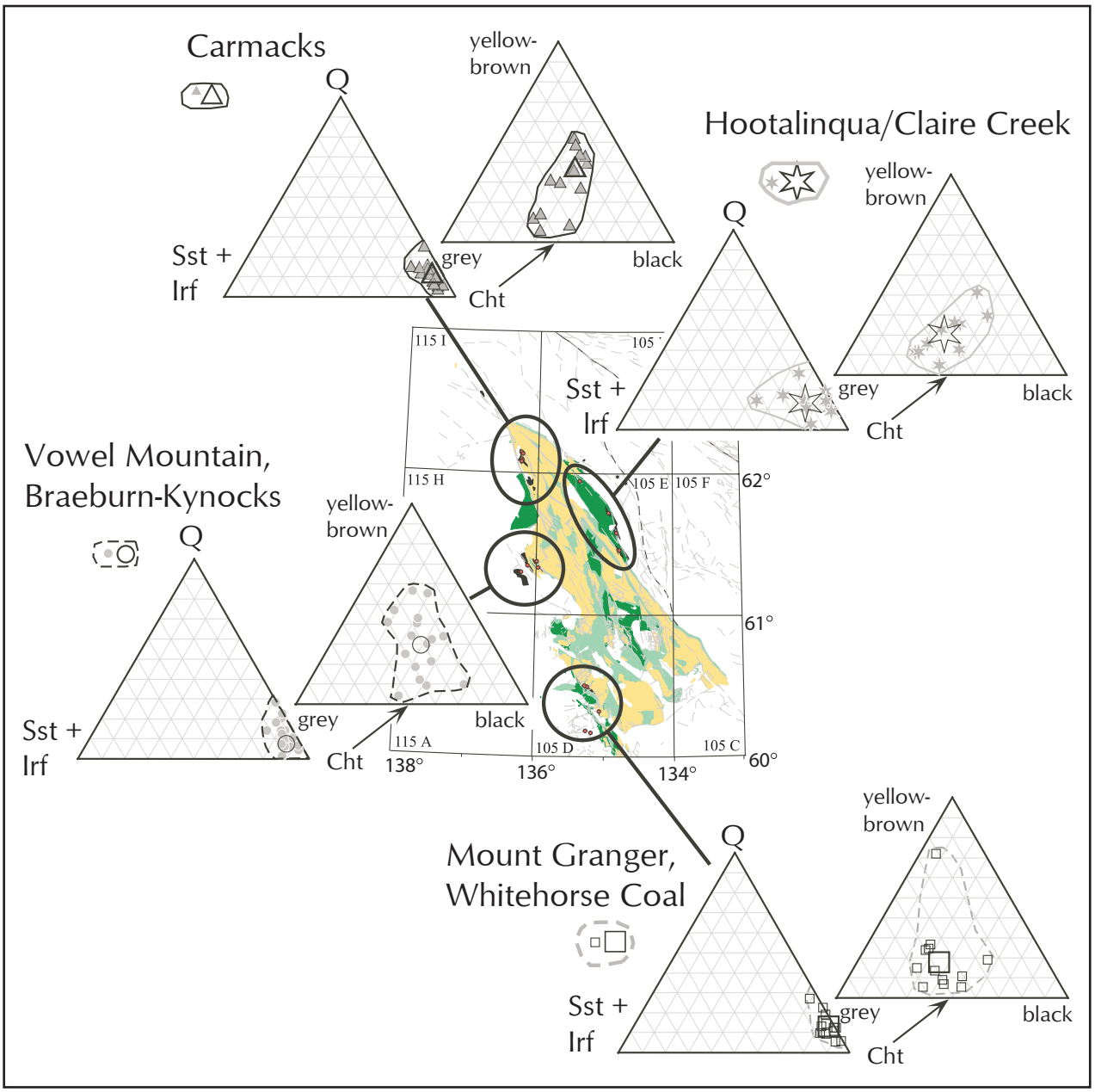

Figure 12. *Petrographic analysis of the >2 mm fraction of cut slabs of conglomerate from the Tantalus Formation from the NE (Hootalinqua/Claire Creek), N (Carmacks), W (Vowel Mountain) and SW (Mount Granger) parts of the basin. The left-hand triangles show the relative proportions of quartz pebbles (Q), chert pebbles (Cht), and sandstone and felsic igneous rock fragments (Sst+Irf). The daughter triangles on the right show the relative abundance of the three main chert types (see Appendix 2, table 1 for further details). Small symbols indicate individual samples, large symbols indicate modes.*

The conglomerate in the Tanglefoot formation contains, on average, a significantly higher abundance of quartz (average 44.0%, range 7-73%) and feldspar (average 25.1%, range 0-63%), and a lower abundance of lithic fragments than the Tantalus Formation (average 30.9%, range 0-88%). Chert constitutes only 52% of the lithic component of the conglomerate in the Tangefoot formation, and is absent in 66% of the conglomerate samples examined. The ratio of monocrystalline to strained quartz is similar to that in the Tantalus Formation, although the abundance of polycrystalline quartz grains is more restricted (Figs. 13 and 14). The range of textural varieties of chert is similar to the Tantalus Formation, although white chert appears to be more abundant.

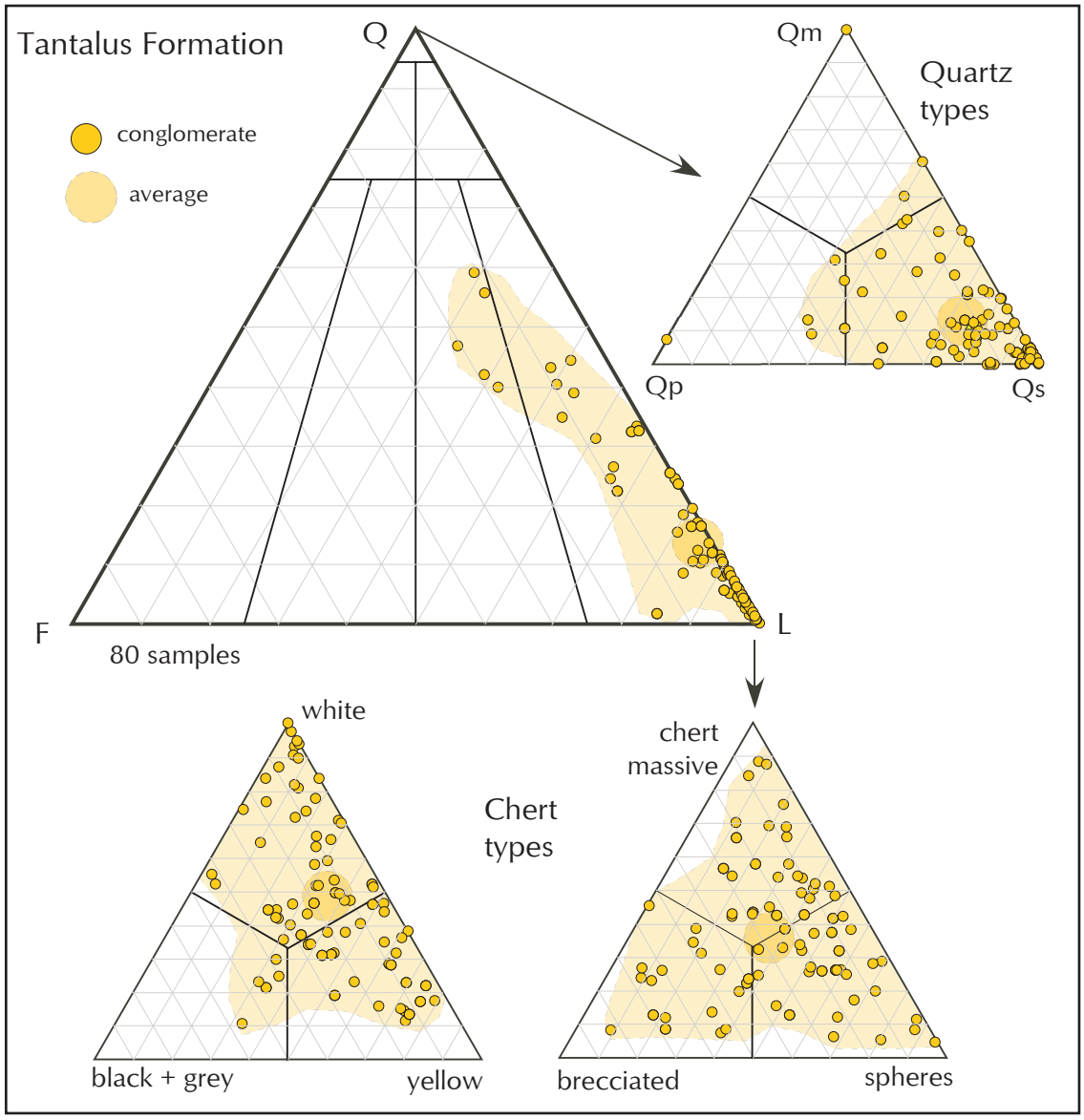

Figure 13. *Petrography of framework grains in thin sections of 80 conglomerate samples from the Tantalus Formation. Primary diagram shows abundance of quartz (Q), feldspar (F) and lithic fragments (L). Daughter triangle at top right shows abundance of quartz types (Qm=monocrystalline; Qp=polycrystalline; Qs=strained). Daughter triangles at bottom indicate relative abundance of the chert component of the lithic fraction, based on colour (left) and texture (right). Small symbols indicate individual samples, large symbols indicate modes. Coloured field indicates range.*

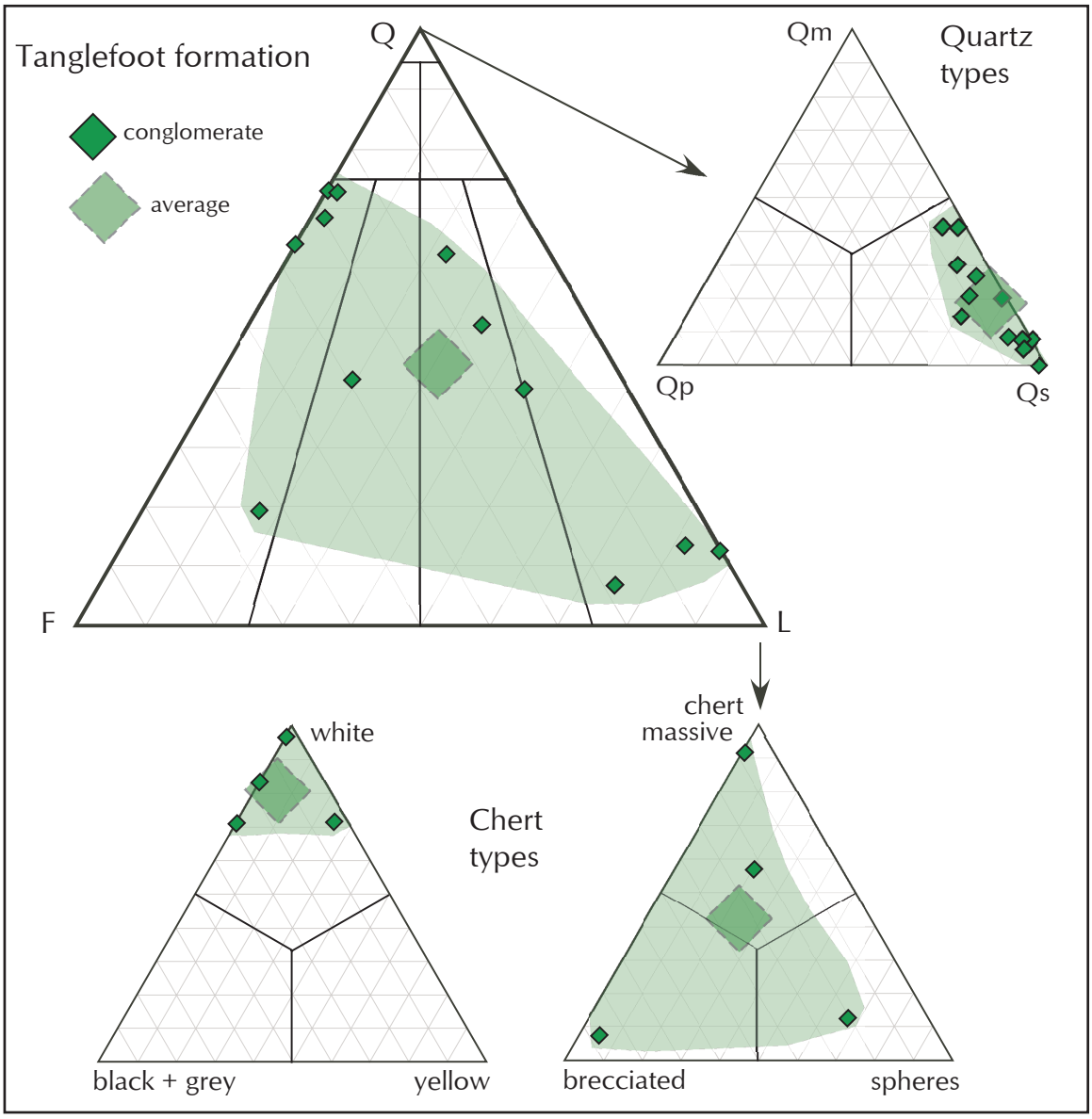

Figure 14. *Petrography of framework grains in 12 conglomerate samples from the Tanglefoot formation. Legend as in Figure 13. Five of the samples contain clay as detrital matrix or cement (Average=2.7% of the whole rock). Voids typically form about 0.1%, ferruginous cements average 7.8%, and carbonate cements average 3.2% of the whole rock.*

Sandstone

Lithology

Sandstone forms less than 10% of exposed strata in the Tantalus Formation, and is dominated by medium to very coarse sand grade material (Fig. 5). Most of the sandstone is moderately well sorted, although pebbly sandstone (*i.e.*, with less than 30% gravel) is common (Fig. 15a,c). Units are from 2 cm to 6.2 m thick (average 0.57 m; mode 0.15 m). They occur as thin beds and cosets in conglomerate dominated sequences (Fig. 15a,b,c), and in sets 0.01 to 1.2 m thick, interbedded with thin mudstone and siltstone units non-conglomeratic intervals (Fig. 15d,e,f,g). Medium to very

coarse sandstone is typically massive or planar cross-stratified, and occurs in beds 10 to 60 cm thick (Fig. 15a,c). Low-angle cross-stratification and planar lamination (with current lineation) are present locally (Fig. 15b). Finer grained sandstone is typically planar laminated or asymmetric ripple cross-stratified (1 to 5 cm; Fig. 15f), with local disruption of sedimentary structures produced by physical displacement of sediment during growth of plant roots (rhizoturbation). Thin laminated examples in places have well-preserved plant material on bedding planes (Fig. 15g).

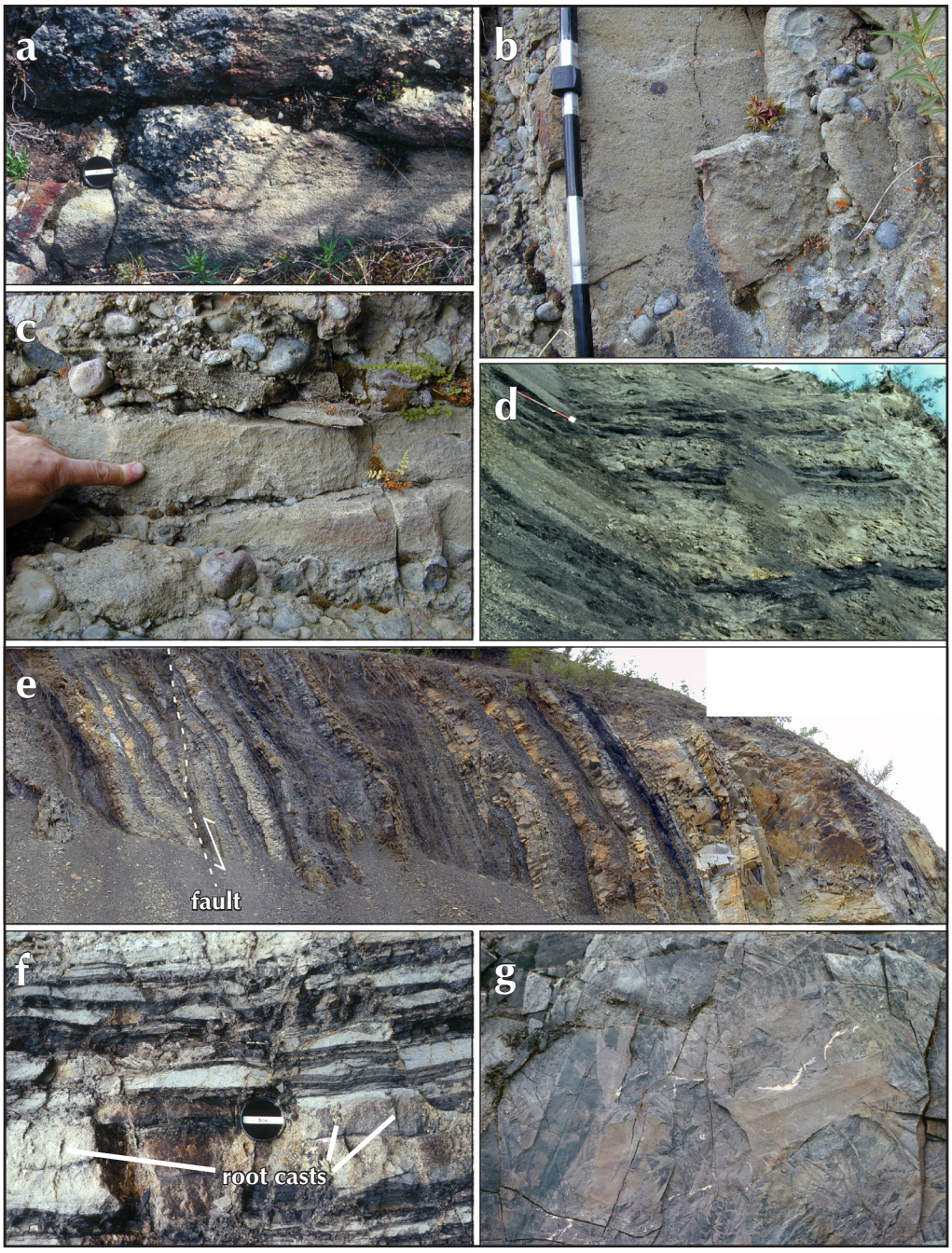

Figure 15. *Sandstones in the Tantalus Formation. a) Planar cross-stratified, and b) plane bedded, coarse to very coarse grained sandstone from between thick conglomerate units, Corduroy Mountain. c) Planar cross-stratified medium to coarse grained sandstone, Tantalus Butte. d, e, f) Inter-bedded medium to fine grained sandstone and mudstone, Tantalus Butte, open pit. g) Well-preserved plant material (ferns) on plane bedded sandstone, Tantalus Butte, open pit.*

Petrography

All the sandstone units in the Tantalus Formation have a speckled "salt and pepper" appearance due to the abundance of chert grains. Petrographic analysis of thin sections of 26 sandstone samples from the Tantalus Formation indicate an average composition of 31% quartz (range 16-55%), 9.7% feldspar (range 0-42%), and 58.9% lithic fragments (range 24-82%), of which 95.4% are chert, with minor igneous (2.9%), sedimentary (1.0%) and metamorphic (0.7%) rock fragments (Fig. 16 and Appendix 2, table 2). As in the associated conglomerate, the quartz is predominantly strained (average 71.3%). Monocrystalline grains appear to be slightly more abundant (average 17.8%) and polycrystalline quartz slightly less abundant (average 10.9%) although the overall range is similar (Fig. 16). In thin section 53.5% of the chert is white (range 33-54%), 26.4% is yellow (range 13-44%), 10.3% is black (range 3-21%) and 9.4% is grey (range 3-27%). The overall distribution of chert colours is more tightly clustered than in the conglomerate (Fig. 13). Chert textures are likewise more tightly clustered, with 75.3% massive textures (range 42-75%), 16.8% containing spheres (range 2-47%) and 7.8% with brecciated textures (range 1-22%). Voids (empty pores) form an average of 4% of the samples examined. Filled pores form a further 7.2% (average) of the thin sections, including 4.6% ferruginous cement, 1.7% carbonate and 0.9% quartz. Chlorite cement was detected in trace amounts in only one sample.

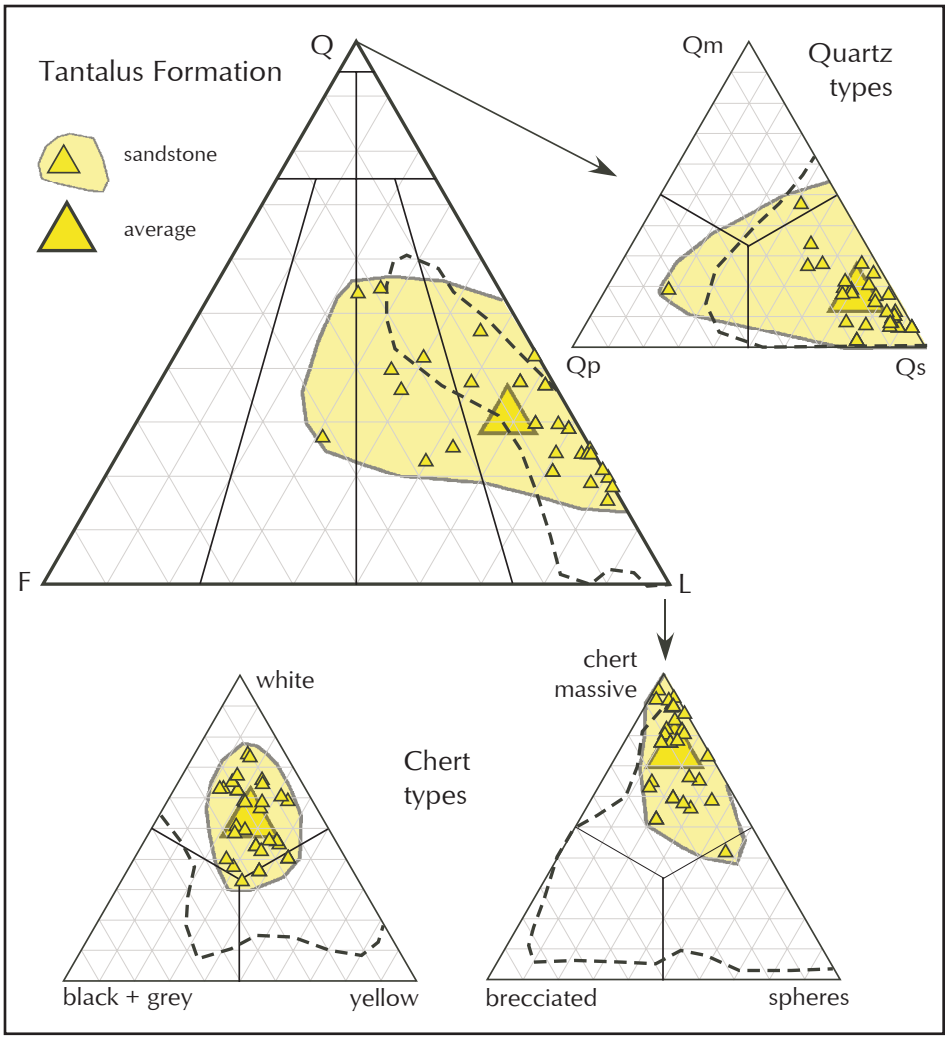

Figure 16. *Petrographic composition of framework grains in 26 samples of sandstone from the Tantalus Formation. Primary diagram shows abundance of quartz (Q), feldspar (F) and lithic fragments (L). Daughter triangle at top right shows abundance of quartz types (Qm=monocrystalline; Qp=polycrystalline; Qs=strained). Daughter triangles at bottom indicate relative abundance of the chert component of the lithic fraction, based on colour (left) and texture (right). Small symbols indicate individual samples, large symbols indicate modes. Coloured field indicates range. Black dashed line indicates limit of data fields of conglomerate in the Tantalus Formation (Fig. 13).*

Sandstone in the underlying Tanglefoot formation can readily be distinguished from that in the Tantalus Formation by its higher quartz (average 51.4%, range 16-87%) and feldspar content (average 33.4%, range 13-52%). Lithic fragments make up only 15.2% (range 0-56%) of the 23 sandstone samples examined from the Tanglefoot formation. Igneous rock fragments are more abundant (average 24.3%) than chert (average 2.1%), which appears in only half the samples examined (Appendix 2, table 2). Sedimentary rock fragments (other than chert) make up an average of 7.6% of the lithic component, and metamorphic rock fragments make up a further 2.1%. Most sandstone plots as arkose, with lesser abundances of lithic arkose, subarkose and feldspathic litharenite, with only one sample plotting as a litharenite (Fig. 17). Polycrystalline quartz is less abundant than in the Tantalus Formation (average 4.5%, range 2-8%), with similar abundances of monocrystalline and strained varieties. Chert varieties are similar to the Tantalus Formation, although the overall distribution is more variable. Clay is present as a matrix component (detrital) or cement in half the samples examined (average 2.2%), with minor voids (average 0.3%), ferruginous cements (average 5.1%), carbonate (average 5.1%) and traces of quartz cement (average 0.5%).

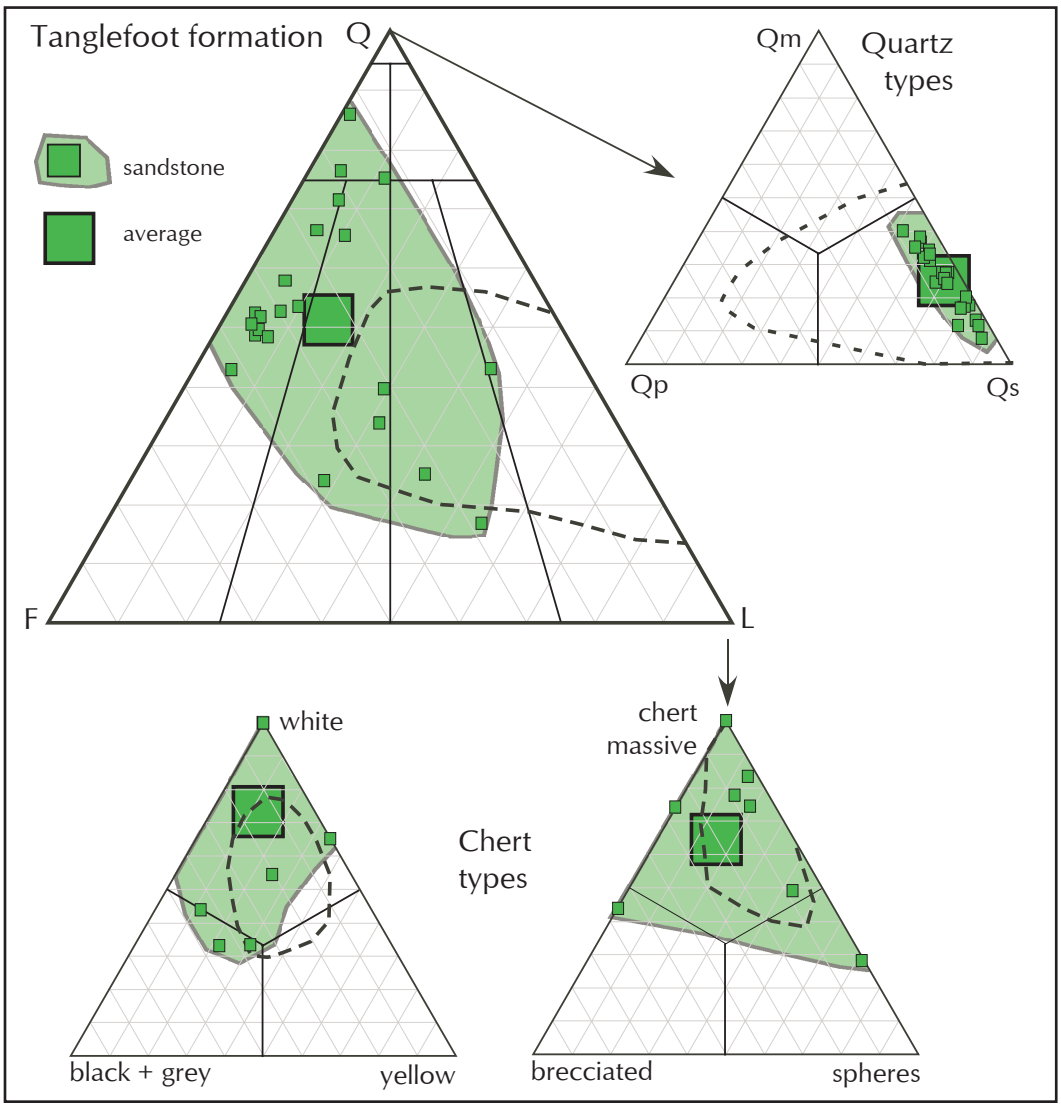

Figure 17. *Petrographic analysis of 23 samples of sandstone from the Tanglefoot formation. Legend as Figure 16. Black dashed line indicates range of composition of sandstone from the Tantalus Formation.*

Mudstone

Mudstone forms only 4.2% of the exposed parts of the Tantalus Formation (Fig. 15d,e,f). It is dominated by siltstone (54%), with lesser amounts of claystone (39%) and mudstone (10%). Most samples are massive, with abundant slickensides (soil crumb texture), or are thin (0-2 mm) to thick (2-10 mm) laminated. Grey mudstone tends to have low organic content, while black samples are organic rich and in places contain plant roots and well preserved leaf and stem material.

Coal

Coal forms only 0.42% of the exposed parts of the Tantalus Formation, although this may be a slight under estimation, as seams typically occur in recessive intervals separating thick conglomerate units, and tend to have high ash (detrital clay) content. Rank is typically high volatile A to B in the north, increasing to sub-anthracite in the southwest (Goodarzi and Jerzykiewicz, 1989; Beaton *et al.*, 1992; Cameron and Beaton, 2000). Thin (1-5 cm) beds of coal (>50% organics) and coaly-mudstone (<50% organics) typically occur in intimate association with ripple laminated sandstone and massive to weakly planar to wavy laminated organic rich mudstone, with traces of root casts or soil crumbs (Figs. 15d,e and 18). Thick seams, exposed in the open pit at Tantalus Butte (Fig. 18b,c,d), are intimately associated with mudstone and sandstone and have high ash (mud) content. Within the open pit, the coal is tectonically thickened along the axis of drag folds. Both at Carmacks and at Mount Granger, thicker coal seams are found only within fine-grained intervals.

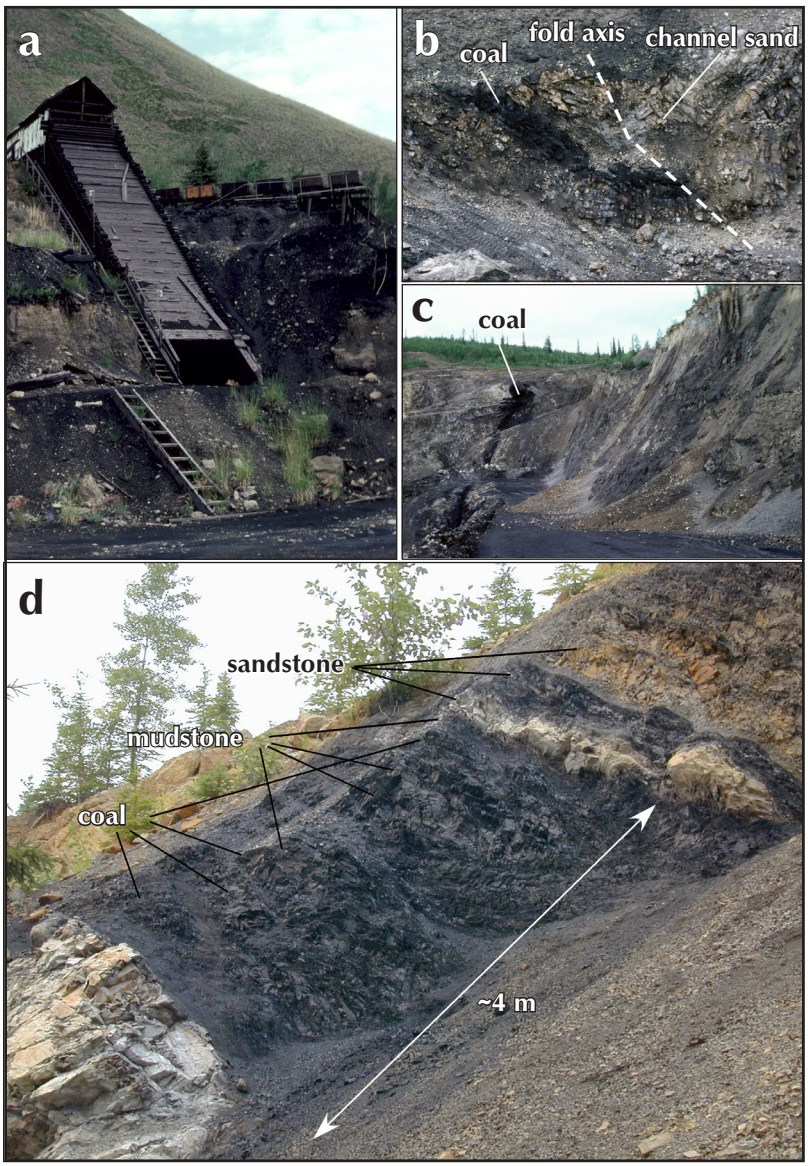

Figure 18. *Carmacks area coal: a) adit to main underground workings at Tantalus Butte (1978), this structure has since been destroyed; b, c) highly deformed coal seams (drag folds) in the open pit at Tantalus Butte; d) thick seam exposed in centre of open pit.*

STRATIGRAPHY

The base of the Tantalus Formation is marked by a significant increase in the chert content of the sandstone and conglomerate, when compared to underlying strata of the Tanglefoot formation. South of the Yukon River at Carmacks, the base of the Tantalus Formation is clearly erosional. This can be demonstrated by truncation of coal seams and sandy channel fill deposits in the underlying Tanglefoot formation (Fig. 19). At other locations, such as Vowel Mountain (T-09), Corduroy Mountain (T-1) and Mount Granger (T-19 and 20), the contact appears to be sharp and conformable, but may still be erosional. At Division Mountain (between Vowel and Corduroy Mountains, at ~61°20'N, 136°08'W) Allen (2000) indicates a sharp lower contact. Drilling by Cash Resources Ltd. in this area indicates that coal seams in the underlying Tanglefoot formation have been truncated at the base of the Tantalus Formation (Fig. 3 in Carne and Gish, 1996).

As strata of the Tantalus Formation are predominantly chert pebble conglomerate, it is difficult to correlate between isolated areas of outcrop, as the (recessive) finer grained units do not appear to be continuous across the basin. On a local scale, it is possible to make correlations based on the first occurrence of exotic pebble types. For example, in the north end of the Whitehorse trough

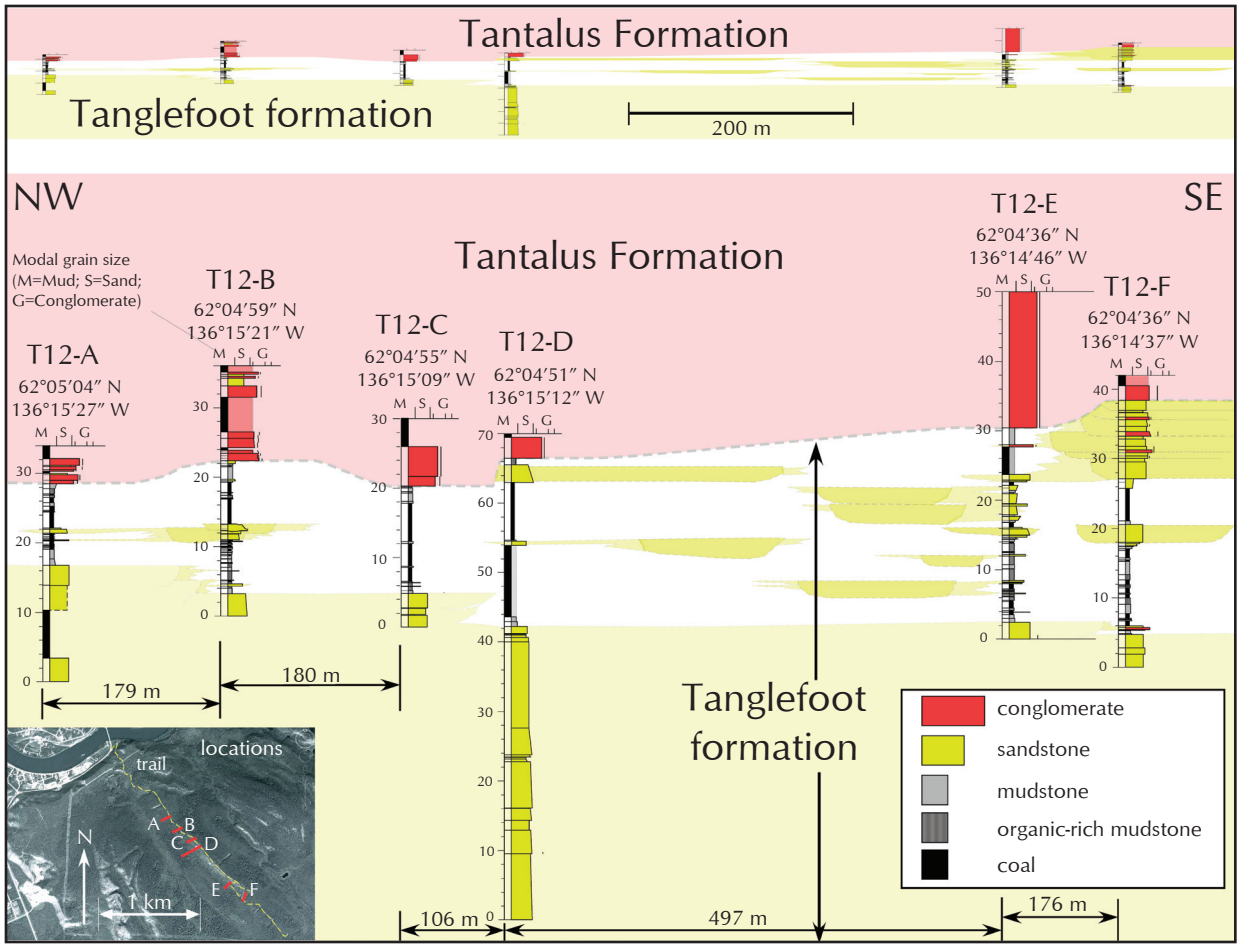

Figure 19. *Detailed correlation of coal-bearing strata in the Tanglefoot formation, south of Carmacks (after Long 2005). Top at true scale. Bottom with vertical exaggeration x6. Base of the Tantalus Formation (Pink/Red – at top of diagram) is estimated at 14 m higher in the southerly exposures, over a distance of 1066 m (for details see Appendix 1). Base map for locations based on Google Earth image.*

at Carmacks (Fig. 20), Long (1986, 2005) suggested that the first occurrence of felsic (plutonic) pebbles, which coincides with a marked increase in clast size (horizon B in Fig. 20), indicated that there is a minimum of 155 m of local relief at the base of the formation. Maximum pebble size may also be used for local correlation, as sediment flux in valley fill settings is often driven by climate shifts (possibly driven by 100 Ka Milankovich cycle: Van der Zwan, 2002; Thamó-Bozsó *et al.*, 2002; Hinderer, 2012; Pepin *et al.*, 2013; Wu *et al.*, 2013), and/or by tectonic events (Miall, 1996; Leeder, 1997; Frostick and Jones, 2002). Surfaces C and D (Fig. 20) indicate how this can be used to confirm local correlations.

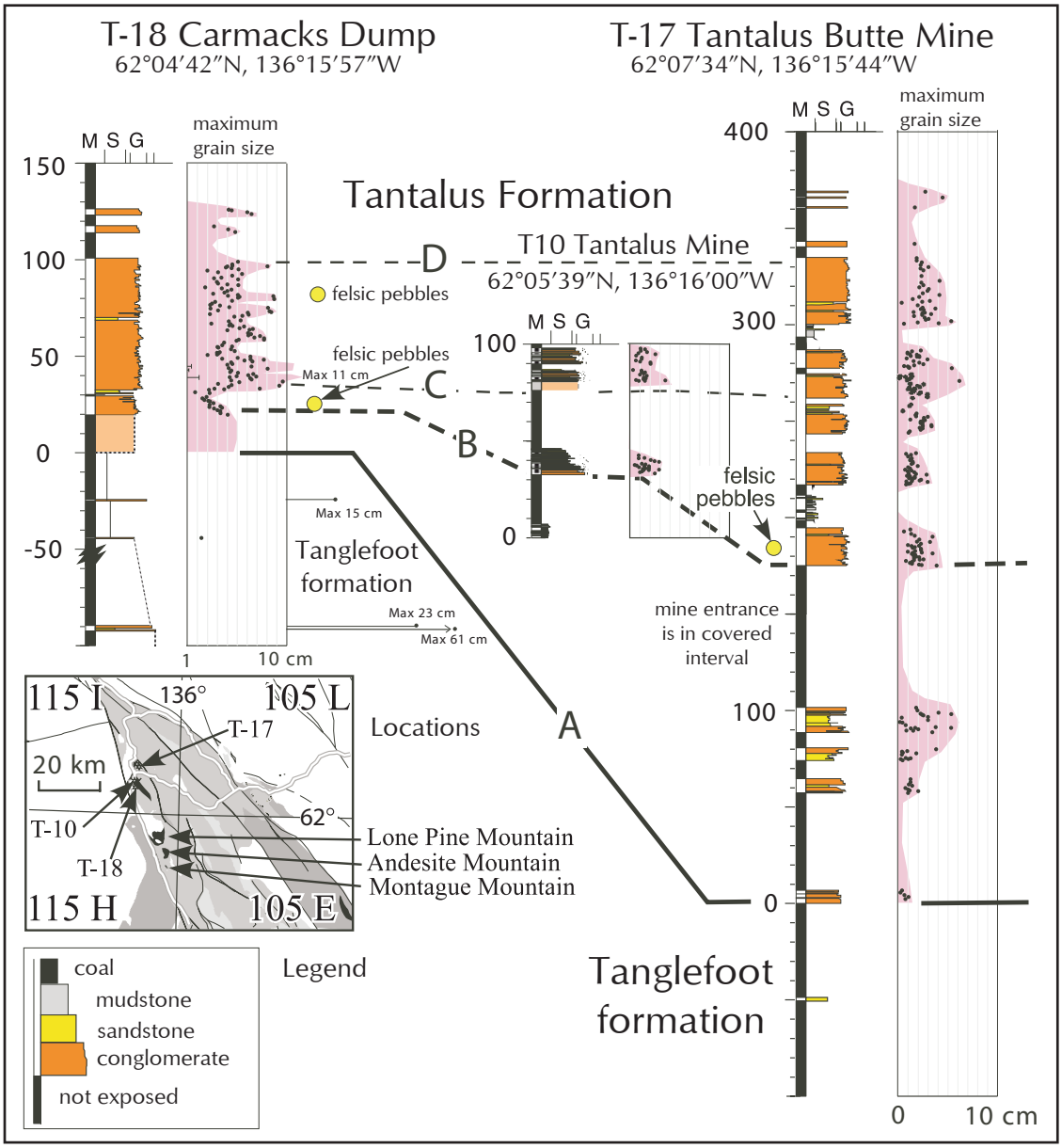

Figure 20. *Correlation of sections in the Carmacks area, based on location of unconformity (A); first occurrence of felsic clasts (B); and initiation of fluctuations in maximum grain size (C, D). North to right. Base of lower conglomerate in section T-10 may correlate with surface B. Bars to right of column indicate bed thickness and sedimentary structures. Arrows to right of these columns indicate paleoflow observations. Dots, and pink envelope indicates maximum grain size in 1 cm divisions. See Appendix 1 for further details of individual sections.*

Cairnes (1910) recorded coal seams associated with conglomeratic strata south of the Carmacks area, south of Montague House, at Lone Pine Mountain (61°56'N, 136°07'W), Andesite Mountain (61°54'N, 136°05"W) and Montague Mountain (61°53'N, 136°05'W: Fig 20, inset). These have been mapped as part of the Tantalus Formation by Colpron (2011), but may include some strata of the Tanglefoot formation (Laberge Group), in road-side exposures west of Lone Pine Mountain where they tend to be finer grained and feldspathic, with lower chert content than samples from the Tantalus Formation.

The basal contact of the Tantalus Formation is not exposed along the northeast side of the Whitehorse trough (Fig. 21). Exposures between Claire Creek (T-11) and Mason Landing (T-15) may be affected by faults. Correlation based on coal or fine grained intervals is not practical, due to the paucity of exposures south of Claire Creek. All sections contain some felsic plutonic pebbles, so this is of little use for correlation. Using peaks in maximum grain size it is possible to correlate over an along strike distance of 50 km (Fig. 21; horizons C, D, E). These may or may not be equivalent to peaks seen in the Carmacks sections (Fig. 20) an additional 50 km to the northwest. Strata at Mason Landing (T-15) are too poorly exposed to allow correlation. Faults in section T-11 have minimal off set. Faults in sections T-6, T-15 and T-16 are difficult to locate in the absence of outcrop, but are probably strike parallel with minimum off set of the stratigraphy.

Correlation of strata in the Braeburn-Kynocks area, along the central western margin of the Whitehorse trough, is more difficult as no significant coal seams have been recognized in the formation in this area (Long, 1986; Carne and Gish, 1996; Allen, 2000), and there are few proven intervals with fines. The basal unconformity is exposed along the western margin of the Whitehorse trough, in the Nordenskiöld River section (T-7) at 61°15'43"N, 136°16'05"W (Fig. 22). At this locality the Tantalus Formation rests directly on a coarse-grained quartz monzonite that Tempelman-Kluit (1974) considered to be of possible Triassic age. Mapping to the west indicates that this pluton is probably of Toarcian age (late Lower Jurassic), corresponding to the Long Lake plutonic suite of Johnston and Timmerman (1994). This has been dated at 179.1 ± 1 by Johnston *et al.* (1996), indicating emplacement during deposition of the lower to middle part of the Laberge Group (Fig. 1). Along the eastern margin of NTS 115H/8 the formation overlies a thick sequence of strata belonging to the Tanglefoot formation (Fig. 22). The contact appears conformable, but as it truncates several coal seams in the underlying strata (Carne and Gish, 1996; Allen, 2000) near Division Mountain, it must have an erosional base.

Fyles (1950), Wheeler (1961), Hart and Radloff (1990), and Hart (1997) show a thin sliver of Tantalus strata preserved between high-angle faults on the east side of the Ibex River (NTS 105D). A 300 m section through these strata, measured in a gully at 60°37'13"N, 135°26'34" (section T-21 in Appendix 1), consists of minor small to medium pebble and granule conglomerate units, associated with massive units of medium and coarse sand, and thick intervals of non-carbonaceous mudstone. The conglomerate contains minor concentrations of black chert and superficially resembles strata of the Tantalus Formation (except that they lack cross-stratification). The average composition of three conglomerate samples examined contained 34.4% quartz (predominantly strained), 11.5% feldspar, and 54.1% lithic fragments, of which 69% were chert (Fig. 23). Associated sandstone is typically quartzo-feldspathic. The three samples examined included both lithic arkose and feldspathic litharenite (Fig. 23), with 27.3% quartz (predominantly strained), 30.3 % feldspar, and 42.5% lithic fragments, of which only 17.9% were chert. In both the conglomerate and sandstone samples concentrations of chert are significantly lower in both absolute and relative abundance than in comparable samples from the Tantalus Formation, hence this strata is more properly assigned to the

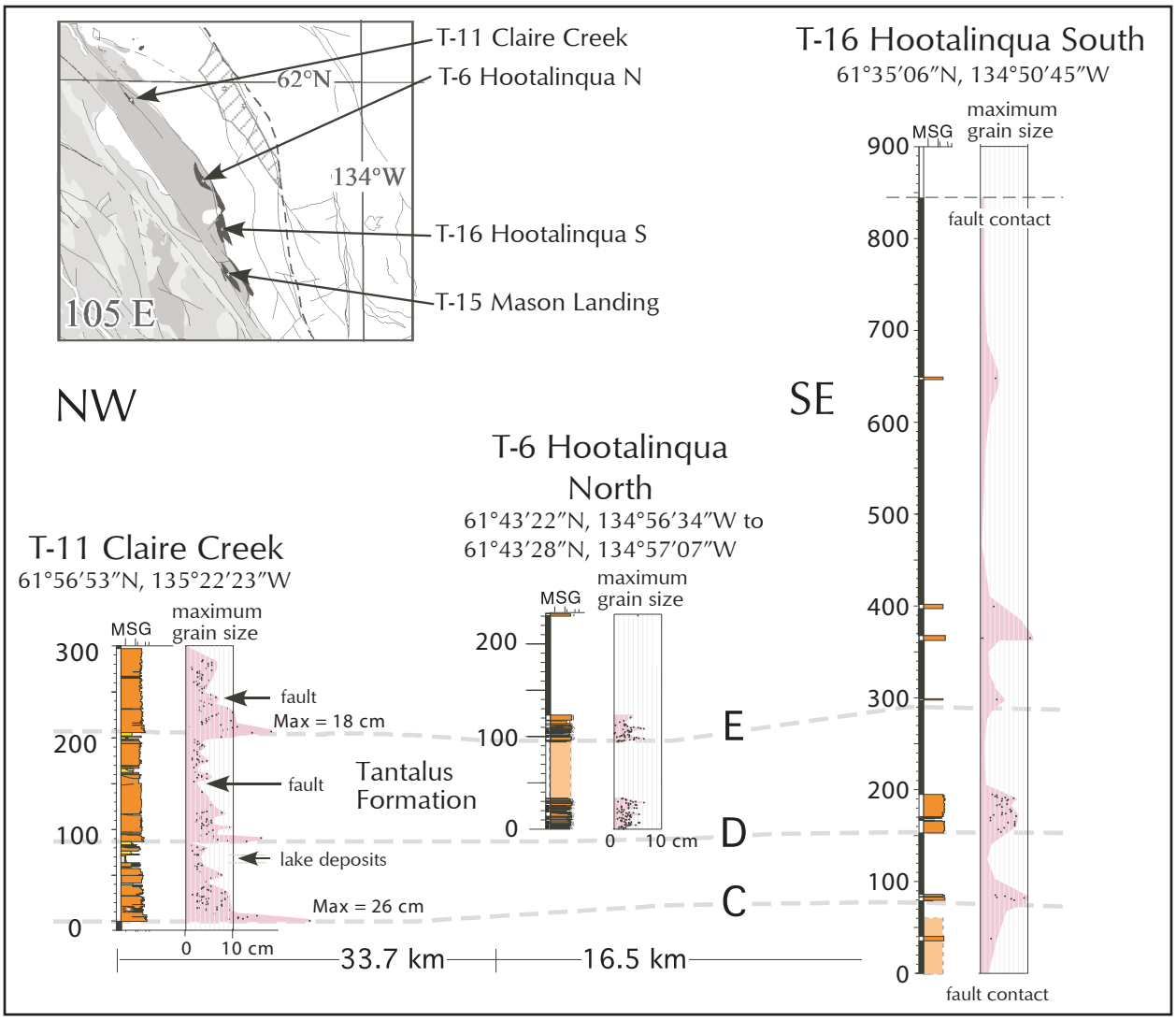

Figure 21. *Correlation of strata in the NE Whitehorse trough. C, D, E are correlations based on fluctuation of maximum grain size. Bars to right of column indicate bed thickness and sedimentary structures. Arrows to right of these columns indicate paleoflow observations. Dots, and pink envelope indicates maximum grain size in 1 cm divisions. The pink envelope projects to the right of the box where maximum grain size exceeds 10 cm: see Appendix 1 for further details of individual sections. Faults exposed in section T-11 are bedding parallel, and have minimal offset. Faults may be present in T-6 and T-16, but could not be identified due to poor outcrop.*

Tanglefoot formation of the Laberge Group. The presence of Kimmeridgian – Oxfordian (lower to mid-Upper Jurassic) palynomorphs in the Ibex River section (Rouse, cited in Hart and Radloff, 1990) indicates that deposition of the Tanglefoot formation may have continued into the Oxfordian, hence the unconformity between the Laberge Group and Tantalus Formation may represent a relatively short period (Fig. 2).

Allen (2000), working in the vicinity of Division Mountain suggested that at least locally, the Tantalus Formation can be divided into upper and lower members, due to an abundance of sandstone intervals in the lower part of the formation. In this study, sections measured at Vowel

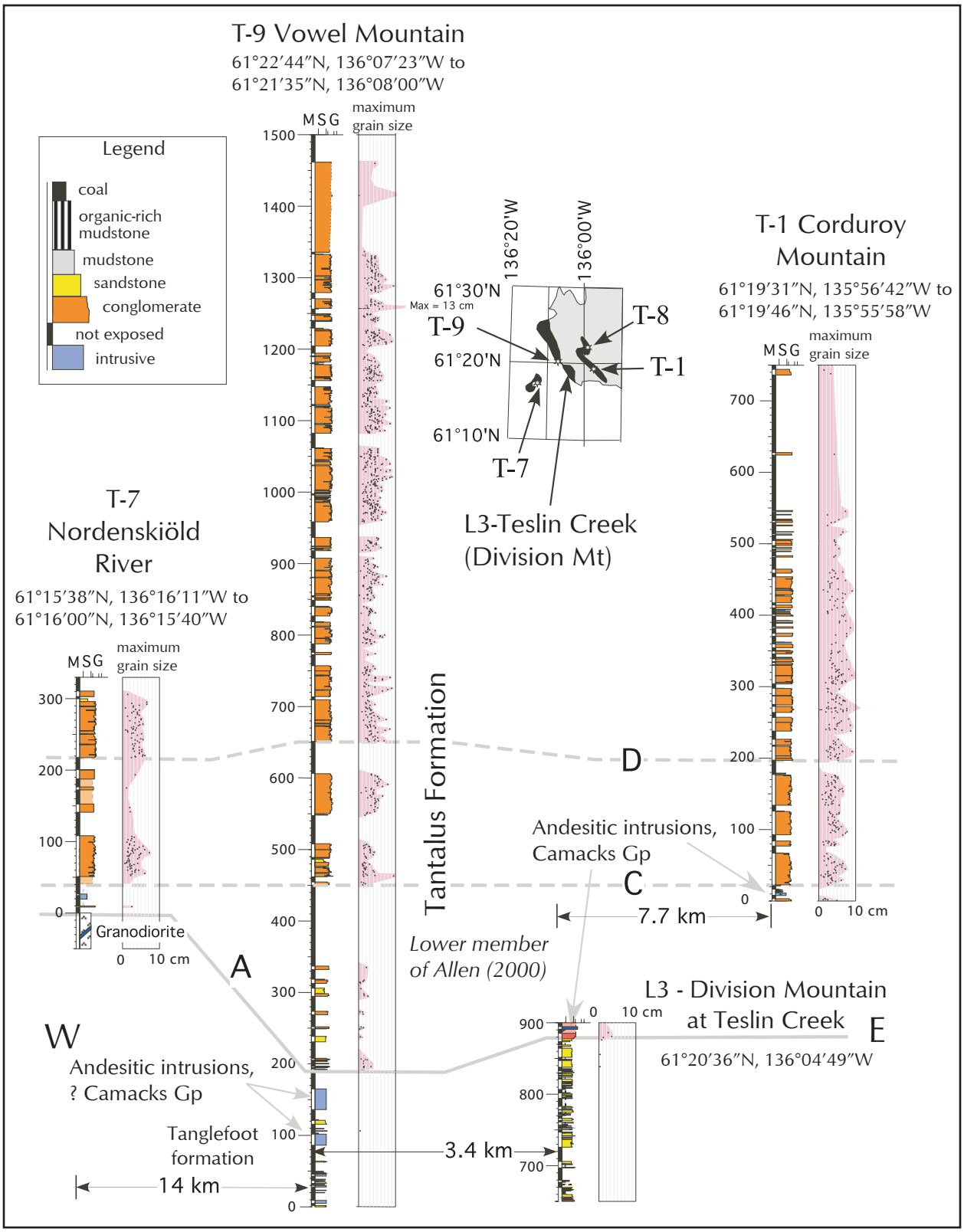

Figure 22. *Correlation of strata in the Braeburn-Kynocks area. A=Unconformity; C, D=possible correlations based on changes in grain size. Bars to right of column indicate bed thickness and sedimentary structures. Dots, and pink envelope indicates maximum grain size in 1 cm divisions. See Appendix 1 for further details of individual sections.*

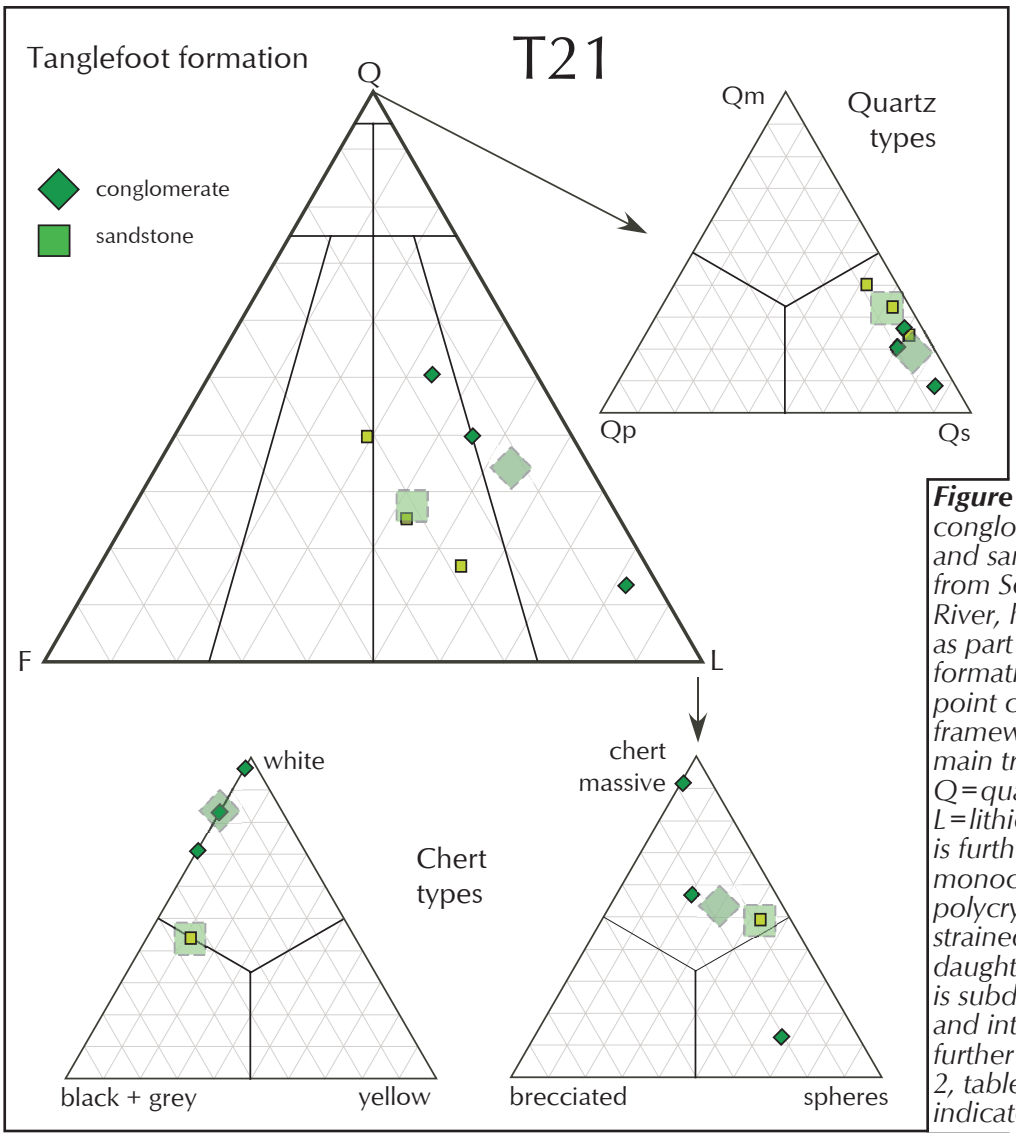

Figure 23. *Petrography of conglomerates (diamonds) and sandstones (squares) from Section T-21, at Ibex River, here interpreted as part of the Tanglefoot formation. Plots based of point counts with ≥500 framework grains. In the main triangle (top left) Q=quartz, F=feldspar, L=lithic fragments. Quartz is further divided into monocrystalline (Qm), polycrystalline (Qp) and strained (Qs). In the lower daughter triangles chert is subdivided by colour and internal texture (for further detail see Appendix 2, table 2). Large symbols indicate average values.*

Mountain (T-9) and alongside the Nordenskiöld River (T-7) appear to have a lower unit with abundant sandstone (Fig. 22). Based on the location of the basal contact with the Tanglefoot formation in the Vowel Mountain section (T-9), this lower unit is estimated to be as much as 260 m thick, thinning to about 42 m to the west (section T-7), and to the east where only 20 m is exposed at the base of the Corduroy Mountain section (T-1). Sills of porphyritic andesite, possibly belonging to the Carmacks Group tend to be concentrated in this unit. Allen (2000) noted the presence of pebbly sandstone of possible debris flow origin in the lower member at Division Mountain. No massive pebbly sandstone was encountered in any of the sections measured during the current study. Felsic plutonic pebbles are not conspicuous in any of the four sections measured, hence cannot be used for local or inter-regional correlation. Plots of maximum clast size may support local correlations in the area (lines C and D in Fig. 22), but cannot be correlated to the Carmacks area or beyond with any confidence.

In the Whitehorse Coal area, to the west of Mount Granger (sections T-19 and 20), the base of the formation is not exposed, but appears, based on local geomorphology, to lie near-conformably on underlying strata of the Laberge Group (Fig. 24). In this area, exploration in the 1980s has indicated up to eight coal seams (some of which may be in the Tanglefoot formation), with a maximum seam thickness of 13.1 m (Bremner, 1988; Cameron and Beaton, 2000). Some of the thicker seams can be traced along strike for distances of 2-11 km (Latour, 1968; Hunt and Hart, 1994; Bremner, 1988; Ricketts, 1984), and may correlate with exposures on Double Mountain (Cairnes, 1910). The abundance of finer grained units (sandstone, mudstone and coal), along with sills of aphanitic volcanic material indicates that much of the section in this area is equivalent to the lower member of the formation in the Braeburn-Kynocks area.

At Bush Mountain (section T-22 in Fig.1), some 23 km SSE of the Whitehorse coal occurrence, Cairnes (1912) reported three coal seams in ~600 m of strata at Idaho Hill (4 km west of Annie Lake) that he initially considered to be part of the Tantalus Formation, but later correlated with the Laberge Group (Cairnes, 1916). Hart and Radloff (1990) described these strata as a "chert/ quartz poor" facies of the Tantalus Formation, and noted that they contain both abundant feldspar and lithic fragments, which are not evident in this formation elsewhere (*see* above). Petrographic analysis of three samples of conglomerate from Bush Mountain (Appendix 2, table 2, samples T22-7, 20, 25), indicate average QLF (quartz, lithic, feldspar), quartz-type, and chert-type, distributions

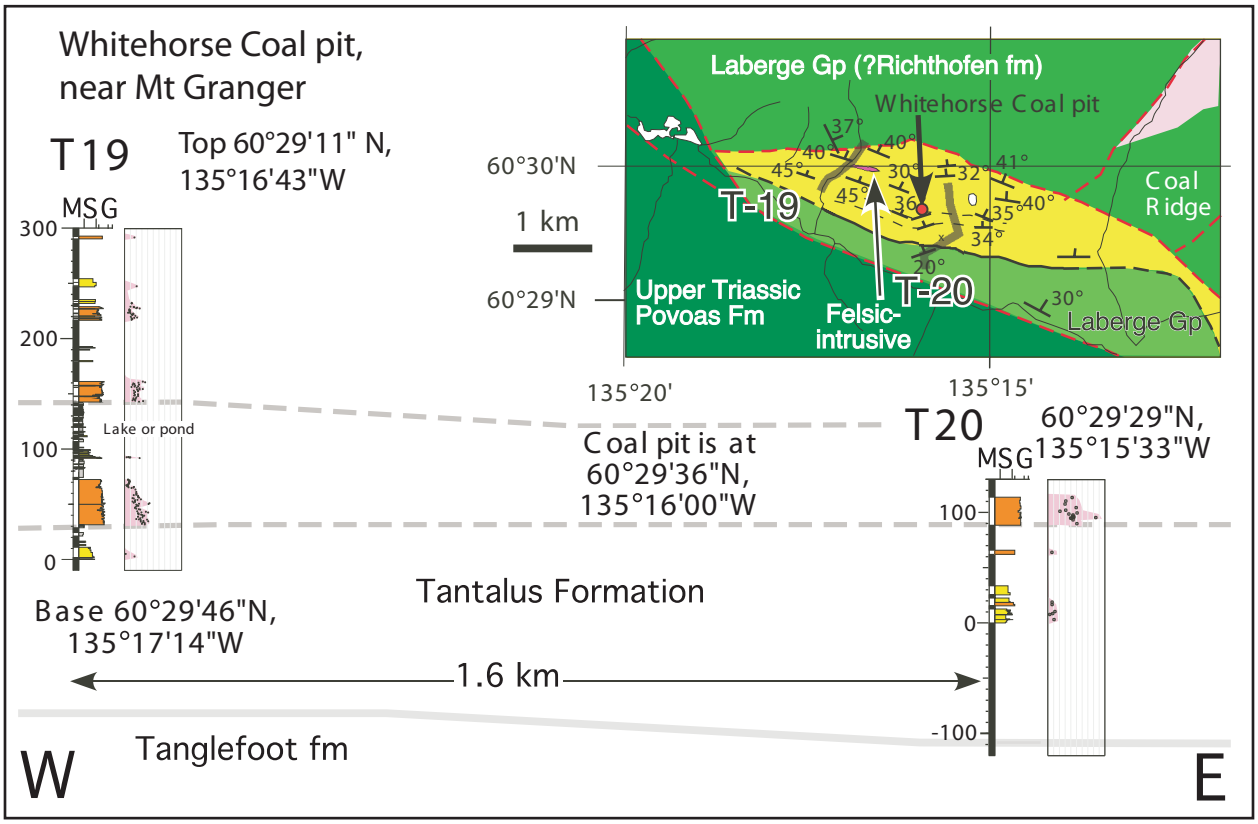

Figure 24. *Correlation of strata near Mount Granger (Whitehorse Coal deposits). Insert shows location of sections measured along with local geology (based on my observations, combined with those of Colpron 2011). Numerous cross-faults may be present (Hart and Radloff 1990) but were not recognised during this study. The pink units in the upper right of the insert map are part of the late-Lower Cretaceous (108-113 Ma: Hart 1997) Whitehorse igneous suite. The thin dike of felsic porphyry near section 19 may be part of the 70 Ma Carmacks Group, or the 54 Ma (Hart 1997) Skukum Group, but has not been dated.*

that are almost identical to those of samples of the Tantalus Formation from the Whitehorse Coal area, although the relative abundance of white (clear) chert clasts is higher. On average both (non-chert) sedimentary rock fragments (6.3% *vs.* 2.1%) and igneous rock fragments (7.3% *vs.* 3.0%) are two to three times more abundant than in the conglomerate of the Tantalus Formation from the Whitehorse Coal area (for further discussion on regional petrographic variations *see* below). The strata at Bush Mountain have been extensively deformed (Fig. 25), and are intruded by andesite sills and dikes that may be part of the Albian (late-Lower Cretaceous) Mount Nansen Group (Hart and Radloff, 1990) or Ypreian (lower Eocene) Skukum Group (Gordey, 2008), that have upgraded the coals to semi-anthracite with a high ash content (Speelman, 1971). Many of the recessive areas along Idaho Ridge may be underlain by sandstone and mudstone, in which case the area may correlate with the lower part of the succession in the Braeburn-Kynocks area. Plant fossils (Fig. 25b), collected from finer grained intervals, included *Cladophlebis virginiensis* (Fontaine). Bell (1956, p. 27 and 173) used examples of this species and associated plant material to indicate a Lower Cretaceous age. Unfortunately this species has a broad age range, spanning the Tithonian (late Upper Jurassic: 152.1-145 Ma) to Aptian (late Lower Cretaceous: 125-113 Ma), so is not age diagnostic (Bell, 1956; Lapasha and Miller, 1985; MacLeod and Hills, 1991).

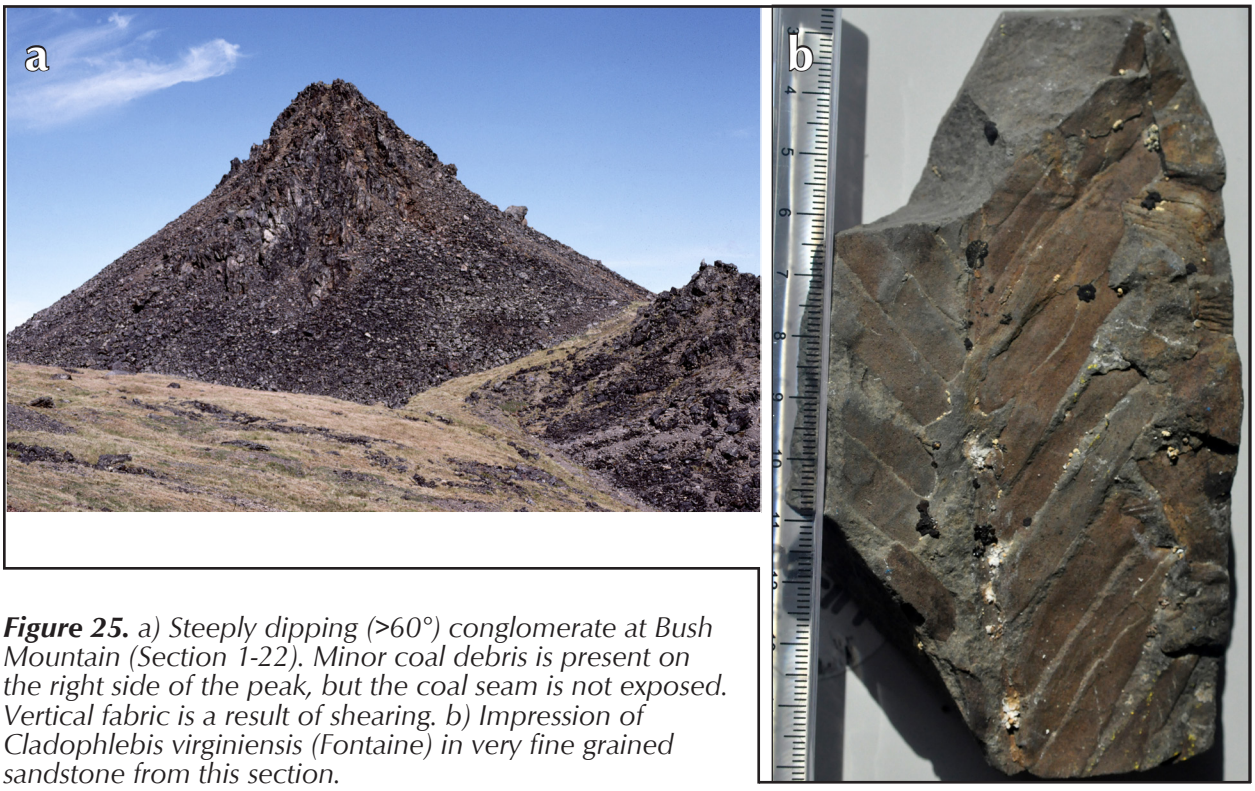

Figure 25. *a) Steeply dipping (>60°) conglomerate at Bush Mountain (Section 1-22). Minor coal debris is present on the right side of the peak, but the coal seam is not exposed. Vertical fabric is a result of shearing. b) Impression of Cladophlebis virginiensis (Fontaine) in very fine grained sandstone from this section.*

Small areas of Tantalus Formation have been mapped on Carbon Hill (T-2) and Mount Bell (T-3), but are poorly exposed. Highly weathered, frost shattered samples of conglomerate collected from Carbon Hill (60°11′21″N, 135°14′21″W) were highly sheared medium pebble conglomerate. Samples on Mount Bell (60°10′22″N, 135°11′06″N) were of small to medium pebble grade. Samples from both sections were exceptionally chert-rich (94-96% of framework grains: Appendix 2, table 2, samples T2-3 and T3-1a), and contained no other sedimentary, metamorphic or igneous

clasts. No coal was found in float at either locality. Thirty-five kilometres southeast of Mount Bell (T-3), Bultman (1979) recorded a fault-bounded area with approximately 300 m of interbedded sandstone and conglomerate (but no coal), in sets 10-30 cm thick. The small pebble conglomerate at this location contains about 65% chert, 23% quartz, 11% sedimentary rock fragments and only 1% volcanic material (Bultman, 1979, p. 113) which plots within the range of composition for Tantalus Formation conglomerate in this study (Fig. 13).

On a regional scale, a lower member of the Tantalus Formation, tentatively equivalent to the lower member of Allen (2000), can be identified along the western margin of the Whitehorse trough, at least between Mount Bush and Tantalus Butte (Fig. 1), and possibly 35 km to the southwest, at Tutshi Lake, British Columbia (Bultman, 1979). The lower member is characterized by a greater abundance of fines, while the upper member is predominantly conglomerate (Fig. 22). In sections near the Whitehorse Coal pit the lower member is represented by about 100 m of poorly exposed strata below the first thick stacks of conglomerate (Fig. 24). It is more difficult to establish the existence of this member with any certainty in the vicinity of Carmacks (Fig. 20; possibly below surface B), and was not detected between Claire Creek (T-11) and Mason Landing (T-15; Fig. 21). Correlations can be made between widely spaced outcrops, based on maximum grain size, but should be used with extreme caution.

DETRITAL ZIRCONS

Zircons from three samples of the Tantalus Formation were examined by Dr. George Gehrels at the University of Arizona LaserChron Centre. Samples TB1 and TB2 are both from the open pit mine at Tantalus Butte (62°08′32″N, 136°15′59″W). Sample TB3 is from Tantalus Butte, from a conglomerate below the mine adit (~60 m level of T-17). Sample TB1 is from a conglomerate, 6 m above the base of the hanging wall conglomerate on the west side of the pit (Fig. 10), and sample TB2 is from sandstone about 20 m below this contact, on the east side of the pit. Sample C1 is from the upper half of the exposed section at the north end of Corduroy Mountain (61°20′33″N, 135°58′45″W). It is from a level roughly equivalent to the 310 m level of section T-1.

The analytical methods and data are reported in Appendix 4. Interpreted ages are based on $^{206}Pb/^{238}U$ for <800 Ma grains and on $^{206}Pb/^{207}Pb$ for >800 Ma grains. Analyses that are >30% discordant (by comparison of $^{206}Pb/^{238}U$ and $^{206}Pb/^{207}Pb$ ages) or >5% reverse discordant (in italics in Appendix 4b) are not considered further. Concordia diagrams for the four samples are shown as Figure 26. The resulting interpreted ages are shown on relative age-probability diagrams (Fig. 27; following Ludwig, 2001). These diagrams show each age and its uncertainty (for measurement error only) as a normal distribution, and sum all ages from a sample into a single curve. Interpretation of the data is provided below (Provenance; Zircons section).

INTERPRETATION

Sedimentology

In this study almost all of the extensive chert pebble conglomerate in the Tantalus Formation is interpreted as a deposit of gravel-bed rivers: this includes deposits of shallow (<3 m) and deep (>3 m) braided gravel-bed rivers, and locally deep meandering gravel-bed rivers (comparable to models B, C, and F of Miall, 1996, p. 203). Overbank (*i.e.*, levee, splay, marsh, swamp and pond) deposits are largely restricted to recessive slope forming intervals. Coal deposits developed locally

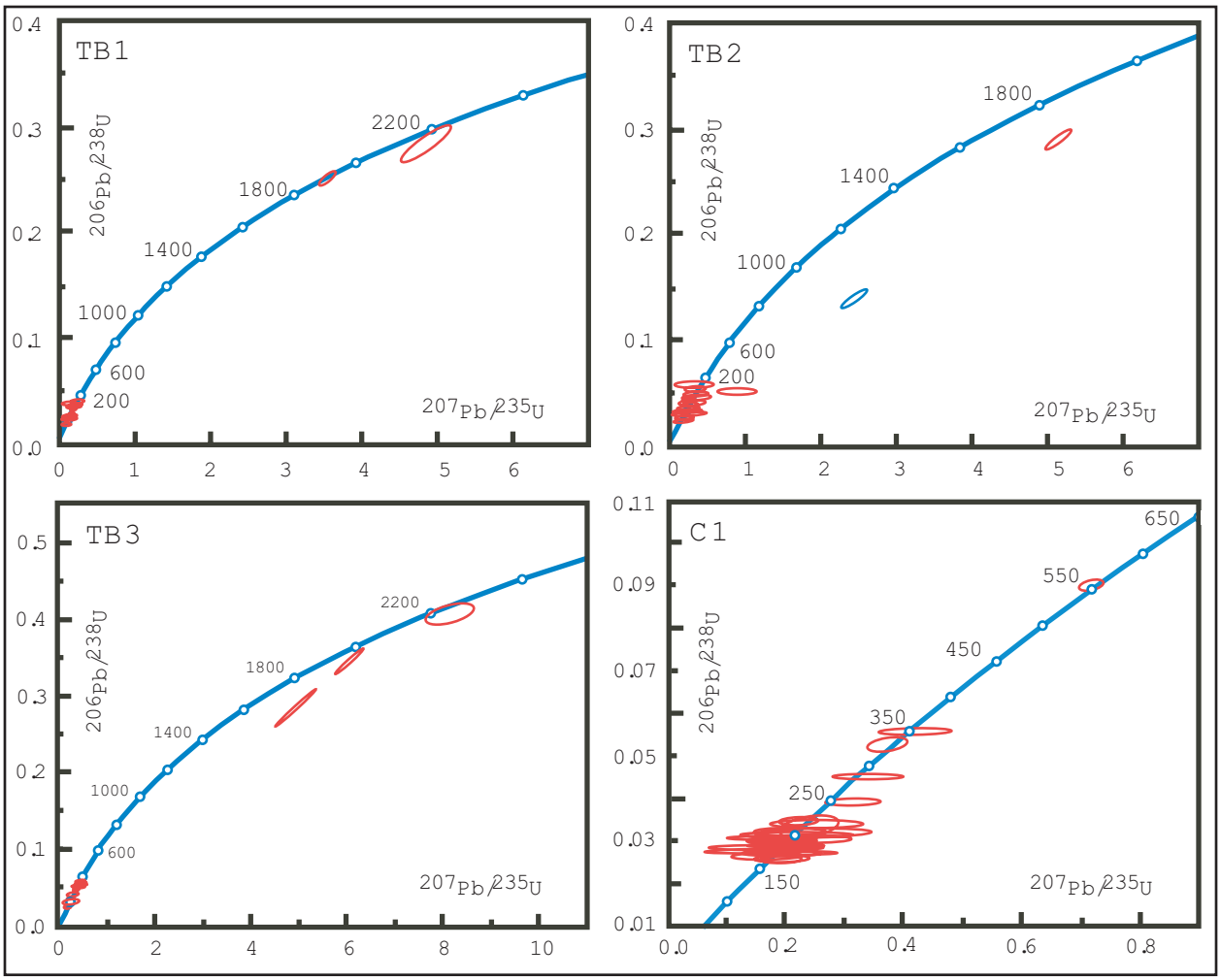

Figure 26. *Concordia plots of zircon data from four samples of the Tantalus Formation. Sample TB1 is from strata 6 m above the coal seams on the western side of the open pit at Tantalus Butte (Fig. 10). Sample TB2 is from strata structurally 20m below this coal seam, with dips to the east rather than west (Fig. 15e). Due to folding and faulting in the pit, TB2 appears to be from a higher stratigraphic level than TB1. Sample TB3 is from a conglomerate at Tantalus Butte in the lower part of the Formation, below the mine entrance (~60 m level of T-17). Sample C1 is from the upper half of the formation at Corduroy Mountain. Data point error ellipses are plotted at the 68.3% confidence limits.*

on abandoned segments of floodplains within confined river valleys, in places associated with high-constructive single or multi-channel (anastomosed) fluvial systems, with sand-filled channels (analogous to model J of Miall, 1996). Minor deltaic facies are preserved where rivers debouched into local floodplain ponds or lakes, to produce Gilbert-type deltas.

Braided gravel-bed river deposits

Most conglomeratic units in the Tantalus Formation are characterized by massive and sub-horizontal bedding, with minor planar and trough cross-bedding (Conglomerate section above). Massive and sub-horizontal bedding is a characteristic of deposition on in-channel macroforms in braided gravel-bed rivers (Miall, 1996; Long, 2011). Absence of marked imbrication reflects paucity of relatively flat clasts (*i.e.*, platy and very platy clast forms of Folk, 1974), rather than inability of subsequent flood

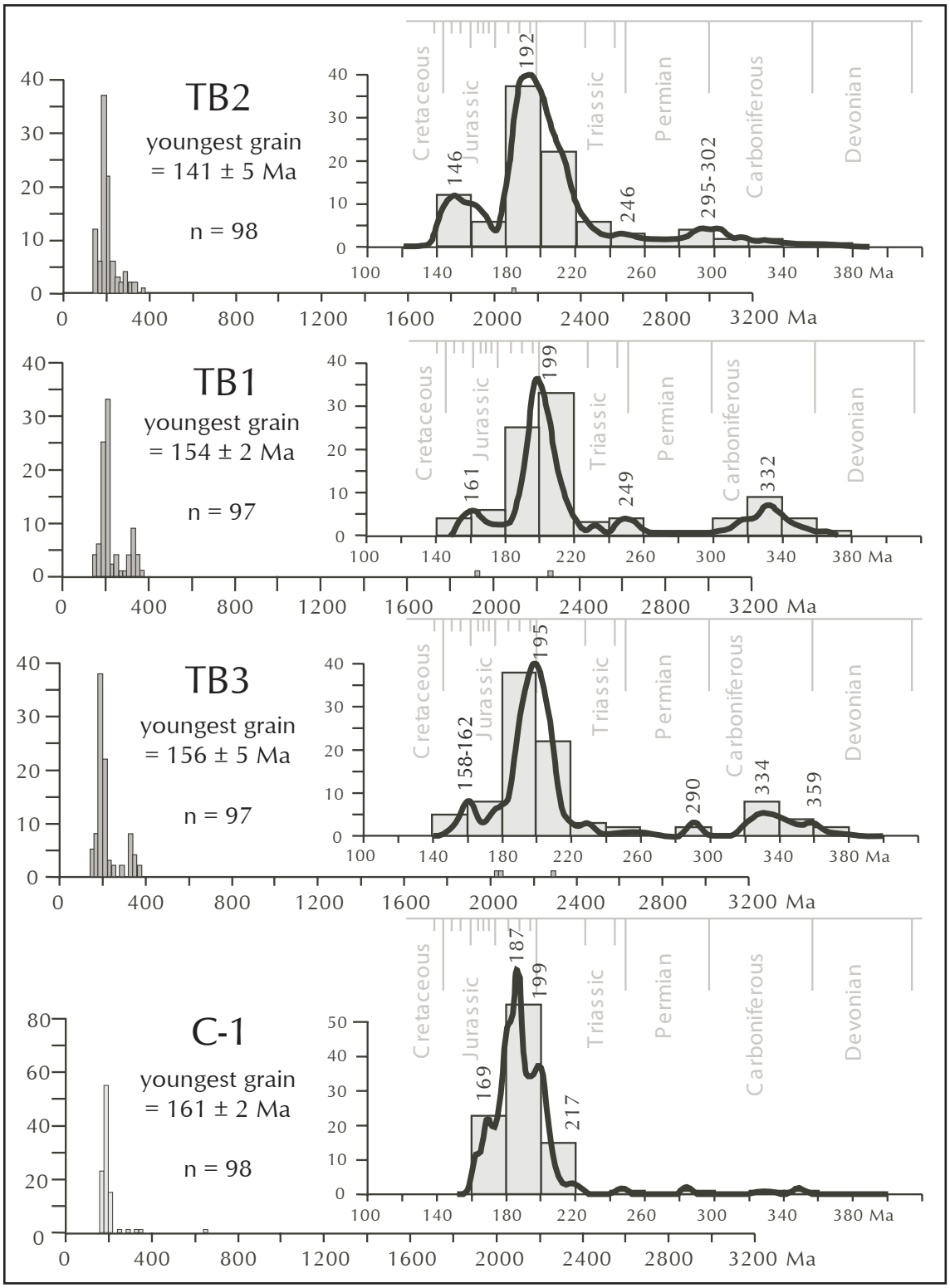

Figure 27. *Relative age probability plots of zircon data from four samples of the Tantalus Formation. Sample TB1 is from 6 m above, and sample TB2 is from 20 m below the hanging wall conglomerate (Fig. 10) exposed in the open pit at Tantalus Butte (62°08′32″N, 136°15′59″W). Due to folding and faulting in the pit TB2 is from a higher stratigraphic level than TB1. Sample TB3 is from a conglomerate at Tantalus Butte in the lower part of the Formation, below the mine entrance (~60 m level of T-17). Sample C1 is from the upper half of the formation at Corduroy Mountain (61°20′33″N, 135°58′45″W).*

events to rework and armour bar-tops. Depth of channels is difficult to estimate, as conglomeratic intervals tend to be stacked. The average bed thickness of massive and weakly planar stratified conglomerate units is 0.79 m, based on measurement of 2418 units (Fig. 28). On a volumetric basis, only 0.04% are very thin bedded (1-5 cm), 25% are thin bedded (5-60 cm), 39% are thick bedded (60-120 cm) and the remaining 38.85% are very thick bedded (>120 cm).

A beach origin for conglomerate units in the Tantalus Formation is rejected, as they typically have sheet-like geometry, rather than developing as linear prisms. In addition none of the conglomerate units is linked to coarsening upwards successions involving shore-face sand or lower shore-face deposits with hummocky cross-stratification or polymodal cross-stratification patterns (*cf.*, Fraser *et al.*, 2005; Castelle *et al.*, 2007; Alegria-Arzaburu and Masselink, 2010). In addition there is no evidence for draped shore-face accretionary architecture (Engels and Roberts, 2005; Bennett *et al.*, 2009; Clemmensen and Nielsen, 2010; Garrison *et al.*, 2010), or berm, runnel, ridge and swale development. In addition there is no evidence of bimodal-opposed cross-stratification (characteristic of tidal influence), or onshore plus along shore, tri-modal paleocurrent patterns characteristic of beaches (Potter and Pettijohn, 1977), nor are there any recognizable washover-fan deposits.

Analysis of a 17 m wide, strike parallel, interval of conglomerate, located 8-10 m above the Whitehorse Coal pit at Mount Granger was undertaken to determine the geometry of the conglomeratic units (Fig. 29). The face, as exposed is oriented nearly normal to local river flow, and shows a cross section of part of a channel with a number of minor scours and reactivation surfaces indicative of repetitive deposition and erosion of in-channel compound bars in a shallow braided gravel-bed river system. The predominant orientation of foresets (0th order surfaces; Table 2) with set and coset boundaries (2nd order surfaces) suggest that most deposition took place by downstream accretion (*cf.*, Miall, 1996), typical of deposition on composite in-channel macroforms (bars). Truncation of first and second-order set boundaries at the base of surface "B" (a 3rd order surface)

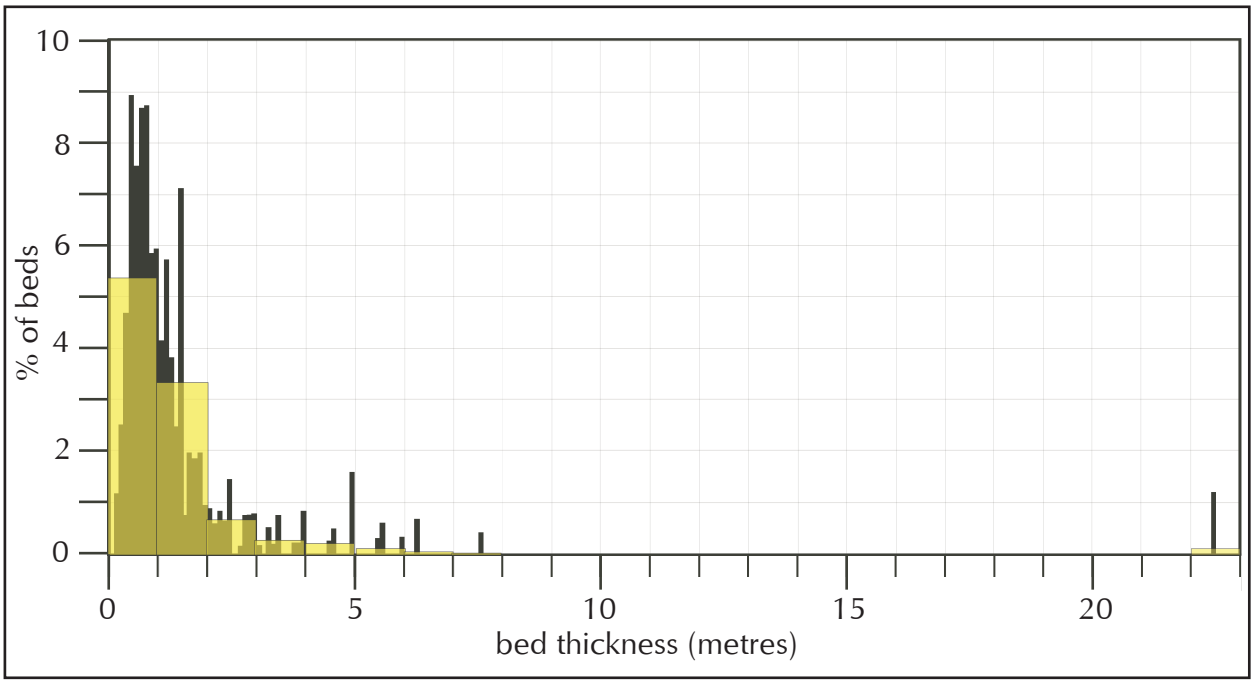

Figure 28. *Thickness distribution (by bed) of 2418 conglomeratic beds or composite bedsets in the Tantalus Formation, shown as numerical percentage in 10 cm intervals (in black) and 1 m intervals (in yellow).*

probably indicates a secondary or tertiary channel thalweg with a minimum depth of 1.2 m (based on exposed thickness). The primary bankfull relief of the braid channel (between surfaces A and F) may have been 2.5 m or more, based on lateral continuity of the exposures on either side of the panel shown. The thinner sub-horizontal elements (1st order surfaces between surfaces C, D, E and F) that cap the channel may reflect products of reworking the tops of a composite bar by repeated flood action. Surface F may represent a 5th or 6th order surface, and may represent the basal contact of the overlying braid channel.

A second small-scale architectural analysis was attempted on steeply dipping strata south of Mount Granger (Fig. 30). This outcrop trends at a high-angle to regional strike, providing a different perspective of the local braided gravel-bed river systems (oriented at about 45° to channel axis).

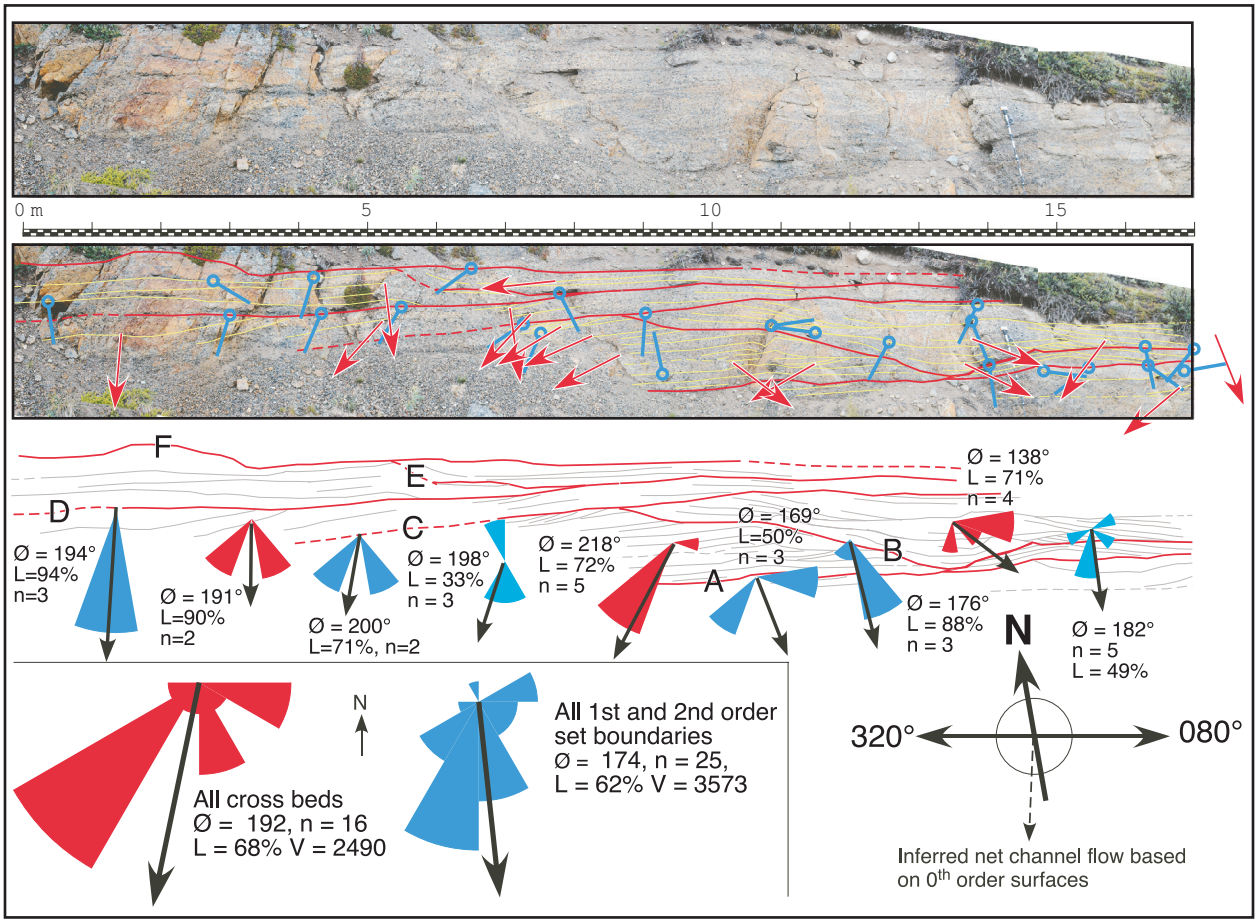

Figure 29. *A 17 m wide panel of conglomerate, exposed at Mount Granger, about 8-10 m above the Whitehorse Coal Pit (strike of exposure is 220-080°). Top panel shows a photo mosaic of the exposure. Middle panel shows exposure, with 3rd and 4th order set boundaries in red, and 1st and 2nd order set boundaries in yellow. Orientation of set boundaries (2nd and 3rd order surfaces) is shown by blue pins. Orientation of 0th order surfaces (foresets) is shown by red arrows. In this, and the next panel, all vector data have been adjusted so that slopes away from the observer point up, and slopes towards the observer point down. In the third panel vector data have been grouped and plotted as rose diagrams with 30° bins oriented in the same way as the vector data. Red roses represent groups of 0th order surfaces (adjusted as above). Light blue roses represent groups of 1st and 2nd order surfaces (set boundaries) and dark blue roses represent groups of 3rd and 4th order coset boundaries. Surface F may be a 5th or 6th order surface. Statistical information is shown next to each rose: Ø=vector mean, n=number of observations, L=vector strength (as percentage). The two roses at the base show the grouped data for the outcrop, plotted with north to the top (V=variance).*

The exposure is dominated by medium pebble conglomerate, with minor small and large pebble conglomerate. There is no evidence of systemic fining upwards, or overbank deposits, consistent with deposition in a braided river system. Foreset directions (0th order surfaces), on average indicate that current flow direction moved obliquely up set boundaries (Figs. 30 and 31). This implies that deposition may in some cases have occurred on the upstream sides of compound barforms as upstream lateral accretion elements (ULA elements of Long, 2011). Upstream accretion on bar-heads (UA elements), and on the upstream end of lateral accretion surfaces (ULA elements) has been recorded in modern gravel-bed wandering (Wooldridge and Hickin, 2005; Burge, 2006) and braided (Miall, 1996; Lunt and Bridge, 2004; Li *et al.*, 2014) river systems, as well as in sandy braided rivers (Skelley *et al.*, 2003; Best *et al.*, 2003; Mumpy *et al.*, 2007; Sambrook Smith *et al.*, 2009). Upstream accretion reflects abandonment of transverse bedforms (dunes) that were migrating over the back and sides of compound bars during high discharge events during falling flow stage (Skelley *et al.*, 2003). ULA elements may consequently indicate accretion of gravel unit bars to the upstream ends of LA surfaces (bar-head lobes of Lunt and Bridge, 2004).

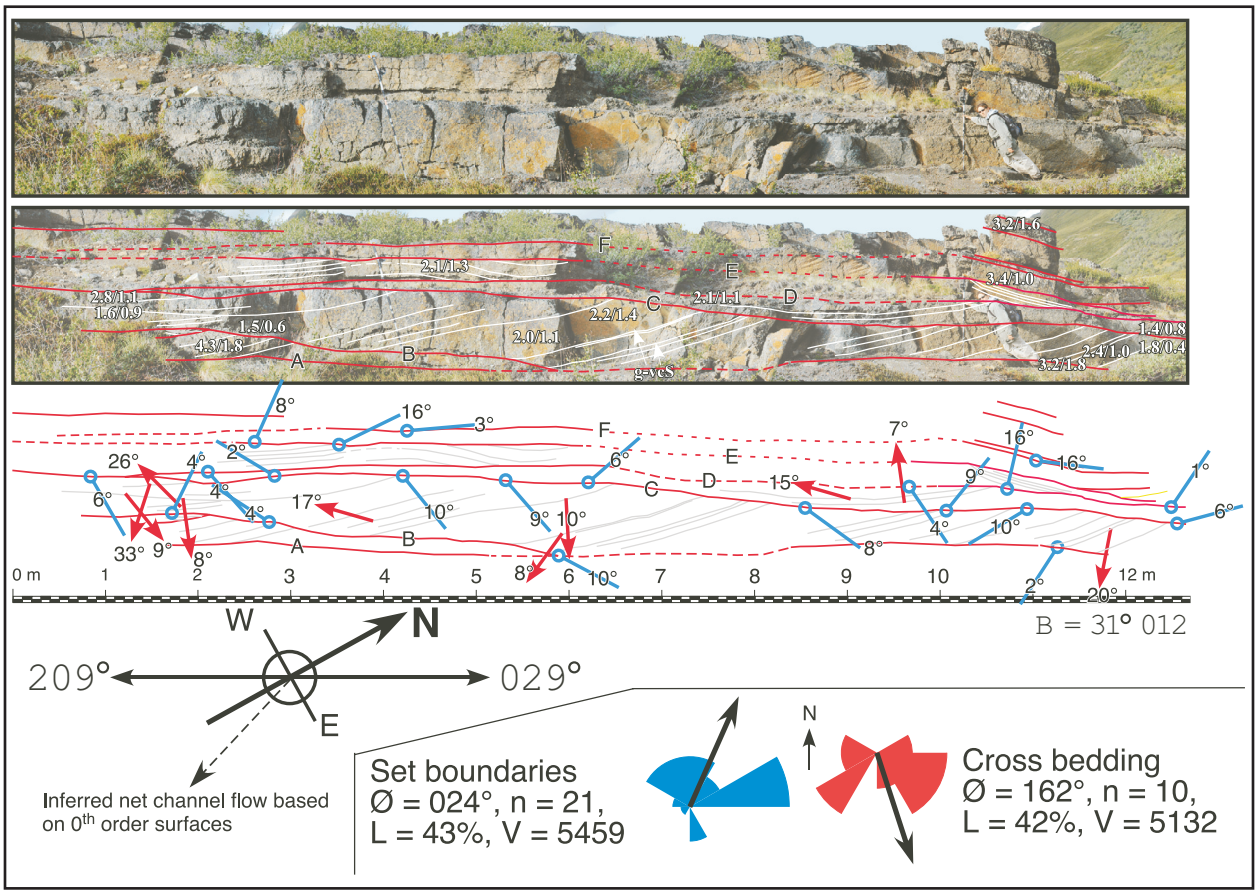

Figure 30. *Architectural analysis of a small panel, south of Mount Granger. Top image shows outcrop, adjusted for structural dip: maximum and / median grain size shown in white (gvcS=granular very coarse sandstone on foreset laminae). In the lower image foreset dip directions (tilt corrected) are shown as red arrows, oriented so that flow away from the observer is up, and flow towards the observer is down (as in Fig. 29). Panel strikes 209-029°. Blue pins indicate dip of selected bedding surfaces (labelled in order of deposition). Lower insert shows grouped orientation data for the face, with rose diagrams (north to top) for all set boundaries (blue) and cross-beds (red).*

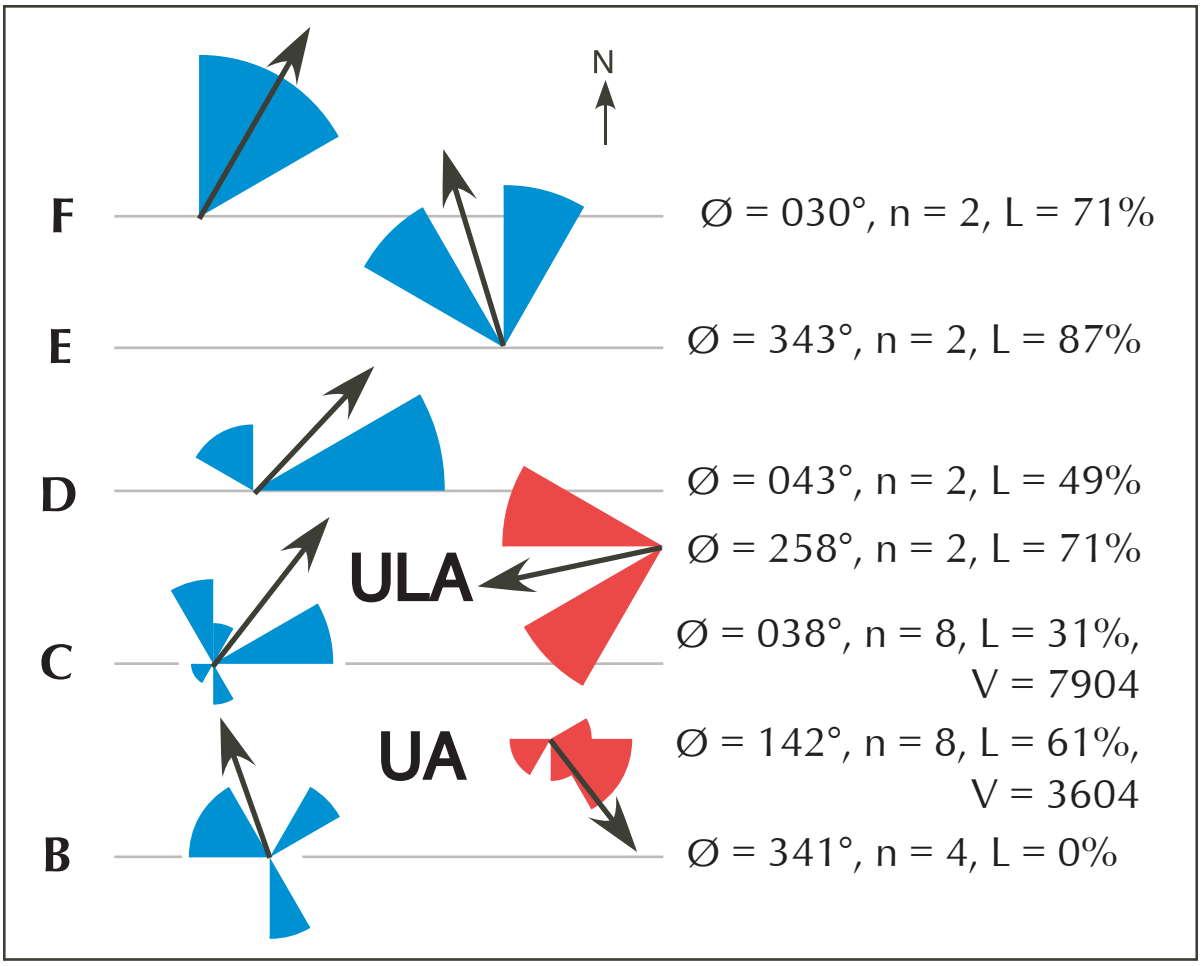

Figure 31. *Relative orientation of crossbeds (red) to set-boundaries in Figure 30. Ø=vector mean, n=number of observations, L=vector magnitude. B, C, D, E, F=set boundaries. UA=upstream accretionary element; ULA=upstream lateral accretion element. North is to the top.*

Miall (1996) divides braided gravel-bed rivers into shallow (less than 3 m water at bankfull flow) and deep (>3 m). In the absence of preserved cut-banks, terrace features, and point bars (LA surfaces), it is difficult to estimate the absolute bankfull depth of the braided rivers that formed the bulk of the Tantalus Formation. Preserved conglomerate units range in thickness from a few centimetres to 22.5 m (Fig. 28): 8.6% of the units are greater than 3 m in thickness. If unit thickness is taken as an approximate measure of bankfull stream depth (*cf.*, Bridge and Tye, 2000), then the average depth would be ~79 cm (*i.e.*, shallow gravel-bed braided). Fielding and Crane (1987) have suggested that bankfull stream depth (d) can be estimated from storey thickness (t) by the formula d=0.55 t. If unit thickness is taken as a proxy for storey thickness, then the average stream depth, based on the average unit thickness of 79 cm, would be in the order of 43 cm, and only ~3.4% of the rivers would be more than 3 m deep at bankfull.

An alternative method to estimate bankfull stream depth is to use preserved cross-bed thickness (Fig. 32). Allen (1970) suggested that modern dune height (H) is related to flow depth (d) by the formula $H=0.086\ d^{1.19}$. This would give an average stream depth for formation of planar cross-stratified gravel units of 5.7 m, and 6.8 m for formation of trough cross-stratified gravel units. This would imply that more than 75% of the rivers would fall into the category of deep gravel-bed

braided rivers. If, as suggested by Leclair and Bridge (2001) that average preserved dune height is ~2.9 x preserved cross-bed thickness, even more of the rivers would be classified as deep (>3 m). As both Allen's (1970) and Leclaire and Bridge's (2001) analysis were based on sand-bed dunes, direct application to preserved thickness of gravel bedforms may not be directly applicable. When thickness data for cross-stratified sandstone is used, the average depth calculated using Allen (1970), is 3.4 m (deep) for planar cross-stratified sandstone and 2.1 m (shallow) for trough cross-stratified sandstone (Fig. 32).

In gravel-bed braided river systems, planar cross-stratified units are typically interpreted as being deposited by avalanches of grains at the downstream end of longitudinal bars (Miall, 1996), hence the maximum preserved thickness records a minimum stream depth. Trough cross-stratified gravel beds may form at the downstream end of chutes, or on sinuous transverse in-channel bedforms.

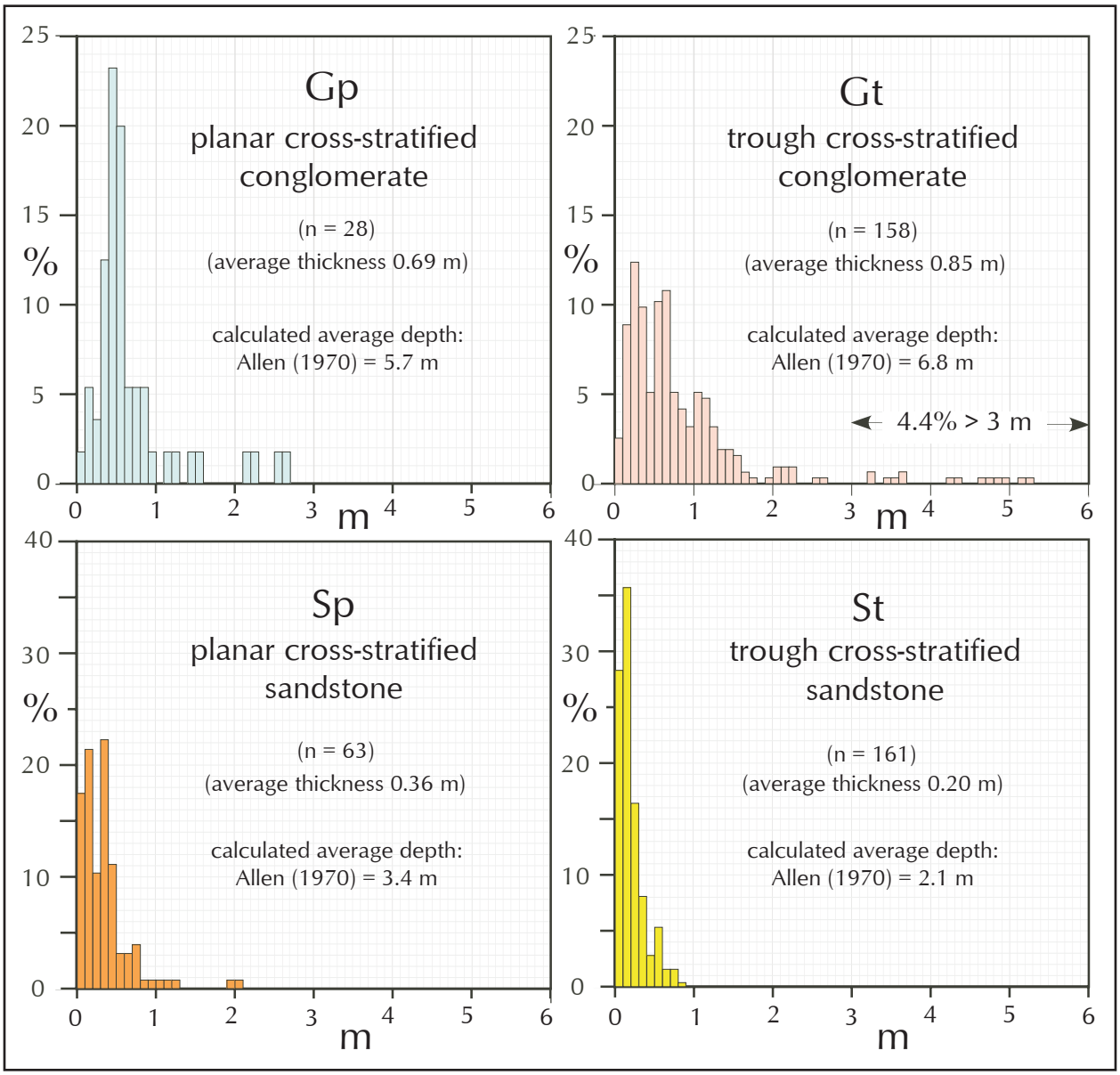

Figure 32. *Thickness distributions (number %) of measured cross-stratified gravel and sandstone units from the Tantalus Formation.*

As ~4.4% of the observed trough cross-stratified conglomerate units are more than 3 m thick, this confirms that at least some, and perhaps many, of the gravel-bed rivers which were active during deposition of the Tantalus Formation can be considered as deep.

Meandering gravel-bed river deposits

Positive evidence for the presence of meandering gravel-bed river systems, similar to those described by Bluck (1971), Gustavson (1978), Blacknell (1982), Arche (1983), Carson (1986), Smith (1986, 1989, 1990), Alonso and Garzón (1994) Gomez *et al.* (2007), Kostic and Aigner (2007), and Wolf *et al.* (2013) was found in exposures at Claire Creek (section T-11; Figs. 33 and 34; Long and Lowey 2006). Despite the difficult access, it is possible to delimit a series of large-scale channel elements based on observed contacts. These are apparent due to local grain size differences of conglomeratic elements and the presence of isolated packages of ripple and cross-stratified sandstone on the lateral accretion (LA) surfaces (Figs. 33 and 35).

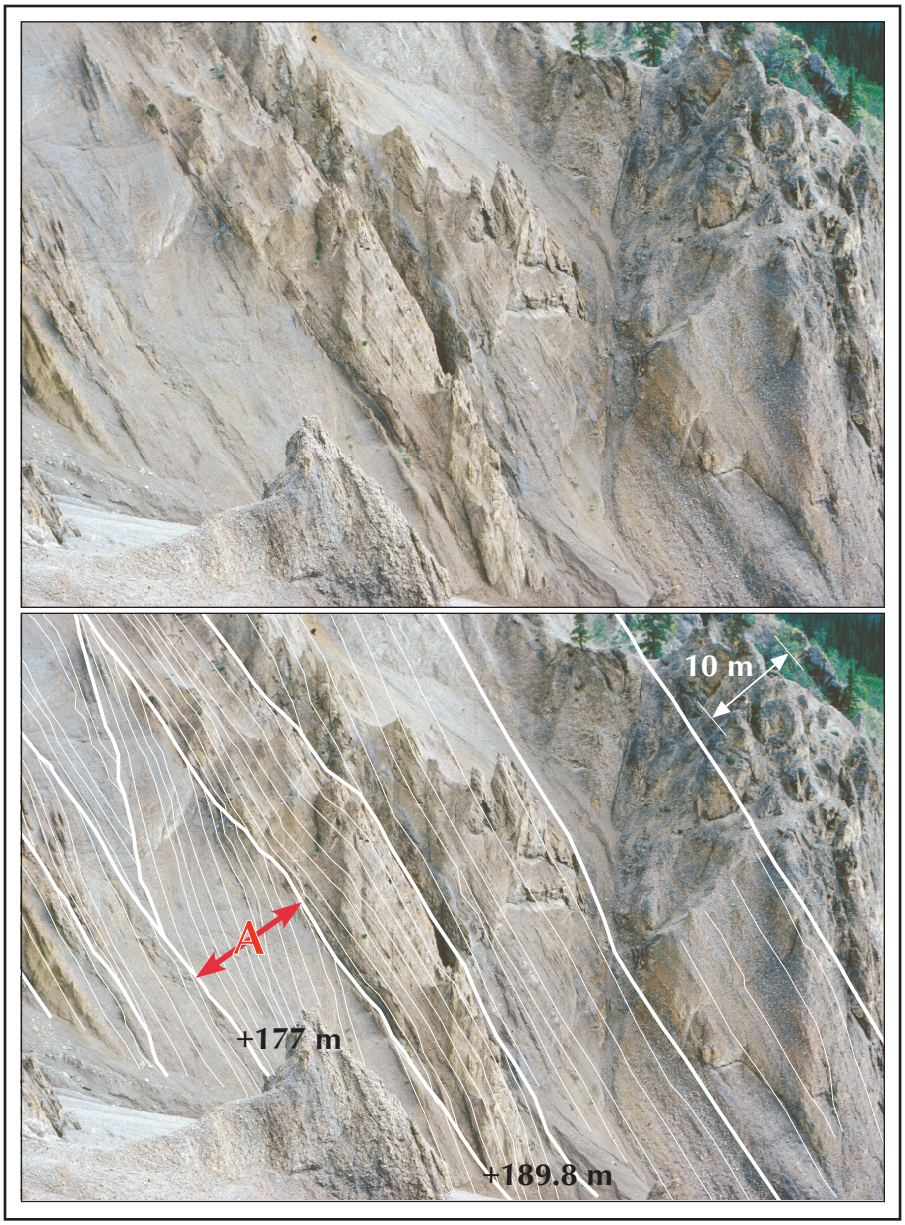

Figure 33. *Exposure of steeply dipping conglomerate units in the Tantalus Formation at Claire Creek (Section T-11) showing stacking of meandering gravel-bed river deposits. See Figure 34 for detailed view of unit A.*

Figure 34. *Detail of LA (thin white) and CH (thick white) surfaces in 12.8 m thick channel fill unit A in Figure 33, rotated to sub-horizontal orientation. Most of the cliff face was too steep and unstable to allow access and detailed paleoslope orientations.*

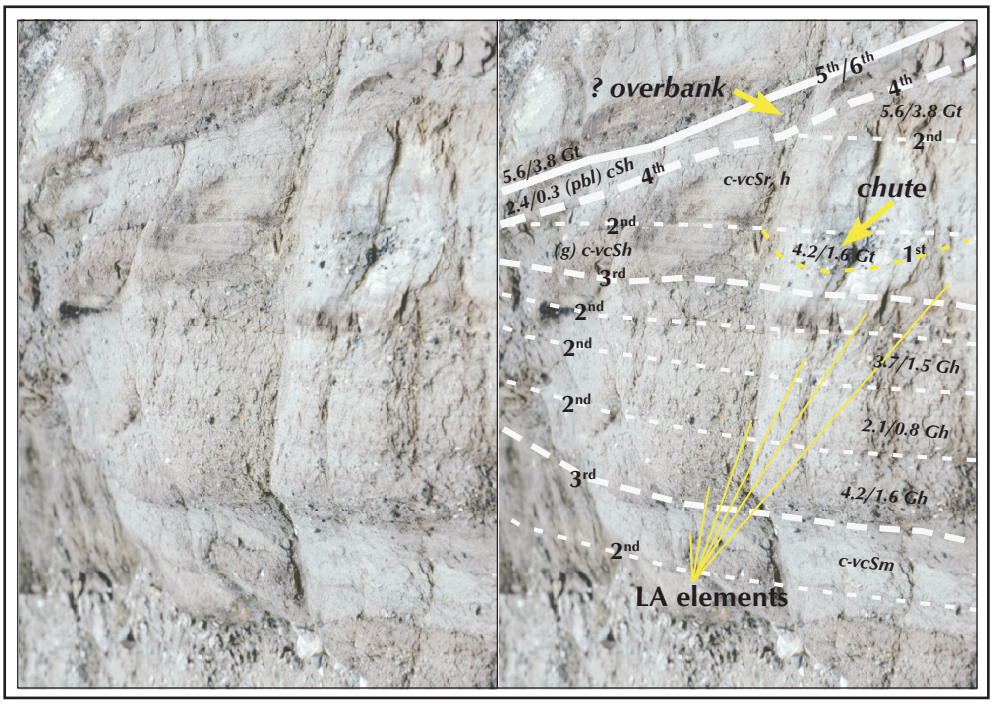

Figure 35. *Close up of top of composite gravel and gravelly sandstone unit, with 2nd and 3rd order surfaces defining lateral accretion (LA) elements in a large-scale gravel-dominated point-bar in the Tantalus Formation at Claire Creek (from Long and Lowey, 2006). This is part of a 5.9 m thick channel unit, starting at the 9.5 m level of section T-11 (Appendix 1). Note limited preservation of possible overbank elements between the 4th and 5th/6th order surfaces, and preservation of an isolated lense of gravel, oriented at right angles to the slope of the lateral accretion surface (upper right) that represents a possible chute deposit.*

In the 5.9 m thick channel shown in figure 7.8 (beginning at the 9.5 m level of section T-11), the orientation of small-scale planar cross-stratification is at 75° (*i.e.*, towards 047°) to the restored dip of the LA surfaces, which had local primary dips of up to 22° towards 122°. This indicates that this developed on the downstream end of the point bar. The small gravel filled channel developed on the upper part of one of the LA surfaces in this channel (Fig. 35) may represent a small chute channel, or an erosive scour formed during rising flow stage. The thin layer of granule conglomerate between the 4th and 5th/6th order surfaces may represent local preservation of overbank deposits (? splay deposits) beneath the overlying channel system. Based on the geometry of the LA surfaces, and the preserved thickness of the channel, it would have been at least 6.5 m deep (assuming 10% compaction: Ito *et al.*, 2006), and about 24 m wide (Leeder, 1973). Given an observed maximum grain size of 9.0 cm, this would indicate flow velocities of 1.08 m/s (method of O'Connor, 1993), 1.13 m/s (method of Koster, 1978) or 1.55 m/s (method of Costa, 1983). Using the continuity equation of Schumm (1968) the calculated maximum bankfull discharge is estimated at 108-155 m^3/s.

In comparison the 12.8 m thick channel complex at the 177-189.9 m level of the section (A in Figs. 33 and 35) has LA surfaces with lower primary dips in the order of 11°. This suggests deposition in a channel at least 14.2 m deep (assuming 10% compaction – Ito *et al.*, 2006), with a width of about 99 m (Leeder, 1973), based on projected extent of the LA surface. Given an observed maximum grain size of 3.2 cm, this would indicate flow velocities of 58 cm/s (method of O'Connor, 1993), 76 cm/s (method of Koster, 1978) or 97 cm/s (method of Costa, 1983). Using the continuity equation of Schumm (1968) the calculated bankfull discharge is estimated at 544-909 m^3/s, well below the estimated discharge recorded for meandering gravel-bed rivers in warm-dry climatic settings by Gustavson (1978), but within that estimated for the temperate-humid Waipaoa River in New Zealand by Gomez *et al.* (2007) and meandering gravel-bed systems in general by Xu (2004). Using the formula provided by Xu (2004, p. 647), the predicted discharge would be achieved by a meandering gravel-bed river with a width of 74-95 m, suggesting that the upper discharge and velocity estimates are most realistic.

Gilbert-type deltas

Large-scale gravel foresets in the Tantalus Formation were not all produced in fluvial settings as downsteam accretion (DA) or lateral accretion (LA) elements. Long and Lowey (2006) demonstrated that local clino-stratified inclined sets of gravelly and sandy strata, lying above laminated mudstone and siltstone in the vicinity of the Whitehorse Coal pit (Fig. 36) are best interpreted as a product of a classic steep-sloped Gilbert-type delta (Gilbert, 1885, 1890; Postma *et al.*, 1988; Sohn *et al.*, 1997), that was fed by a fluvial distributary system with closely spaced, highly mobile bed-load channels (Type B – deeper water Gilbert-type model of Postma, 1990). Further details and discussion of this outcrop are provided by Long and Lowey (2006).

The delta appears to have prograded directly into a lake that was at least 6 m deep. This may represent a large floodplain pond, or a temporary lake formed when local uplift or local fan progradation temporarily blocked river flow (*cf.*, Smith and Smith, 1980). Progradation of the delta-front appears to have taken place over a number of flood seasons, each of which produced down-lapping packages of foreset strata, and are capped by finer material near the delta toe. There is no evidence for flash-flood induced progradation, such as marked inverse grading of foresets (Postma *et al.*, 1988), hence distributary channels were probably dominated by individual flood events with moderate discharge (Postma, 2001).

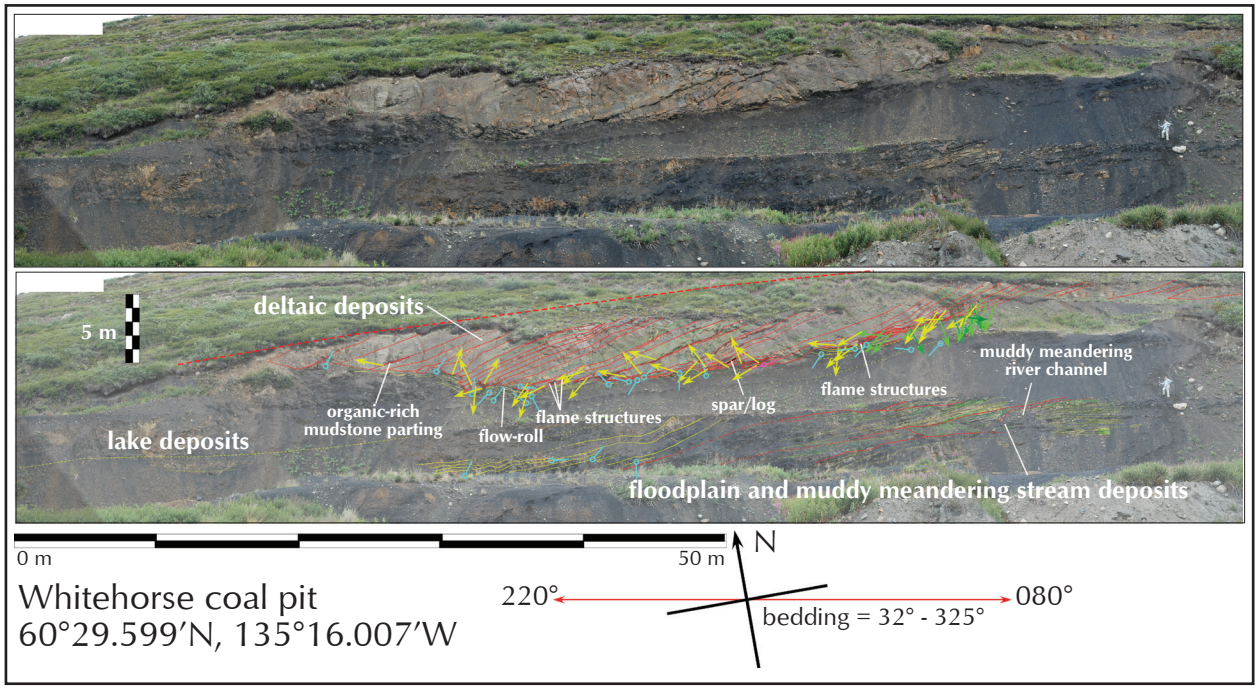

Figure 36. *Architectural reconstruction of the Whitehorse Coal Pit exposure, near Mount Granger. The dashed line, at the top, represents a 5th or 6th order surface. In the deltaic facies the red lines represent 1st order surfaces, which bound foreset elements. Green lines between these are 0th order surfaces. Yellow lines at base represent 1st and 2nd order surfaces within bottom set and lacustrine units. Arrows (yellow and green) reflect the orientation of 0th and 1st order foreset surfaces. These have been rotated so that arrows directed above the horizontal reflect slopes away from the observer, and arrows below the horizontal represent slopes towards the observer (after correction for tectonic dip). Blue pins represent dips of 1st and 2nd order set boundaries, reoriented as above.*

Floodplain, levee, splay, lake, pond, marsh and swamp facies

Most of the recessive (covered) intervals associated with the Tantalus Formation may be developed over floodplain facies. Poorly defined thick laminated to thin bedded, dark grey to grey, massive mudstone, with abundant slickensides, and occasional preserved plant root casts, are here interpreted as floodplain soils. The lighter grey colours, and the slickensides indicate a seasonally variable groundwater table. This would allow the organic content of the soils to oxidize, and develop crumb textures (Donahue *et al.*, 1958; Fitzpatrick, 1980). Organic rich mudstone (<50% organics) represents marsh deposits, that are typically found beneath and between coal deposits. Coal deposits, represent riverine-swamps that developed in valley bottom settings where the groundwater table was near surface all year. A riverine influence is indicated by the high ash (mud) content (11-47% according to Cameron and Beaton, 2000), which indicates introduction of suspended mud into the swamps during flood events (Stach *et al.*, 1982; Morozova and Smith, 2003). Thin sandstone units with ripples and root casts associated with floodplain deposits are here interpreted as splay deposits (Fig. 15d,e,f,g).

Thin cosets (<1 m) of well defined, laminated mudstone are here interpreted as floodplain pond deposits. They are typically associated with overbank fines and minor sandstone, as at the 1179 m level of section T-9 at Vowel Mountain (Appendix 1), where 50 cm of thin to thick planar laminated mudstone is exposed.

Thicker (>1 m) successions of planar laminated mudstone may represent larger floodplain ponds or lakes. They are conspicuous only in the Whitehorse Coal pit (Fig. 36) and at the 64-73 m levels of section T-11 at Claire Creek (Appendix 1). At Claire Creek the lacustrine interval is dominated by black (organic rich) thin to thick laminated silty-mudstone in bed sets 10-20 cm thick, separated by 2-5 cm thick bed sets of flat laminated very fine grained sandstone, with local concentration of siderite as a cement in very fine grained sandstone near the top of the interval, indicating passage of oxygenated meteoric groundwater through the sand during early diagenesis (Baker *et al.*, 1995). The laminated sandstone beds may represent suspension deposits associated with major overbank flooding events. In the Whitehorse Coal pit 2-6 m of uniform, poorly exposed, dark grey, thin to thick laminated, silty mudstone (with no siderite) is preserved above floodplain muds, and below deltaic conglomerate (Fig. 36).

Sandy meandering and anastomosed stream deposits

Minor meandering and possible stable channel anastomosed river channels are preserved within the floodplain facies. In the Tantalus Butte coal mine highly deformed small sand-filled channels (width to depth ratio ~3:1) are preserved in the nose of drag folds (Fig. 18b) The abundance of overbank splay deposits adjacent to this channel, and in other parts of the pit (Fig. 15d,e,f,g) indicates that these may be stable channel (possibly anastomosed) systems in which bank stability was maintained by plant roots (*cf.*, Smith and Smith, 1980; Long and Graham, 1993; Miall, 1996; Long, 2000, 2005; Long and Lowey, 2006). Overbank splay deposits may contain casts of plant roots as well as reworked woody material. In the Whitehorse Coal pit, amalgamated sets of small channels with lateral accretions elements consisting of interbedded sandstone and mudstone (Fig. 36, lower right) may represent stacked deposits of small sandy-muddy meandering streams (Miall, 1996; Ghosh *et al.*, 2006). The low lateral extent of the channels, combined with the abundance of associated splay sand sheets, suggest these too had high bank stability.

Paleocurrents

Plots of dip-corrected (grouped) paleocurrent distributions of cross-stratified units within the Tantalus Formation show a general tendency of northeasterly to westerly (? basin transverse) flow in the Carmacks and Claire Creek areas, and predominantly southeasterly (? axial) with minor local deviations in areas to the south (Fig. 37). In all cases the data dispersion (measured as variance – V in Figure 37) is high, due to some extent to grouping of data through the whole formation. A similar trend is obtained (blue dashed arrows on Figure 37) when weighted vector strengths are determined (method of Miall, 1976). A general south to southeasterly transport path is also supported by an overall decrease in maximum grain size to the south, from 26 cm intermediate diameter at Claire Creek, to 2 cm at Carbon Hill (Fig. 8).

Provenance

Provenance information can be inferred from pebble and cobble clast counts of slabbed material, point counts of thin sections, and dating of zircon populations. Both the pebble counts and point counts indicate contributions from local (feldspar, lithic fragments) and more exotic sources (chert). Framework grains in all samples are predominantly chert; this means that most sandstone samples plot as litharenite, and conglomerate samples plot as lithrudite, on standard petrographic plots (Folk, 1974; Figs. 13 and 16). This is in marked contrast to the underlying strata of the Laberge Group that typically have less lithic fragments and more feldspar (Figs. 14 and 17). Where lithic fragments are common in Laberge strata, clasts are predominantly plutonic and volcanic, with lesser

metamorphic and sedimentary varieties (Dickie, 1989; Dickie and Hein, 1995; Johannson *et al.*, 1997). Chert rarely exceeds 2% of the lithic component, and is most abundant in the upper parts of the Laberge Group (Dickie, 1989; Clapham *et al.*, 2002). Minor regional differences occur in the petrography of the Tantalus Formation between the north and south of the Whitehorse trough (Fig. 38). In the north and northeast (Carmacks, Hootalinqua and Claire Creek) all data plot in the field of lithic arenite or rudite. To the south and southwest (Vowel Mountain and Whitehorse Coal area)

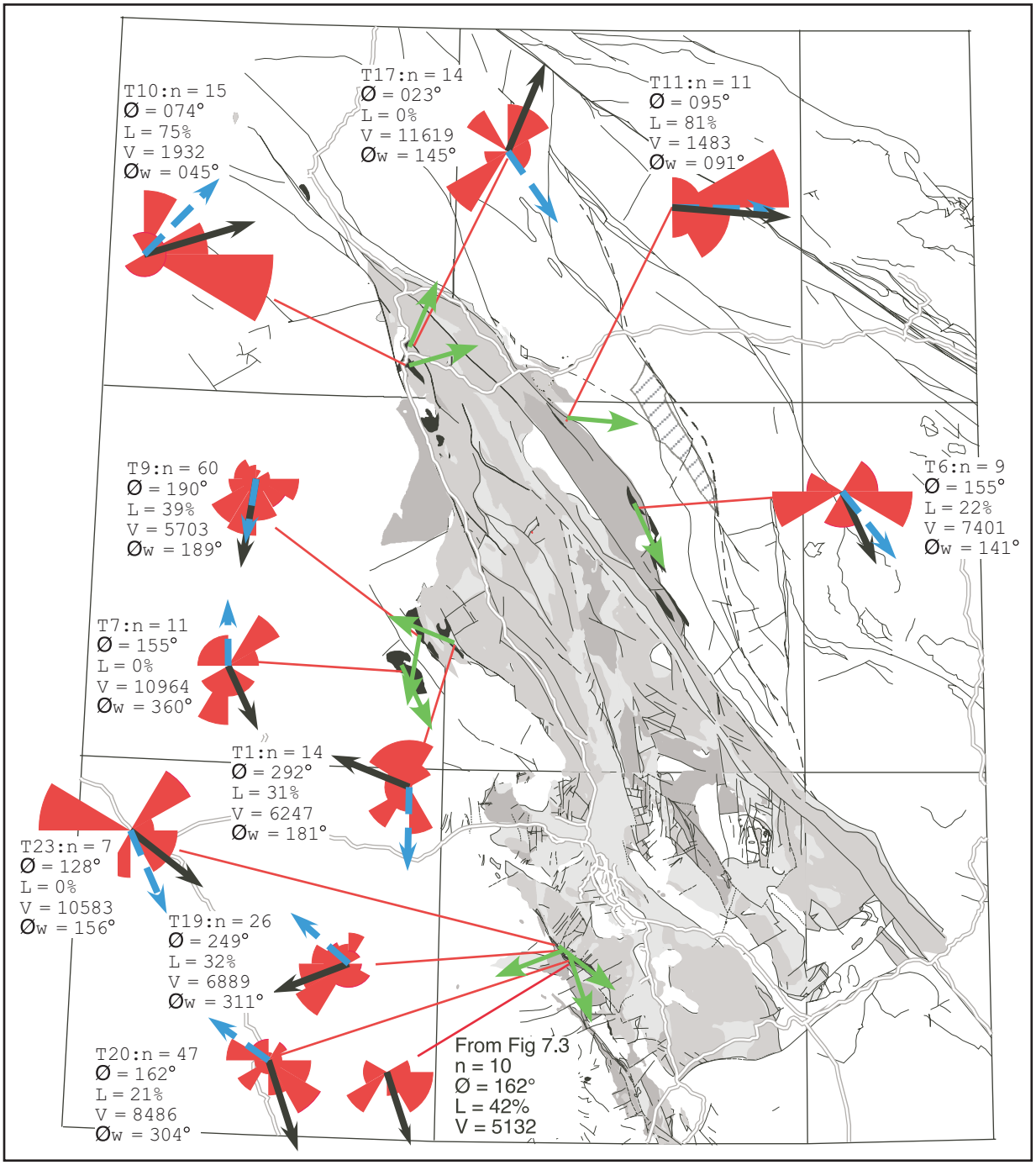

Figure 37. *Dip corrected paleocurrent data for the Tantalus Formation (with section numbers). Data are presented as a paleocurrent rose (in red) with the vector mean (Ø) in black (and green), and weighted vector mean (Øw) in blue. n=number of cross-beds; L=Vector strength; V=Circular Variance.*

feldspar, and to a lesser extent quartz, appears to be more abundant, such that some sandstone and conglomerate plot in the field of feldspathic (arkosic) litharenite or lithrudite. This may indicate a greater contribution of local detritus to the Tantalus rivers from plutonic sources in this part of the basin, perhaps from exposed parts of Stikinia.

Quartz

Quartz pebbles form an average of 11.8% of pebbles in the 54 slabs of Tantalus Formation conglomerate examined during this study (Appendix 2, table 1). Most are well rounded, translucent to white (Fig. 11a,b), with some evidence of fracturing (which may have in part been developed post lithification). In thin section, quartz is seen to make up 13.4% of framework grains in the conglomerate, and 31.4% in the sandstone. This is significantly less than conglomerate and sandstone in the Tanglefoot formation that contain an average of 44.0% and 51.4% of quartz respectively (Appendix 2, tables 6 to 9). The quartz in the Tantalus Formation is dominated by strained varieties (Figs. 13 and 16), indicating that it was derived predominantly from highly deformed (metamorphic sources), possibly within the Yukon-Tanana terrane (*cf.*, Colpron *et al.*, 2006b, 2007b). As conglomerate and sandstone in the underlying Tanglefoot formation also contain a similar ratio of strained quartz (Figs. 14 and 17) they may both alternatively be derived in part from deformed Permian and older plutonic sources within Stikinia, and/or Quesnellia, and/or

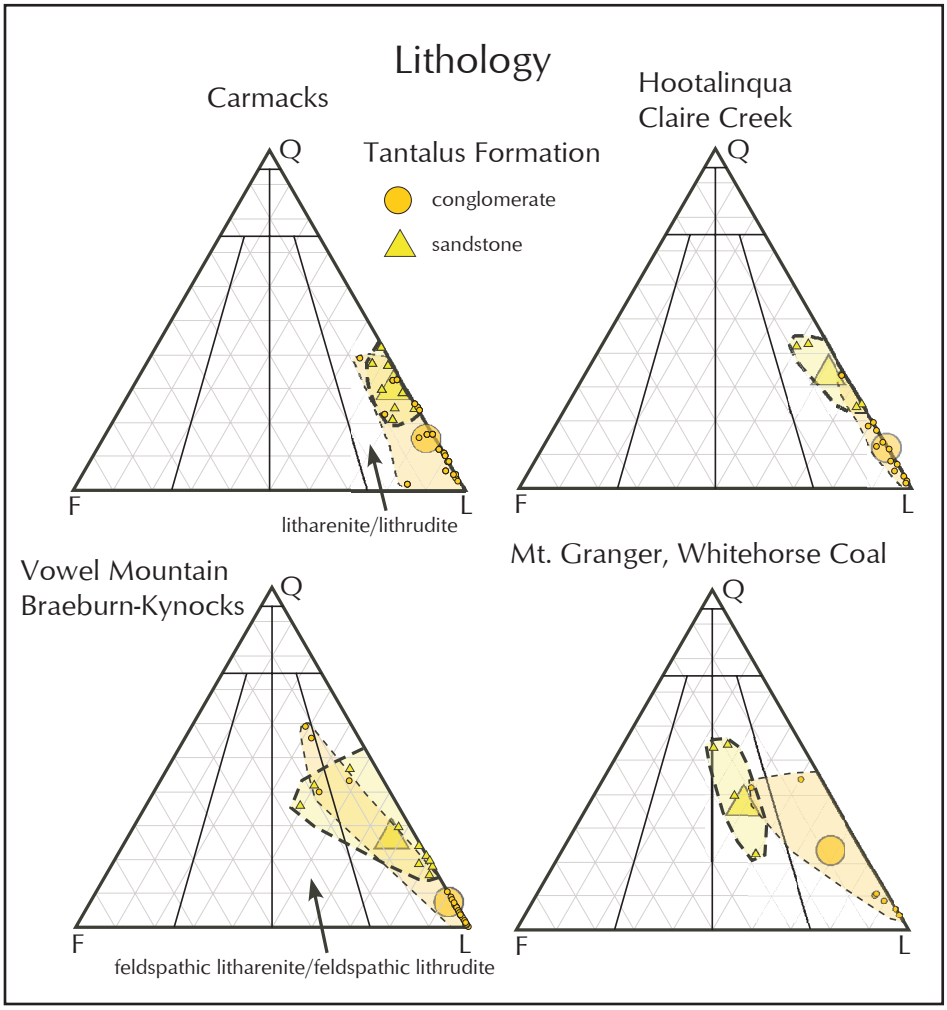

Figure 38. *Framework lithology of sandstone and conglomerate of the Tantalus Formation by region (data in Appendix 2).*

Yukon-Tanana (*see* paleocurrents above), or may have been deformed *in situ* during later tectonic events. Monocrystalline quartz grains are typically considered to be derived from undeformed igneous sources (Folk, 1974). They form 13.3% and 17.8% of the quartz content of the Tantalus Formation conglomerate and sandstone, compared with 18.7% and 25.3% of conglomerate and sandstone in the underlying Laberge Group. In both cases the most obvious primary source of igneous quartz would be Upper Triassic and early Lower Jurassic intrusions in the roots of the Stikine arc, and adjacent parts of the Yukon-Tanana and Quesnellia terranes. In the case of the Tantalus Formation some of this monocrystalline quartz was probably reworked from underlying strata of the Laberge and Lewes River groups. The relative abundance of polycrystalline quartz is more than twice as abundant in the Tantalus Formation (12.7% in conglomerate, and 10.9% in sandstone) than in the Tanglefoot formation (4.7% in conglomerate and 4.5% in sandstone). This is typically ascribed to annealing of metamorphic quartz during retrograde metamorphism: this could indicate an increased contribution from the Yukon-Tanana terrane, or metasedimentary rocks in the core of Stikinia or Quesnellia. The overall abundance of quartz appears to be partly dependent on grain size (Fig. 39). Regression analysis of all 112 Tantalus samples (Appendix 2) shows a moderate positive relationship (% quartz = 29.4 + 4.7 Ø), that is significant at the p <0.05 level (*i.e.*, overall finer grained samples contain more quartz). Plots of quartz *vs* grain size do not appear to differ significantly between sub-areas within the Whitehorse trough (Fig. 39).

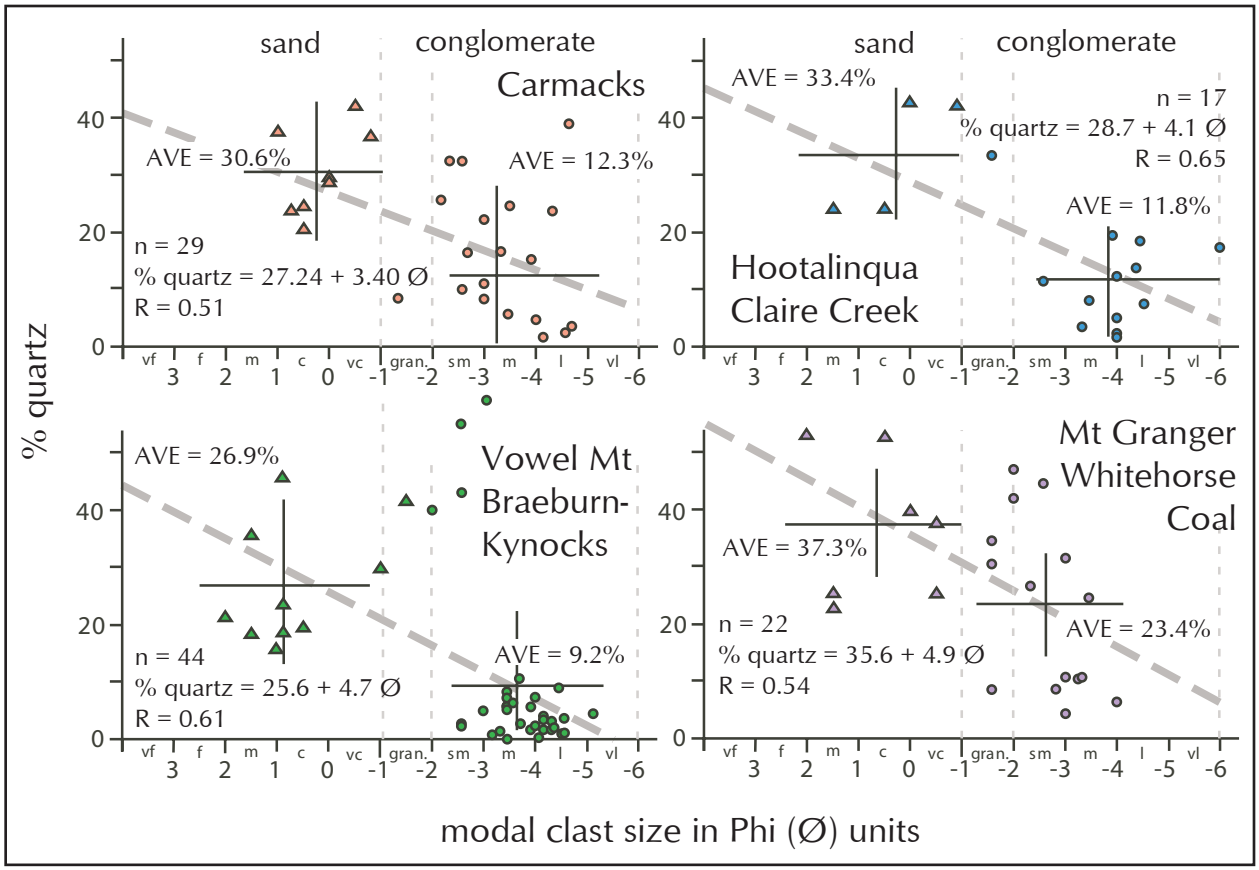

Figure 39. *Regional plots of quartz abundance vs modal grain size (as Phi units). AVE=Average; n=number of point counts; R=Pearson's R statistic (data in Appendix 2). Regression analysis indicates that the calculated correlation is significant at the p <0.05 level in the Vowel Mountain, Braeburn-Kynocks area, but not at the other locations.*

Plots of quartz types from four different sub-areas show minor differences (Fig. 40). Strained quartz is dominant in all areas, with slightly reduced abundance in the Vowel Mountain area, presumably reflecting input from weathering of local non-deformed igneous sources within Stikinia, or from reworking of underlying strata of the Laberge Group. The greater abundance of polycrystalline quartz in this area may indicate greater contributions from the Yukon-Tanana terrane.

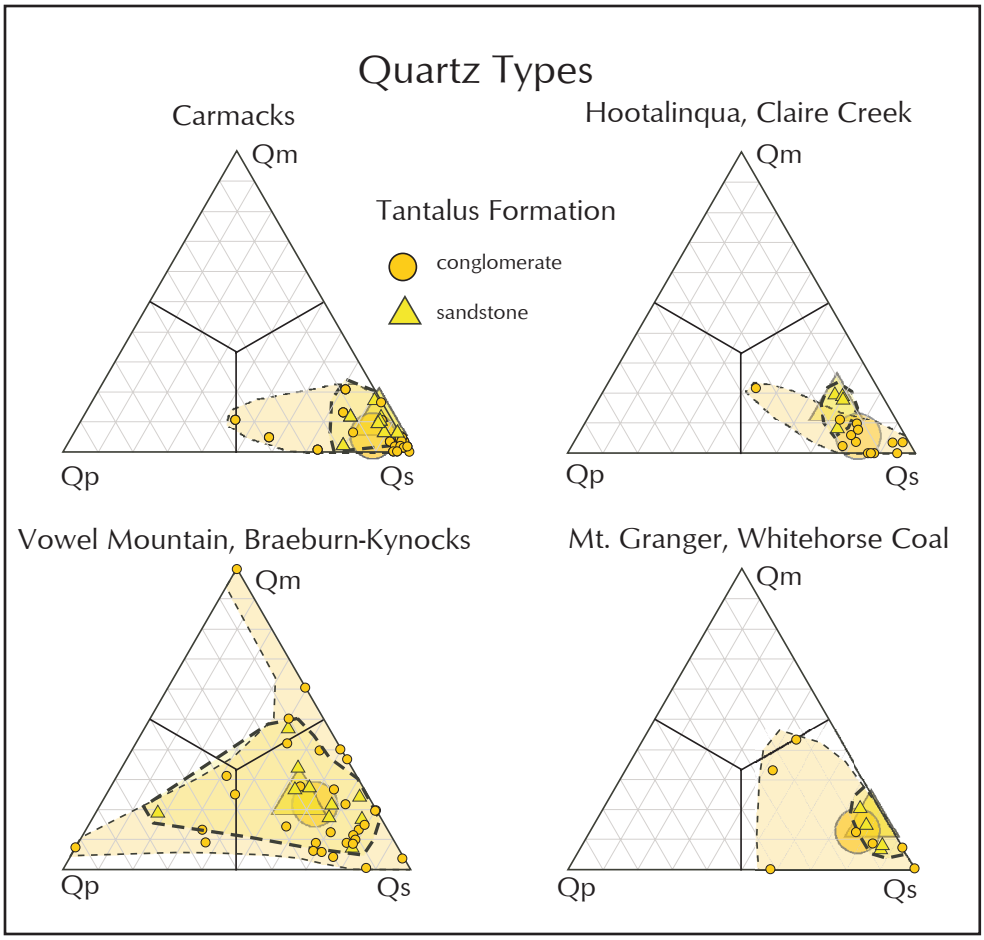

Figure 40. *Regional differences in quartz types (data in Appendix 2).*

Feldspar

Petrographic analysis indicates that 2.4% of framework grains in conglomerate and 9.7% of grains in the sandstone from the Tantalus Formation are, or were, feldspar (Appendix 2, tables 6 and 7). This is significantly lower than in the Tanglefoot formation where they form 25% of framework grains in the conglomerate samples, and 33.4% of the framework grains in the sandstone samples (Figs. 13 and 16). Microcline is present in only minor quantities, representing 0.5% of the conglomerate samples and 0.2% of the feldspar in the sandstone samples. Plagioclase forms 2.2% of the feldspar in the conglomerate samples and 4.1% in the sandstone samples. Non-twinned potassium feldspar are the most abundant recognizable feldspar in the conglomerate (30.4%) and sandstone samples (38.7%). It is notable that only 14% of the Tantalus Formation conglomerate and 62% of the sandstone samples contained recognizable feldspar: this is increased to 48% and 84% when epimatrix (patches of clay replacing feldspar; Dickinson, 1970) is included. In contrast, conglomerate and sandstone samples in the Tanglefoot formation almost all contain some feldspar and/or epimatrix (Fig. 41; Appendix 2).

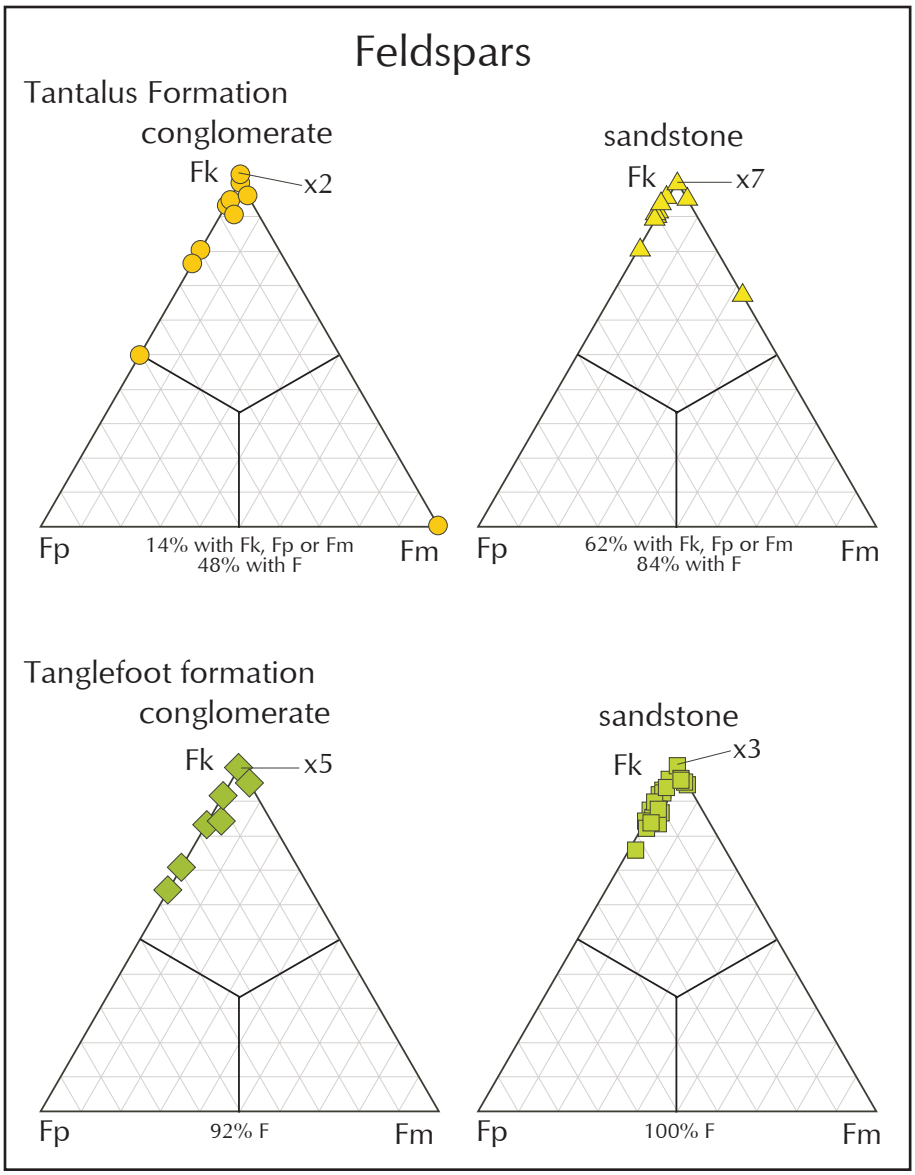

Figure 41. *Relative abundance of recognizable feldspar grains (excludes epimatrix) in strata of the Tantalus (top) and Tanglefoot formations (data in Appendix 2). Note similarity in feldspar types in both formations.*

The overall abundance of feldspar (including epimatrix) is weakly dependent on grain size. Regression analysis of all 112 Tantalus samples (Appendix 2) shows a weak positive relationship (% feldspar = 8.6 + 1.8 Ø), that appears to be significant at the p <0.05 level (*i.e.*, overall finer grained samples contain more feldspar). Regional plots show a strong positive correlation between feldspar abundance and grain size for samples from the Mount Granger, Whitehorse Coal area, along the south eastern part of the Whitehorse trough, but only moderate to very weak positive relations elsewhere (Fig. 42).

The similarity of feldspar types in the Tantalus and Tanglefoot formations indicates that they were derived from a similar source (Upper Triassic and early Lower Jurassic plutons within Stikinia, Quesnellia or Yukon-Tanana), or that the feldspar preserved in strata of the Tantalus Formation was produced largely by reworking of the Tanglefoot formation. As microcline tends to be more resistant to weathering than orthoclase and plagioclase (Folk, 1974), the general paucity of

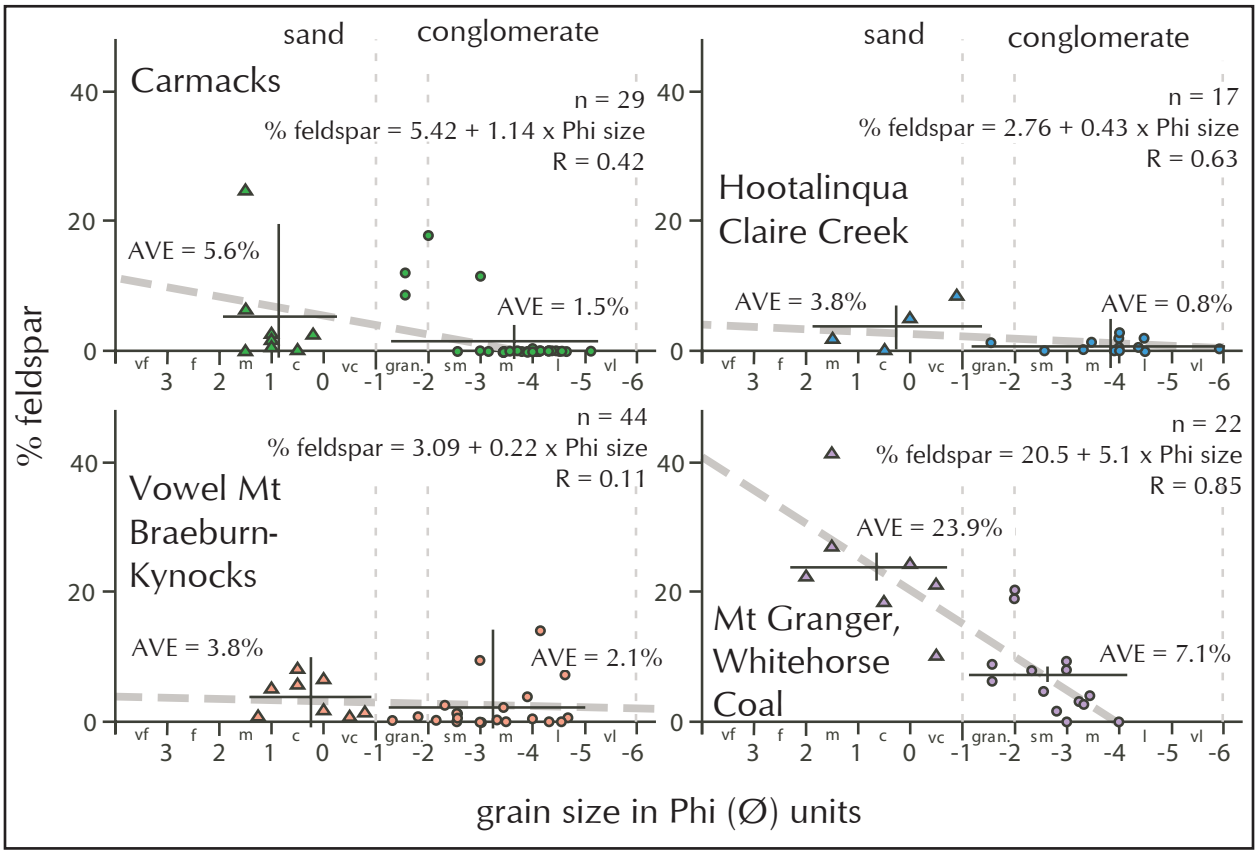

Figure 42. *Regional plots of feldspar abundance (including epimatrix) vs modal grain size (as Phi units). AVE=Average; n=number of point counts; R=Pearson's R statistic (data in Appendix 2). Regression analysis indicates that the calculated correlation are significant at the p < 0.05 level in all areas, except around Carmacks.*

microcline suggests that pegmatite was not especially abundant in the source area, even though it is locally significant within the Aishihik batholith and younger plutons of the Long Lake plutonic suite, to the west of the Whitehorse trough (Johnston *et al.*, 1996). Although orthoclase is currently far more abundant than plagioclase, this may not represent the primary detrital composition. In the Tantalus Formation conglomerate, 67% of the feldspar has been converted to clay to form patches of epimatrix (57% in the sandstone). This is much higher than in the underlying Tanglefoot formation, where only 16% of the feldspar in the conglomerate is represented by epimatrix (20% in the sandstone) indicating more intense in situ weathering by groundwater following deposition and shallow burial. Feldspar probably converted to clay in a humid temperate setting (*cf.*, Bauluz *et al.*, 2014). Folk (1974) and Nesbitt *et al.* (1997) suggest that microcline and orthoclase are more resistant to both weathering and *in situ* diagenetic alteration than plagioclase, consequently the relative abundance of plagioclase plus epimatrix in the Tantalus Formation tends to support a dominantly volcanic source area (Stikinia or Quesnellia) with more aggressive diagenetic alteration of feldspar *in situ*, than in the Tanglefoot formation.

Lithic fragments (non-chert)

The range of non-chert lithic fragments in the sandstone and conglomerate includes sandstone, silicified mudstone, felsic igneous (plutonic plus minor volcanic), and metamorphic rock fragments. Volcanic rock fragments are comparatively rare in the Tantalus Formation, reflecting a greater tendency to break down during weathering and transport, prior to burial and possibly deeper erosion of older arc systems.

Analysis of conglomeratic slabs indicates that non-chert fragments typically form about 3% of the total clast population (max = 23%; Appendix 2, table 1). Petrographic analysis of 79 samples indicates that they make up 7.3% of framework grains, while analysis of 26 samples of sandstone indicate that they make up 2.7% of sand-grade framework grains (Appendix 2, tables 6 and 7). Sedimentary rock fragments are slightly more abundant in the Tantalus Formation conglomerate than the sandstone (Fig. 43), indicating that many of these were labile, and hence decomposed during transport. In contrast, both conglomerate and sandstone samples in the Tanglefoot formation are dominated by igneous rock fragments, including many of volcanic origin. This, and the greater contribution of metamorphic rock fragments in the Tantalus samples, may indicate a greater contribution of material from Yukon-Tanana and other metamorphic sources, and deeper weathering of the Stikine arc. Minor regional differences include a greater abundance of sedimentary and metamorphic rock fragments in the Vowel Mountain – Braeburn-Kynocks area (Table 3) supporting an increased contribution of material from the Yukon-Tanana terrane.

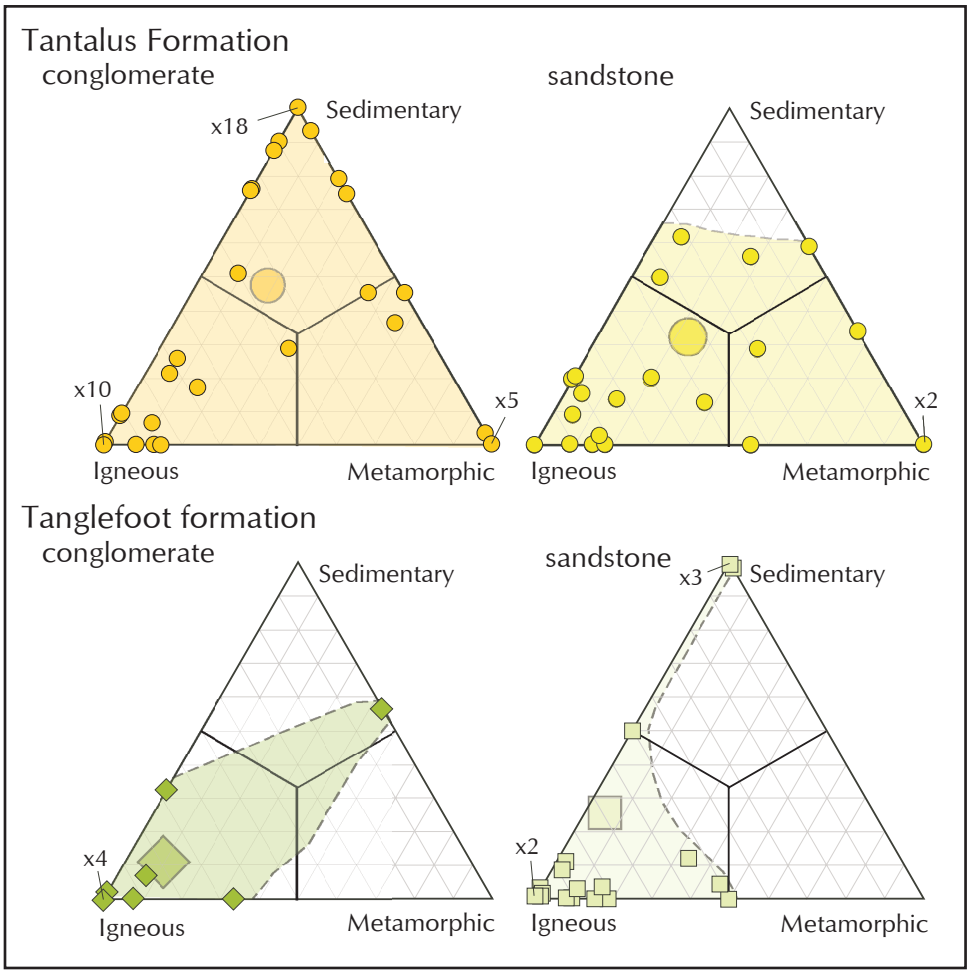

Figure 43. *Relative abundance of non-chert lithotypes in conglomerate and sandstone of the Tantalus (top) and Tanglefoot (bottom) formations (data in Appendix 2). 26% of the conglomerate in the Tantalus Formation and 8% of conglomerate in the Tanglefoot formation contained no non-chert rock fragments. Only 4% of the sandstone in the Tantalus Formation, and 5% of the Tanglefoot formation sandstone had no non-chert rock fragments.*

Table 3. *Relative abundance of minor grain types. Igneous includes volcanic plus plutonic grains (range indicated in brackets). For data see Appendix 2.*

Area/Grain type	Sedimentary		Metamorphic		Igneous	
Tantalus Fm	Sst	Cong	Sst	Cong	Sst	Cong
Mt Granger- Whitehorse Coal	6.7 (0-19.4)	21.4 (0-79.4)	7.9 (0-15.7)	18.1 (0-97.4)	85.4 (80.4-92.3)	60.5 (0-100)
Braeburn-Kynocks Vowel Mountain	0.3 (0-0.9)	0.1 (0-2.0)	1.3 (0-3.8)	1.0 (0-10.9)	1.3 (0-3.8)	98.9 (88.2-100)
Carmacks	0.3 (0-0.6)	0.9 (0-6.4)	2.6 (0-14.0)	0.1 (0-2.0)	97.0 (85.2-100)	99.0 (97.3-100)
Hootalinqua Claire Creek	0.4 (0-1.0)	0.6 (0-4.9)	0 (0-0)	0 (0-0)	99.6 (99.4-100)	99.4 (95.1-100)
Tanglefoot fm						
Mt Granger	1.9 (0-11.8)	2.4 (0-7.4)	1.9 (0-9.1)	2.4 (0-7.4)	96.3 (86.3-100)	95.2 (85.2-100)
Braeburn-Kynocks Vowel Mountain	0.5 (0-1.9)	0.4 (0-0.9)	21.8 (10.2-27.3)	20.3 (0-25.5)	77.7 (72.0-89.8)	79.3 (73.6-85.6)
Carmacks	0 (0-0)	0.6 (0-3.3)	17.4 (9.1-24.4)	18.5 (0-35.5)	82.6 (75.6-90.9)	81.0 (64.5-96.7)
Hootalinqua Claire Creek	0	-	10.2	-	89.8	-

Chert

Chert is by far the most abundant lithic fragment preserved in the Tantalus Formation, making up 77% of the framework grains in the conglomerate, and 56% in the sandstone. In contrast, in the Tanglefoot formation, only 16% of the framework grains in the conglomerate and 5.5% in the sandstone consist of chert. This means that most of the chert must be extra-basinal. Although 110 varieties of chert were observed during this study (Appendices 2 and 3), it is difficult to locate specific sources. When chert types are grouped based on colour (white, black and grey, and yellow), there is little difference between sub areas of the basin (Fig. 44), although yellow chert seems to be slightly less abundant in the vicinity of Mount Granger. When chert types are grouped by texture (massive, brecciated, sphere bearing), sandstone has similar distributions in all areas of the Whitehorse trough (Fig. 45). In the conglomerate, brecciated and sphere bearing chert types are slightly more abundant (Fig. 45). In northern areas massive varieties are dominant, less so in the vicinity of the Mount Granger - Whitehorse Coal area.

Wheeler (1961) suggested that the Cache Creek terrane may have been the main source of chert in the Tantalus Formation, as did Hart and Radloff (1990), who specifically indicated the Kedahda Formation as a probable source (Fig. 46). Cordey (1992) reported Permian radiolaria in a pebble from the Whitehorse Coal area, but found only Middle to Upper Triassic radiolaria in pebbles from the Carmacks area. He suggested that these were most likely derived from the northeastern belt of the Cache Creek terrane, where Triassic and Jurassic chert is present (Cordey *et al.*, 1991), but Pennsylvanian and Permian radiolarian chert are more abundant (Monger, 1975; Table 4). This suggested provenance presents major problems, as none of the pebbles examined by Cordey (1992) from Tantalus Butte contained any Paleozoic radiolaria. In addition, both paleocurrent trends (Fig. 37), and a southerly decrease in maximum grain size of clasts within the Tantalus Formation (Fig. 8) indicate that potential sources should be located to the north or northwest of

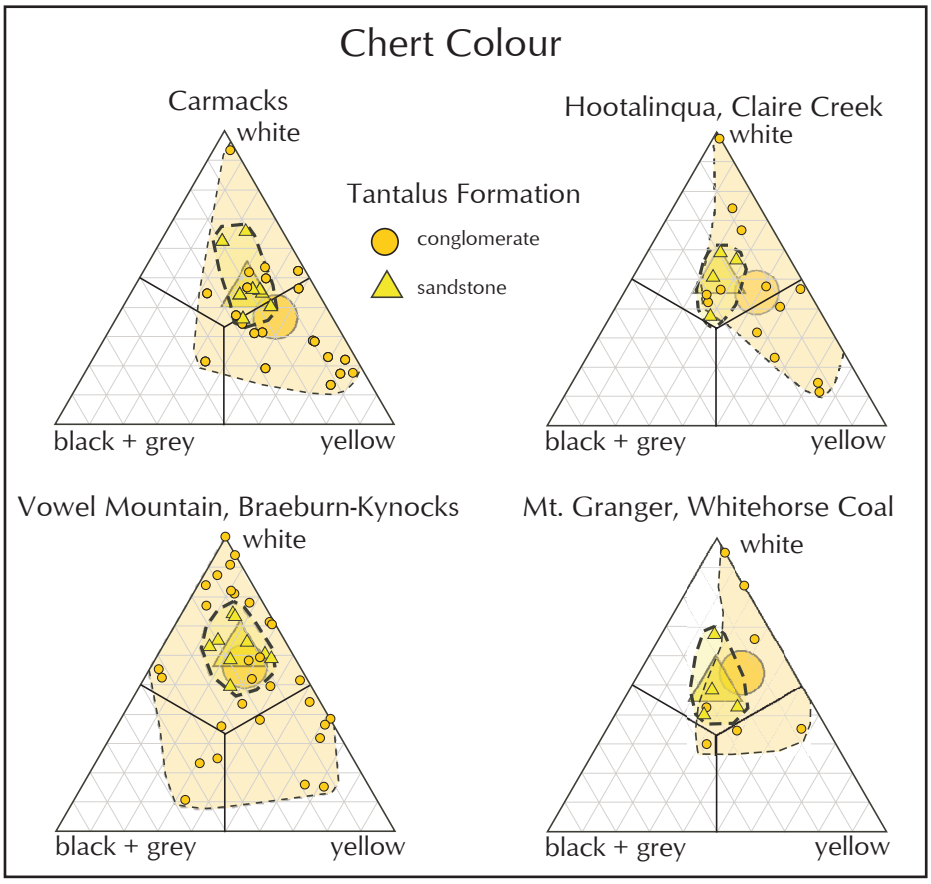

Figure 44. *Relative abundance of chert types by colour, in thin section (data in Appendix 2).*

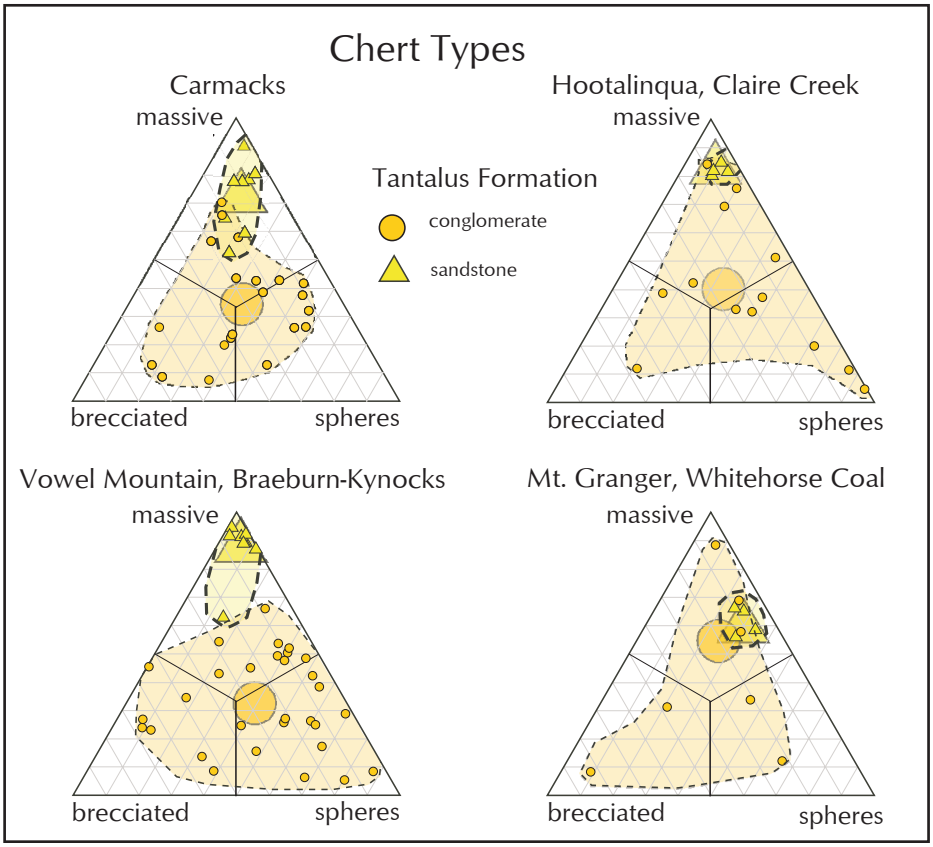

Figure 45. *Relative abundance of chert types by texture (data in Appendix 2). The spherical clusters of microcrystalline quartz, 0.05-0.2 mm diameter are taken to indicate the past presence of radiolarian tests in the chert protolith.*

the Whitehorse trough. Remnants of the Slide Mountain terrane located west of the Yukon-Tanana terrane, about 100 km west of the north end of the Whitehorse trough (Israel *et al.*, 2014), do contain vari-coloured Triassic chert in the Wellesley Lake Formation (Murphy *et al.*, 2008) and might be a viable source of some of the sphere bearing (? Radiolarian) chert grains (Table 4).

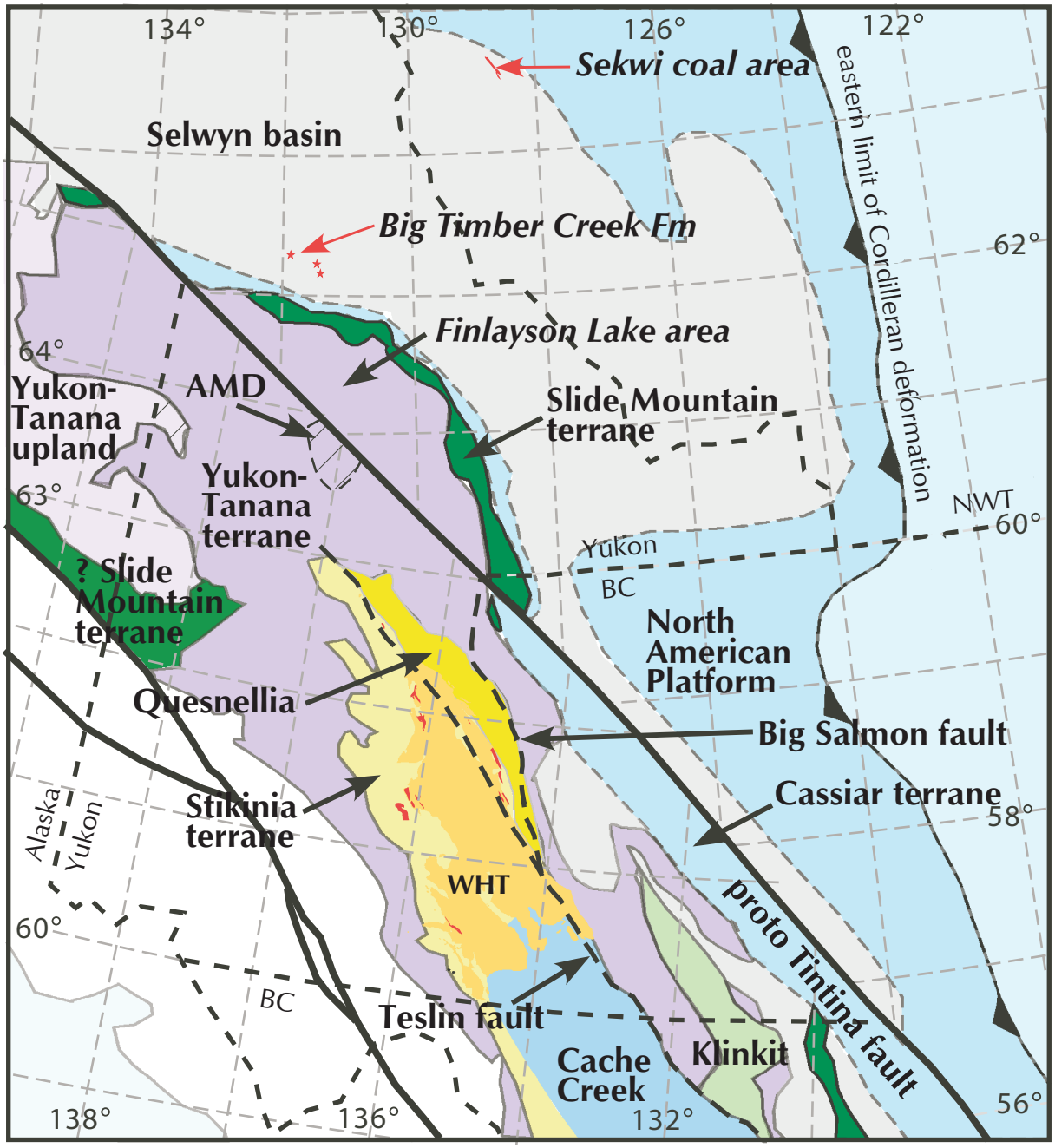

Figure 46. *Tectonic framework of the Whitehorse trough, based on Colpron et al. (2007b), adjusted for ~430 km of Eocene displacement along the Tintina fault (Gabrielse et al., 2006). Red areas within Stikina indicate location of exposures of the Tantalus Formation in the Whitehorse trough (WHT). Red areas in the Selwyn basin indicate isolated basins of Cretaceous clastic strata of the Big Timber Creek Formation (Gordey, 2013), and Sekwi coal area (Martel et al., 2011). Cross-hatch indicates areas with known Lower Cretaceous metamorphism: AMD=Australian Mountain domain (Staples et al., 2013, 2014).*

The exact source of individual chert varieties is difficult to identify based on petrography, using either colour or texture. Most populations include clasts with casts of spherical microfossils, presumably representing recrystallized radiolaria. Chert is most abundant in platformal and proximal slope facies of cratonic North America, especially in slope facies of the Middle Ordovician to Silurian Road River Group (Gordey, 2013; Table 4). Radiolaria have been identified in the Permian Fantasque Formation, as well as the Devonian Canol Formation, and the Upper Ordovician to Silurian Mount Kindle Formation (Bamber and Waterhouse, 1971; Beauchamp and Baud, 2002; Martel *et al.*, 2011). These sources appear to have contributed to isolated bodies of chert pebble conglomerate in the Big Timber Creek Formation (Gordey, 2008, 2013). They may not have been available to the Tantalus rivers during the late Upper Jurassic and early Lower Cretaceous as they would have been on the far side of the mountain ranges generated by thrusting of the Slide Mountain and Yukon-Tanana terranes onto North America (Fig. 46).

Vari-coloured radiolarian chert is a conspicuous component of the Slide Mountain terrane in Devonian to Lower Permian units, including the Mount Aho, Rose Mountain, Fortin Creek and Campbell Range formations (Table 4; Plint and Gordon, 1997; Pigage, 2004; Colpron *et al.*, 2006b; Murphy *et al.*, 2006). This would have been to the north of the Whitehorse trough at the time of deposition of the Tantalus Formation (Fig. 46), but does not contain any known Triassic chert. The Yukon-Tanana terrane, which surrounds the northern Whitehorse trough contains minor vari-coloured chert of Devonian to Triassic age (Table 4). Unfortunately none of these has been shown to contain radiolaria. The Stikine terrane, which underlies the Whitehorse trough contains minor chert bearing units in the Devonian–Permian Stikine Assemblage (including the Permian Ambition Formation in northern British Columbia: Gunning *et al.*, 1994; Evenchick and Thorkelson, 2005), as do the Pennsylvanian Boswell and Semenof formations, east of the trough, and Middle Triassic intervals within the Joe Mountain Formation, within and west of the trough (Hart and Orchard, 1996; Simard and Devine, 2003). Within the Whitehorse trough, Triassic strata of the Hancock member of the Aksala formation contain minor grey and white chert, but in insufficient quantities to have been a major supplier to the Tantalus Formation. Red (or pink) chert is present in 8% of the samples from the Tantalus Formation, and makes up less than 1% of the total chert population (Appendix 2). Pink manganiferous chert is present locally in the Yukon-Tanana terrane to the east of the Whitehorse trough, in the Little Salmon area (Colpron and Reinecke, 2000; Colpron *et al.*, 2006b), and southeast of the trough in northern British Columbia (Big Salmon complex; Mihalynuk and Peter, 2001).

The Cache Creek terrane, located south of the northern Whitehorse trough contains abundant vari-coloured chert of Pennsylvanian to Jurassic age (Monger, 1975; Cordey *et al.*, 1991; Jackson, 1992; Bickerton *et al.*, 2013). It is considered to be the main supplier of chert to the Bowser basin, which overlaps and lies above Stikinia in northern British Columbia, and developed following obduction of the Cache Creek terrane onto Stikinia in the late Lower, to early Middle Jurassic (Evenchick and Thorkelson, 2005). For the currently exposed remnants of the Cache Creek terrane (south of the Whitehorse trough) to have provided significant quantities of chert to the northern Whitehorse trough, major north flowing rivers would have to have developed east of Stikinia, within major intermontane valleys to link with rivers at the north end of the trough. This is considered unlikely, although the modern Columbia River in southern British Columbia, which follows the southern Rocky Mountain trench northwards for 375 km from Columbia Lake, before diverting to the southwest towards Revelstoke, has a similar pattern.

The Wellesely Lake Formation, located in the Slide Mountain terrane, northwest of the Whitehorse trough (Fig. 46), contains some vari-coloured Triassic chert (Murphy *et al.*, 2008), although radiolaria

Table 4. *Potential chart sources.*

Terrane/Age	Unit	Red	Green	Grey	Black	White/Clear	Yellow-Brn.	Clay/ Mica	Radiolaria	References
North American Platform (Mackenzie Mountains)										
Permian	Fantasque Fm			X	X		X		X	MacNaughton 2002; Martel *et al.* 2011
Permian	Jungle Creek Fm					X				Bamber and Waterhouse 1971
Late Mississippian	Hart River Fm						X			Bamber and Waterhouse 1971; Dixon 1992
Early Mississippian	Ford Lake Fm			X	X					Richards *et al.* 1997
Early Mississippian	Tischu Gp					X				Martel *et al.* 2011
Devonian	Imperial Fm			X	X	X	X	X		Norris 1968; Pyle and Jones 2009
Devonian	Canol Fm			X	X		X	X	X	Mackenzie 1974; Martel *et al.* 2011
Mid-Early Devonian	Sombre Fm				X					Martel *et al.* 2011
Late Silurian - Early Devonian	Tsetso Fm (Delorme Gp)					X				Martel *et al.* 2011
Late Ordovician - Silurian	Mt Kindle Fm			X	X	X	X		X	Pyle and Jones 2009; Martel *et al.* 2011
Ordovician-Silurian	Bouvette Fm			X	X	X	X	X		Morrow 1999
Late Cambrian - Early Ordovician	Franklin Mountain Fm			X		X	X			Pyle and Jones 2009; Martel *et al.* 2011
Cambrian	Slats Creek Fm					X				Morrow 1999
Cambrian	Illtyd Fm			X	X			X		Gordey and Makepeace 2001
Neoproterozoic	Coates Lake Gp		X	X	X					Martel *et al.* 2011
Mesoproterozoic	Mackenzie Mts SGp			X	X	X				Martel *et al.* 2011
Paleoproterozoic	Wernecke SGp		X	X	X					Delaney 1981
North American Slope (Selwyn basin)										
Early Permian	Mount Christie Fm	tr	X	X	X					Martel *et al.* 2011; Gordey 2013
Mississippian	Tay Fm				X					Gordey 2013
L.ate Devonian - Early Mississippian	Prevost Fm			X	X					Martel *et al.* 2011
Devonian	Portrait Lake Fm			X		Tr				Martel *et al.* 2011; Gordey 2013
Late Silurian	Steel Fm (Road River Gp)		X	X	Tr	Tr				Gordey 2013
Middle Ordovician - Early Silurian	Duo Lake Fm (Road River Gp)			X	X					Martel *et al.* 2011; Gordey 2013
Late Cambrian - Early Devonian	Rabbitkettle Fm		X	X	X					Gordey 2013
Neoproterozoic	Yusezyu Fm				Tr					Gordey 2013
Slide Mountain terrane										
Mississippian - Early Permian	Campbell Range Fm	X	X						X	Plint and Gordon 1997; Pigage 2004; Murphy *et al.* 2006
Late Pennsylvanian - Early Permian	Fortin Creek Fm		X	X					X	Murphy *et al.* 2006

Terrane/Age	Unit	Red	Green	Grey	Black	White/Clear	Yellow-Brn.	Clay/Mica	Radiolaria	References
Mississippian - Early Permian	Rose Mountain Fm	X	X	X	X	X	X		X	Pigage 2004
Devonian - Early Mississippian	Mount Aho Fm	X	X		X	X	X			Pigage 2004
Southwest Yukon and Alaska										
Triassic	Wellesley Lake Fm	X	X		X		X			Murphy *et al.* 2008
Yukon-Tanana terrane										
Late Triassic?	Faro Peak Fm			X	X					Pigage 2004
Early Permian	Gatehouse Fm	X	X	X		X				Murphy *et al.* 2006
Early Permian	Money Creek Fm	X	X	X			X			Murphy *et al.* 2006
Carboniferous	White Lake/King Arctic fms	X	X			X	X			Murphy *et al.* 2006
Early Mississippian	Tuchitua River Fm									Murphy *et al.* 2006
Late Devonian	Waters Creek Fm									Murphy *et al.* 2006
Late Devonian - Early Mississippian	Cleaver Lake Fm									Murphy *et al.* 2006
Southern Yukon (including Klinkit Assemblage)										
Triassic	Teh and Logjam Fms				X					Roots *et al.* 2006
Late Mississippian – Middle Permian	Little Salmon Fm	X	X	X						Colpron *et al.* 2006
Late Mississippian	Screw Creek Lst -Klinkit Gp	X	X							Roots *et al.* 2006
Devonian-Mississippian?	Swift River Group		X	X	X					Roots *et al.* 2006
Late Mississippian	Big Salmon Complex	X								Mihalynuk and Peter 2001
Early Mississippian	Ram Creek Complex		X	X		X				Roots *et al.* 2006
Mississippian	Little Kalzas Fm (S. Yukon)	X	X	X						Colpron *et al.* 2006
Stikine terrane										
Late Triassic	Hancock mbr, Aksala Fm			X		X				This study
Middle Triassic	Joe Mountain Fm									Hart and Orchard 1996
Early-Mid Pennsylvanian	Boswell and Semminof Fms		X		X	X				Simard and Devine 2003
Early Permian	Ambition Fm (Astika Gp)			X	X					Gunning *et al.*1994
Devonian-Permian	Stikine Assemblage									Evenchick and Thorkelson 2005
Cache Creek terrane										
Middle Triassic - Early Jurassic	Teenah Lake Assemblage		X	X	X	X			X	Jackson 1992
Jurassic	unnamed									Cordey 1991
Triassic	Kedahda Fm	X	X		X	X	X		X	Cordey 1991; Mihalynuk 1999
Permian	Teslin Fm				X				X	Monger 1975
Pennsylvanian-Permian	Horsefeed Fm			X	X				X	Monger 1975
Pennsylvanian-Permian	Kedahda Fm		X	X		X	X		X	Monger 1975; Bickerton *et al.* 2013

have yet to be documented. Given that lithic fragments recovered from the Claire Creek exposures of the Tantalus Formation contain pebbles and cobbles of schistose Yukon-Tanana material, it is possible that the Wellesley Lake Formation, could have been a source of at least some of the chert within the formation.

Given the observed southerly decrease in maximum grain size (Fig. 8) and the overall southerly paleocurrent trends (Fig. 37) it is considered unlikely that any of the known sources discussed above contributed more than minor amounts of chert to the Tantalus basins. The most viable alternative is that much of the chert was derived from a segment of the Cache Creek terrane that had been emplaced onto the Yukon-Tanana terrane north of the Whitehorse trough that was uplifted during accretion of Stikinia and Quesnellia with the North American craton, and has since been completely eroded. Possible evidence for crustal stacking in the area north of the trough comes from the presence of high-grade metamorphic rocks in Yukon-Tanana both to the north, in the Stewart River area (Berman *et al.*, 2007), and to the north-northeast on the other side of the Tintina trench, in the Finlayson Lake area (Staples *et al.*, 2013, 2014; Fig. 46). The Finlayson Lake area is currently located to the east of the Whitehorse trough, but was originally located to the north, prior to ~430 km of dextral strike slip movement along the Tintina fault in the Eocene (Gabrielse *et al.*, 2006). Most of the Yukon-Tanana west of the Tintina fault was metamorphosed in the Longpingian (Upper Permian) and Lower to Middle Triassic (260-239 Ma: Berman *et al.*, 2007), with a further phase of burial between 195 and 187 Ma. To the west of the trough Johnston *et al.* (1996) suggested rapid following emplacement of the Aishihik batholiths during the Pleinsbachian at ~186 Ma and intrusion of the Long Lake plutonic suite at ~187 Ma. They also suggested that cooling ages of 160 to 165 Ma might indicate a second burial event associated with obduction of part of the Cache Creek terrane in this area. Staples *et al.* (2013, 2014) identified a broad area of Middle Jurassic to early Lower Cretaceous (Berrisian; 169-142 Ma) prograde metamorphism in the Yukon-Tanana terrane in the Finlayson Lake area east of the Tintina fault that indicate burial to ~25 km. West of the Tintina trench, Staples *et al.* (2013, 2014) identified a possible core complex in the Australian Mountain domain where prograde metamorphism occurred at ~30 km depth during the Lower Cretaceous (Berrisian to Aptian; 146-118 Ma). The presence of these high-grade metamorphic rocks in the area north of the Whitehorse trough may indicate that the Yukon Tanana terrane in this area could have been overridden by a plate of Cache Creek terrane during closure of the Whitehorse trough, and hence this may be the most viable source for the abundant chert in the Tantalus Formation.

Zircons

Zircon populations within the Tantalus Formation (Fig. 47) appear to be largely derived from older strata within Stikinia and/or Quesnellia. The main peaks (between 200 and 170 Ma) are apparent in underlying strata of the Laberge Group (Colpron *et al.*, 2007c) and indicate a common (direct or indirect) source in the Lewes River - Stuhini arcs (Fig. 46). The minor peak around 250 Ma coincides with ages from the Klondike schist, which occurs as remnants in the Yukon-Tanana terrane north of the trough (Colpron *et al.*, 2006a,b), or may indicate a contribution from strata in the Cache Creek terrane analogous to the Kutcho assemblage in northern British Columbia, which has yielded ages of 242 to 246 Ma (Childe and Thompson, 1997; Childe *et al.*, 1998; Schiarizza, 2012). Peaks between 300 and 280 Ma are present in two of the three Tantalus samples, but are absent in the underlying Laberge Group. These Upper Pennsylvanian and Permian zircons are rare in Yukon terranes (Breitsprecher and Mortensen, 2004), but could come from part of the Klinkit assemblage in the Yukon-Tanana terrane (Colpron *et al.*, 2006a; Beranek and Mortensen, 2011), or some as yet undated source in the Slide Mountain terrane to the northwest (Murphy *et al.*, 2008). Zircons with dates between 350 and 310 Ma may have been recycled from strata of the Laberge Group

or from the Yukon-Tanana terrane (Colpron *et al.*, 2006a). The absence of abundant Archean zircons suggests that cratonic strata from North America did not contribute significantly to the Tantalus Formation. Six Paleoproterozoic zircons (2292-1925 Ma) were recorded from the Tantalus Formation (Appendix 4). These Rhyacian and Orosirian grains may have been from distal parts of the North American craton within the Yukon-Tanana terrane (Beranek and Mortensen, 2011), or may be inherited cores from Paleozoic intrusions in the Yukon-Tanana terrane, or Upper Triassic to Lower Jurassic plutons that intrude Stikinia, Quesnellia and the Yukon Tanana terranes (Mortensen, 1990; Colpron *et al.*, 2006a,b).

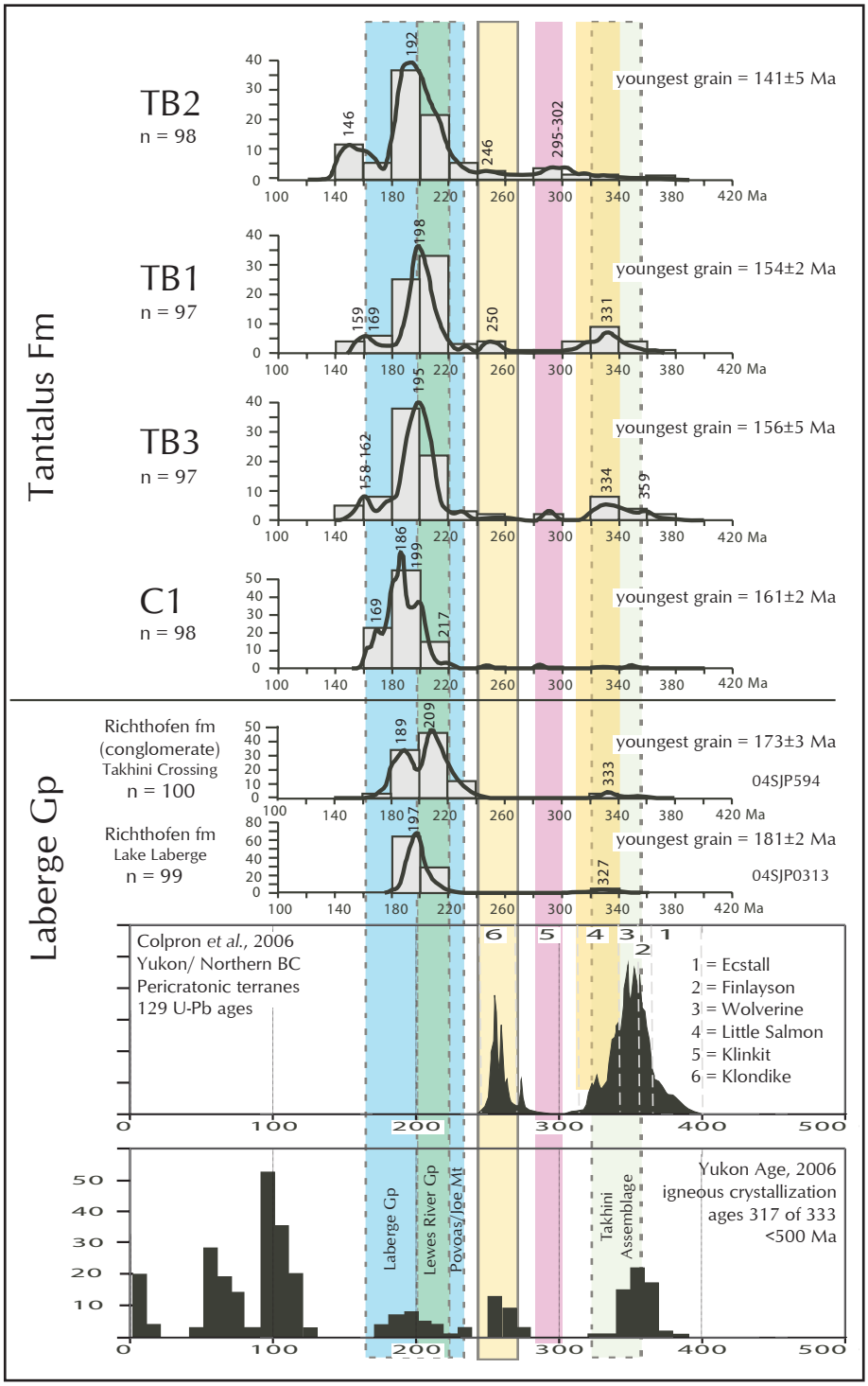

Figure 47. *Zircon provenance for strata from the Tantalus Formation (this paper) and Laberge Group (from Colpron et al., 2007c), with comparative information for ages of pericratonic terranes (Colpron et al., 2006) and igneous crystallization ages in the Yukon based on the age database of Breitsprecher and Mortensen (2004).*

The youngest three grains in the Tantalus samples overlap with the suspected time of deposition of the unit (Fig. 2). The YukonAge database (Breitsprecher and Mortensen, 2004), includes no record of igneous crystallization ages within the time span of 156 ± 6 to 141 ± 5 Ma within the Yukon, although as yet undated rocks of this age may be present west of the Denali fault. These younger grains must have been contributed as wind-born ash from more westerly or more southerly terranes within the Coast Ranges, or farther to the south, in central British Columbia. Strata within the Bowser Basin typically contain zircons that are the same age as the host strata: for example, strata in the upper part of the Todagin Formation contain an ash horizon dated at 158 ± 1 Ma, and strata of the Devils Claw Formation contain an ash horizon dated at 141 ± 1 Ma (McNicoll, pers. comm. 2007), hence a common (airborne) source, in the Skeena arch, south of the Bowser basin, is possible (McNicoll *et al.*, 2005; Evenchick *et al.*, 2007, 2010).

Climate

The climate history of the Cordillera is not well documented in the Upper Jurassic and Lower Cretaceous (Haggart *et al.*, 2006). Sellwood and Price (1993) indicate that the CO_2 content of the atmosphere was about four times greater than the current levels, so global climate would have been more equitable than the present. Global climate modeling by Hallam (1993) suggests that the Whitehorse trough was in a zone characterized by warm-wet conditions in the Upper Jurassic (Kimmeridgian). This is supported by the presence of coal accumulations, which indicate that humid conditions prevailed on a year-round basis (Sellwood and Price, 1993), with annual precipitation between 3 and 5 mm per day (Price *et al.*, 1995) and no dry periods. Mean average temperatures would be between 4 and 12°C (Sellwood and Price, 1993; Sellwood *et al.*, 2000). Similar conditions would have prevailed up to the early Valanginian, when a brief period of cooling is indicated by a shift to more positive carbon isotope content in terrestrial plants (Gröcke *et al.*, 2005). This trend towards cooler and wetter climates is also indicated towards the craton, in the Svedrup basin, by changes in plant communities (Galloway *et al.*, 2013). The climate model suggested above is based on a Tithonian paleolatitude of the Whitehorse trough of ~55-65°N, and assumes that Stikinia was firmly anchored to the North American craton by 140 Ma (prior to ~430 km northward dextral displacement in the Eocene: Gabrielse *et al.*, 2006). This is a situation supported by Haggart *et al.* (2006), who notes that during the Lower Cretaceous most of the terrestrial basins west of the Cordilleran foreland basin (including the Bowser basin) have a similar paleoflora, indicative of a humid temperate climate. If the Whitehorse trough was significantly farther south as is implied in the models of Johnston (2001, 2008), and Kent and Irving (2010), then warmer, semi-arid to arid conditions should have prevailed, and pedogenic calcretes should be present (Haywood *et al.*, 2004). In this more arid model accumulation of coal deposits would be minimal.

The high resistate (quartz, chert) content of the Tantalus Formation indicates intense weathering in the provenance area. This is supported by the paucity of feldspar and abundant evidence of *in situ* alteration of feldspar to epimatrix during deposition (*cf.*, Haywood *et al.*, 2004). Feldspar probably converted to clay in a humid temperate setting (Bauluz *et al.*, 2014), possibly equivalent to a modern Cf_b Koppen Climate zone, which Peel *et al.* (2007) suggest records a temperate climate, without a dry season, and with warm summers (temperature range between 4 and 22°C).

Paleogeography/tectonics

The Tantalus basins are superimposed on earlier piggyback basins, developed during the final stages of counterclockwise rotation of Stikinia against North America (Gordey and Stevens, 1994b; White *et al.*, 2012; Bickerton *et al.*, 2013). The elongate pattern of the basins, along with

generally southerly paleocurrents and decrease in maximum grain size, suggests deposition in elongate intermontane, valley-confined basins, possibly coeval with orogen parallel thrusting of the Intermontane terranes onto the North American craton during early stages of development of the Cordilleran mountain belt. As such the Tantalus basins represent a second phase of piggyback basin development in the area, as this model has also been applied to the late stages of deposition of the Laberge Group (Mihalynuk *et al.*, 1994, 2004; White *et al.*, 2012). Local deviations in paleocurrents may reflect deposition in orogen transverse segments of the river systems, or may reflect local tectonic uplift deflecting river patterns. Considerable local subsidence, either by load induced subsidence or local tectonic mechanisms, is required to provide the accommodation space to allow preservation of thick sequences, such as those preserved at Vowel Mountain. Some of this subsidence could have been associated with trans-tension related to dextral strike-slip faulting during deposition as suggested earlier by Tempelman-Kluit (2009). If the Tantalus Formation had been deposited as a uniform wedge of strata away from a rising mountain front (*i.e.*, a foreland or hinterland basin fill) it would have more uniform orogen normal paleocurrents, and not the more irregular orogen parallel patterns seen in the Tantalus Formation, which mimic the pattern of modern intermontane river systems, like the Fraser River in British Columbia.

Local sources can be used to explain much of the feldspar and igneous (volcanic plus plutonic) components in the Tantalus Formation, and were probably provided by valley normal tributaries. The large volumes of chert in the formation cannot be explained by local sources, and appear to have been derived from an extension of the Cache Creek terrane that once occupied highlands to the north of the Whitehorse trough, in an area now characterized by highly metamorphosed strata of the Yukon-Tanana terrane (*see* above). North of this area Gordey (2013) has recorded the presence of up to 120 m of Lower Cretaceous chert pebble conglomerate, with clasts up to 20 cm in diameter, in the Tay River area (NTS 105J), east of the Tintina fault. These strata of the Big Timber Creek Formation would have been due north of the Whitehorse trough in the Tithonian to Valanginian (Fig. 46), and probably derived most of their chert fragments from the Selwyn basin. Isolated Barremian to early Cenomanian (mid-Lower Cretaceous to early Upper Cretaceous) coal bearing strata in the Sekwi area on the margins of the Selwyn basin (Fig. 46) contain only local siliciclastic clasts and chert derived from the Devonian Landry Formation and Permian Fantasque Formation (Martel *et al.*, 2011). Likewise mid-Albian to Cenomanian strata adjacent to the Tintina fault are dominated by locally derived siliciclastic material, with only minor chert, and were derived from local strata within the Yukon-Tanana terrane (Long *et al.*, 2001; Long and Lowey, 2011). All that these basins, and the isolated outcrops of Upper Jurassic strata and the Tantalus Formation have in common is that they appear to have been deposited in narrow valley-confined systems during intervals of (? oblique) regional convergence of Stikinia, Quesnellia, and the Yukon-Tanana terranes with the North American craton. Deformation of the pre-Tantalus strata in the Whitehorse trough began by the Bajocian and continued during deposition of the Tantalus Formation, continuing into the Paleogene (Ricketts *et al.*, 1992; Murphy *et al.*, 1995). The *en échelon* pattern of folds in the Yukon segment of the Whitehorse trough suggests that some dextral strike-slip movement may have occurred during Upper Jurassic to Lower Cretaceous folding (Colpron, 2011; White *et al.*, 2012), and that this may have directly influenced the geometry of the Tantalus basins. Strike-slip movement on the Teslin fault (Fig. 46) was concentrated between 115 and 95 Ma (Gabrielse *et al.*, 2006), hence additional folding and burial of the Tantalus Formation may have occurred at this time (White *et al.*, 2012). Lowey (2008) and Lowey *et al.* (2009) used homogenization temperatures of petroleum fluid inclusions to estimate that strata of the Tantalus and Tanglefoot formations in the northern part of the Whitehorse trough must have been buried by a about 3-4 km of strata, prior to Aptian to Albian uplift, erosion and deposition of volcanic strata of the (Albian) Mount Nansen and overlying (Maastrichtian) Carmacks groups.

The Tantalus Formation appears to have been deposited in elongate, structurally controlled, intermontane valley fills. These narrow piggyback basins developed at the same time as strata in the Bowser Lake Group were being deposited to the south in a broad, more extensive, successor basin (Fig. 48). The Bowser basin is interpreted as a broken retroforeland basin (in the sense of Ingersol, 2012), created by subsidence associated with westward obduction of the Cache Creek terrane onto Stikinia (Evenchick and Thorkelson, 2005; Evenchick *et al.*, 2007, 2010; Gagnon *et al.*, 2009). The Cache Creek terrane, south of the Whitehorse trough, provided chert to the Upper Jurassic Bowser Lake Group, that was subsequently reworked to form conglomeratic deposits in the Devils Claw Formation and the Sustut Group in elongate intermontane piggyback basins in Aptian to Maastrichtian times (Fig. 48). Deposition of the Sustut Group appears to be coeval with tensional and/or transtensional events in the Whitehorse trough in Yukon, which is marked by emplacement of volcanic rocks of the Mount Nansen and Carmacks groups during this time.

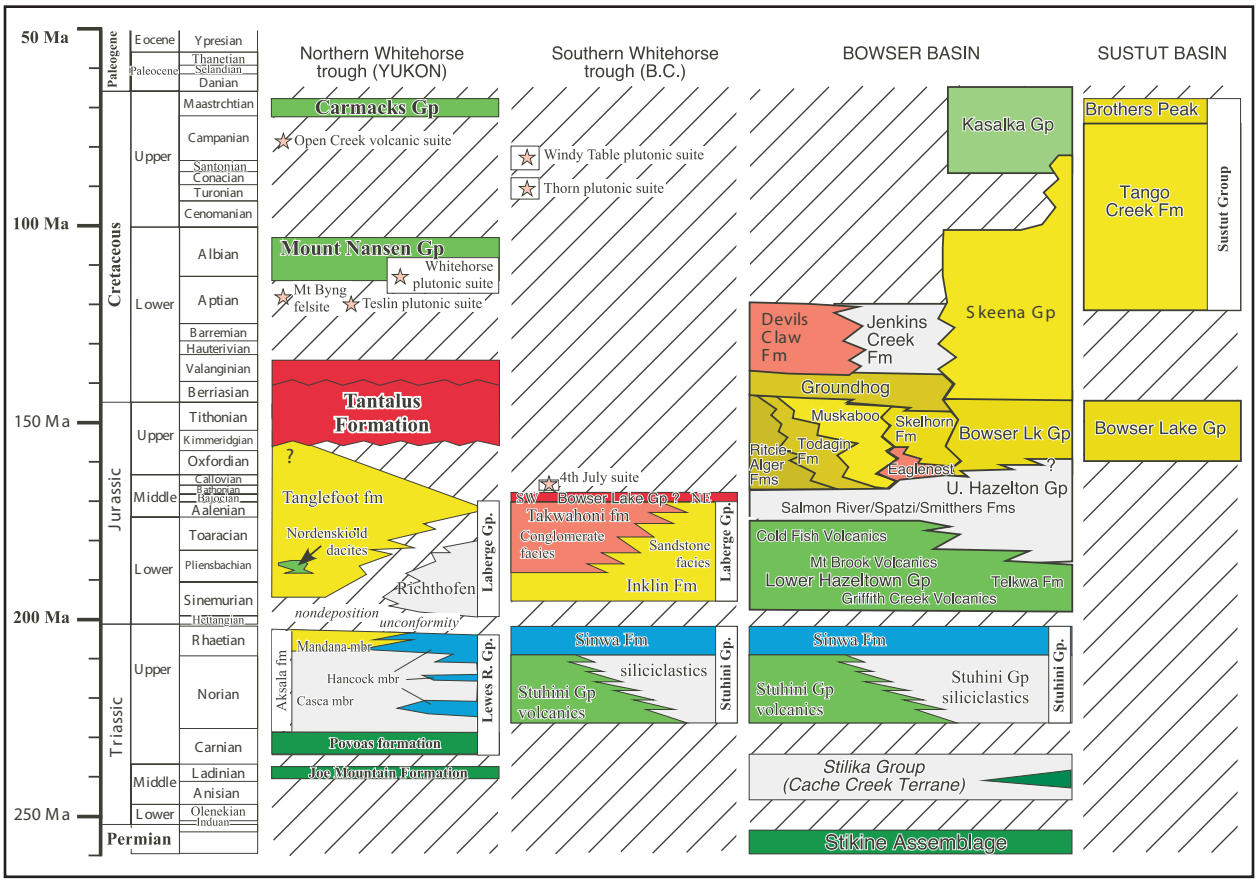

Figure 48. *Correlation of strata in the northern Whitehorse trough, with strata in northern British Columbia, based on this publication and data presented by Evenchick and Thorkelson (2005), Evenchick et al. (2007, 2010) and Gagnon et al. (2009). Stars indicate dated volcanic and plutonic suites.*

CONCLUSIONS

The Tantalus Formation represents high-energy fluvial deposition in an intermontane valley fill setting that may represent a series of piggyback basins developed during compression of underlying strata within the Whitehorse trough. Conglomerate reflects deposition in shallow to deep braided river systems, with local development of meandering gravel-bed rivers. Correlation between sub-basins may be possible due to fluctuation in the maximum grain size in individual sub-basins, which may have been driven by tectonically driven episodes of uplift (*cf.*, Leeder, 1997; Frostick and Jones, 2002; Kumar *et al.*, 2007), or by climatically induced fluctuation in rainfall or maximum storm intensity. The latter is indicated in part by strong evidence for Milankovitch cyclicity (~100 ka) in the Lower Cretaceous (Dean and Arthur, 1999; Mutterlose and Ruffell, 1999; Kujau *et al.*, 2013; Wu *et al.*, 2013) and studies of sediment flux in older basins (Cecil, 1990).

Overbank, marsh, swamp and pond deposits in the Tantalus Formation are restricted to recessive intervals. Coal deposits developed locally on abandoned segments of floodplains within confined river valleys, and in places are associated with high constructive river deposits. This might have occurred in response to local capture of headwaters by other rivers, or local reduction in stream gradients by downstream progradation of valley-transverse fan systems, although this would be difficult to prove given the predominance of chert clasts in the sands and gravels.

Based on the observed paleocurrents, distribution of potential chert sources, and observed zircon assemblages, it is probable that strata of the Tantalus Formation were derived in part from weathering of uplifted blocks of older Triassic and Jurassic strata within the Whitehorse trough and the adjacent arc terrains (Stikinia, Quesnellia), with contributions from Yukon-Tanana to the north. As clasts within the Tantalus Formation are predominantly chert, silicified mudstone and quartz, with only minor labile lithic fragments it is clear that much of the lithic material was derived from a source other than the underlying arc-derived strata. The source of chert clasts is enigmatic: early interpretations suggested that they may have come from strata within the Cache Creek terrane. As preserved parts of this currently lies to the south of the Whitehorse trough this (southern) source is highly unlikely. A minor peak of zircon ages around 250 Ma in the Tantalus samples indicates that at least some of the drainage basin that fed the Tantalus rivers was located in the Yukon-Tanana terrane, or alternatively could be derived from strata equivalent to the Kutcho assemblage in the Cache Creek of northern British Columbia. Some of the chert could have been derived from now eroded strata preserved within the upper parts of the Yukon-Tanana (as seen in southern Yukon and British Columbia: Table 4). A problem with this interpretation is that none of the chert from Yukon-Tanana in southern Yukon or British Columbia is known to contain radiolarians (*i.e.*, sphere bearing chert). In contrast radiolarians are abundant in most of the chert from the Cache Creek terrane (Table 4).

It is here suggested that most of the chert in the Tantalus Formation was derived from supracrustal rocks of Cache Creek affinity that were emplaced at the north end of the Whitehorse trough during rotational closure (*cf.*, Mihalynuk *et al.*, 1994, 2004), and were subsequently eroded from the top of the Yukon-Tanana terrane. The chert from the Cache Creek terrane have a similar range of colours (Table 4) to those seen in the Tantalus Formation, indicating that the main source may have been a now eroded segment of the Cache Creek terrane, that was, centered over an area of intense Lower Cretaceous metamorphism in the Australian Mountain domain. Staples *et al.* (2013, 2014) suggest that this area has been exhumed about 30 km since peak metamorphism, while rocks to the north of the Tintina trench and to the west of the Whitehorse have been exhumed about 20 to 25 km (Johnston *et al.*, 1996; Staples *et al.*, 2014: Fig. 46). The dominance of stable rock fragments reflects

intense weathering in a warm humid climatic setting that would have removed much of the labile feldspars and high-temperature minerals derived from the local basement. Wet (humid) summer and winter conditions are also supported by the presence of coal deposits.

The hydrocarbon potential of the Tantalus Formation is considered to be limited to negligible given the predominance of conglomerates (all highly jointed) and lack of suitable cap rocks, although there may some, as yet undiscovered, coal resources, and a limited (unproven) potential for coal-bed methane.

ACKNOWLEDGEMENTS

This project was initiated while I was in the Coal Geology section of the Geological Survey of Canada. Subsequent research was funded by NSERC Discovery grants, with additional direct funding and logistical support from the Yukon Geological Survey. I thank Dirk Tempelman-Kluit for introducing me to the area in 1978, and George Gehrels for dating zircons from the Tantalus Formation. I thank Maurice Colpron, Don Murphy, Lee Pigage, Charlie Roots, Steve Gordey, Grant Lowey, Phillipe Erdmer, Tiffani Fraser, Julie Hunt, Jim Monger, Steve Piercey, Pamela Read, Steve Johnston, and many others for stimulating discussions and sharing their insight into Yukon geology. I thank Tiffani Fraser, Matt Hutchison and Maurice Colpron for critically reviewing this paper and providing constructive criticism. Any remaining errors and misconceptions are my own.

REFERENCES

Alegria-Arzaburu, A.R. de. and Masselink, G., 2010. Storm response and beach rotation on a gravel beach, Slapton Sands, UK. Marine Geology, vol. 278, p. 77-99.

Allen, J.R.L., 1970. Physical Processes in Sedimentology. Allen and Unwin, London, 248 p.

Allen, T.L., 2000. An evaluation of coal-bearing strata at Division Mountain (115H/8 east-half, 105E/5 west-half), southcentral Yukon. *In:* Yukon Exploration and Geology 1999, D.S. Emond and L.H. Weston (eds.), Exploration and Geological Services Division, Yukon, Indian and Northern Affairs Canada, p. 177-198.

Alonso, A. and Garzón, G., 1994. Quaternary evolution of a meandering gravel bed river in central Spain. Terra Nova, vol. 6, p. 465-475.

Appel, V.L., 1998. Geological, geochronological and Pb isotopic constraints on the age and origin of the Mount Nansen epithermal Au-Ag vein deposit, eastern Dawson Range, Yukon. Unpublished BSc thesis, University of British Columbia, Vancouver, BC.

Arche A., 1983. Coarse-grained Meander Lobe Deposits in the Jarama River Madrid (Spain). *In:* Modern and ancient fluvial systems, J.D. Collinson and U. Lewin (eds.), International Association of Sedimentologists, Special Publication, no. 6, p. 313-321.

Baker, J.C., Kassan, J. and Hamilton, P.J., 1995. Early diagenetic siderite as an indicator of depositional environment in the Triassic Rewan Group, southern Bowen Basin, eastern Australia. Sedimentology, vol. 43, p. 77-88.

Bamber, E.W. and Waterhouse, J.B., 1971. Carboniferous and Permian Stratigraphy and Paleontology, Northern Yukon Territory, Canada. Bulletin of Canadian Petroleum Geology, vol. 19, p. 29-250.

Bauluz, B., Yusye, A., Mayayo, M.J. and Canudo, J.I., 2014. Early kaolinization of detrital Weald facies in Galve sub-basin (Central Iberian Chain, northeast Spain) and its relationship to paleoclimate. Cretaceous Research, vol. 50, p. 214-227.

Beaton, A.P., Cameron, A.R. and Goodarzi, F., 1992. Petrography, geochemistry and utilization potential of the Division Mountain coal occurrences, Yukon Territory. *In:* Current Research, Part E, Geological Survey of Canada, Paper 92-1E, p. 23–32.

Beauchamp, B. and Baud, A., 2002. Growth and demise of Permian biogenic chert along northwest Pangea: evidence for end-Permian collapse of thermohaline circulation. Palaeogeography, Palaeoclimatology, Palaeoecology, vol. 184, p. 37–64.

Bell, W.A., 1956. Lower Cretaceous floras of western Canada. Geological Survey of Canada, Memoir 285, 331 p.

Bennett, M.R., Cassidy, N.J. and Pile, J., 2009. Internal structure of a barrier beach as revealed by ground penetrating radar (GPR): Chesil Beach, UK. Geomorphology, vol. 104, p. 218-229.

Beranek, L.P. and Mortensen, J.K., 2011. The timing and provenance of the Late Permian Klondike orogeny in northwestern Canada and arc-continent collision along western North America. Tectonics, vol. 30, cit. no. TC5017, <http://www.agu.org> [accessed January 15, 2014]. doi:10.1029/2010TC002849.

Berman, R.G., Ryan, J.J., Gordey, S.P. and Villeneuve, M., 2007. Permian to Cretaceous polymetamorphic evolution of the Stewart River region, Yukon-Tanana terrane, Yukon, Canada: P-T evolution linked with in situ SHRIMP monazite geochronology. Journal of Metamorphic Geology, vol. 25, p. 803–827.

Best, J.L., Ashworth, P.J., Bristow, C.S. and Roden, J., 2003. Three-dimensional sedimentary architecture of a large, mid-channel sand braid bar, Jamuna River, Bangladesh. Journal of Sedimentary Research, vol. 73, p. 516-530.

Bickerton, L., Colpron, M. and Gibson, D., 2013. Cache Creek terrane, Stikinia, and overlap assemblages of the eastern Whitehorse (NTS 105D) and western Teslin (NTS 105C) map areas. *In:* Yukon Exploration and Geology 2012, K.E. MacFarlane, M.G. Nordling and P.J. Sack (eds.). Yukon Geological Survey, p. 1-17.

Blacknell, C., 1982. Morphology and surface sedimentary features of point bars in Welsh gravel-bed rivers. Geological Magazine, vol. 119, p. 181-192

Bluck, B.J., 1971. Sedimentation in the meandering River Endrich. Scottish Journal of Geology, vol. 7, p. 93-138.

Bond, D.P.G. and Chapman, R.J., 2006. Evaluation of the origins of gold hosted by the conglomerates of the Indian River formation, Yukon, using a combined sedimentological and mineralogical approach. *In:* Yukon Exploration and Geology 2006, D.S. Emond, L.L. Lewis and L.H. Weston (eds.). Yukon Geological Survey, p. 93-103.

Bostock, H.S., 1936. Carmacks District, Yukon. Canada, Department of Mines, Geological Survey, Memoir 187, 67 p.

Bostock, H.S. and Lees, E.J., 1938. Laberge map-area, Yukon. Canada Department of Mines and Resources, Geological Survey Memoir, 217, 32 p.

Breitsprecher, K. and Mortensen, J.K. (compilers), 2004. YukonAge 2004: A database of isotopic age determinations for rock units from Yukon Territory. Yukon Geological Survey, CD-ROM.

Bremner, T., 1988. Geology of the Whitehorse Coal Deposit. *In:* Yukon Geology Volume 2, J.G. Abbott (ed.). Exploration & Geological Services Division, Indian and Northern Affairs Canada, p. 1-7.

Bridge, J.S. and Tye, R.S., 2000. Interpreting the dimensions of ancient fluvial channel bars, channels, and channel belts from wireline-logs and cores. American Association of Petroleum Geologists, Bulletin 84, p. 1205-1228.

Bultman, T.R., 1979. Geology and tectonic history of the Whitehorse trough west of Atlin, British Columbia. PhD thesis, Yale University, New Haven, Connecticut, 296 p.

Burge, L.M., 2006. Stability, morphology, and surface grain size patterns of channel bifurcation in gravel-cobble bedded anabranching rivers. Earth Surface Processes and Landforms, vol. 31, p. 1211-1226.

Cairnes, D.D., 1910. Lewes and Nordenskiöld Rivers coal district. Canada Department of Mines, Geological Survey Branch, Memoir 5.

Cairnes D.D., 1912. Wheaton District, Yukon Territory. Geological Survey of Canada, Memoir 31.

Cairnes D.D., 1916. Wheaton District, southern Yukon; Supplement to Geological Survey of Canada Memoir 31. Geological Survey of Canada, Summary Report for 1915.

Cameron, A. R. and Beaton, A. P., 2000. Coal resources of Northern Canada with emphasis on Whitehorse Trough, Bonnet Plume Basin and Brackett Basin. International Journal of Coal Geology, vol. 43, p. 187-210.

Carne, R.C. and Gish, R.F., 1996. Geology of the Division Mountain coal deposit of Cash Resources Ltd. *In:* Yukon Exploration and Geology 1995. Exploration and Geological Services Division, Yukon, Indian and Northern Affairs Canada, p. 37-42.

Carson, M.A., 1986. Characteristics of high-energy ''meandering'' rivers: the Canterbury Plains, New Zealand. Geological Society of America, Bulletin, vol. 97, p. 886–895.

Castelle, B., Bonneton, P., Dupuis, H. and Sénéchal, N., 2007. Double bar beach dynamics on the high-energy meso-macrotidal French Aquitanian coast: a review. Marine Geology, vol. 245, p. 141-159.

Cecil, C.B., 1990. Paleoclimate controls on stratigraphic repetition of chemical and siliciclastic rocks. Geology, vol. 18, p. 533-536.

Childe, F.C. and Thompson, J.F.H., 1997. Geological setting, U-Pb geochronology, and radiogenic isotope characteristics of the Permo-Triassic Kutcho assemblage north-central British Columbia. Canadian Journal of Earth Sciences, vol. 34, p. 1310-1324.

Childe, F.C., Thompson, J.F.H., Mortensen, J.K., Friedman, R.M., Schiarizza, P., Bellefontaine, K. and Marr, J.M., 1998. Primative Permo-Triassic volcanism in the Canadian Cordillera: tectonic and metallogenic implications. Economic Geology, vol. 93, p. 224-231.

Clapham, M.E., Smith, P.L. and Tipper, H.W., 2002. Lower to Middle Jurassic stratigraphy, ammonoid fauna and sedimentary history of the Laberge Group in the Fish Lake syncline, northern Whitehorse trough, Yukon, Canada. *In:* Yukon Exploration and Geology 2001, D.S. Emond, L.H. Weston, and L.L. Lewis (eds.). Yukon Geological Survey, p. 73-85.

Clemmensen, L.B. and Nielsen, L., 2010. Internal architecture of a raised beach ridge system (Anholt, Denmark) resolved by ground-penetrating radar investigations. Sedimentary Geology, vol. 223, p. 281-290.

Cohen, K.M., Finney, S.C., Gibbard, P.L. and Fan, J.-X., 2013. The ICS International Chronostratigraphic Chart. Episodes, vol. 36, p. 199-204.

Colpron, M. (compiler), 2011. Geological compilation of the Whitehorse Trough – Whitehorse (105D), Lake Laberge (105E), and parts of Carmacks (115I) and Teslin (105C). Yukon Geological Survey, Geoscience Map 2011-1, 3 maps, legend and appendices.

Colpron, M. and Friedman, R.M., 2008. U-Pb zircon ages for the Nordenskiöld formation (Laberge Group) and Cretaceous intrusive rocks, Whitehorse trough, Yukon. *In:* Yukon Exploration and Geology 2007, D.S. Emond, L.R. Blackburn, R.P. Hill and L.H. Weston (eds.). Yukon Geological Survey, p. 139-151.

Colpron, M., Gordey, S.P., Lowey, G.W., White, D. and Piercey, S.J., 2007a. Geology of the northern Whitehorse trough, Yukon (NTS 105E/12, 13, and parts of 11 and 14; 105L/4 and parts of 3 and 5; parts of 115H/9 and 16; 115I/1 and part of 8) (1:150 000 scale). Yukon geological Survey, Open File 2007-6.

Colpron, M., Mortensen, J.K., Gehrels, G.E. and Villeneuve, M., 2006b. Basement complex, Carboniferous magnetism and Paleozoic deformation in Yukon-Tanana terrane of central Yukon: field, geochemical and geochronological constraints from Glenyon map area. *In:* Paleozoic Evolution and Metallogeny of Pericratonic Terranes at the Ancient Pacific Margin of North America, Canadian and Alaskan Cordillera, M. Colpron and J.L. Nelson (eds.). Geological Association of Canada, Special Paper, no. 45, p. 131–151.

Colpron, M., Murphy, D.C., Nelson, J.L., Roots, C.F., Gladwin, K., Gordey, S.P., Abbott, G. and Lipovsky, P.S., 2002. Preliminary geological map of Glenlyon (105L/1-7, 11-14) and northeast Carmacks (115I/9, 16) areas, Yukon Territory, scale 1:125 000. Indian and Northern Affairs, Canada, Exploration and Geological Services Division, Yukon Region, Open File 2002-9/ Geological Survey of Canada, Open File 1457.

Colpron, M. and Nelson, J.L., 2009. A Palaeozoic Northwest Passage: incursions of Caledonian, Baltican and Siberian terranes into eastern Panthalassa, and the early evolution of the North American Cordillera. *In:* Earth Accretionary Systems in time and Space, P.A. Cawood and A. Kröner (eds.). Geological Society (London), Special Publication 318, p. 273-307.

Colpron, M., Nelson, J.L. and Israel, S., 2007c. A transect through accreted terranes of the northern Canadian Cordillera: from Cassiar, British Columbia to Kluane Lake, Yukon. Arizona Geological Society ores and orogenesis symposium field trip no. 15. Yukon Geological Survey, Open File 2007-3.

Colpron, M., Nelson, J.L. and Murphy, D.C., 2006a. A tectonostratigraphic framework for the pericratonic terranes of the northern Cordillera. *In:* Paleozoic Evolution and Metallogeny of Pericratonic Terranes at the Ancient Pacific Margin of North America, Canadian and Alaskan Cordillera, M. Colpron and J.L. Nelson (eds.). Geological Association of Canada, Special Paper, no. 45, p. 1-23.

Colpron, M., Nelson, J.L. and Murphy, D.C., 2007b. Northern Cordilleran terranes and their interactions through time. GSA Today, vol. 17, issue 4/5, p. 4-10.

Colpron, M. and Reinecke, M., 2000. Glenlyon project: Coherent stratigraphic succession of Yukon-Tanana terrane in the Little Salmon Range, and its potential for volcanic-hosted massive sulphide deposits, central Yukon. *In:* Yukon Exploration and Geology 1999, D.S. Emond and L.H. Weston (eds.). Exploration and Geological Services Division, Yukon, Indian and Northern Affairs Canada, p. 87-100.

Cordey, F., 1992. Radiolarian ages from chert pebbles of the Tantalus Formation, Carmacks area, Yukon Territory. Geological Survey of Canada, Paper 92-1E, p. 53-59.

Cordey, F., Gordey, S.P. and Orchard, M.J., 1991. New biostratigraphic data for the northern Cache Creek terrane, Teslin map area, southern Yukon. *In:* Current Research, Part E. Geological Survey of Canada, Paper 91-1E, p. 67-76.

Costa, J.E., 1983. Paleohydraulic reconstruction of flash-flood peaks from boulder deposits in the Colorado Front Range. Geological Society of America, Bulletin, vol. 94, p. 986-1004.

Dean, W.E. and Arthur, M.A., 1999. Sensitivity of the North Atlantic basin to cyclic climatic forcing during the Early Cretaceous. Journal of Foraminiferal Research, vol. 29, p. 465-486.

Delaney, G.D., 1981. The Mid-Proterozoic Wernecke Supergroup, Wernecke Mountains, Yukon Territory. Geological Survey of Canada, Paper 81-10, p. 1-23.

Dickie, J.R., 1989. Sedimentary response to arc-continent transpressional tectonics: Laberge conglomerates (Jurassic), Whitehorse trough, Yukon Territory. MSc thesis, Dalhousie University, Halifax, NS, 361 p.

Dickie, J.R. and Hein, F.J., 1995. Conglomerate fan deltas and submarine fans of the Jurassic Laberge Group, Whitehorse trough, Yukon Territory, Canada: fore-arc sedimentation and unroofing of a volcanic island arc complex. Sedimentary Geology, vol. 98, p. 263-292.

Dickinson, W.R., 1970. Interpreting detrital modes of greywacke and arkose. Journal of Sedimentary Petrology, vol. 40, p. 695-707.

Dixon, J., 1992. Stratigraphy of Mesozoic strata, Eagle Plain area, northern Yukon. Geological Survey of Canada, Bulletin, vol. 408, 58 p.

Donahue, R.L., Miller, R.W. and Shikluna, J.C., 1958. Soils, an introduction to soils and plant growth. Prentice-Hall, Inc., New Jersey, USA.

Engels, S. and Roberts, M.C., 2005. The architecture of prograding sandy-gravel beach ridges formed during the last Holocene highstand: southwestern British Columbia, Canada. Journal of Sedimentary Research, vol. 75, p. 1052-1064.

English, J.M. and Johnston, S.T., 2005. Collisional orogenesis in the northern Canadian Cordillera: implications for Cordilleran crustal structure, ophiolite emplacement, continental growth, and the terrane hypothesis. Earth and Planetary Science Letters, vol. 232, p. 333-344.

English, J.M., Johannson, G.G., Johnston, S.T., Mihalynuk, M.G., Fowler, M. and Wight, K.L., 2005. Structure, stratigraphy and petroleum resource potential of the central Whitehorse Trough, northern Canadian Cordillera. Bulletin of Canadian Petroleum Geology, vol. 53, issue 2, p. 130-153.

Evenchick, C.A., McMechan, M.E., McNicoll, V.J. and Carr, S.D., 2007. A synthesis of the Jurassic-Cretaceous tectonic evolution of the central and southeastern Canadian Cordillera: exploring links across the orogeny. *In:* Whence the Mountains? Inquiries into the evolution of orogenic systems: a volume in honor of Raymond A Price, J.W. Sears, T.A. Harms, and C.A. Evenchick (eds.). Geological Society of America, Special Paper, no. 433, p. 117-145.

Evenchick, C.A., Poulton, T.P. and McNicoll, V.J., 2010. Nature and significance of the diachronous contact between the Hazelton and Bowser Lake Groups (Jurassic), north-central British Columbia. Bulletin of Canadian Petroleum Geology, vol. 58, p. 235-267.

Evenchick, C.A. and Thorkelson, D.J., 2005. Geology of the Spatsizi River map area, north-central British Columbia. Geological Survey of Canada, Bulletin, vol. 577, 276 p.

Fielding, C.R. and Crane, R.C., 1987. An application of statistical modeling to the prediction of hydrocarbon recovery factors in fluvial reservoir sequences. *In:* Recent Developments in Fluvial Sedimentology, F.G. Ethridge, R.M. Flores, and M.D. Harvey, M.D., (eds.). SEPM, Special Publication, no. 39, p. 321–327.

Fillmore, J.A., 2006. Character and origin of the Lower Jurassic (Pliensbachian) Nordenskiöld dacite, Whitehorse trough, Yukon Territory, Canada. Unpublished Honours BSc thesis, Laurentian University, Sudbury, Ontario, 28 p.

Folk, R.L., 1974. Petrology of sedimentary rocks. Hemphill Publishing Co., Austin, Texas, USA.

Fitzpatrick, E.A., 1980. Soils, their formation, classification and distribution. Longman Inc., New York, USA. 353 p.

Fraser, C., Hill, P.R. and Allard, M., 2005. Morphology and facies architecture of a falling sea level strandplain, Umiujaq, Hudson Bay, Canada. Sedimentology, vol. 52, p. 141-160.

Frostick, L.E. and Jones, S.J., 2002. Impact of periodicy on sediment flux in alluvial systems: grain to basin scale. *In:* Sedimentary flux to basins: causes, controls and consequences, S.J. Jones and L.E. Frostick (eds.). Geological Society, London, Special Publication no. 191, p. 81-95.

Fyles, J.G., 1950. Geology of the northwest quarter of Whitehorse Map-Area, Yukon and studies of weathered granitic rocks near Whitehorse. MSc thesis, University of British Columbia, Vancouver, B.C.

Gabrielse, H., Murphy, D.C. and Mortensen, J.K., 2006. Cretaceous and Cenozoic dextral orogen-parallel displacements, magmatism and paleogeography, north-central Canadian Cordillera. *In:* Paleogeography of the North American Cordillera: Evidence For and Against Large-Scale Displacements, J.W. Haggart, J.W.H. Monger and R.J. Enkin (eds.). Geological Association of Canada, Special Paper, no. 46, p. 255–276.

Gagnon, J.-F., Evenchick, C.A., Waldron, J.F.W., Cordey, F. and Poulton, T.P., 2009. Jurassic subsidence history of the Hazelton trough – Bowser Basin in the area of Todagin Mountain, north-central British Columbia, Canada. Bulletin of Canadian Petroleum Geology, vol. 57, p. 430-448.

Galloway, J.M., Sweet, A.R., Swindles, G.T., Dewing, K., Hadlari, T., Embry, A.F. and Sanei, H., 2013. Middle Jurassic to Lower Cretaceous paleoclimate of Sverdrup Basin, Canadian Arctic Archipelago inferred from the palynostratigraphy. Marine and Petroleum Geology, vol. 44, p. 240-255.

Garrison, J.R., Jr., Williams, J., Miller, S.P., Weber, E.T., McMechan, G. and Zeng, X., 2010. Ground-penetrating radar study of North Padre Island: implications for barrier island internal architecture, model for growth of progradational microtidal barrier islands, and Gulf of Mexico sea-level cyclicity. Journal of Sedimentary Research, vol. 80, p. 303-319.

Gehrels, G.E. and Kapp, P.A., 1997. Detrital zircon geochronology and regional correlation of metasedimentary rocks in the Coast Mountains, southeastern Alaska. Canadian Journal of Earth Sciences, vol. 35, p. 269-279.

Ghosh, P., Sarkar, S. and Maulik, P., 2006. Sedimentology of a muddy alluvial deposit: Triassic Denwa Formation, India. Sedimentary Geology, vol. 191, p. 3-36.

Gilbert, G.K., 1885. The topographic features of lake shores. United States Geological Survey, Annual Report, vol. 5, p. 69-123.

Gilbert, G.K., 1890. Lake Bonneville. United States Geological Survey, Monograph, vol. 1, 438 p.

Gomez, B., Coleman, S.E., Sy, W.V.K., Peacock, D.H. and Kent, M., 2007. Channel change, bankfull and effective discharges on a vertically accreting, meandering, gravel-bed river. Earth Surface Processes and Landforms, vol. 32, p. 770-785.

Goodarzi, F. and Jerzykiewicz, T., 1989. The nature of thermally altered coal from Mount Granger, Whitehorse area, Yukon Territory. *In:* Contributions to Canadian Coal Geoscience, Geological Survey of Canada, Paper 89-8, p. 104-107.

Gordey, S.P., 2008. Bedrock geology, Whitehorse (105D). Yukon. Geological Survey of Canada, Open File 5640, scale 1: 250000.

Gordey, S.P., 2013. Evolution of the Selwyn Basin region, Sheldon Lake and Tay River map areas, central Yukon. Geological Survey of Canada, Bulletin, vol. 599, 176 p.

Gordey, S.P. and Irwin, S.E.B., 1987. Geology, Sheldon Lake and Tay River map areas, Yukon Territory. Geological Survey of Canada, Map 19-1987 (3 sheets), scale 1: 250000.

Gordey, S.P. and Makepeace, A.J., 2001. Bedrock Geology, Yukon Territory. Geological Survey of Canada, Open File 3754.

Gordey, S.P. and Stevens, R.A., 1994a. Preliminary interpretation of the bedrock geology of the Teslin area (105 C), southern Yukon. Geological Survey of Canada, Open File 2886, scale 1: 250000.

Gordey, S.P. and Stevens, R.A., 1994b. Tectonic framework of the Teslin region, southern Yukon Territory. Geological Survey of Canada, Current Research 1994-A, 11-18.

Gröcke, D.R., Price, G.D., Robinson, S.A., Baraboshkin, E.Y., Mutterlose, J. and Ruffell, A.H., 2005. The Upper Valanginian (Early Cretaceous) positive carbon–isotope event recorded in terrestrial plants. Earth and Planetary Science Letters, vol. 240, p. 495-509.

Gunning, M.H., Bamber, E.W., Brown, D.A., Rui, L., Mamet, B.L. and Orchard, M.J., 1994. The Permian Ambition Formation of northwestern Stikinia, British Columbia. *In:* Pangea: global environments and resources, A.F. Embry, B. Beauchamp and D.J. Glass (eds.). Canadian Society of Petroleum Resources, Memoir 17, p. 589-619.

Gustavson, T.C., 1978. Bed forms and stratification types of modern gravel meander lobes, Nueces River, Texas. Sedimentology, vol. 25, p. 401-426.

Haggart, J.W., Matsukawa, M. and Ito, M., 2006. Paleogeographic and paleoclimatic setting of Lower Cretaceous basins of East Asia and Western North America, with reference to the nonmarine strata. Cretaceous Research, vol. 27, p. 149-167.

Hallam, A., 1993. Palaeoclimates and their modelling with special reference to the Mesozoic Era. Philosophical Transactions, Royal Society of London, Biological Sciences, vol. 341, no. 1297, p. 287-296.

Hannigan, P., Lee, P.J. and Osadetz, K.G., 1995. Oil and gas resource potential of the Bowser – Whitehorse area of British Columbia. British Columbia, Ministry of Energy and Mines, GeoFile 2001-5, 190 p. <http://www.empr.gov.bc.ca/Mining/Geoscience/PublicationsCatalogue/GeoFiles/Pages/2001-5.aspx> [accessed on 26th March 2014].

Hart, C.J.R., 1997. A transect across northern Stikinia: geology of the northern Whitehorse map area, southern Yukon Territory (105D/13-16). Exploration and Geological Services Division, Yukon Region, Indian and Northern Affairs Canada, Bulletin 8, 112 p.

Hart, C.J.R. and Orchard, M.J., 1996. Middle Triassic (Ladinian) volcanic strata in southern Yukon Territory, and their Cordilleran correlatives. Geological Survey of Canada, Current Research 1996-A, p. 11-18.

Hart, C.J.R. and Pelletier, K.S., 1989. Geology of the Whitehorse (105D/11) map area. Indian and Northern Affairs Canada, Yukon Region, Open File 1989-2.

Hart, C.J.R. and Radloff, J.K., 1990. Geology of Whitehorse, Alligator Lake, Fenwick Creek, Carcross and part of Robinson map areas (105D/11, 6, 3, 2, and 7). Indian and Northern Affairs Canada, Yukon Region, Open File 1990-4, 113 p.

Hayes, B.J.R., 2012. Petroleum resource assessment of Whitehorse Trough, Yukon, Canada. Yukon Geological Survey, Miscellaneous Report 6, 52 p.

Hayes, B.J.R. and Archibald, H.B., 2012. Scoping study of unconventional oil and gas potential, Yukon. Yukon Geological Survey, Miscellaneous Report 7, 100 p.

Haywood, A.M., Valdes, P.J. and Marwick, P.J., 2004. Cretaceous (Wealden) climates: a modelling perspective. Cretaceous Research, vol. 25, p. 303-311.

Hinderer, M., 2012. From gullies to mountain belts: a review of sediment budgets at various scales. Sedimentary Geology, vol. 280, p. 21-59.

Hunt, J.A. and Hart, C.J.R., 1994. Thermal maturation and hydrocarbon source rock potential of Tantalus Formation coals in the Whitehorse area, Yukon Territory. *In:* Yukon Exploration and Geology, 1993. Exploration and Geological Services Division, Yukon, Indian and Northern Affairs, Canada, p. 67-77.

Ingersol, R.V., 2012. Tectonics of sedimentary basins, with revised nomenclature. *In:* Tectonics of sedimentary basins: recent advances, C. Busby and A. Azor (eds.). Wiley-Blackwell Publishing Ltd, Chichester, U.K., p. 3-43.

Israel, S., 2004. Geology of Southwestern Yukon (1:250 000 scale). Yukon Geological Survey, Open File 2004-16.

Israel, S., Beranek, L., Friedman, R.M. and Crowley, J.L., 2014. New ties between the Alexander terrane and Wrangellia and implications for North American Cordilleran evolution. Lithosphere, vol. 6, p. 270-276

Ito, M., Matsukawa, M, Takahiro Saito, T. and Nichols, D.J., 2006. Facies architecture and paleohydrology of a synrift succession in the Early Cretaceous Choyr Basin, southeastern Mongolia. Cretaceous Research, vol. 27, p. 226-240.

Jackson, J.L., 1992. Tectonic analysis of the Nisling, northern Stikine and northern Cache Creek terranes, Yukon and British Columbia. PhD thesis, University of Arizona, 200 p.

Johannson, G.G., Smith, P.L. and Gordey, S.P., 1997. Early Jurassic evolution of the northern Stikinian arc: Evidence from the Laberge Group, northwestern British Columbia. Canadian Journal of Earth Sciences, vol. 34, p. 1030-1057.

Johnston, S.T., 2001. The great Alaskan terrane wreck: reconciliation of paleomagnetic and geological data in the northern Cordillera. Earth and Planetary Science Letters, vol. 193, p. 259–72.

Johnston, S.T., 2008. The Cordilleran ribbon continent of North America. Annual Review of Earth and Planetary Sciences, vol. 36, p. 495–530.

Johnston, S.T., Mortensen, J.K. and Erdmer, P., 1996. Igneous and metaigneous age constraints for the Aishihik metamorphic suite, southwest Yukon. Canadian Journal of Earth Sciences, vol. 33, p. 1543-1555.

Johnston, S.T. and Timmerman, J., 1994. Geological map of the Hopkins Lake map area, southwest Yukon (115 H/7). Exploration and Geological Services Division, Yukon. Indian and Northern Affairs Canada, Open File 1994-2(g).

Kent D.V. and Irving, E., 2010. Influence of inclination error is sedimentary rocks on the Triassic and Jurassic apparent polar wander paths for North America and implications for Cordilleran tectonics. Journal of Geophysical Research, vol. 115, B10103, doi:10.1029/2009JB007205,

Koster, E.H., 1978. Transverse ribs: their characteristics, origin, and paleohydraulic significance. *In:* Fluvial Sedimentology, A.D. Miall (ed.). Canadian Association of Petroleum Geologists, Memoir 5, p. 161-186.

Kostic, B. and Aigner, T., 2007. Sedimentary architecture and 3D ground-penetrating radar analysis of gravely meandering river deposits (Neckar Valley, S.W. Germany). Sedimentology, vol. 54, p. 789-808.

Kujau, A., Heimhofer, U., Hochuli, P.A., Pauly, S., Morales, C., Adatte, T., Föllmi, K., Ploch, I. and Mutterlose, J., 2013. Reconstructing Valanginian (Early Cretaceous) mid-latitude vegetation and climate dynamics based on spore-pollen assemblages. Review of Paleobotany and Palynology, vol. 197, p. 50-69.

Kumar, R., Suresh, N., Sangode, S.J. and Kumaravel, V., 2007. Evolution of the Quaternary alluvial fan system in the Himalayan foreland basin: implications for climatic and tectonic decoupling. Quaternary International, vol. 159, p. 6-20.

Lapasha, C.A. and Miller, C.N., Jr., 1985. Flora of the Early Cretaceous Kootenai Formation in Montana, bryophytes and tracheophytes excluding conifers. Palaeontographica. Abteilung B: Palaeophytologie, vol. 196, p. 111-145, plus 15 plates.

Latour, B.A., 1968. Coalfields and potential coal areas of Yukon Territory. Yukon Mining Assessment Report 019838, <http://yma.gov.yk.ca/019838.pdf> [accessed on 25th March 2014].

Leclair, S.F. and Bridge, J.S., 2001. Quantitative interpretation of sedimentary structures formed by river dunes. Journal of Sedimentary Research, vol. 71, p. 713-716.

Leeder, M.R., 1973. Fluviatile fining-upward cycles and the magnitude of paleochannels. Geological Magazine, vol. 3, p. 265–276.

Leeder, M.R., 1997, Sedimentary basins: tectonic recorders of sediment discharge from drainage catchments. Earth Surface Processes and Landforms, vol. 22, p. 229-237.

Lees, E.J., 1934. Geology of the Laberge area, Yukon. Transactions of the Royal Canadian Institute, vol. 20, issue 1, p. 1-48, 6 plates.

Li, Z., Wang, Z., Pan, H. and Li, W., 2014. The development mechanism of gravel bars in rivers. Quaternary International, vol. 336, p. 73-79.

Long, D.G.F., 1980. Coals of the Yukon, their depositional environment, tectonic setting and resource potential. Seventh Geoscience Forum, Whitehorse, Yukon, December 2-4, 1979, p.16.

Long, D.G.F., 1982a. Depositional framework of coal deposits in forearc basin and molasse sequences of the Whitehorse Trough, Yukon Territory, Canada. *In:* 11th International Congress on Sedimentology: Abstracts of Papers, J.O. Nriagu and R. Troost (eds.). International Congress on Sedimentology, Hamilton, Ontario, Canada, August 22-27, 1982, p. 55.

Long, D.G.F., 1982b. Depositional style in a Late Jurassic-Early Cretaceous molasse sequence; the Tantalus Formation, Yukon Territory, Canada. Geological Society of America, Abstracts with Programs, vol. 14, issue 4, p. 181.

Long, D.G.F., 1983a. Depositional setting of coal deposits in the Whitehorse Trough, Yukon Territory, Canada. *In:* The Mesozoic of Middle North America, Canadian Society of Petroleum Geologists, Program and Abstracts, p. 57.

Long, D.G.F., 1983b. Coal in the Yukon. *In:* Mineral Deposits of northern Cordillera, abstracts. Canadian Institute of Mining and Metallurgy, December 5-7, Whitehorse, Yukon, p. 22-23.

Long, D.G.F., 1984. Depositional setting of coal deposits in the Whitehorse Trough, Yukon Territory, Canada (abstract). *In:* The Mesozoic of middle North America, D.F. Stott, and D.J. Glass (eds.). Canadian Society of Petroleum Geologists, Memoir, vol. 9, p. 558.

Long, D.G.F., 1986. Coal in Yukon. *In:* Mineral deposits of the northern Cordillera, J.D. Morin (ed.). Canadian Institute of Mining and Metallurgy, Special Paper, no. 37, p. 311-318.

Long, D.G.F., 2000. Cretaceous fluvial strata in the Moose River basin of Ontario, Canada, as a source of kaolin for paper and ceramic industries. Applied Clay Science, vol. 16, p. 97-115.

Long, D.G.F., 2005. Sedimentology and hydrocarbon potential of fluvial strata in the Tantalus and Aksala formations, northern Whitehorse Trough, Yukon. *In:* Yukon Exploration and Geology 2004, D.S. Emond, L.L. Lewis and G.D. Bradshaw (eds.). Yukon Geological Survey, p. 165-174.

Long, D.G.F., 2006. Architecture of pre-vegetation sandy-braided perennial and ephemeral river deposits in the Paleoproterozoic Athabasca Group, northern Saskatchewan, Canada as indicators of Precambrian fluvial style. Sedimentary Geology, vol. 190, p. 71-95.

Long, D.G.F., 2011. Architecture and depositional style of fluvial systems before land plants: a comparison of Precambrian, Early Paleozoic, and Modern river systems. *In:* From river to rock record: the preservation of fluvial sediments and their subsequent interpretation, S.K. Davidson, S. Leleu and C.P. North (eds.). SEPM Special Publication, no. 97, p. 37-61 plus appendix.

Long, D.G.F. and Graham, P.S.W., 1993. Sedimentology and coal resources of the Early Oligocene Australian Creek Formation, near Quesnel, British Columbia. Geological Survey of Canada, Paper 93-11, 73 p.

Long, D.G.F. and Lowey, G.M., 2006. Anatomy of a Late Jurassic Gilbert-type delta in basal strata of the Tantalus Formation, Whitehorse Trough, Yukon, Canada. *In:* Yukon Exploration and Geology 2005, D.S. Emond, G.D. Bradshaw, L.L. Lewis and L.H. Weston (eds.). Yukon Geological Survey, p. 195-205.

Long, D.G.F. and Lowey, G.M., 2011. Wandering gravel-bed rivers and high-constructive stable channel fluvial systems in the Ross River area, Yukon Territory, Canada. Geoscience Frontiers, vol. 2, issue 3, p. 277-288.

Long, D.G.F., Lowey, G.M. and Sweet, A.R., 2001. Age and setting of dinosaur trackways, Ross River area, Yukon Territory (105F/15). *In:* Yukon Exploration and Geology 2000, D.S. Emond and L.H. Weston (eds.). Exploration and Geological Services Division, Yukon, Indian and Northern Affairs Canada, p. 181-198.

Lowey, G.W., 1984. The stratigraphy and sedimentology of siliciclastic rocks, west central Yukon, and their tectonic implications. PhD thesis, Department of Geology and Geophysics, University of Calgary, AB, 329 p.

Lowey, G.W., 2004a. Exploration of the Whitehorse Trough (Yukon, Canada); petroleum potential of a frontier basin. American Association of Petroleum Geologists, Annual Meeting Expanded Abstracts, vol. 13, p. 87.

Lowey, G.W., 2004b. Mopping up the stratigraphic mess; reinvestigation of the stratigraphy of the Laberge Group (Jurassic), south-central Yukon, provides new insights in the exploration for gas and oil in the Whitehorse Trough. CSPG Annual Convention 2004. I.C.E. 2004 CSPG/CHOA/CWLS joint conference; abstract archive, <http://www.cspg.org/conventions/abstracts/2004abstracts/019S0123.pdf> [accessed September 6, 2005].

Lowey, G.W., 2005. Sedimentology, stratigraphy and source rock potential of the Richthofen Formation (Jurassic), Laberge Group, northern Whitehorse Trough, Yukon, Canada. Annual Meeting - American Association of Petroleum Geologists, Abstracts, vol. 14, p. A82.

Lowey, G.W., 2007a. Hydrocarbon source rock potential of the Whitehorse Trough, a frontier basin in southern Yukon, Canada. Annual Meeting - American Association of Petroleum Geologists Abstracts, 2007, p. 84-85.

Lowey, G.W., 2007b. Summary of the stratigraphy, sedimentology and hydrocarbon potential of the Laberge Group (Lower-Middle Jurassic), Whitehorse trough, Yukon. *In:* Yukon Exploration and Geology 2007, D.S. Emond, L.R. Blackburn, R.P. Hill and L.H. Weston (eds.). Yukon Geological Survey, p. 179-197.

Lowey, G.W., 2008. A petroleum events chart for the Whitehorse Trough, Yukon. Reservoir, vol. 35, issue 1, p. 32-35.

Lowey, G.W., 2011. The Lewes River Group (Triassic) arc-fringing carbonate platform; sedimentological evidence Whitehorse Trough was an east-facing forearc basin. Abstracts with Programs - Geological Society of America, vol. 43, issue 5, p. 440.

Lowey, G.W. and Hills, L.V., 1988. Lithofacies, petrography and environments of deposition, Tantalus Formation (Lower Cretaceous) Indian River area, west-central Yukon. Bulletin of Canadian Petroleum Geology, vol. 36, p. 296–310.

Lowey, G.M. and Long, D.G.F., 2006. Summary of Roc-Eval data for the Whitehorse Trough, Yukon: implications concerning the hydrocarbon potential of a frontier basin. *In:* Yukon Exploration and Geology 2005, D.S. Emond, G.D. Bradshaw, L.L. Lewis and L.H. Weston (eds.). Yukon Geological Survey, p. 207-230.

Lowey, G.W., Long, D.G.F., Fowler, M.G., Sweet, A.R. and Orchard, M.J., 2009. Petroleum source rock potential of Whitehorse Trough; a frontier basin in south-central Yukon. Bulletin of Canadian Petroleum Geology, vol. 57, issue 3, p. 350-386.

Ludwig, K.R., 2001. Isoplot/Ex, rev.2.49. Berkeley Geochronology Center, Special Publication, no. 1a, 56 p.

Lunt, I.A. and Bridge, J.S., 2004. Evolution and deposits of a gravelly braid bar, Sagavanirtok River, Alaska. Sedimentology, vol. 51, p. 415-432.

Mackenzie, W.S., 1974. Radiolaria from the Canol Formation, Northwest Territories. Geological Survey of Canada, Paper 74-1, p. 319.

MacLeod, S.E. and Hills, L.V., 1991. Worldwide stratigraphic and geographic distribution of selected Jurassic—Cretaceous plant macrofossils and their significance to the northern Bowser Basin, British Columbia, Canada. Review of Paleobotany and Palynology, vol. 70, p. 47-65.

MacNaughton, R.B., 2002. Sedimentology of Triassic siliciclastic strata in the Mount Martin and Mount Merrill map areas, Yukon Territory. *In:* Geological Survey of Canada, Current Research 2002-A4, 10 p.

Martel, E., Turner, E.C. and Fischer, B.J., 2011. Geology of the central Mackenzie Mountains of the northern Canadian Cordillera, Sekwi Mountain (106P), Mount Eduni (106A), and northern Wigley Lake (95M) map-areas, Northwest Territories. Northwest Territories Geoscience Office, NWT Special Volume, no. 1, 423 p.

Massari, F., 1983. Tabular cross-bedding in Messinian fluvial channel conglomerates, southern Alps, Italy. *In:* Modern and Ancient Fluvial Systems, J.D. Collinson, and J. Lewin (eds.). International Association of Sedimentologists, Special Publication 6, p. 287-300.

McConnell, R.G., 1909. The Whitehorse Copper Belt. Geological Survey of Canada, Separate Report no. 1050, 63 p.

McKee, E.D. and Weir, G.W., 1953. Terminology for stratification and cross-stratification in sedimentary rocks. Geological Society of America Bulletin, vol. 64, p. 381-390.

McNicoll, V.J., Evenchick, C.A. and Mustard, P.S., 2005. Provenance studies on the depositional histories of the Bowser and Sustut basins and their implications for tectonic evolution of the northern Canadian Cordillera. Geological Association of Canada, Annual Meeting Abstracts, vol. 30, p. 133.

Miall, A.D., 1976. Palaeocurrent and palaeohydrologic analysis of some vertical profiles through a Cretaceous braided stream deposits, Banks Island, Arctic Canada. Sedimentology, vol. 23, p. 459-483.

Miall, A.D., 1996. The Geology of fluvial deposits. Springer-Verlag, Berlin, 582 p.

Mihalynuk, M.G., 1999. Geology and mineral resources of the Tagish Lake area (NTS 104M/8, 9, 10E, 15 and 104N/12W) Northwestern British Columbia. BC Ministry of Energy and Mines, Energy and Minerals Division, Geological Survey Branch, Bulletin, no. 105.

Mihalynuk, M.G., Erdmer, P., Ghent, E.D., Cordey, F., Archibald, D.A., Friedman, R.M. and Johannson, G.G., 2004. Coherent French Range blueschist: subduction to exhumation in <2.5 m.y.? Geological Society of America Bulletin, vol. 116, p. 910-922.

Mihalynuk, M.G., Nelson, J. and Diakow, L.J., 1994. Cache Creek terrane entrapment: oroclinal paradox within the Canadian Cordillera. Tectonics, vol. 13, no. 2, p. 575-595.

Mihalynuk, M.G. and Peter, J.M., 2001. A hydrothermal origin for "crinkle chert" of the Big Salmon Complex. *In:* Geological Fieldwork 2000, British Columbia Geological Survey, Paper 2001-1, p. 83-84.

Monger, J.W.H., 1975. Upper Paleozoic rocks of the Atlin terrane, northwestern British Columbia and south-central Yukon. Geological Survey of Canada, Paper 74-47, 63 p.

Monger, J.W.H. and Price, R.A., 1979. Geodynamic evolution of the Canadian Cordillera, progress and problems. Canadian Journal of Earth Sciences, vol. 16, p. 770-791.

Monger, J.W.H., Price, R.A. and Tempelman-Kluit, D.J., 1982. Tectonic accretion and the origin of the two major metamorphic and plutonic welts in the Canadian Cordillera. Geology, vol. 10, p. 70-75.

Morozova, G.S. and Smith, N.D., 2003. Organic matter deposition in the Saskatchewan River floodplain (Cumberland Marshes, Canada): effects of progradational avulsions. Sedimentary Geology, vol. 157, p. 15-29.

Morrow, D.W., 1999. Lower Paleozoic stratigraphy of Northern Yukon Territory and northwestern District of Mackenzie. Geological Survey of Canada, Bulletin 538, 202 p.

Mortensen, J.K., 1990. Geology and U-Pb geochronology of the Klondike district, west-central Yukon Territory. Canadian Journal of Earth Sciences, vol. 27, p. 903-914.

Mumpy, A.J., Jol, H.M., Kean, W.F. and Isabell, J.L., 2007. Architecture and sedimentology of an active braid-bar in the Wisconsin River based on 3-D ground penetrating radar. *In:* Stratigraphic analysis using GPR, G.S. Baker and H.M. Jol (eds.). Geological Society of America, Special Paper, no. 432, p. 111-131.

Murphy, D.C., Mortensen, J.K., Piercey, S.J., Orchard, M.J. and Gehrels, G.E., 2006. Mid-Paleozoic to early Mesozoic tectonostratigraphic evolution of Yukon-Tanana and Slide Mountain terranes and affiliated overlap assemblages, Finlayson Lake massive sulphide district, southeastern Yukon. *In:* Paleozoic Evolution and Metallogeny of Pericratonic Terranes at the Ancient Pacific Margin of North America, Canadian and Alaskan Cordillera, M. Colpron, and J.L. Nelson (eds.). Geological Association of Canada, Special Paper, vol. 45, p. 75-105.

Murphy, D.C., van der Heyden, P., Parrish, R.R., Klepacki, D.W., McMillan, W., Struik, L.C. and Gabites, J., 1995. New geochronological constraints on Jurassic deformation of the western edge of North America, southeastern Canadian Cordillera. *In:* Jurassic Magmatism and Tectonics of the North American Cordillera, D.M. Miller and C. Busby (eds.). Geological Society of America, Special Paper, no. 299, p. 159–171.

Murphy, D.C., van Stall, C. and Mortensen, J.K., 2008. Windy McKinley terrane, Stevenson Ridge area (115JK), western Yukon: composition and proposed correlations, with implications for mineral potential. *In:* Yukon Exploration and Geology 2007, D.S. Emond, L.R. Blackburn, R.P.Hill and L.W. Weston (eds.). Yukon Geological Survey, p. 225-235.

Mutterlose, J. and Ruffell, A., 1999. Milankovitch-scale palaeoclimate changes in pale-dark bedding rhythms from the Early Cretaceous (Hauterivian and Barremian) of eastern England and northern Germany. Palaeogeography, Palaeoclimatology, Palaeoecology, vol. 154, p. 133-160.

National Energy Board, 2001. Petroleum resource assessment of the Whitehorse Trough, Yukon Territory, Canada. Oil and Gas Resource Branch. Department of Economic Development, Government of the Yukon, 59 p.

Nelson, J. and Colpron, M., 2007. Tectonics and metallogeny of the British Columbia, Yukon and Alaskan Cordillera, 1.8 Ga to present. *In:* Mineral deposits of Canada: a synthesis of major deposit-types, district metallogeny, the evolution of geological provinces, and exploration methods, W.D. Goodfellow (ed.). Geological Association of Canada, Special Publication, no. 5, p. 755-791.

Nelson, J.L., Colpron, M. and Israel, S., 2013. The Cordillera of British Columbia, Yukon and Alaska: tectonics and metallogeny. *In:* Tectonics, metallogeny, and discovery: the North American Cordillera and similar accretionary settings, M. Colpron, T. Bissig, B.G. Rust and J.F.H. Thompson (eds.). Society of Economic Geologists, Special Publication 17, p. 53-109.

Nesbitt, H.W., Fedo, C.M. and Young, G.M., 1997. Quartz and feldspar stability, steady and non-steady state weathering and petrogenesis of siliciclastic sands and muds. Journal of Geology, vol. 105, p. 173-192.

Norris, A.W., 1968. Reconnaissance Devonian stratigraphy of northern Yukon Territory and northwestern District of MacKenzie. Geological Survey of Canada, Paper 67-53.

O'Connor, J.E., 1993. Hydrology, hydraulics and geomorphology of the Bonneville Flood. Geological Society of America, Special Paper 274.

Passega, R., 1964. Grain size representation by C M patterns as a geological tool. Journal of Sedimentary Petrology, vol. 34, p. 830-847.

Peel, M.C., Finlayson, B.L. and McMahon, T.A., 2007. Updated world map of the Köppen-Geiger climate classification. Hydrology and Earth System Sciences, vol. 11, p. 1633-1644.

Pepin, E., Guyot, L.J., Armijos, E., Fraizy, P., Moquet, J.S., Noriega, L., Lavado, W., Pombosa, R. and Vauchel, P., 2013. Climatic control on eastern Andean denudation rates (Central Cordillera from Ecuador to Bolivia). Journal of South American Earth Sciences, vol. 44, p. 85-93.

Pigage, L.C., 2004. Bedrock geology compilation of the Anvil District (parts of NTS 105K/2, 3, 5, 6, 7 and 11), central Yukon. Yukon Geological Survey, Bulletin, no. 15, 103 p.

Plint, H.E. and Gordon, T.M., 1997. The Slide Mountain terrane and structural evolution of the Finlayson Lake Fault Zone, southeastern Yukon. Canadian Journal of Earth Sciences, vol. 34, p. 105-126.

Postma, G., 1990. Depositional architecture and facies of river and fan deltas: a synthesis. *In:* Coarse-grained deltas, A. Colella and D.B. Prior (eds.). International Association of Sedimentologists, Special Publication 10, p. 13-27.

Postma, G., 2001. Physical climate signatures in shallow and deep-water deltas. Global and Planetary Change, vol. 28, p. 93-106.

Postma, G., Babic, L., Zupanic, J. and Roe, S.L., 1988. Delta-front failure and associated bottomset deformation in a marine, gravelly Gilbert-type fan delta. *In:* Fan deltas: sedimentology and tectonic settings, W. Nemec and R.J. Steel (eds.). Blackie, Glasgow and London, UK, p. 91-10.

Potter, P.E. and Pettijohn, F.J., 1977. Paleocurrents and basin analysis (2nd edition). Springer-Verlag, Berlin, Germany, 424 p.

Price, G.D., Sellwood, B.W. and Valdes, P.J., 1995. Sedimentological evaluation of general circulation model simulations for the "greenhouse" Earth: Cretaceous and Jurassic case studies. Sedimentary Geology, vol. 100, p. 159-180.

Pyle, L.J. and Jones, A.L., 2009. Regional geoscience studies and petroleum potential, Peel plateau and plain, Northwest Territories and Yukon: Project Volume. Northwest Territories Geoscience Office, and Yukon Geological Survey, NWT Open File 2009-02/YGS Open File 2009-25, 540 p.

Reid, R.P., 1981. Report of field work on the Upper Triassic reef complex of Lime Peak, Laberge map-area, Yukon. *In:* Yukon geology and exploration 1979-80, Exploration and Geological Sciences Division, Yukon Region, Indian and Northern Affairs Canada, p. 110-114.

Reid, R.P., 1988. Lime Peak reef complex, Norian age, Yukon. *In:* Reefs; Canada and adjacent areas, H.J. Helmut, N.J. Geldsetzer and G.E. Tebbutt (eds.). Canadian Society of Petroleum Geologists, Memoir 13, p. 758-765.

Reid, R.P. and Ginsburg, R.N., 1986. The role of framework in Upper Triassic patch reefs in the Yukon. Palaios, vol. 1, issue 6, p. 590-600.

Richards, B.C., Bamber, E.W. and Utting, J., 1997. The geology, mineral and hydrocarbon potential of northern Yukon Territory and northwestern District of Mackenzie. Geological Survey of Canada, Bulletin, no. 422, p. 201-251.

Ricketts, B.D., 1984. A coal index for Yukon and District of Mackenzie, Northwest Territories. Geological Survey of Canada, Open File 1115, 83 p.

Ricketts, B.D., Evenchick, C.A., Anderson, R.G. and Murphy, D.C., 1992. Bowser basin, northern British Columbia: constraints on the timing of initial subsidence and Stikinia-North America terrane interactions. Geology, vol. 20, p. 1119-1122.

Roots, C.F., Nelson, J.L., Simard, R.-L. and Harms, T.A., 2006. Continental fragments, mid-Paleozoic arcs and overlapping late Paleozoic arc and Triassic sedimentary strata in the Yukon-Tanana terrane of northern British Columbia and southern Yukon. *In:* Paleozoic evolution and metallogeny of pericratonic terranes at the ancient Pacific margin of North America, Canadian and Alaskan Cordillera, M. Colpron and J.L. Nelson (eds.). Geological Association of Canada, Special Paper, no. 45, p. 153-177.

Schiarizza, P., 2012. Geology of the Kutcho Assemblage between Kehlechoa and Tucho rivers, northern British Columbia. British Columbia Geological Survey, Geological Fieldwork 2011, Paper 2012-1, p. 75-98.

Schumm, S.A., 1968. Speculations concerning paleohydrologic controls of terrestrial sedimentation. Geological Society of America, Bulletin, vol. 79, p. 1573-1588.

Sambrook Smith, G.H., Ashworth, P.J., Best, J.L., Lunt, I.A., Orfeo, O. and Parsons, D.R., 2009. The sedimentology and alluvial architecture of a large braid bar, Río Paraná, Argentina. Journal of Sedimentary Research, vol. 79, p. 629-642.

Sellwood, B.W. and Price, G.D., 1993. Palaeoclimates and their modelling with special reference to the Mesozoic Era. Philosophical Transactions, Royal Society of London, Biological Sciences, vol. 341, no. 1297, p. 225-233.

Sellwood, B.W., Valdes, P.J. and Price, G.D., 2000. Geological evaluation of multiple general circulation model simulations of Late Jurassic palaeoclimate. Palaeogeography, Palaeoclimatology, Palaeoecology, vol. 156, p. 147-160.

Simard, R.-L. and Devine, F., 2003. Preliminary geology of the southern Semenof Hills, central Yukon (105E/1,7,8). *In:* Yukon Exploration and Geology 2002, D.S. Emond and L.L. Lewis (eds.). Exploration and Geological Services Division, Yukon Region, Indian and Northern Affairs Canada, p. 213-222.

Skelley, R.L., Bristow, C.S. and Etheridge, F.G., 2003. Architecture of channel-belt deposits in an aggrading shallow sandbed braided river: the lower Niobrara River, northeast Nebraska. Sedimentary Geology, vol. 158, p. 249-270.

Smith, D.G. and Smith, N.D. 1980. Sedimentation in anastomosed river systems: examples from alluvial valleys near Banff, Alberta. Journal of Sedimentary Petrology, vol. 50, p. 157-164.

Smith, S.A., 1986. Meandering gravel-bed rivers: the sedimentology of selected modern and ancient examples. PhD thesis, University of Reading, UK, 288 p.

Smith, S.A., 1989. Sedimentation in a meandering gravel-bed river: the River Tywi, South Wales. Geological Journal, vol. 24, issue 3, p. 193–204.

Smith, S.A., 1990. The sedimentology and accretionary styles of an ancient gravel-bed stream: the Budleigh Salterton Pebble Beds (Lower Triassic), southwest England. Sedimentary Geology, vol. 67, p. 199–219.

Sohn, Y.K., Kim, S.B., Hwang, I.G., Bahk, J.J., Choe, M.Y. and Chough, S.K., 1997. Characteristics and depositional processes of large-scale gravelly Gilbert-type foresets in the Miocene Doumsan fan delta, Pohang basin, SE Korea. Journal of Sedimentary Research, vol. 67, p. 130-141.

Speelman, E.L., 1971. Report on Bush Mountain graphitic anthracite prospect, 1971 field season. Yukon Geology Assessment File, no. 019865, 64 p. http://yma.gov.yk.ca/019865.pdf [accessed on 5th March 2014].

Stach, E., Mackowsky, M.-Th., Teichmüller, M., Taylor, G.D., Chandra, D. and Teichmüller, R., 1982. Stach's textbook of coal petrology, 2nd edition. Gebrüder Borntraeger, Berlin, Germany, 535 p.

Staples, R.D., Gibson, H.D., Berman, R.G., Ryan, J.J. and Colpron, M., 2013. A window into the Early to mid-Cretaceous infrastructure of the Yukon-Tanana terrane recorded in multi-stage garnet of west-central Yukon. Journal of Metamorphic Geology, vol. 31, p. 729-753.

Staples, R.D., Murphy, D.C., Gibson, H.D., Colpron, M., Berman, R.G. and Ryan, J.J., 2014. Middle Jurassic to earliest Cretaceous mid-crustal tectono-metamorphism in the northern Canadian Cordillera: recording foreland-directed migration of an orogenic front. Geological Society of America, Bulletin, vol. 126, p. 1511-1530.

Tempelman-Kluit, D.J., 1974. Reconnaissance geology of Aishihik Lake, Snag and part of Stewart River map-areas, west-central Yukon. Geological Survey of Canada, Paper 73-41.

Tempelman-Kluit, D.J., 1978. Laberge (106E) map area, Yukon. Geological Survey of Canada, Open File 578.

Tempelman-Kluit, D.J., 1979. Transported cataclasite, ophiolite and granodiorite in Yukon: evidence of arc-continent collision. Geological Survey of Canada, Paper 79-14, 27 p.

Tempelman-Kluit, D.J., 1984. Geology, Laberge (105E) and Carmacks (115I), Yukon Territory. Geological Survey of Canada, Open File 1101, 10 p.

Tempelman-Kluit, D.J., 2009. Geology of Carmacks and Laberge Map areas, central Yukon: incomplete draft manuscript on stratigraphy, structure and its early interpretation (*ca.* 1986). Geological Survey of Canada, Open File 5982, 399 p.

Thamó-Bozsó, Kercsmár, Z. and Nádor, A., 2002. Tectonic control on changes in sediment supply: Quaternary alluvial systems, Körös sub-basin, SE Hungary. *In:* Sedimentary flux to basins: causes, controls and consequences, S.J. Jones and L.E. Frostick (eds.). Geological Society, London, Special Publication no. 191, p. 37-53.

Tipper, H.W. and Woodsworth, G.J., 1981. Tectonic assemblage map of the Canadian Cordillera. Geological Survey of Canada, Map 1505A, scale 1:2 000 000.

Tozer, E.T., 1958. Stratigraphy of the Lewes River Group (Triassic), central Laberge area, Yukon Territory. Geological Survey of Canada, Bulletin, vol. 43, 28 p.

Van der Zwan, C.J., 2002. The impact of Milankovitch-scale climatic forcing on sediment supply. Sedimentary Geology, vol. 147, p. 271-294.

Wheeler, J.O., 1956. Evolution and history of the Whitehorse Trough as illustrated by the geology of Whitehorse map-area, Yukon. PhD thesis, Columbia University, New York, 194 p.

Wheeler, J.O., 1961. Whitehorse map-area, Yukon Territory, 105D. Geological Survey of Canada, Memoir 312, 156 p.

White, D., Colpron, M. and Buffett, G., 2012. Seismic and geological constraints on the structure and hydrocarbon potential of the northern Whitehorse trough, Yukon Canada. Bulletin of Canadian Petroleum Geology, vol. 60, issue 4, p. 239-255.

White, D., Colpron, M., Buffett, G. and Roberts, B., 2006. Structural constraints for oil and gas assessments in the Whitehorse Trough: new results from seismic profiling. *In:* Yukon Exploration and Geology 2007, D.S. Emond, G.D. Bradshaw, L.L. Lewis and L.H. Weston (eds.), Yukon Geological Survey, p. 139-151.

Wolf, D., Seim, A., Diaz de Olmo, F. and Faust, D., 2013. Late Quaternary fluvial dynamics of the Jarama River in central Spain. Quaternary International, vol. 302, p. 20-41.

Wooldridge, C.L. and Hickin, E.J., 2005. Architecture and evolution of channel bars in wandering gravel-bed rivers: Fraser and Squamish rivers, British Columbia, Canada. Journal of Sedimentary Research, vol. 75, p. 844-860.

Wu, H., Zhang, S., Jiang, G., Yang, T., Guo, J. and Li, H., 2013 Astrochronology for the Early Cretaceous Jehol biota in northeastern China. Palaeogeography, Palaeoclimatology, Palaeoecology, vol. 385, p. 221–228.

Xu, J., 2004. Comparison of hydraulic geometry between sand- and gravel-bed rivers in relation to channel pattern discrimination. Earth Surface Processes and Landforms, vol. 29, p. 645-657.

APPENDIX 1 - Stratigraphic sections

Note: many of these sections are over-sized.

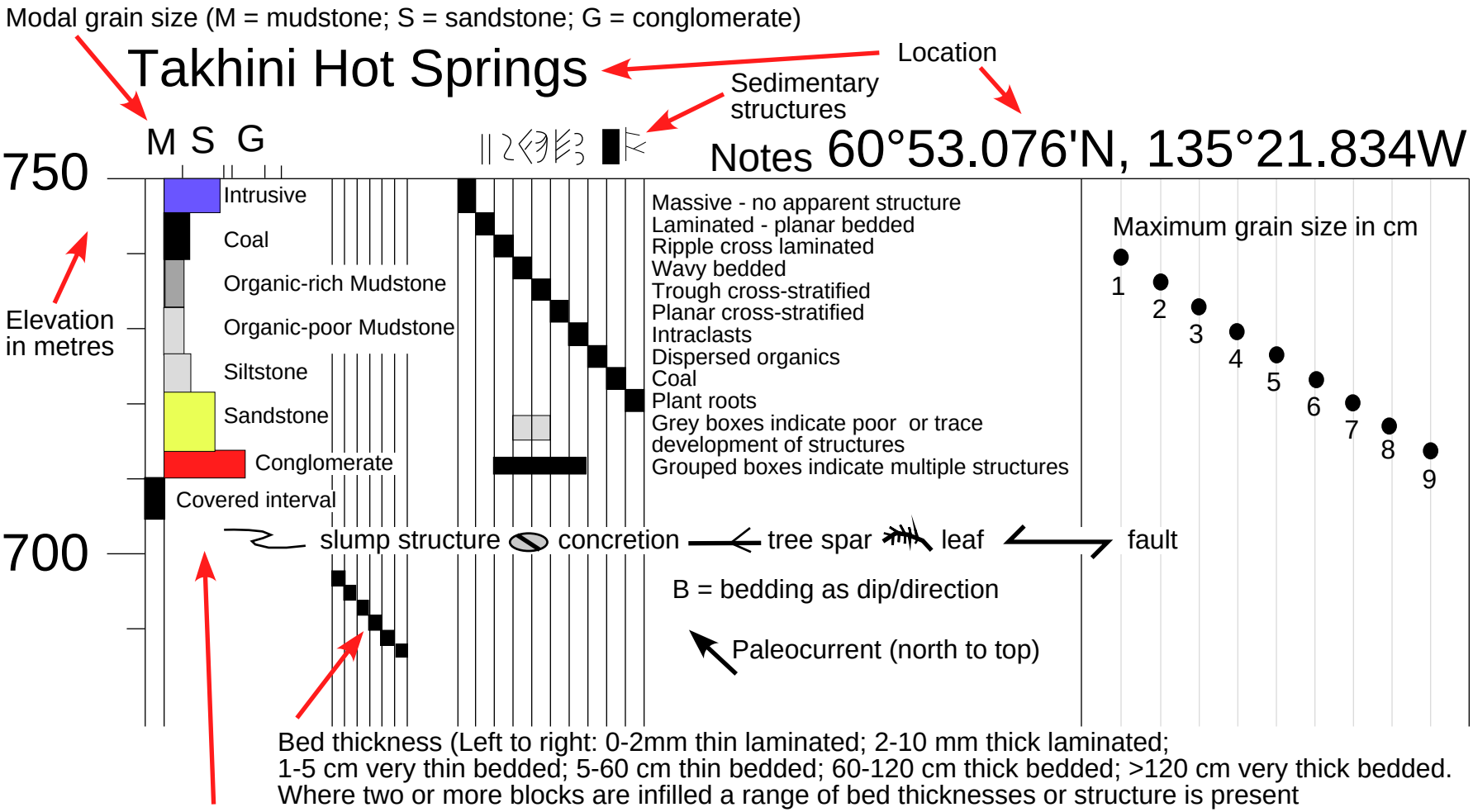
Modal grain size (M = mudstone; S = sandstone; G = conglomerate)
Takhini Hot Springs
Location
Sedimentary structures
M S G
Notes 60°53.076'N, 135°21.834W
750
700
Elevation in metres
Intrusive
Coal
Organic-rich Mudstone
Organic-poor Mudstone
Siltstone
Sandstone
Conglomerate
Covered interval
Massive - no apparent structure
Laminated - planar bedded
Ripple cross laminated
Wavy bedded
Trough cross-stratified
Planar cross-stratified
Intraclasts
Dispersed organics
Coal
Plant roots
Grey boxes indicate poor or trace development of structures
Grouped boxes indicate multiple structures
Maximum grain size in cm
1
2
3
4
5
6
7
8
9
slump structure
concretion
tree spar
leaf
fault
B = bedding as dip/direction
Paleocurrent (north to top)
Bed thickness (Left to right: 0-2mm thin laminated; 2-10 mm thick laminated;
1-5 cm very thin bedded; 5-60 cm thin bedded; 60-120 cm thick bedded; >120 cm very thick bedded.
Where two or more blocks are infilled a range of bed thicknesses or structure is present
Faint colours = lithology implied

T-1: Corduroy Mountain

Top = 61°19'45"N, 125°55'58"W
Base = 61°19’31"N, 125°55’42"W

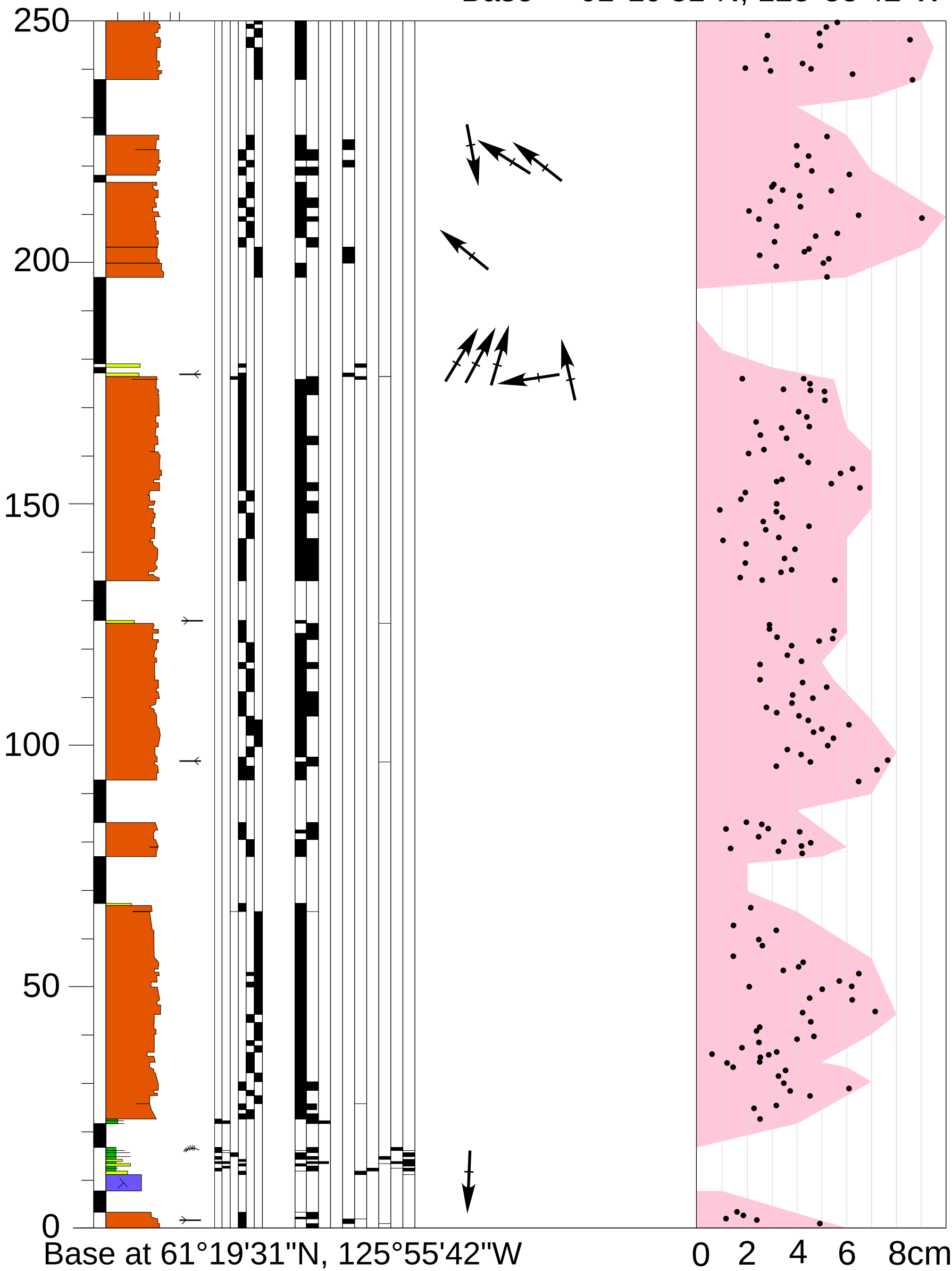

T-1: Corduroy Mountain

Top = 61°19'45"N, 125°55'58"W
Base = 61°19’31"N, 125°55’42"W

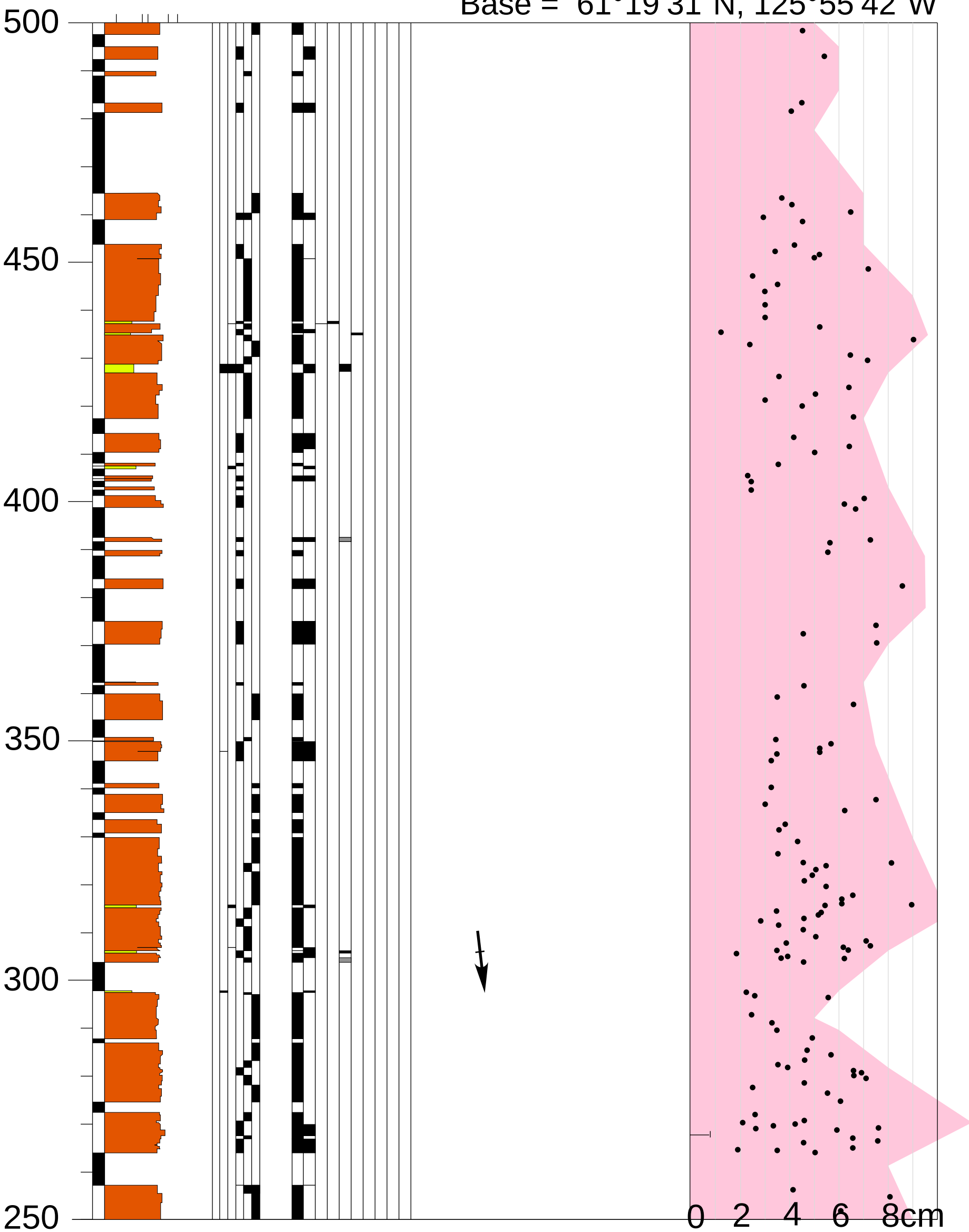

T-1: Corduroy Mountain

Top = 61°19'45"N, 125°55'58"W
Base = 61°19’31"N, 125°55’42"W

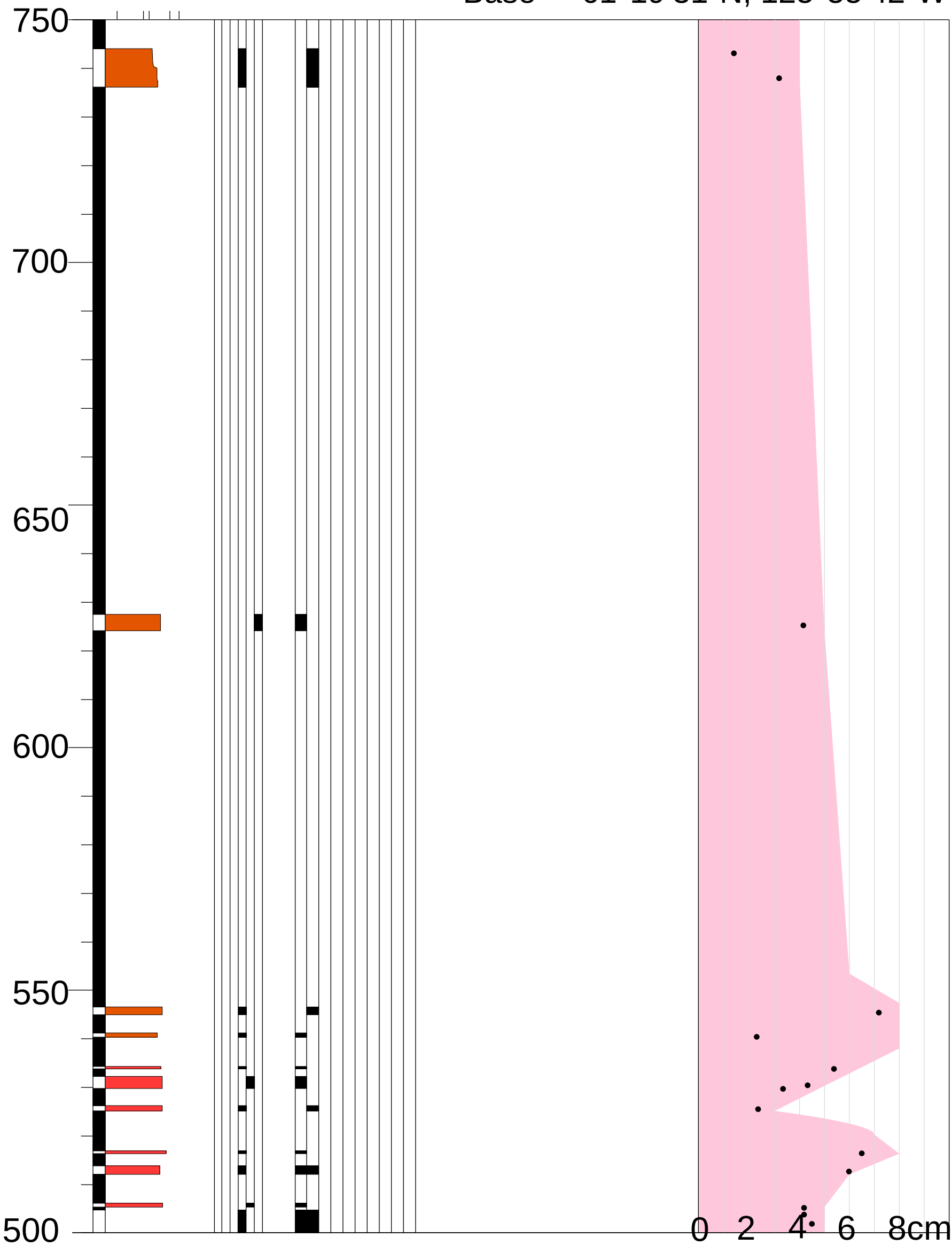

T-1: Corduroy Mountain

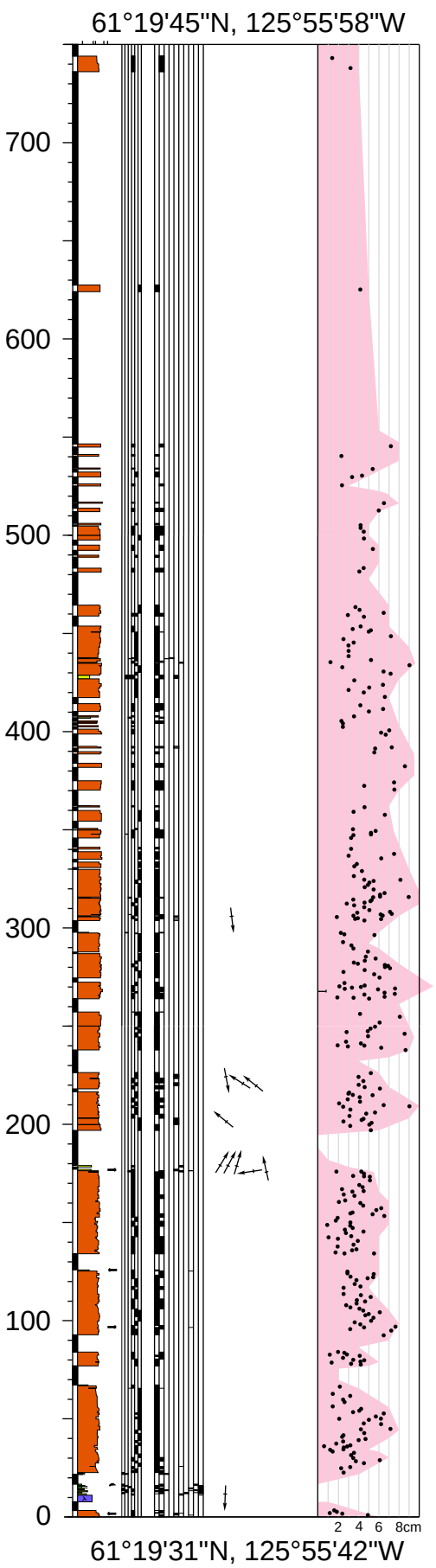

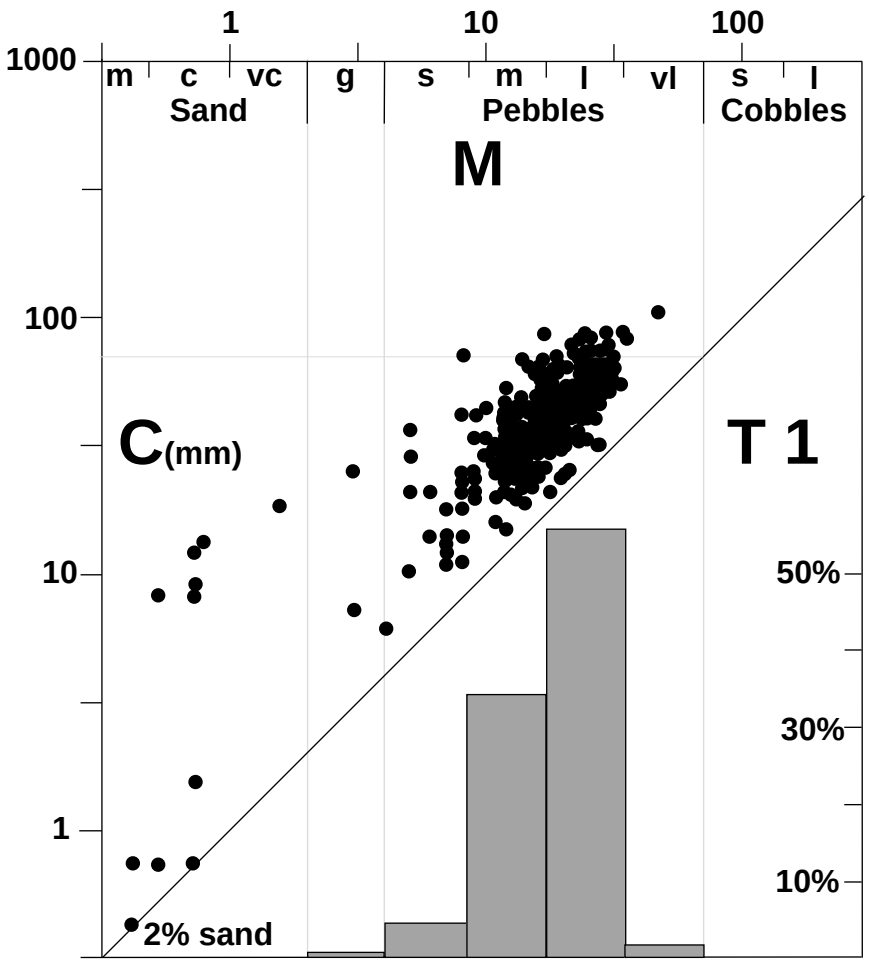

T4 South of Walsh Creek

61°55'29"N, 134°40'57"W

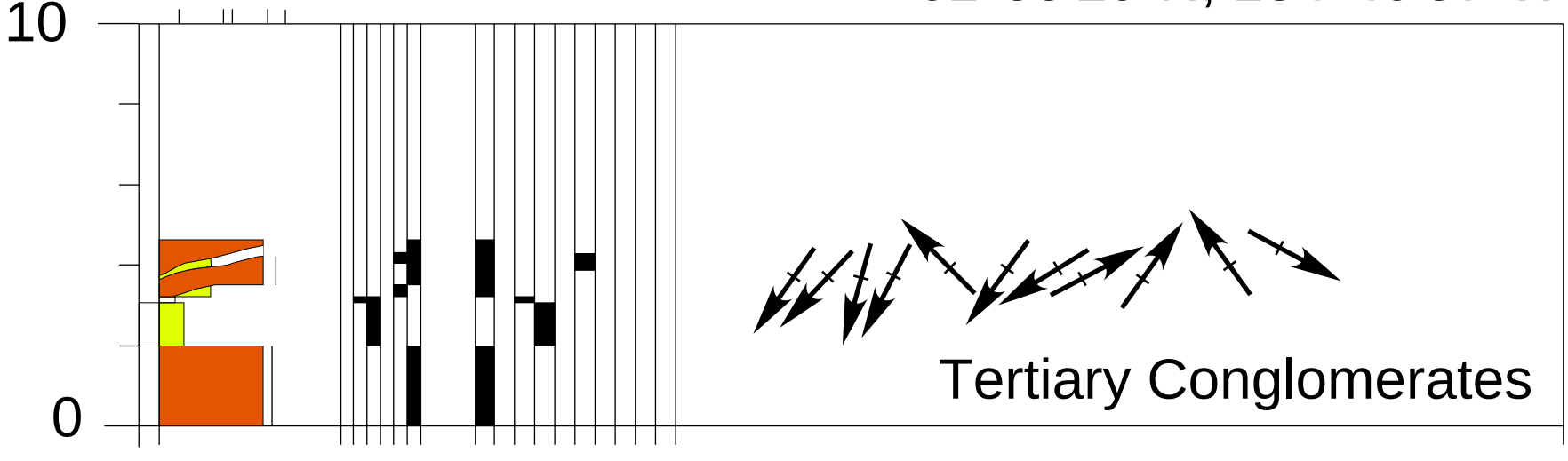

T6a. Hootalinqua

61°43'22"N, 134°56'34"W

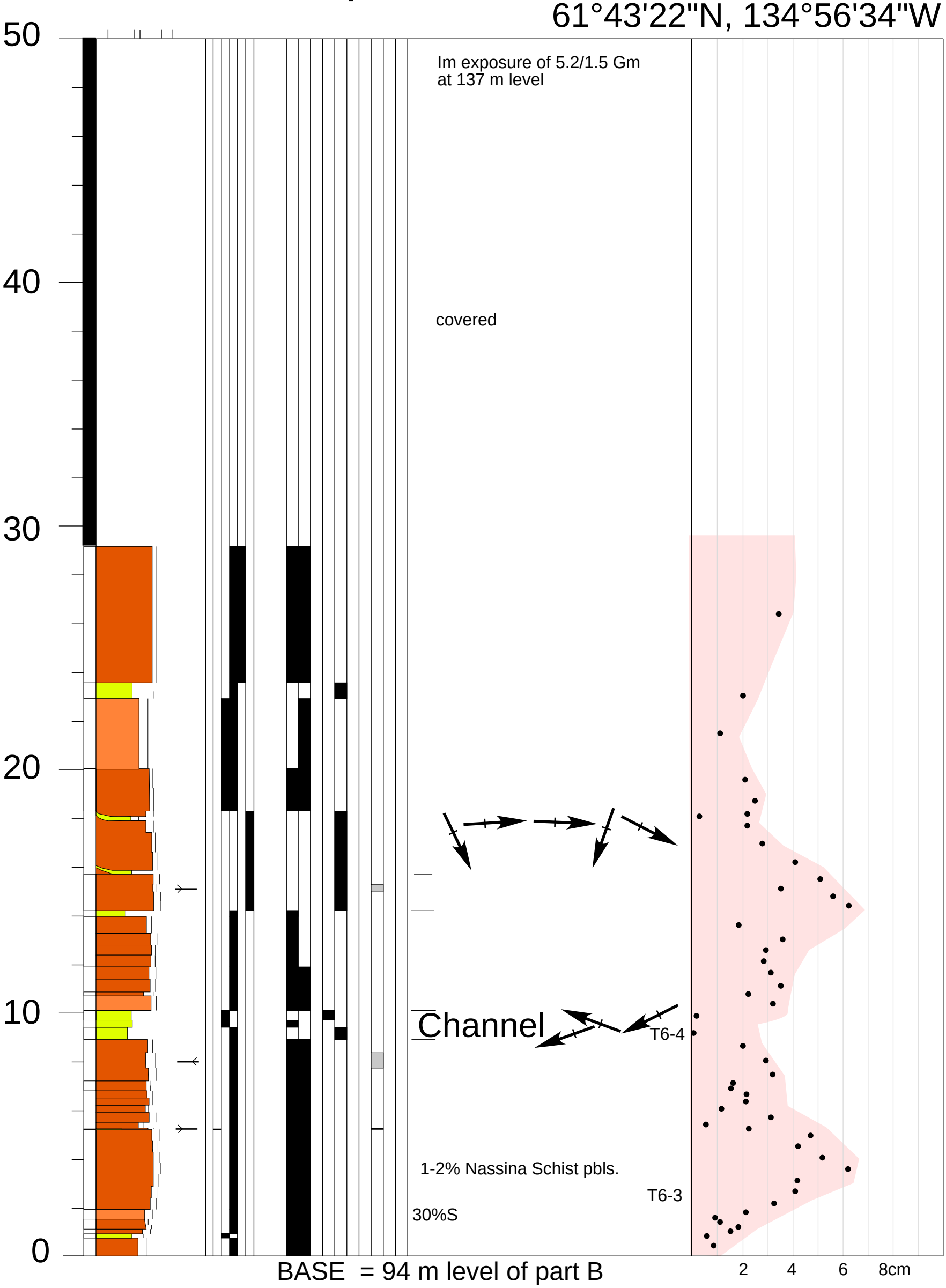

T6b. Hootalinqua

61°43'28"N, 134°57'07"W

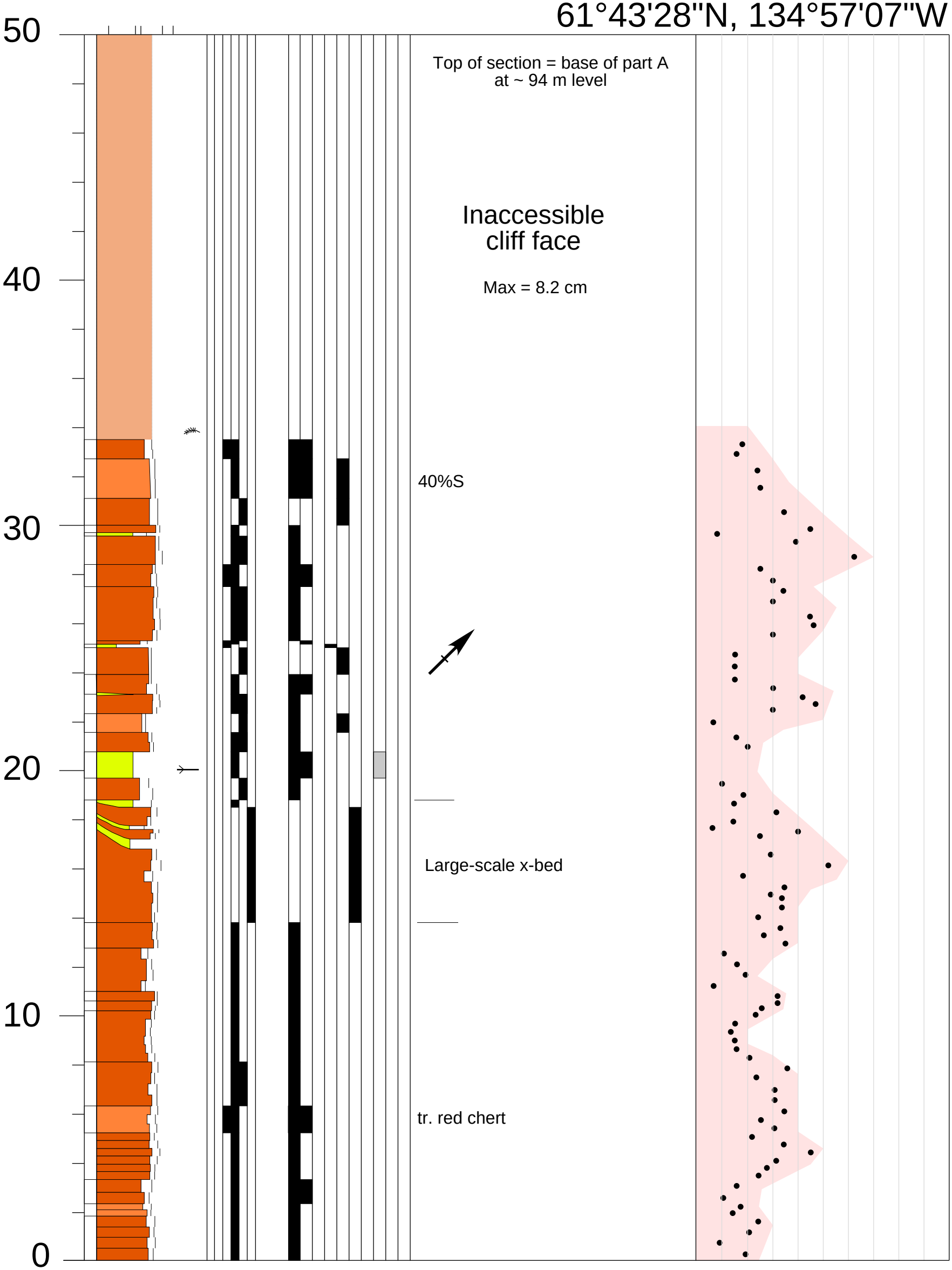

T6 Hootalinqua North

61°43'22"N, 134°56'34"W

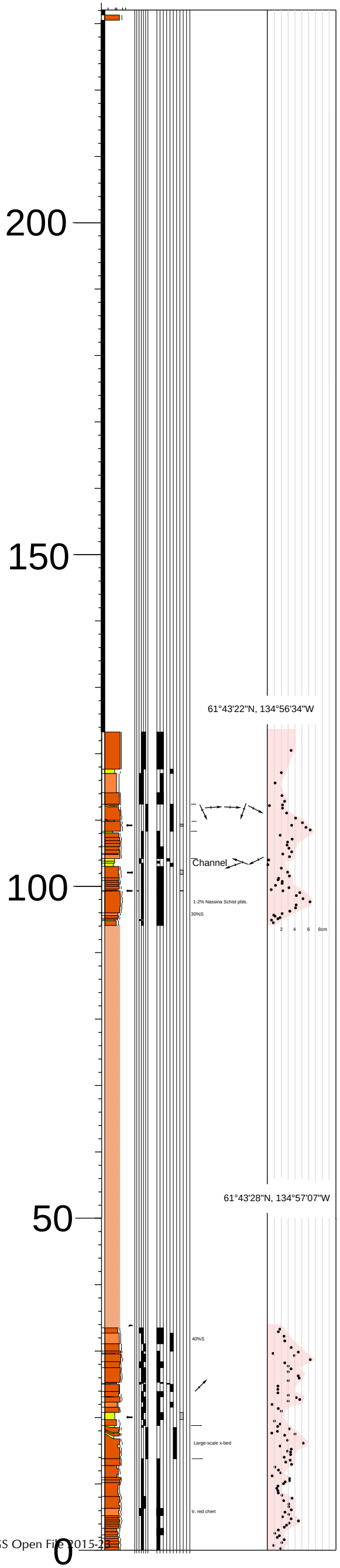

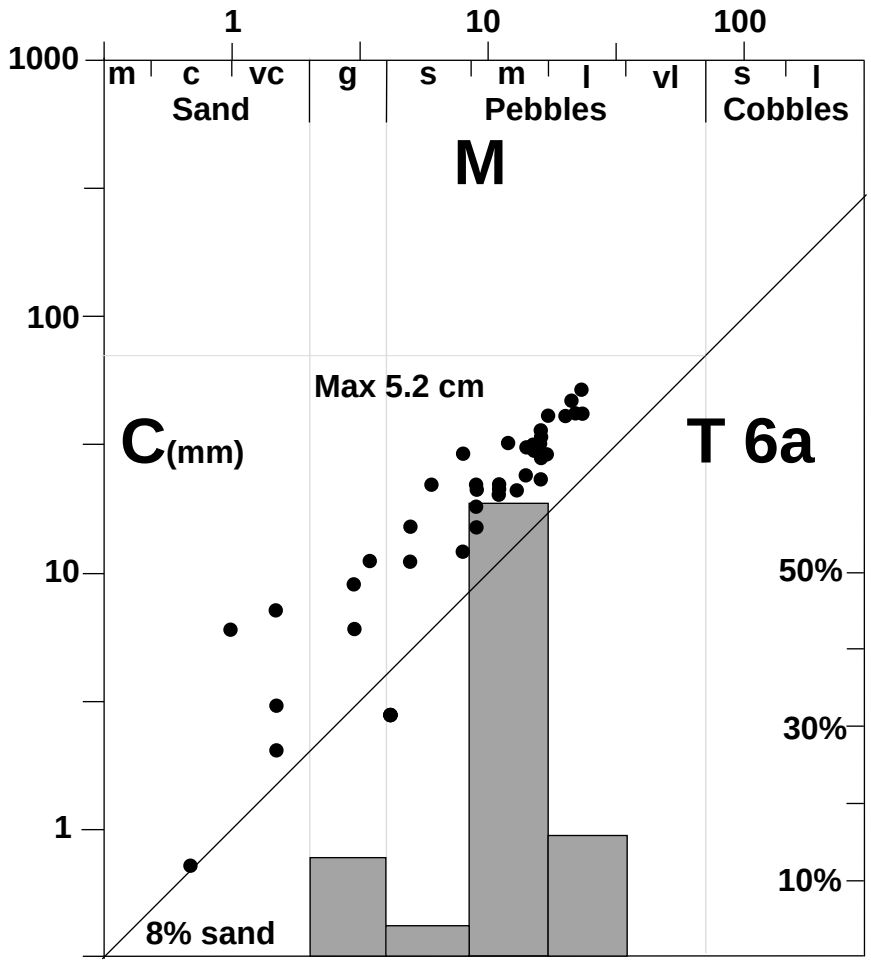

T 6a: Hootalinqua (north)

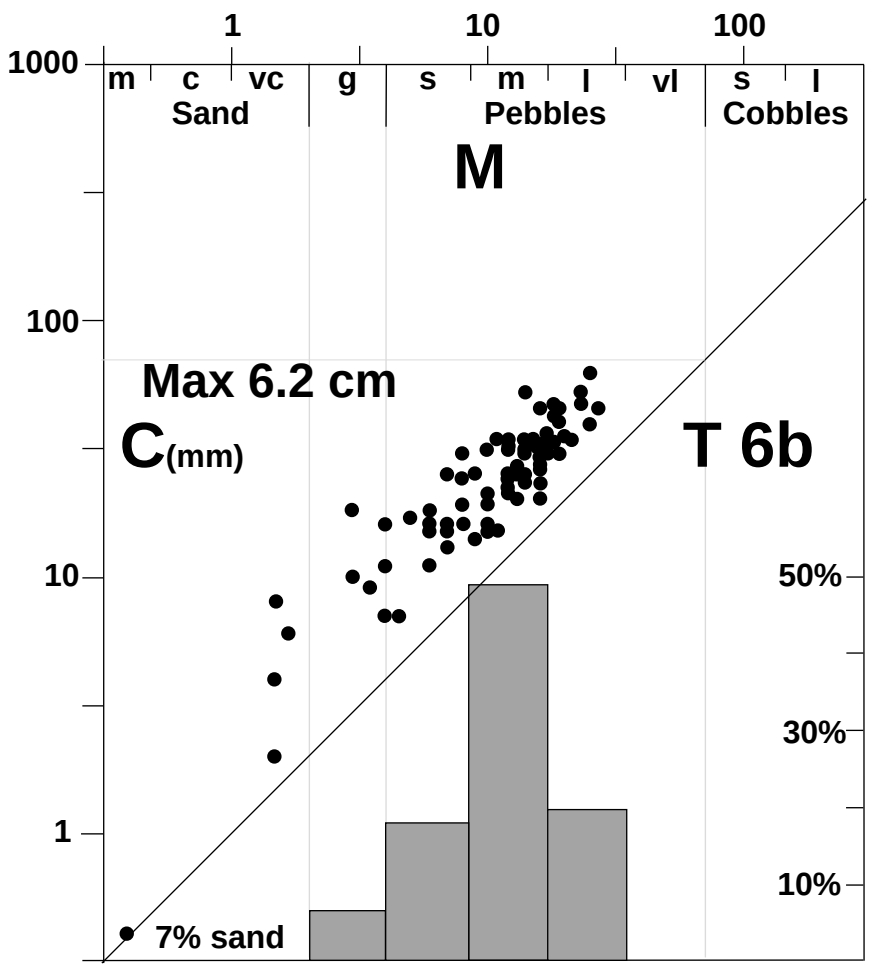

T 6b: Hootalinqua (north)

T-7: Nordenskoid River

Top = 61°16'00"N, 136°15'40"W
Base = 61°15‘38"N, 136°16’11W

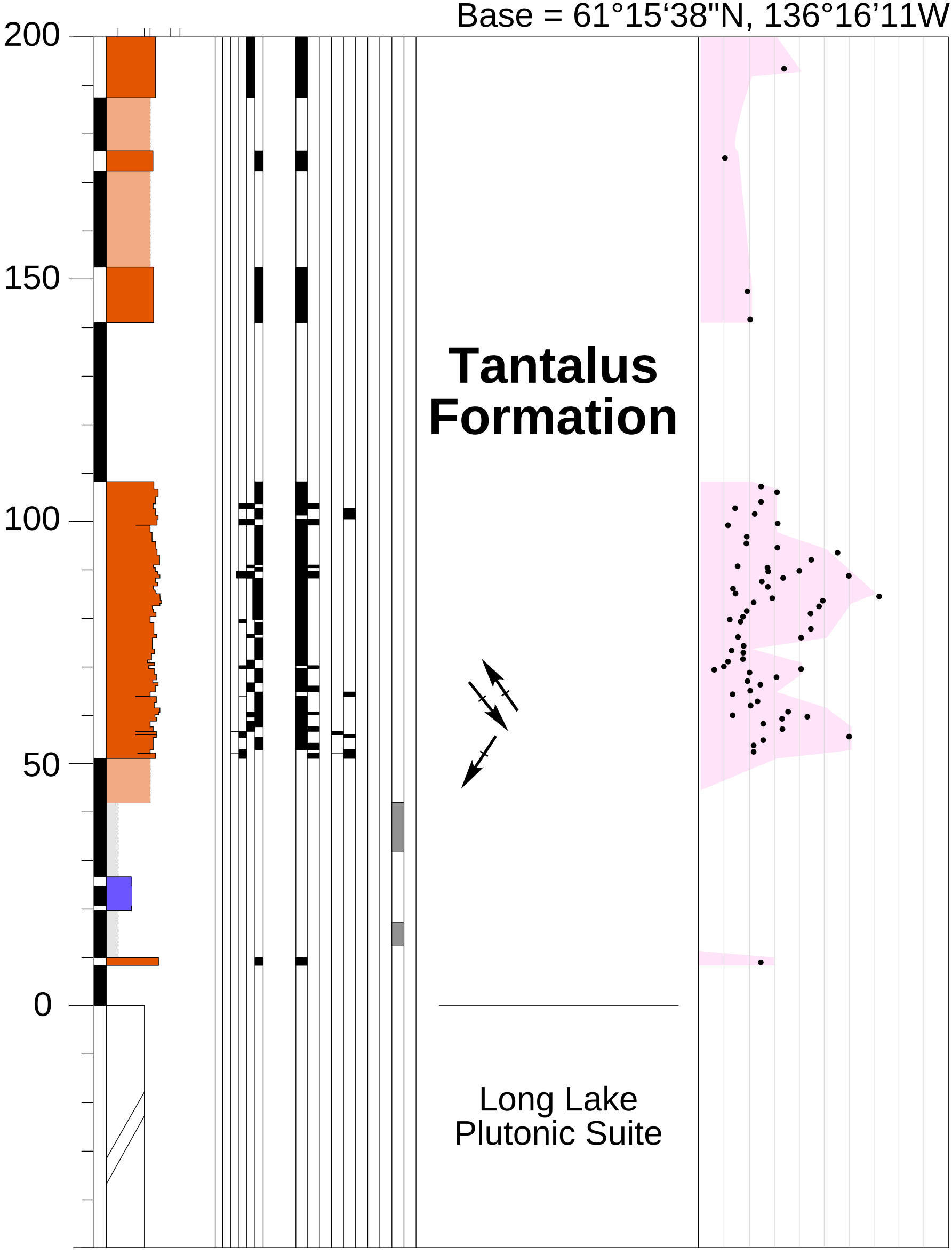

T-7: Nordenskoid River

Top = 61°16'00"N, 136°15'40"W
Base = 61°15‘38"N, 136°16’11W

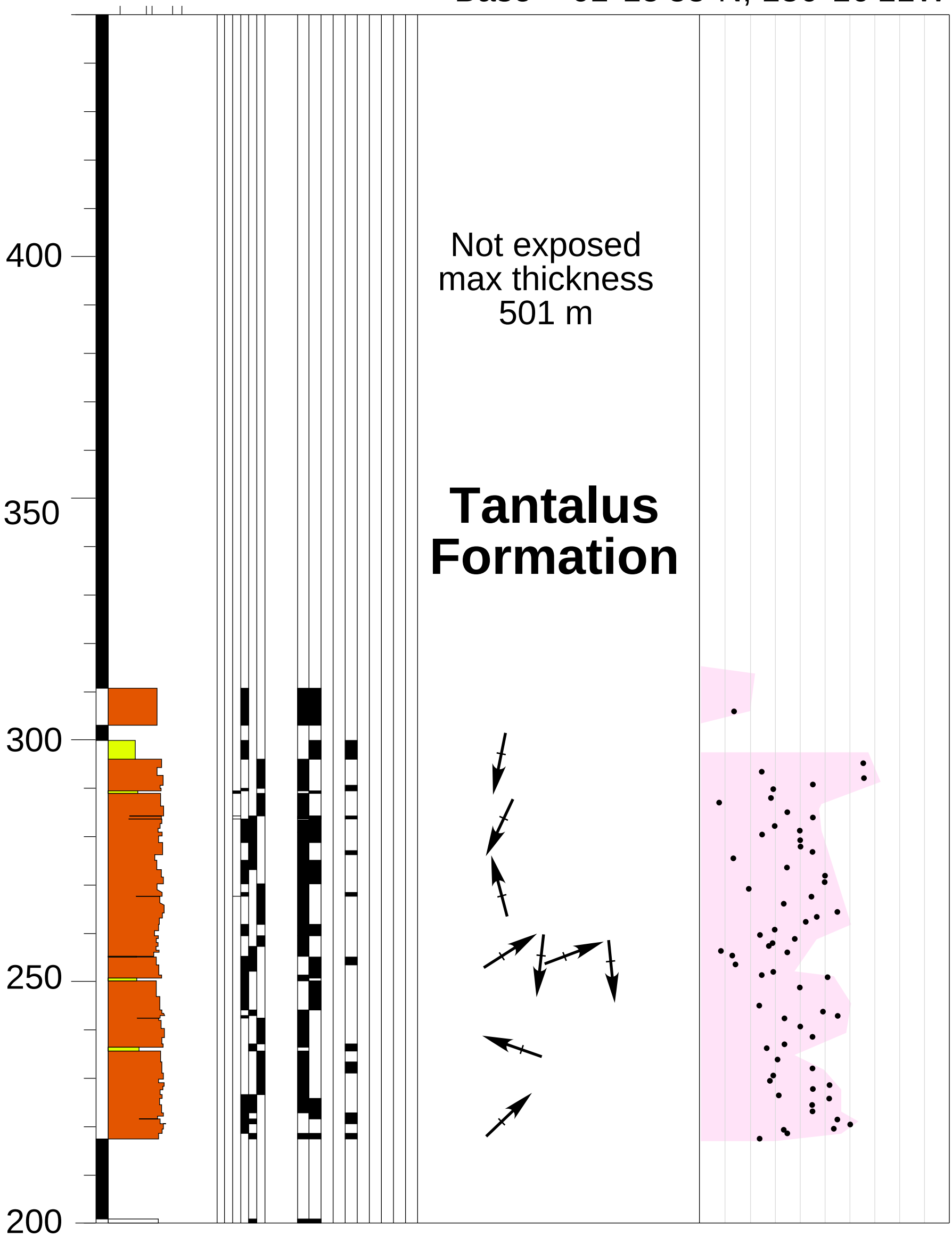

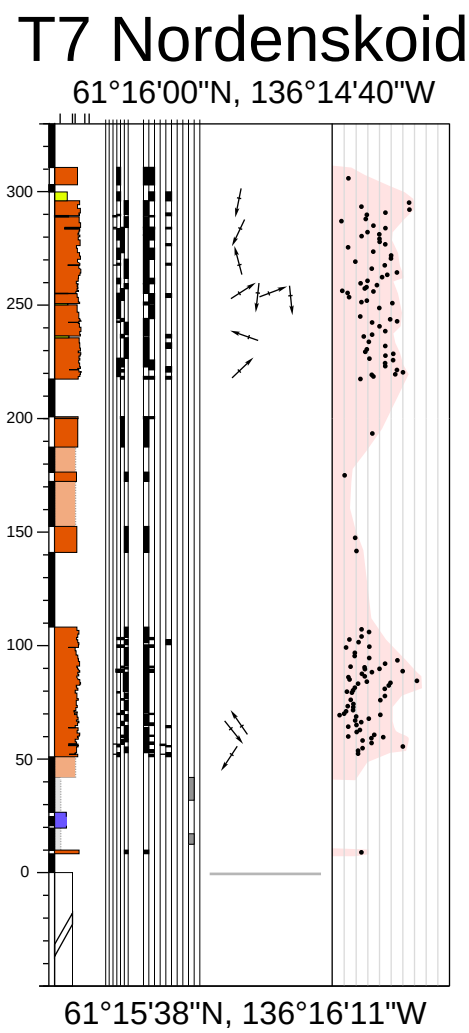

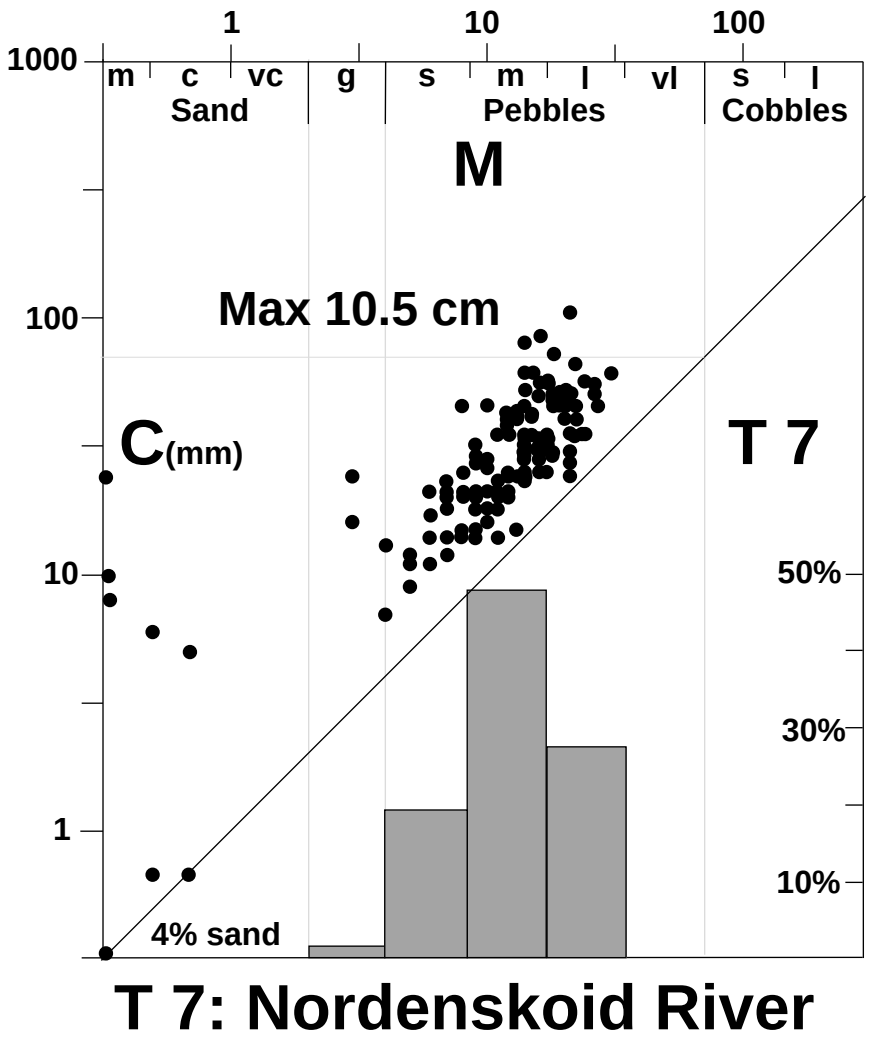

T 7: Nordenskoid River

T8 Cub Mountain

61°23'07"N, 135°59'26"W

50

40

30

20

10

0

265 m
not exposed

Feldspathic sst

T8 Cub Mountain

61°23'07"N, 135°59'26"W

310

300

290

280

270

260

Gap ~136 m
not exposed

Laberge

B = 23°090

T8 Cub Mountain

61°23'07"N, 135°59'26"W

450

440

430

420

410

400

78 m
not exposed

? Nordenskiod

Fine grained dacite

T8 Cub Mountain

61°23'07"N, 135°59'26"W

500

490

480

470

460

450

70 m
not exposed

B = 38°080

T8 Cub Mountain

61°23'07"N, 135°59'26"W

600

590

580

570

560

550

poor exposure

Minor low-angle x-beds

B = 58°085

T8 Cub Mountain

61°23'07"N, 135°59'26"W

650

640

630

620

610

600

not exposed
~110 m

poor exposure

not exposed

T8 Cub Mountain

61°23'07"N, 135°59'26"W

800

790

780

770

760

750

not exposed
40 m

T8 Cub Mountain

61°23'07"N, 135°59'26"W

1310

1300

GAP ESTIMATED AT 500 M
Not exposed

820

810

Trace coal in soil

800

T8 Cub Mountain

61°23'07"N, 135°59'26"W

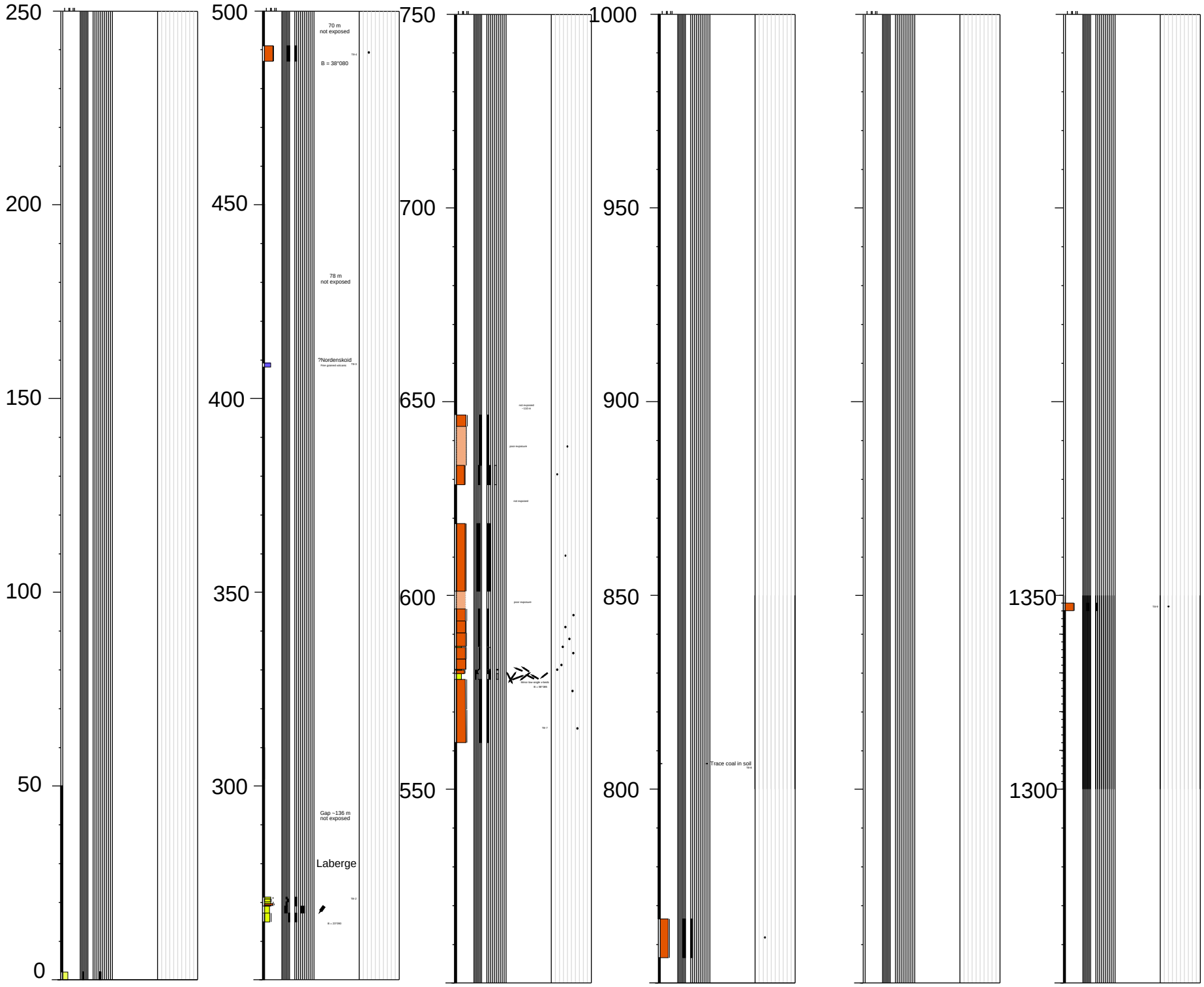

T9 Vowel Mountain

61°21'N, 136°08'W

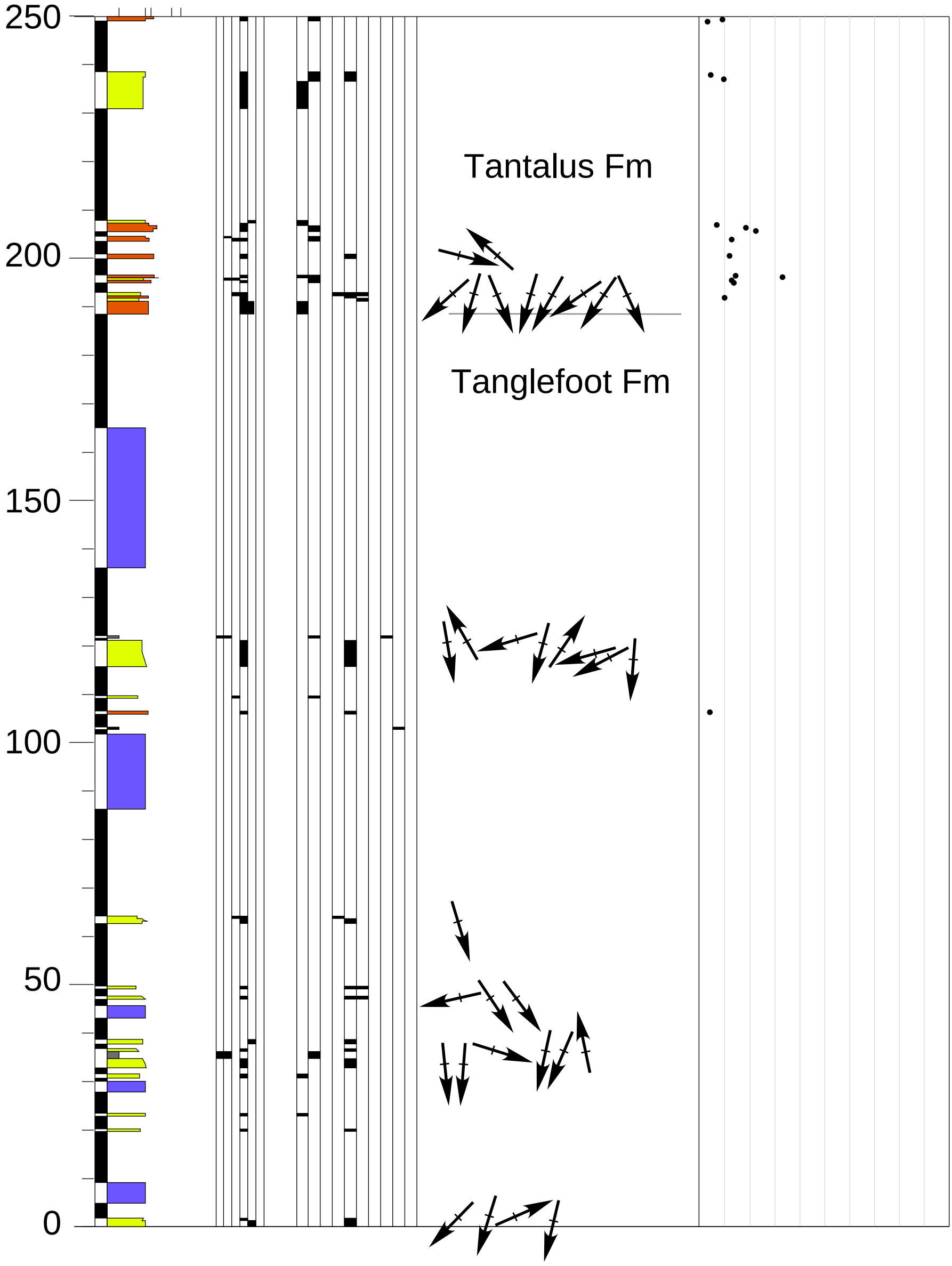

T9 Vowel Mountain

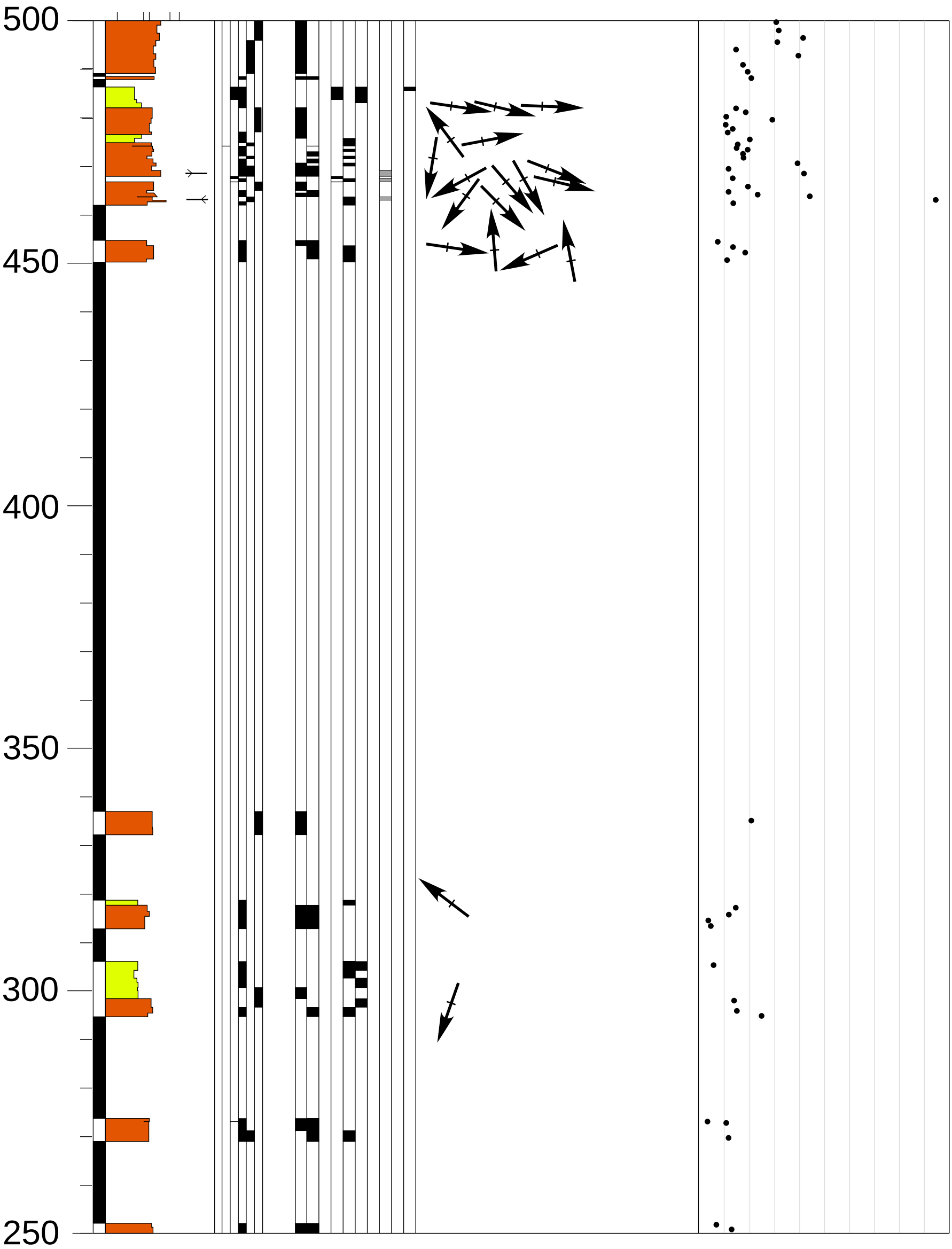

T9 Vowel Mountain

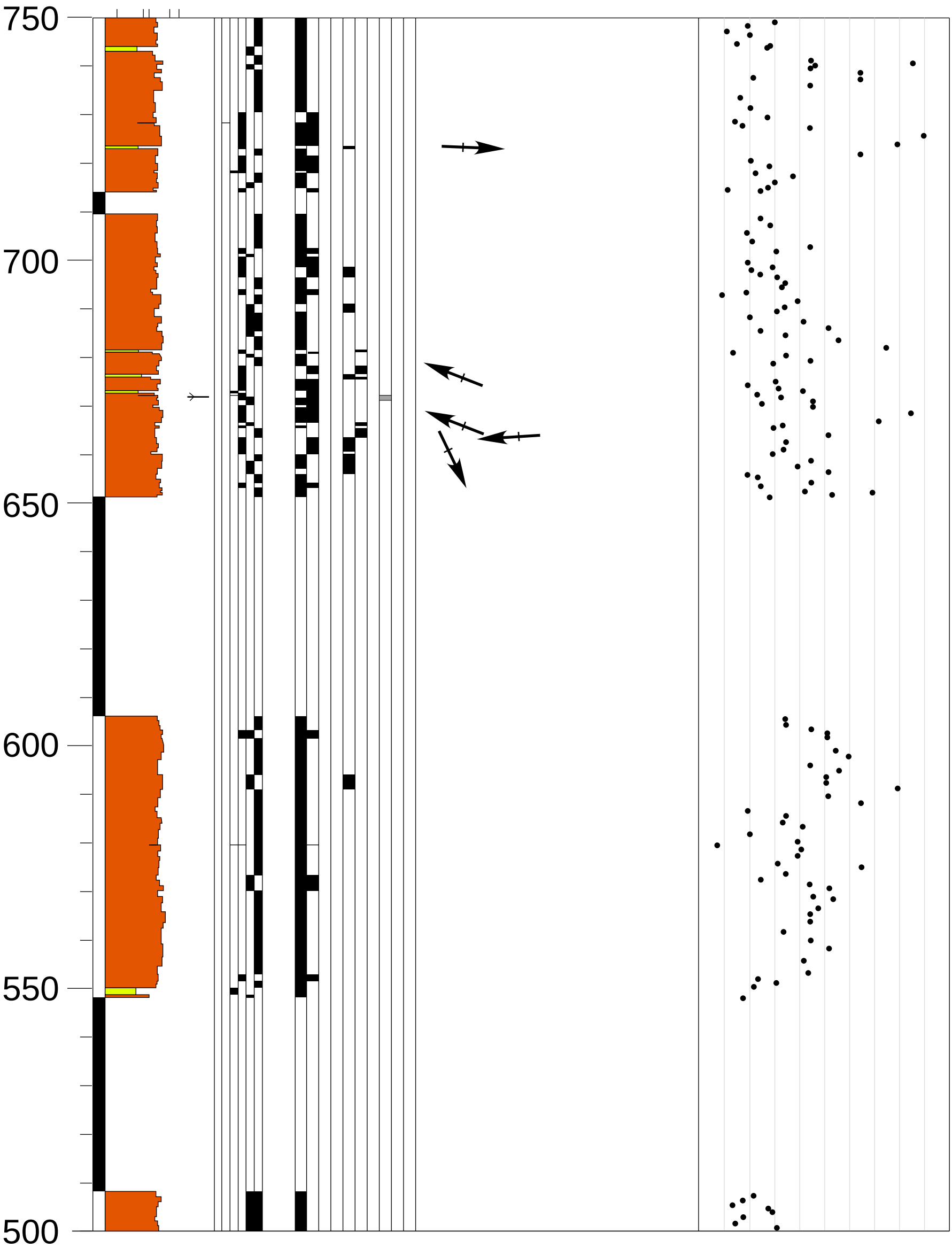

T9 Vowel Mountain

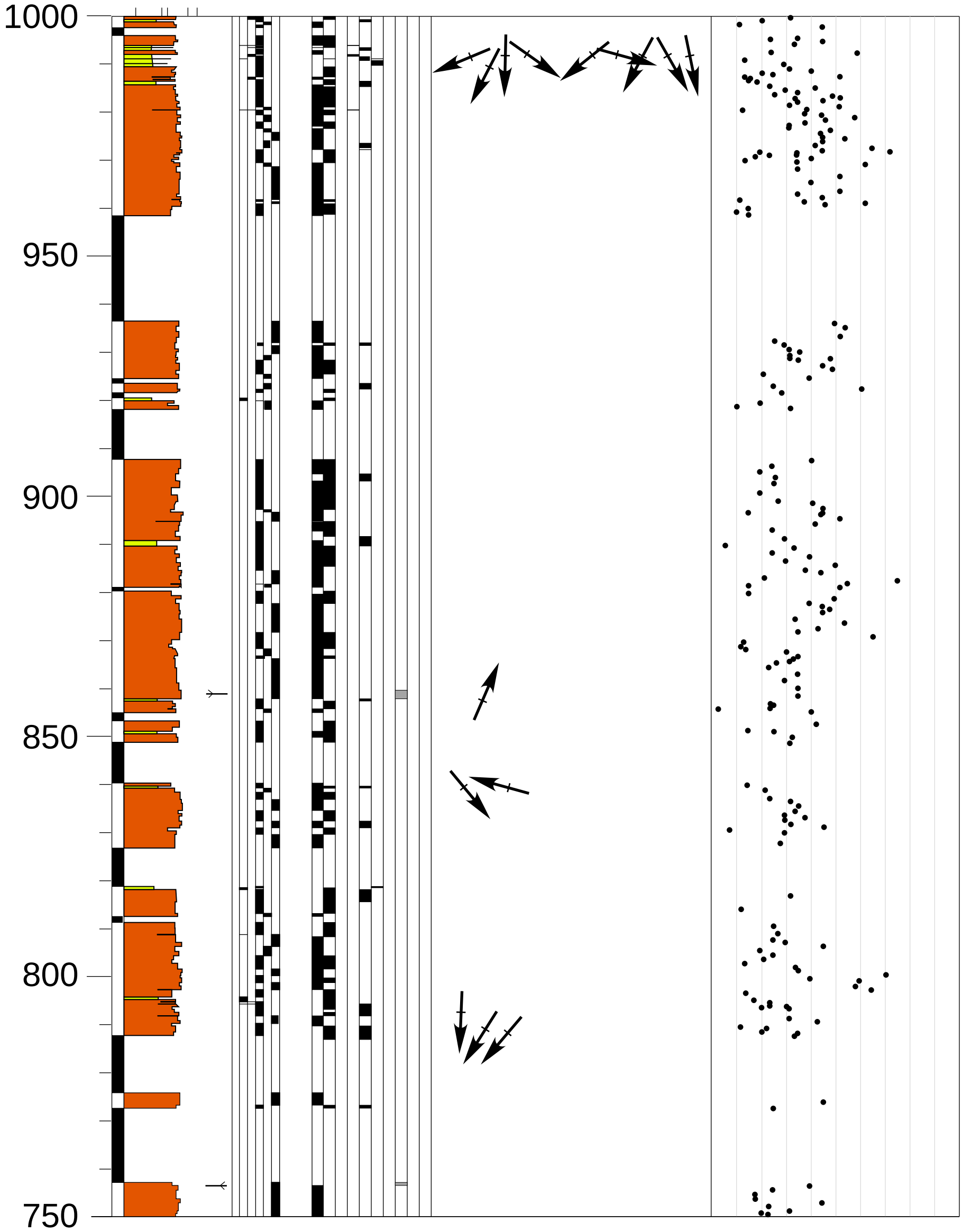

T9 Vowel Mountain

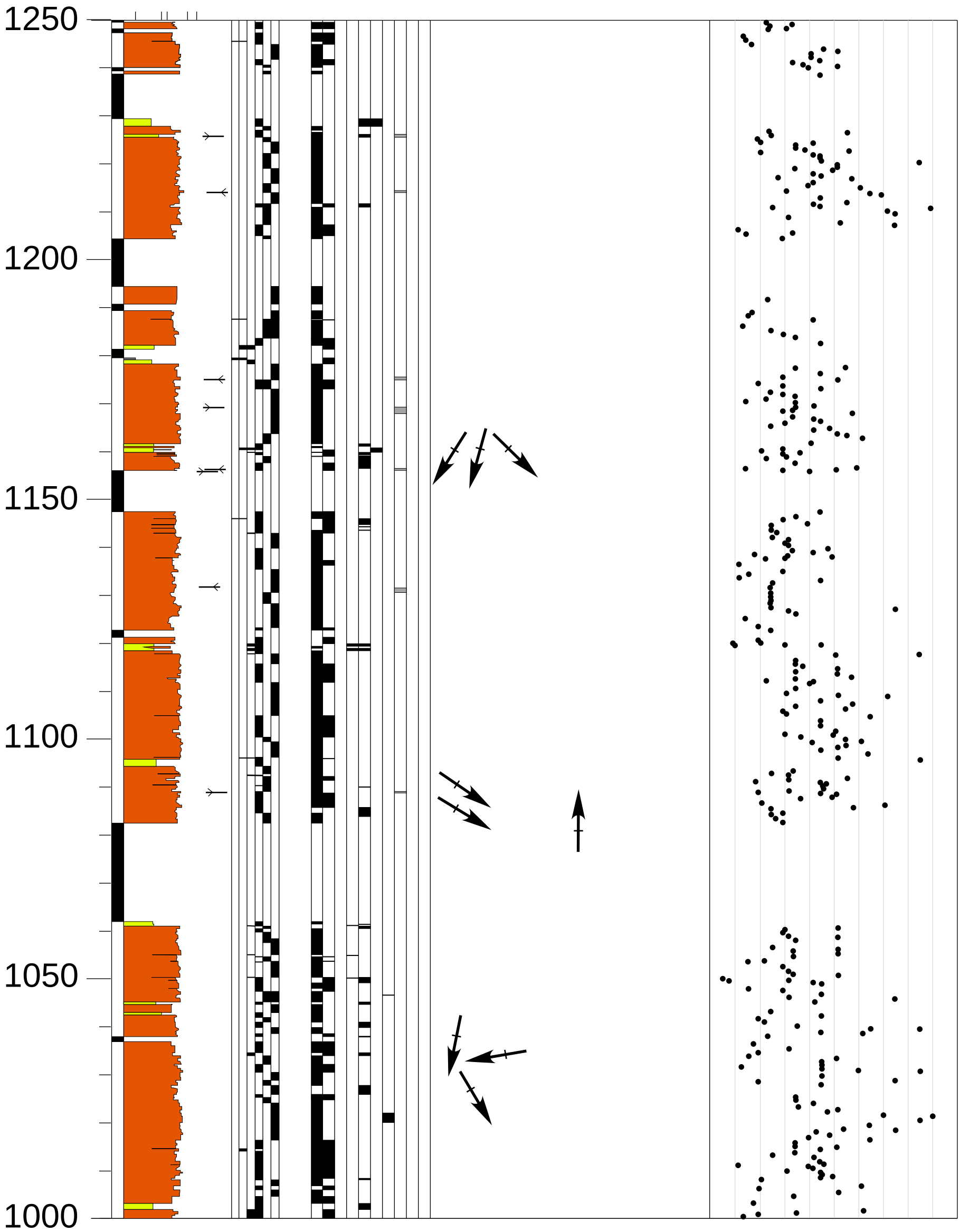

T9 Vowel Mountain

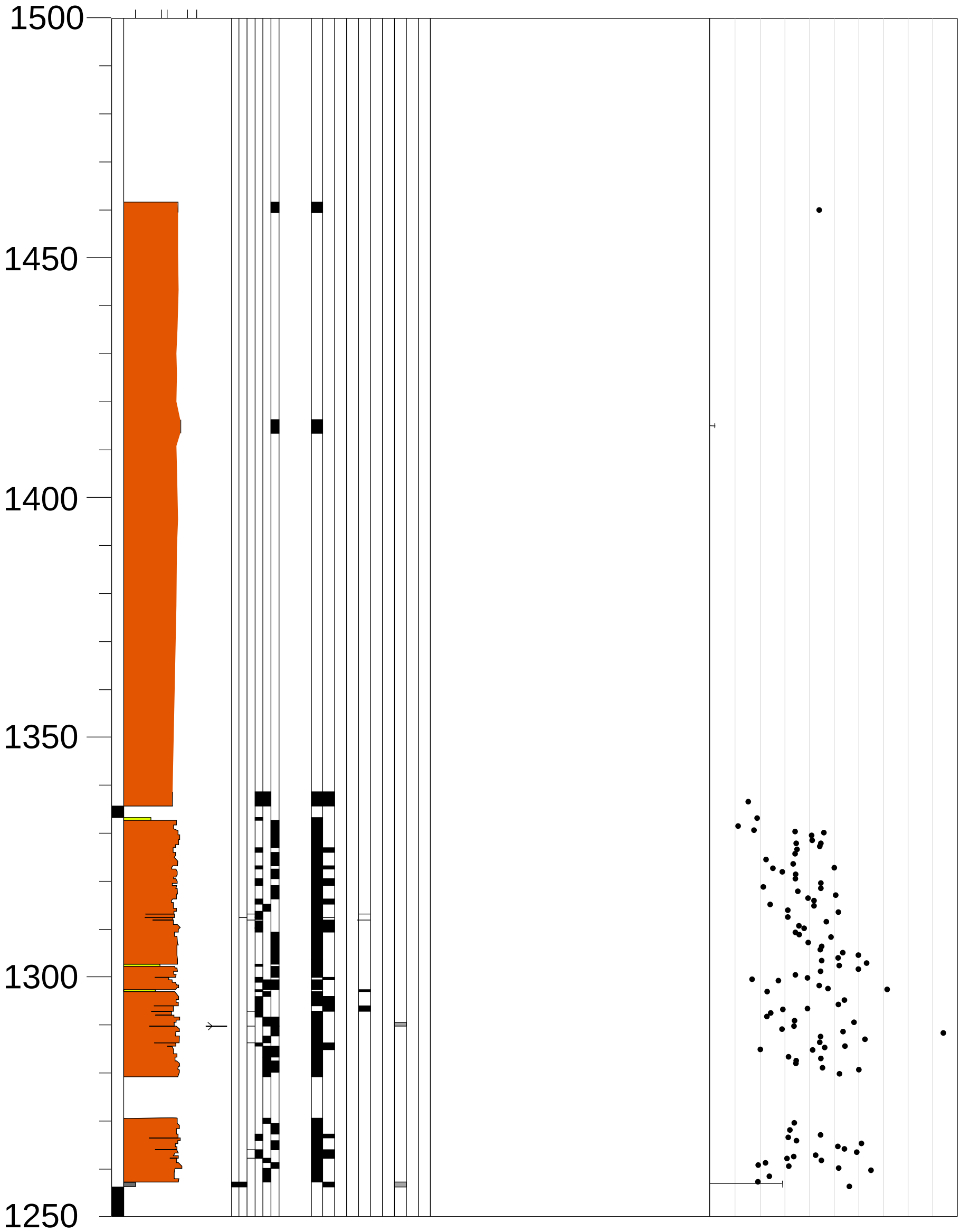

T9-Vowel Mountain

61°21'N, 136°08'W

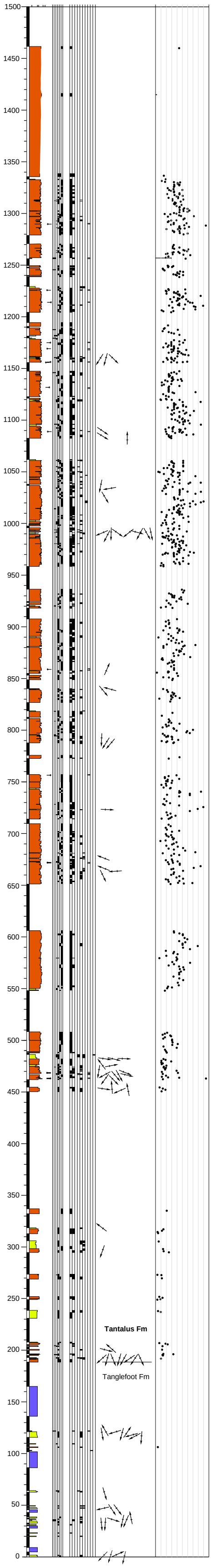

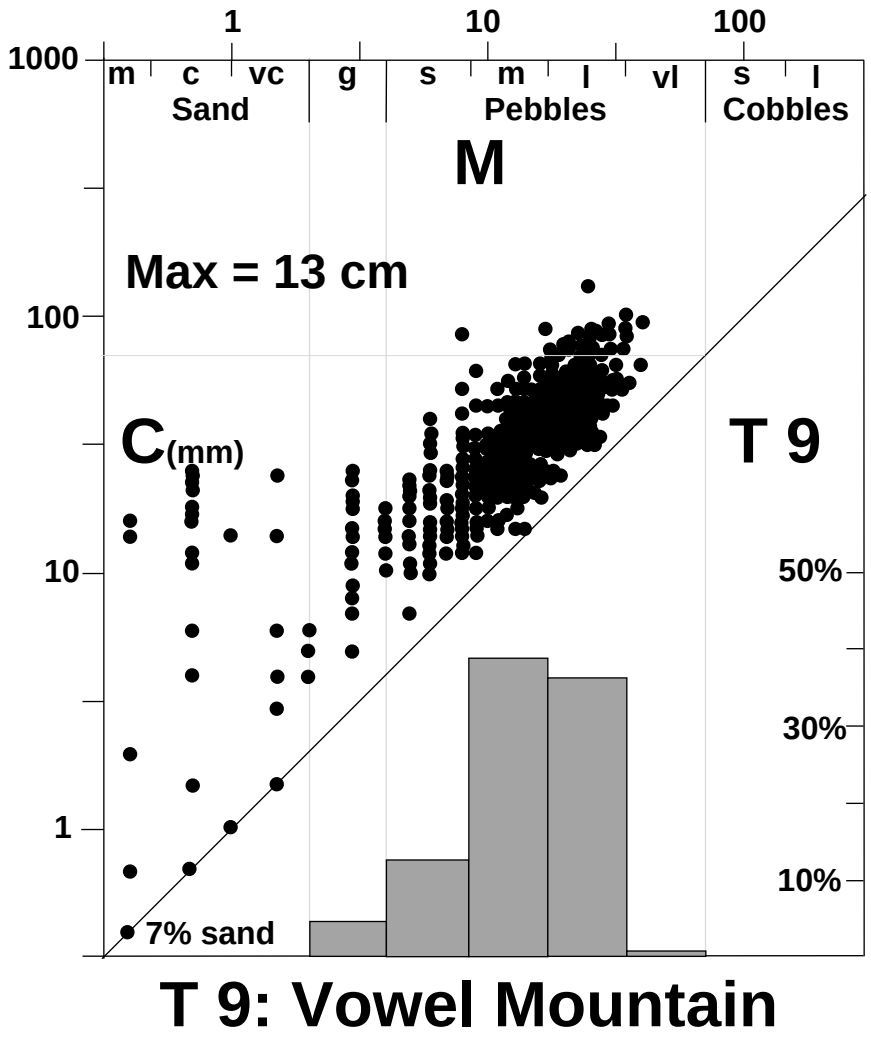

T 9: Vowel Mountain

T10 Tantalus Mine (Old)

62°05'41"N, 136°15'48"W

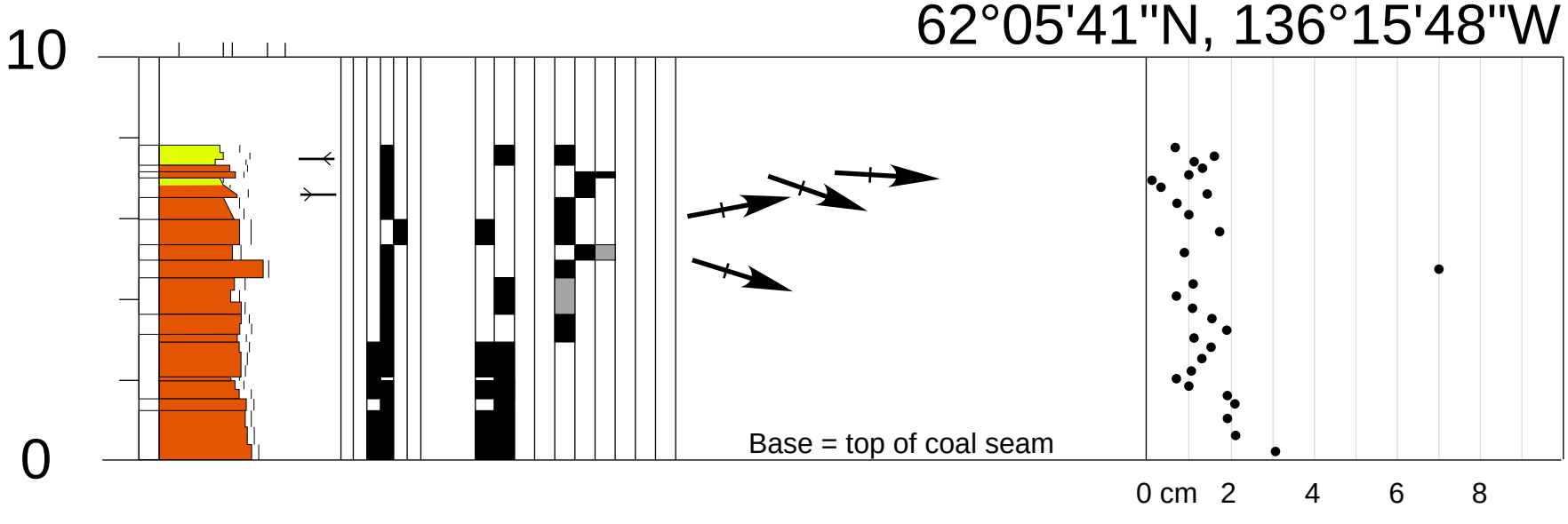

T10 Tantalus Mine (Old) East Side

62°05'39"N, 136°16'00"W

50

40

30

20

10

0

Covered

tr coal in scree

Composite bedform

Covered interval, (burning coal)

T10 Tantalus Mine (Old) East Side

62°05'39"N, 136°16'00"W

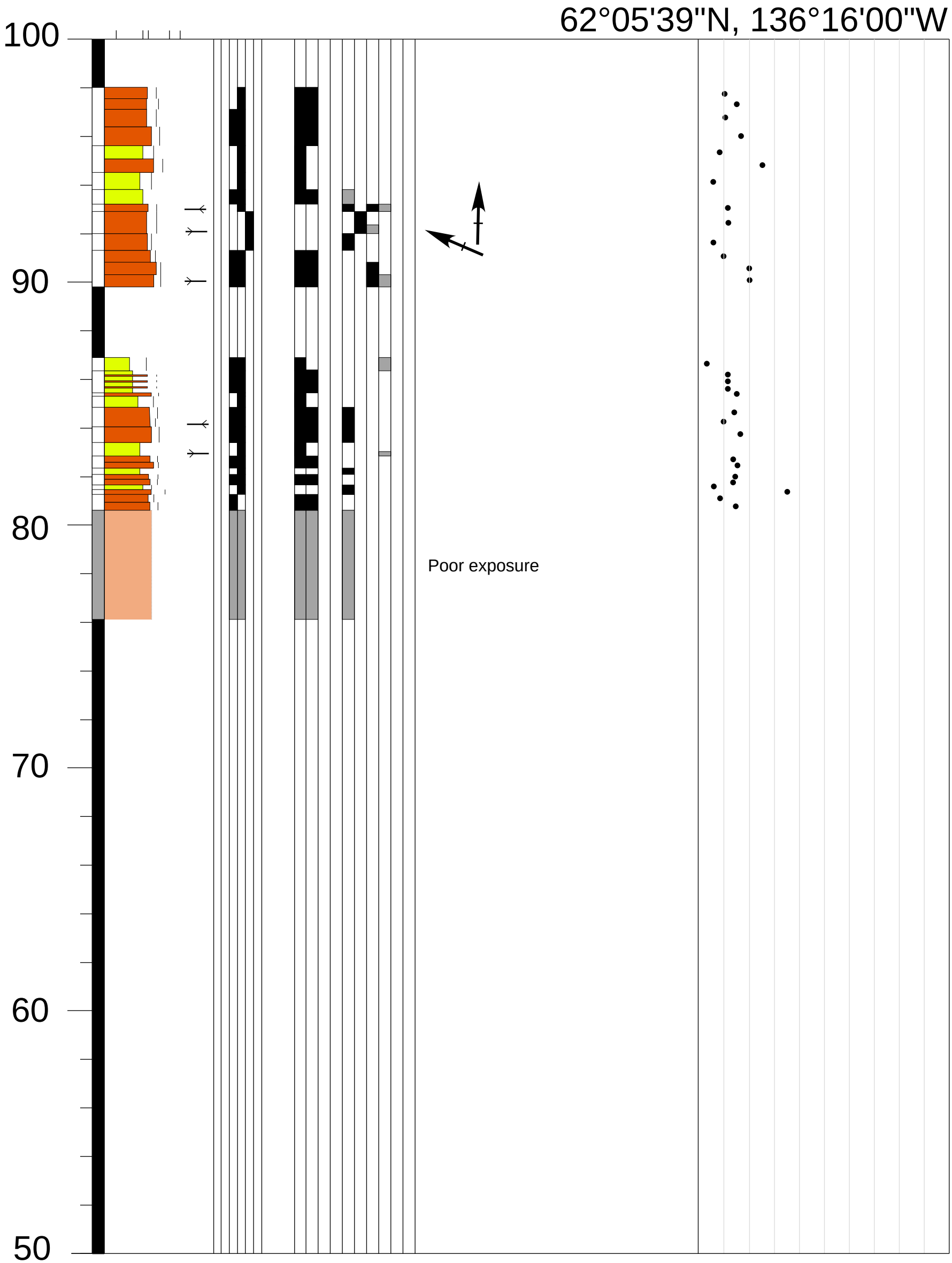

T10 Tantalus Mine (Old) East Side
62°05'39"N, 136°16'00"W

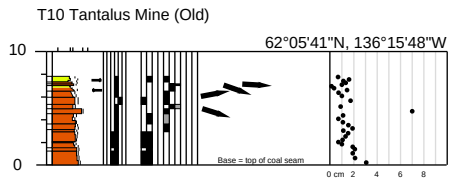

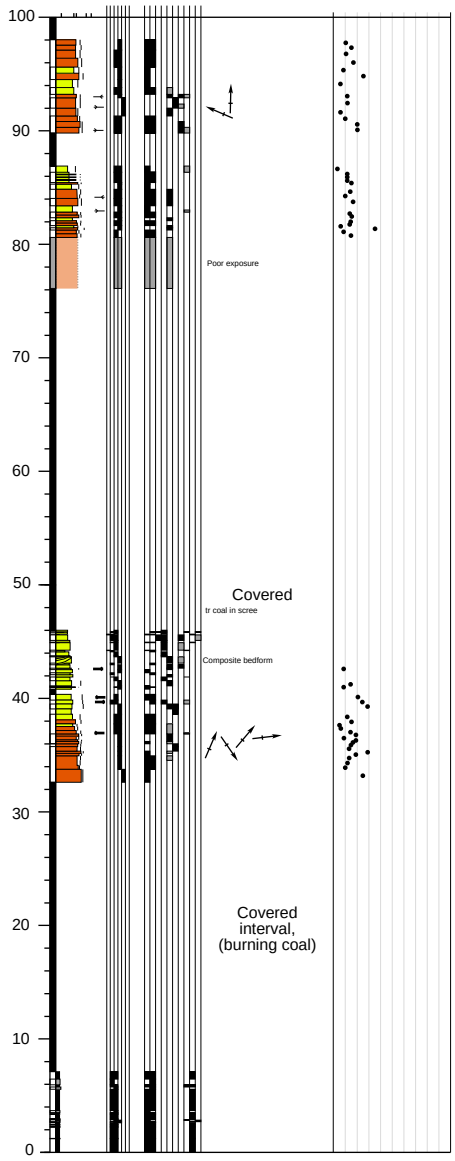

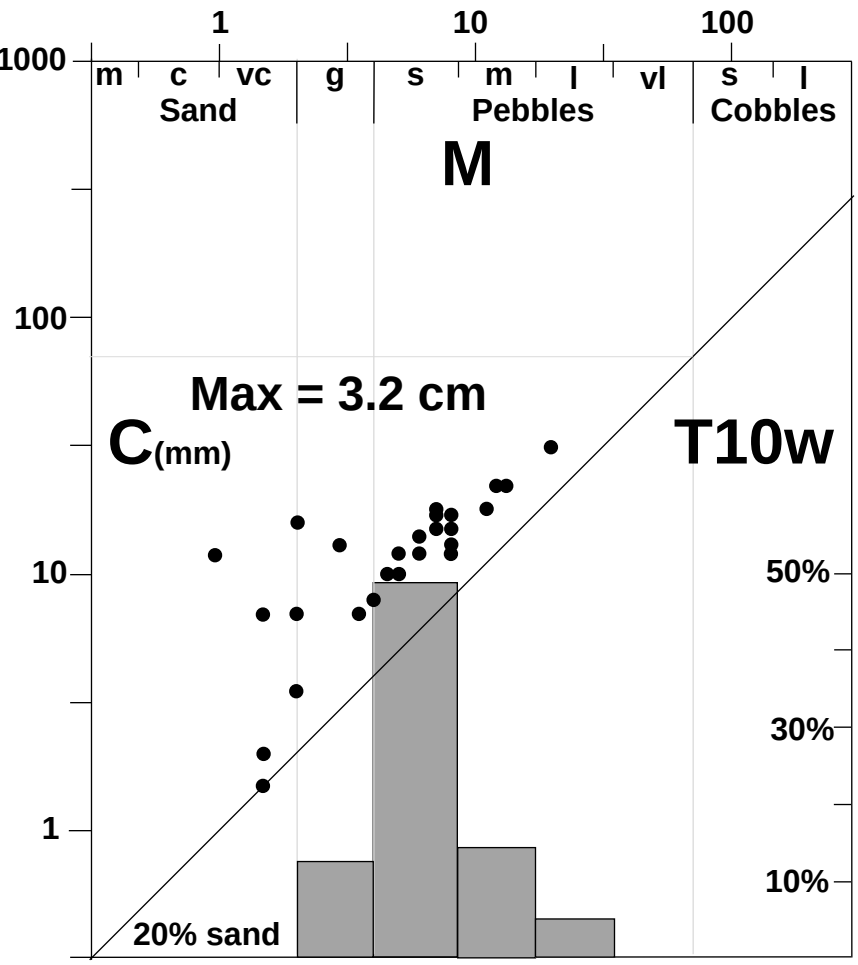

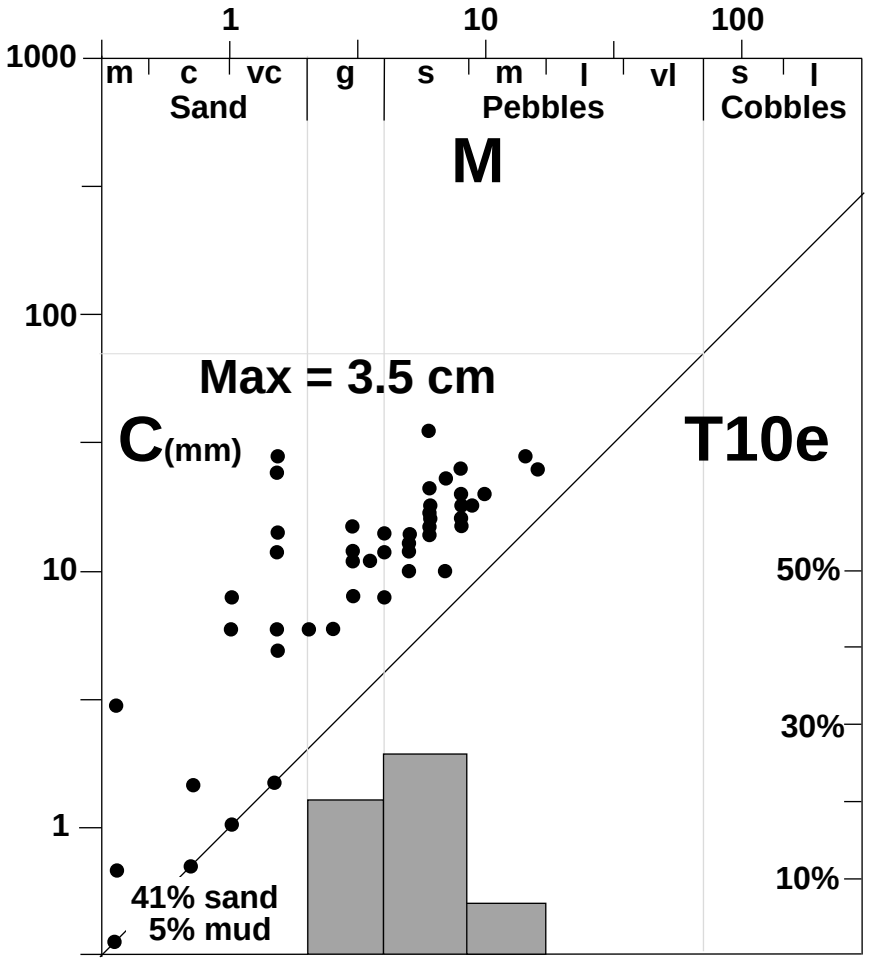

T10: Carmacks Old Mine (west) T10: Carmacks old mine (East)

T11 Claire Creek 50-300m

61°56'53"N,
135°22'23"W

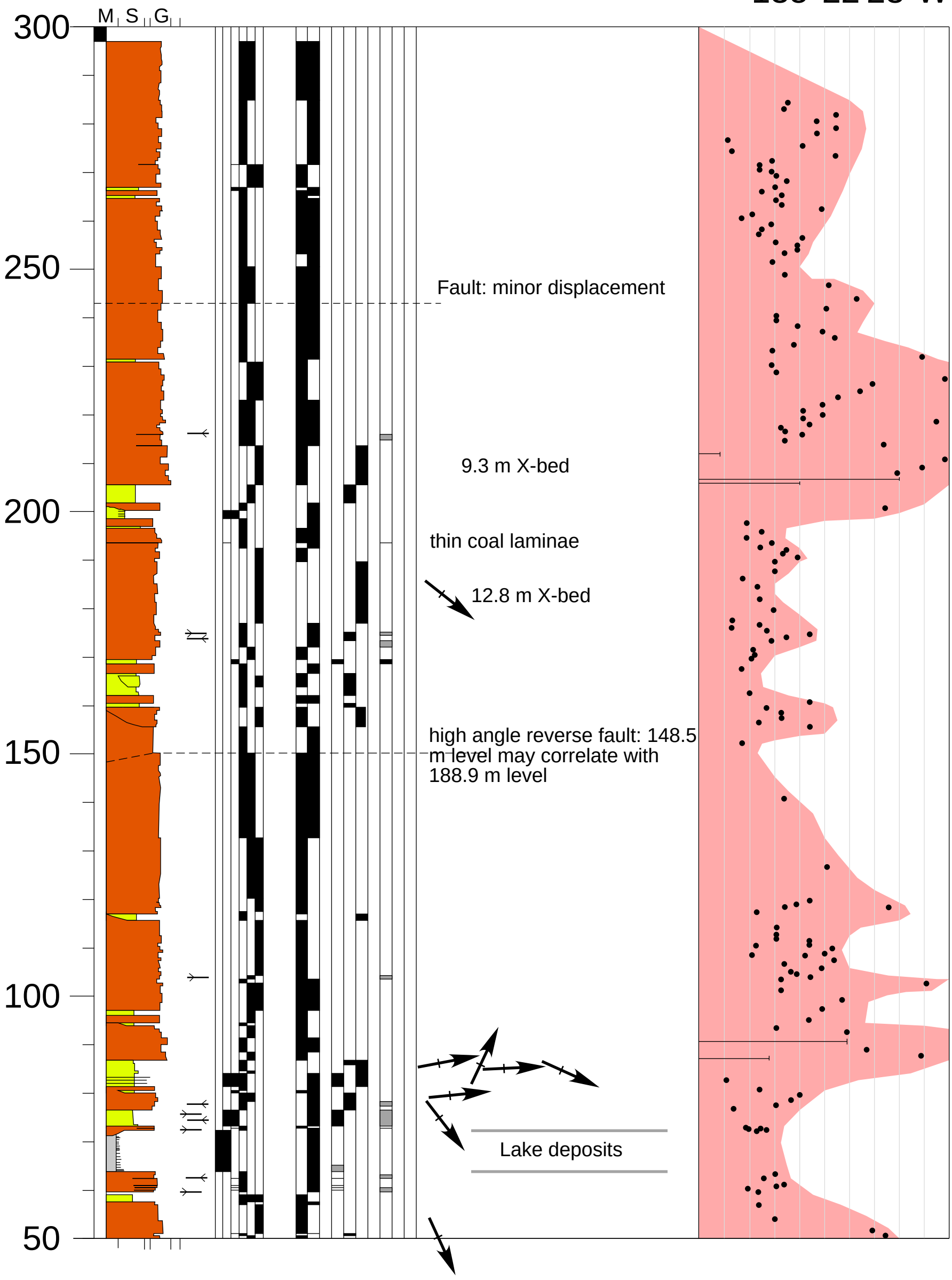

T11 Claire Creek 0-50 m

61°56'53"N, 135°22'23"W

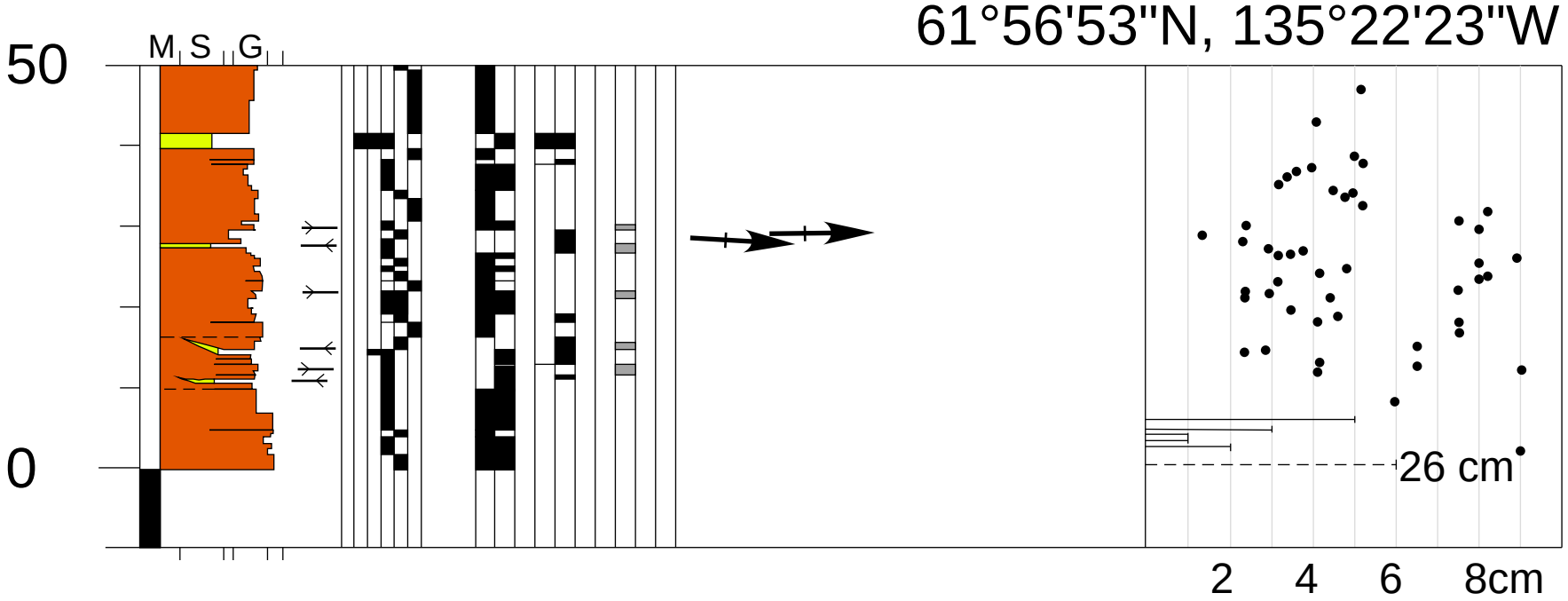

T-11 Claire Creek
61°56'53"N, 135°22'23"W

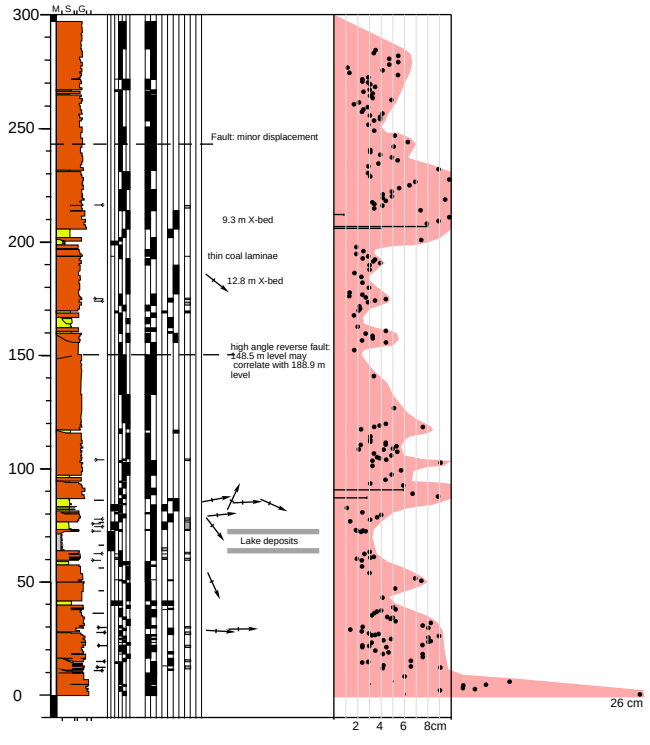

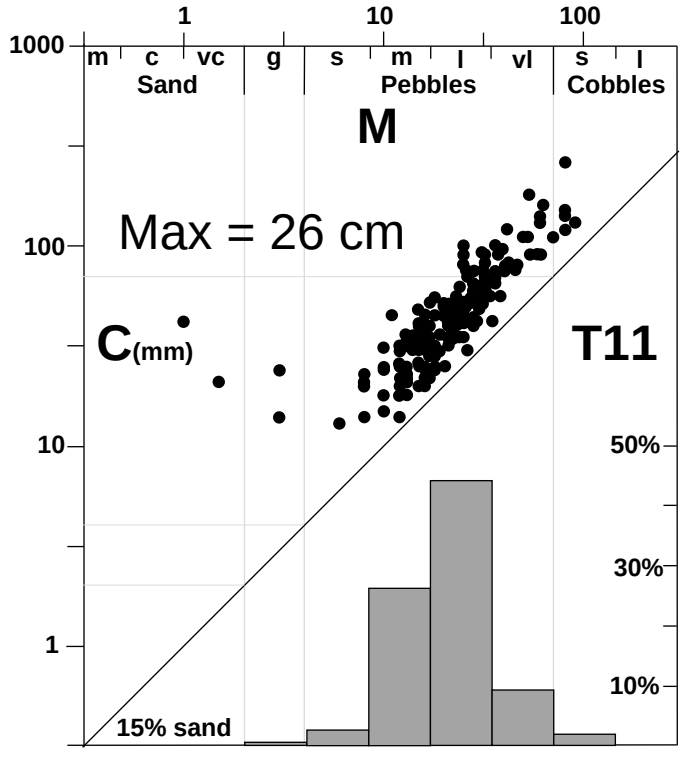

T12-A South of Carmacks

62°05'04"N, 136°15'27"W

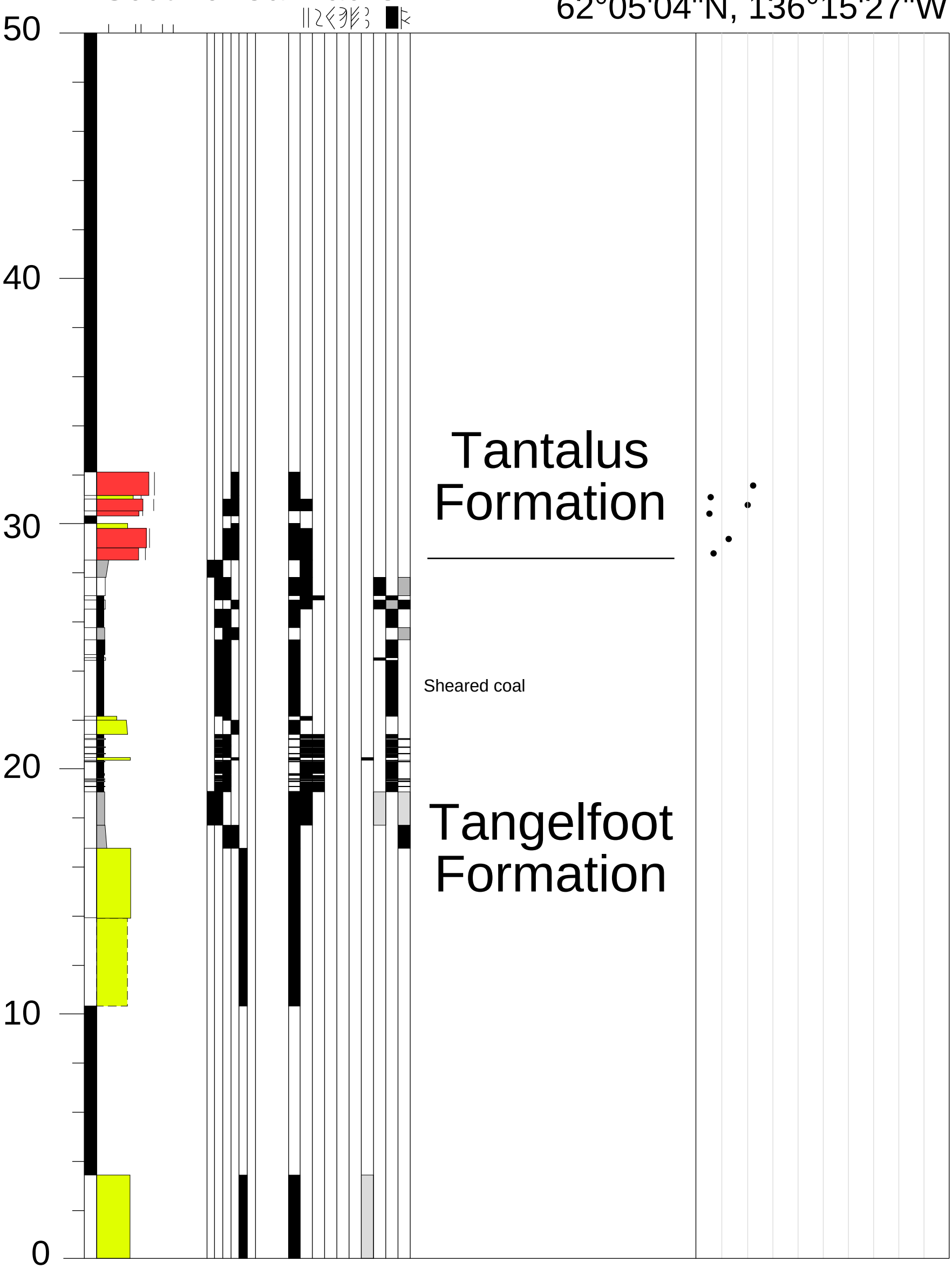

T12-B South of Carmacks

62°04'59"N, 136°15'21"W

50

40

30

20

10

0

Tantalus Formation

Sheared coal

Sheared coal

Tangelfoot Formation

T12-C South of Carmacks

62°04'55"N, 136°15'09"W

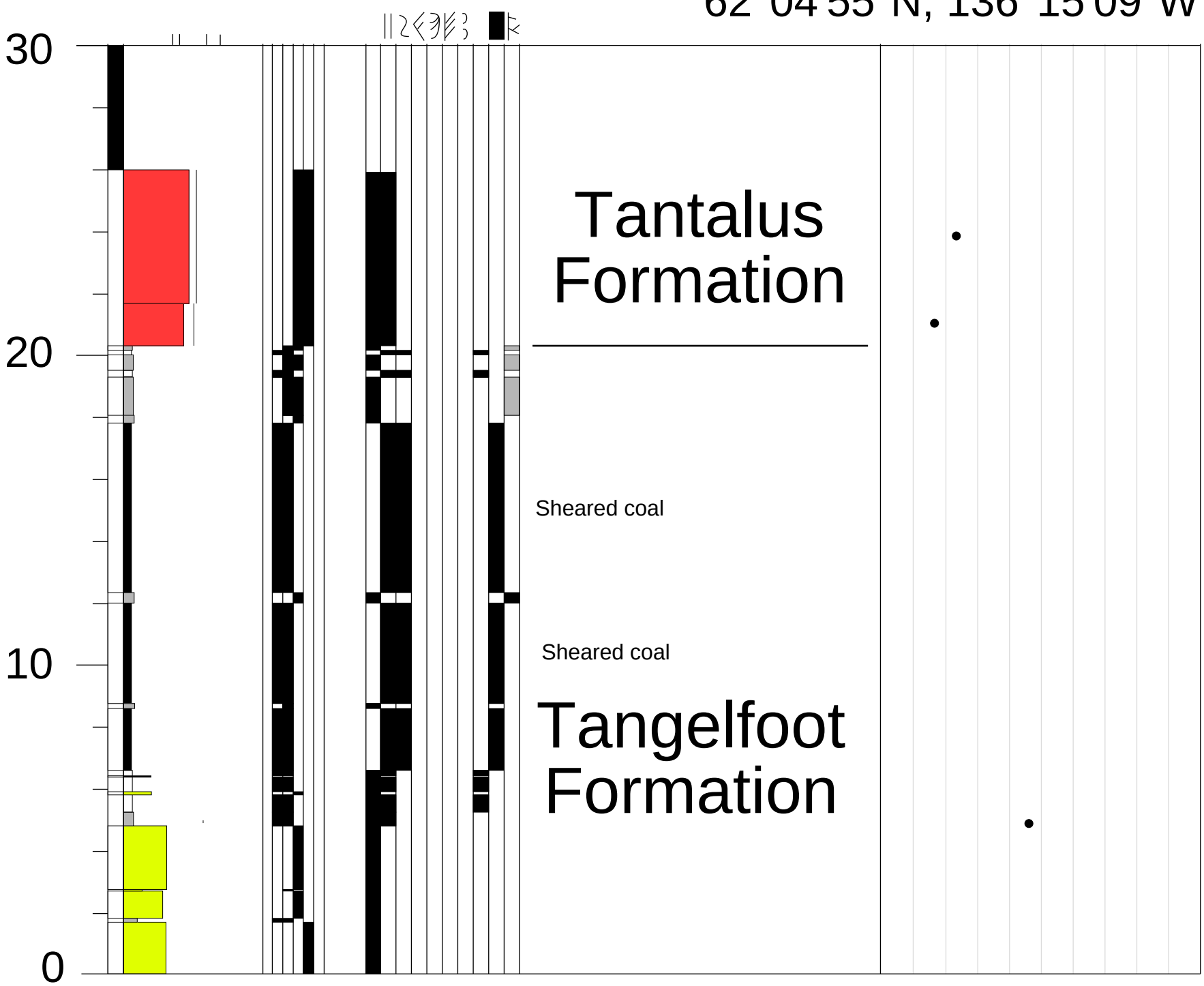

T12-D South of Carmacks

62°04'51"N, 136°15'12"W

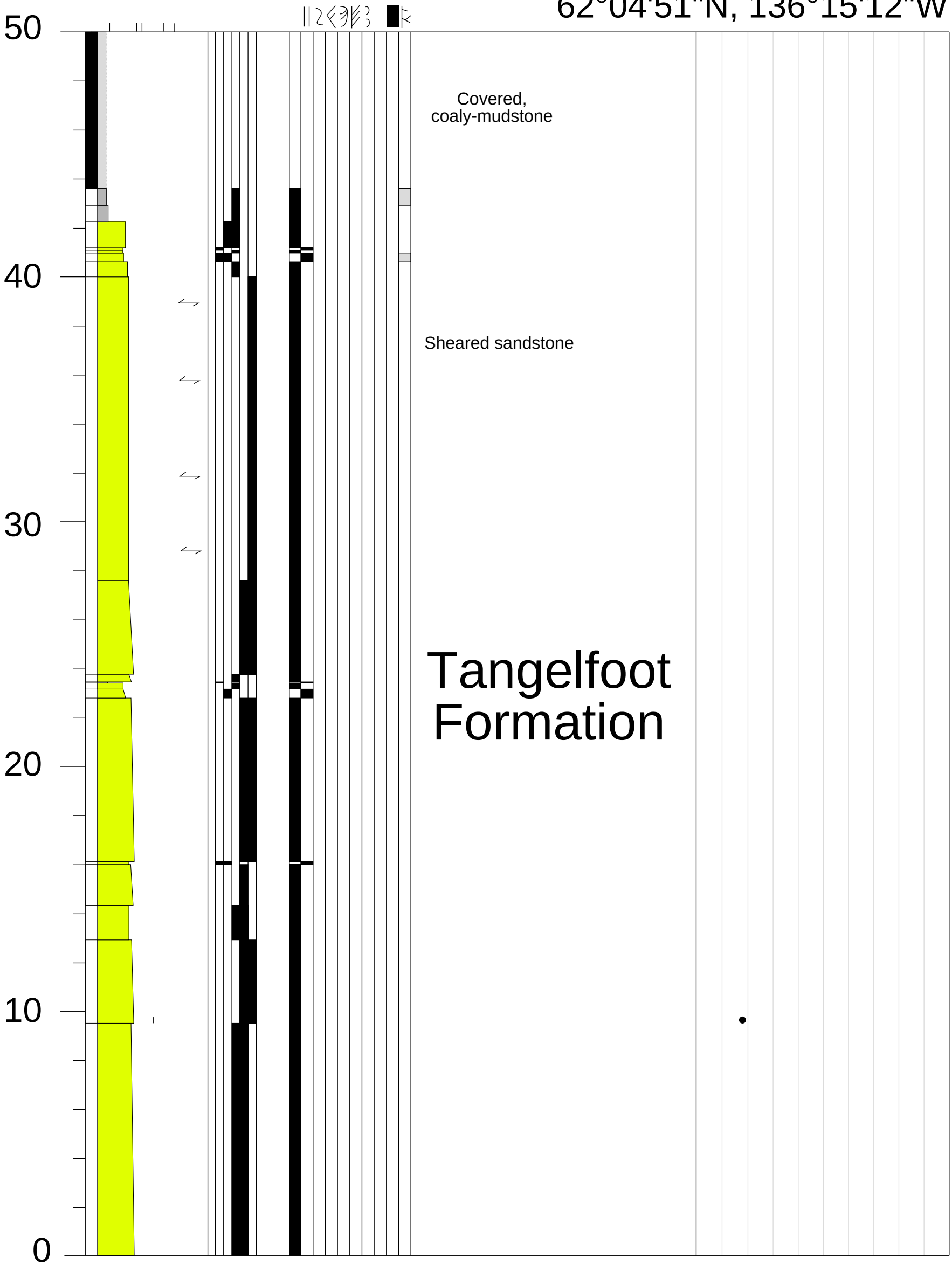

T12-D South of Carmacks

62°04'51"N, 136°15'12"W

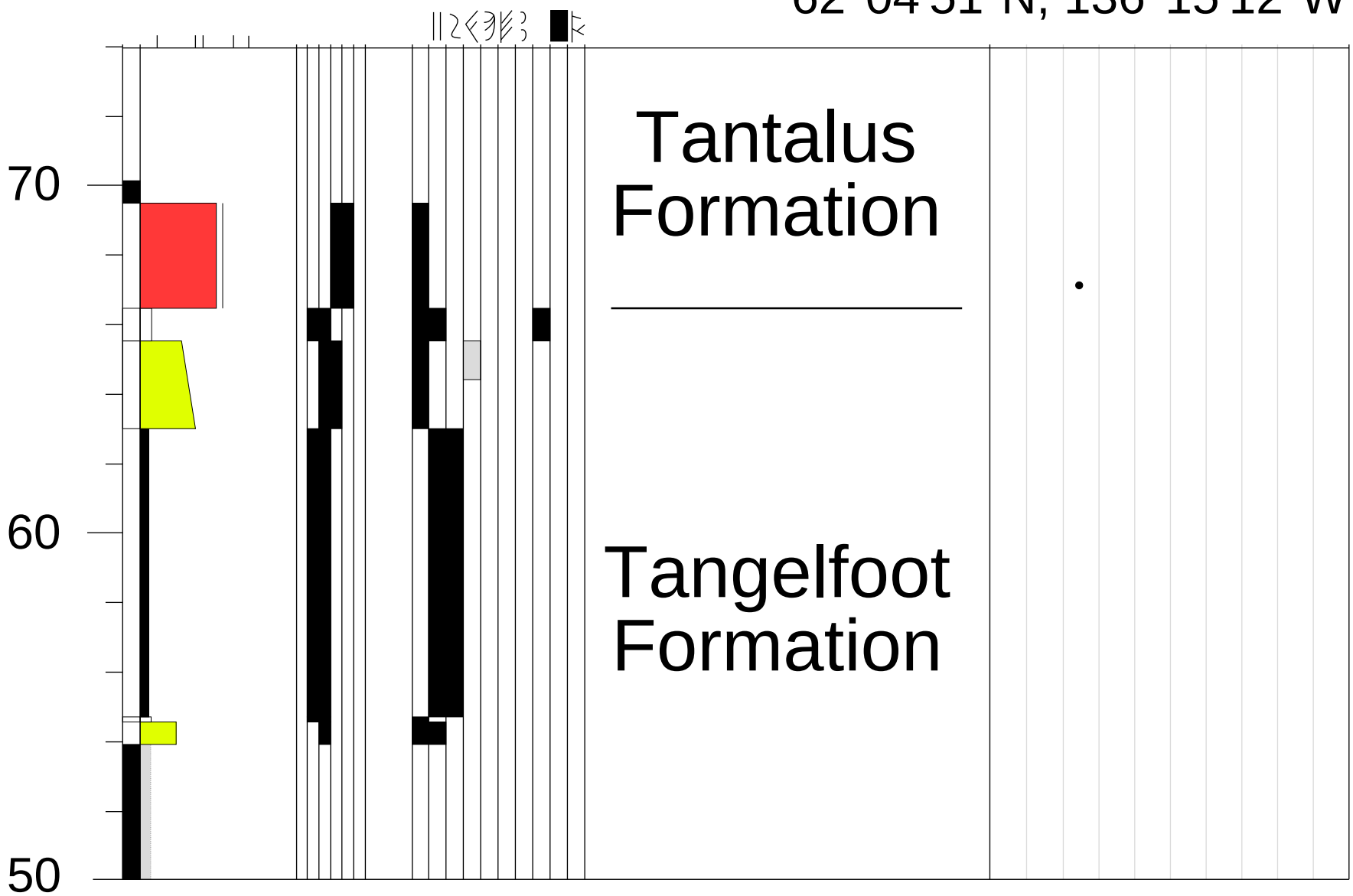

T12-E South of Carmacks

62°04369"N, 13614'46"W

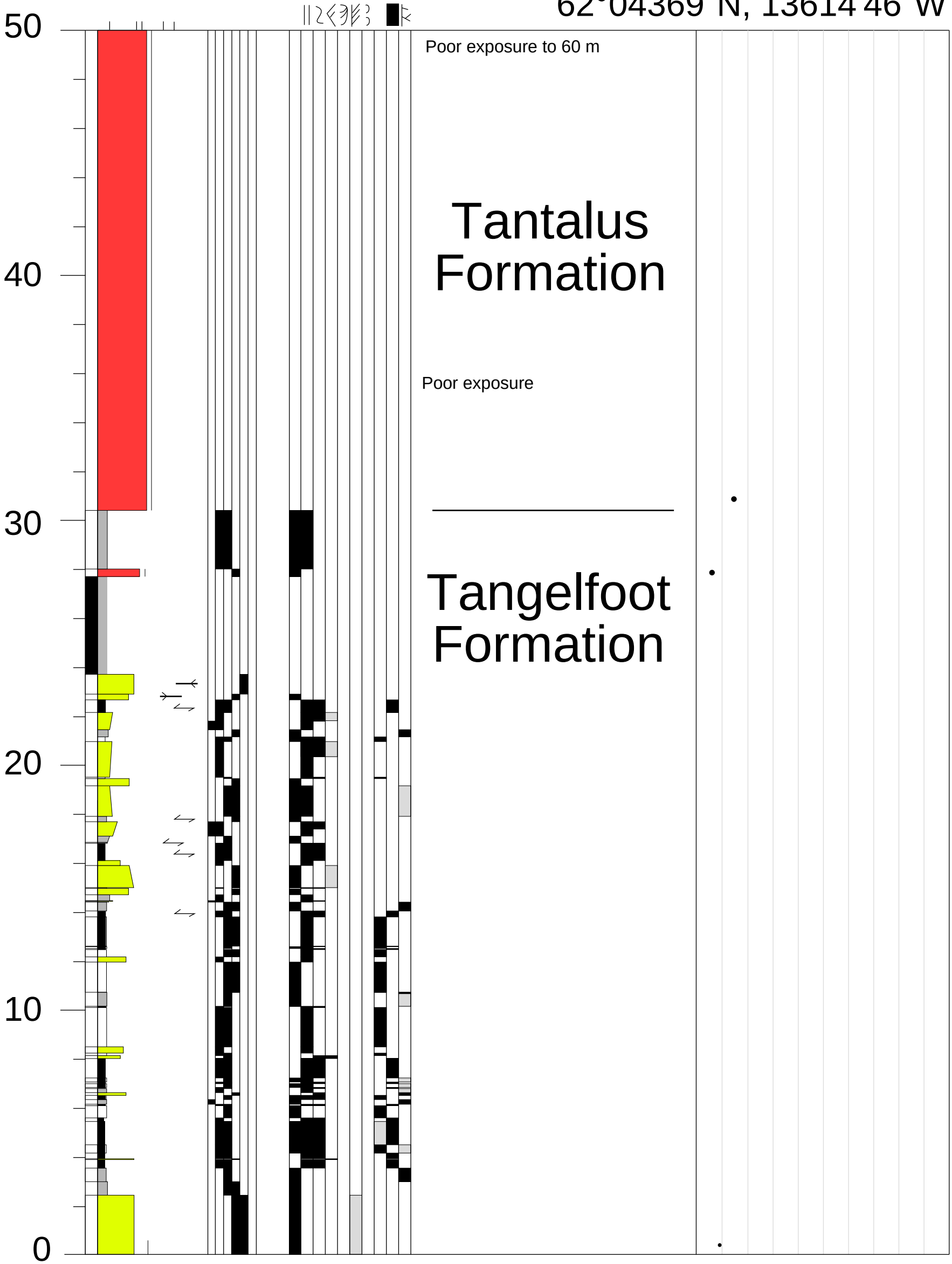

T12-F South of Carmacks

62°04'36"N, 136°14'37"W

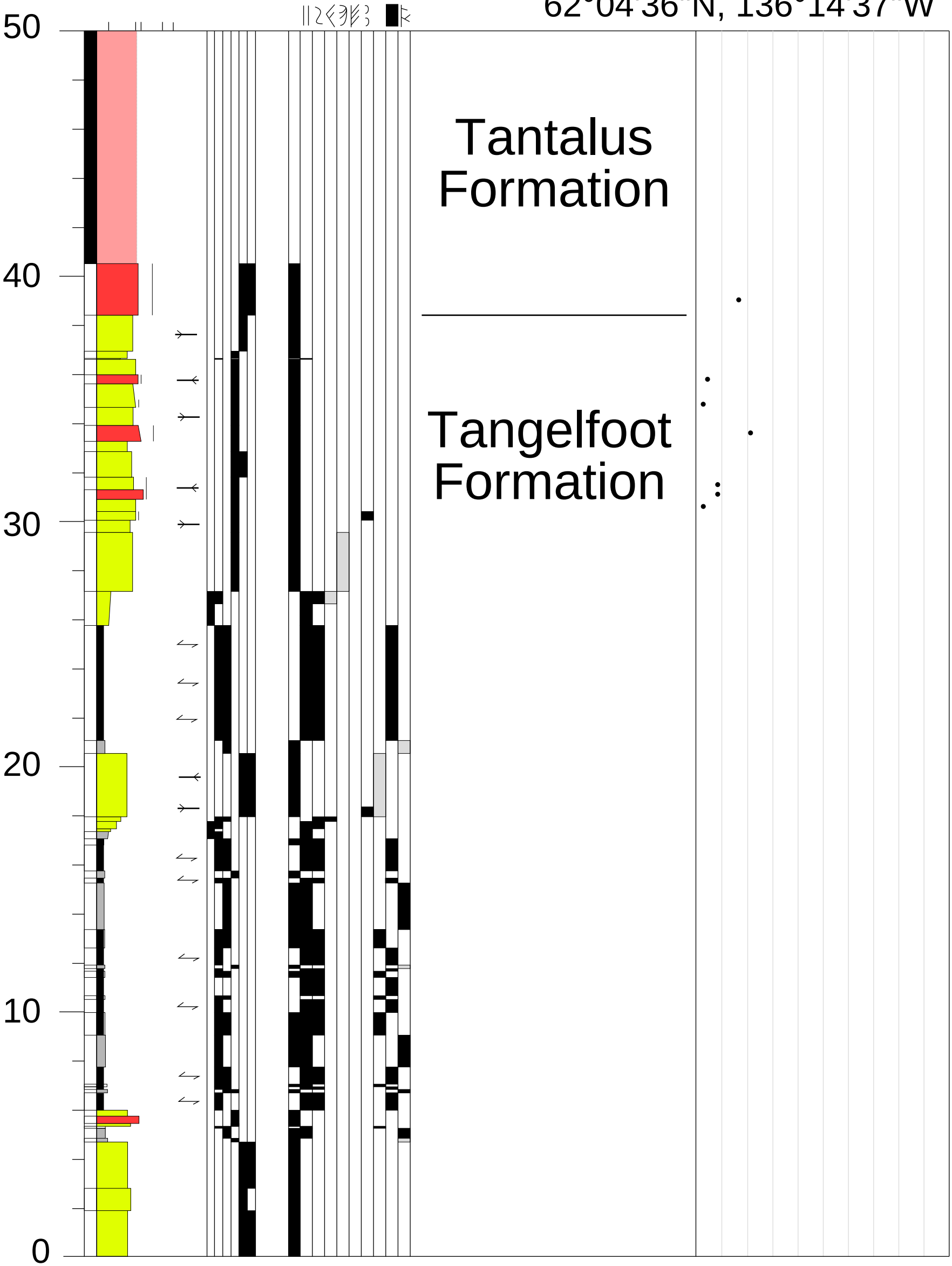

T13b Tantalus Butte mine, Open Pit

62°08'14"N, 136°15'51"W

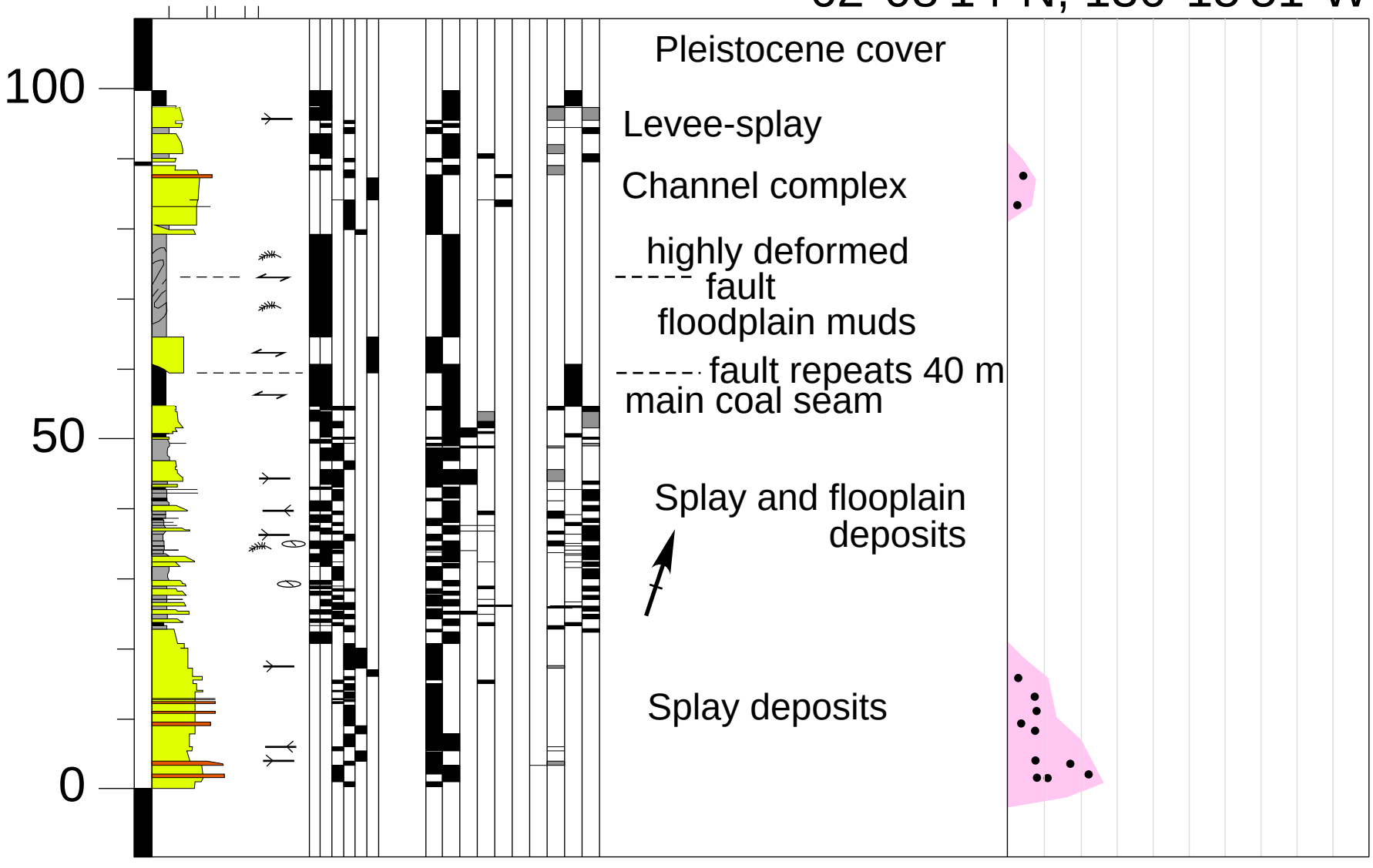

T13a Tantalus Butte, East side of Open Pit.

62°08'23"N, 136°15'50"W

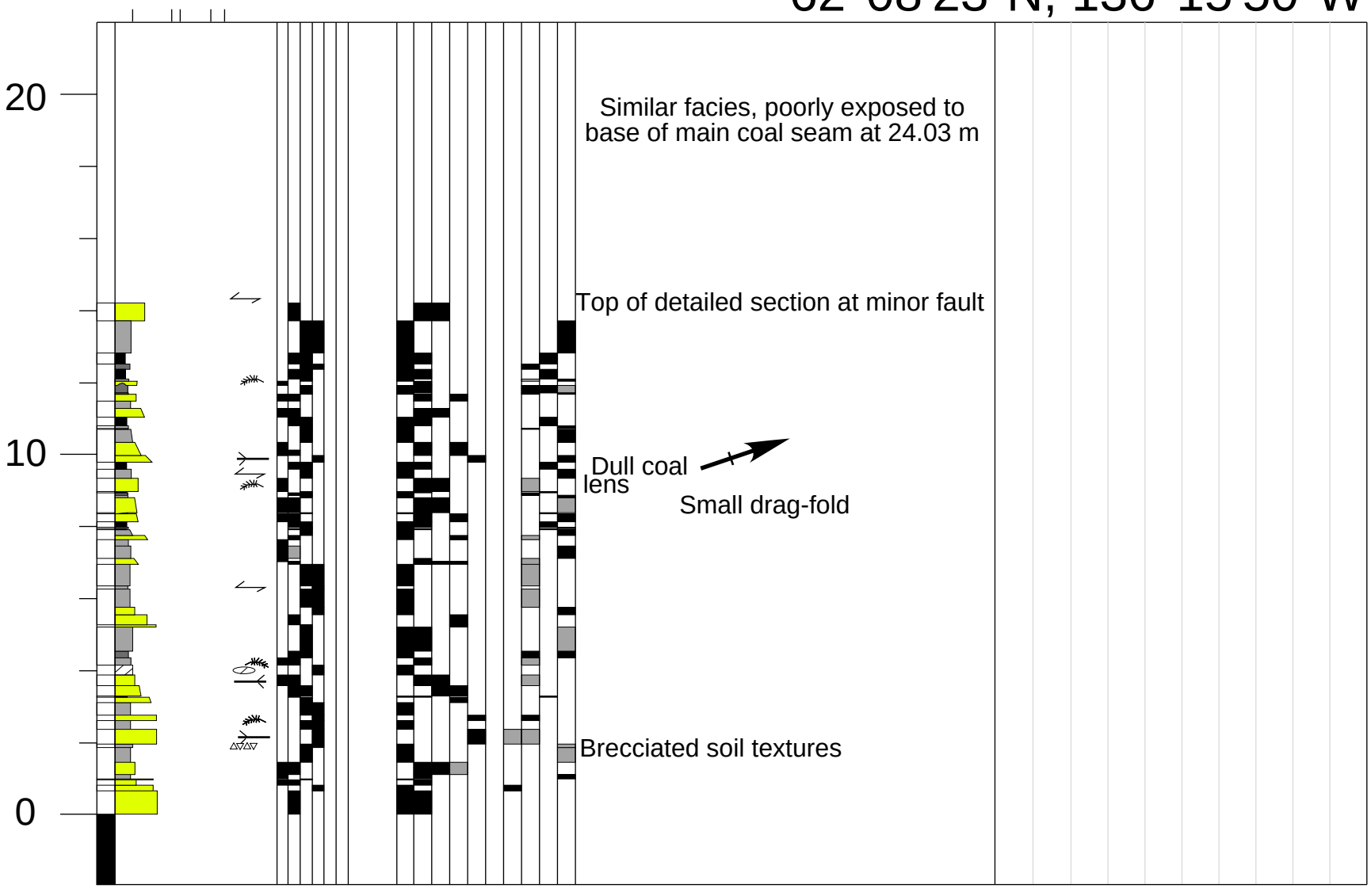

T13b Tantalus Butte mine, Open Pit

62°08'14"N, 136°15'51"W

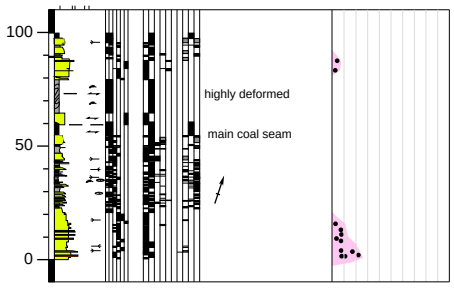

T13a Tantalus Butte, East side of Open Pit.

62°08'23"N, 136°15'50"W

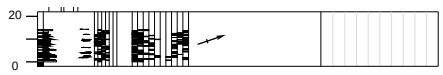

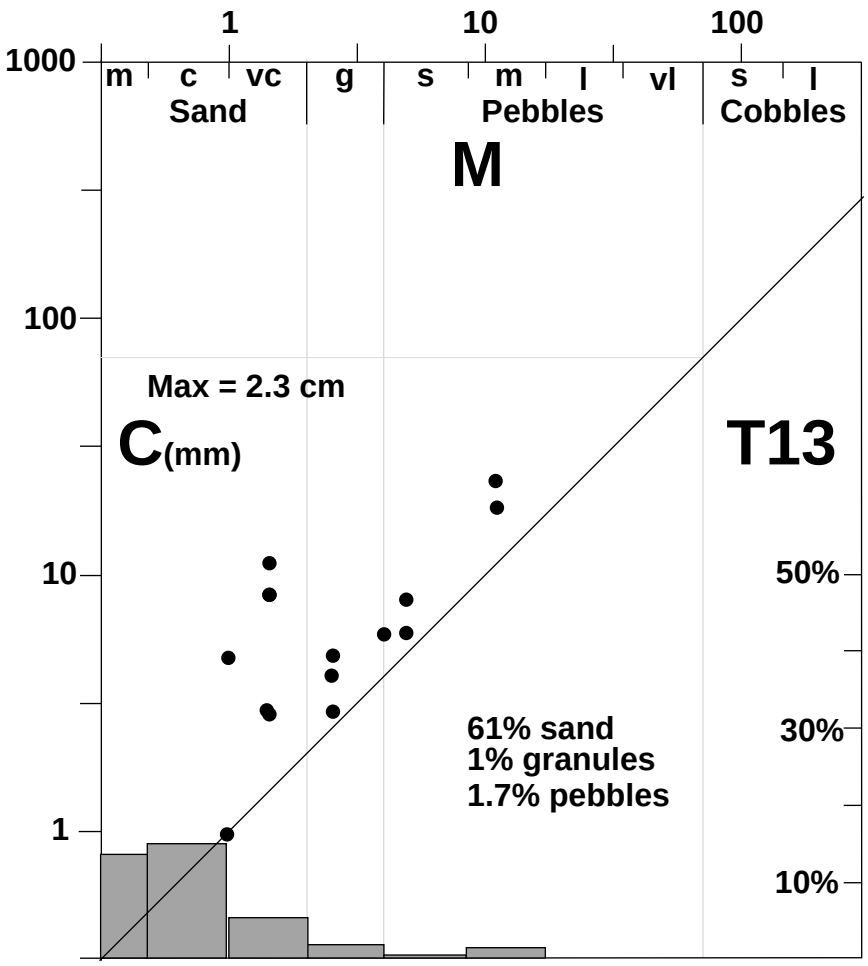

T14 Tantalus Butte, Trench

62°08'20"N, 136°15'33"W.

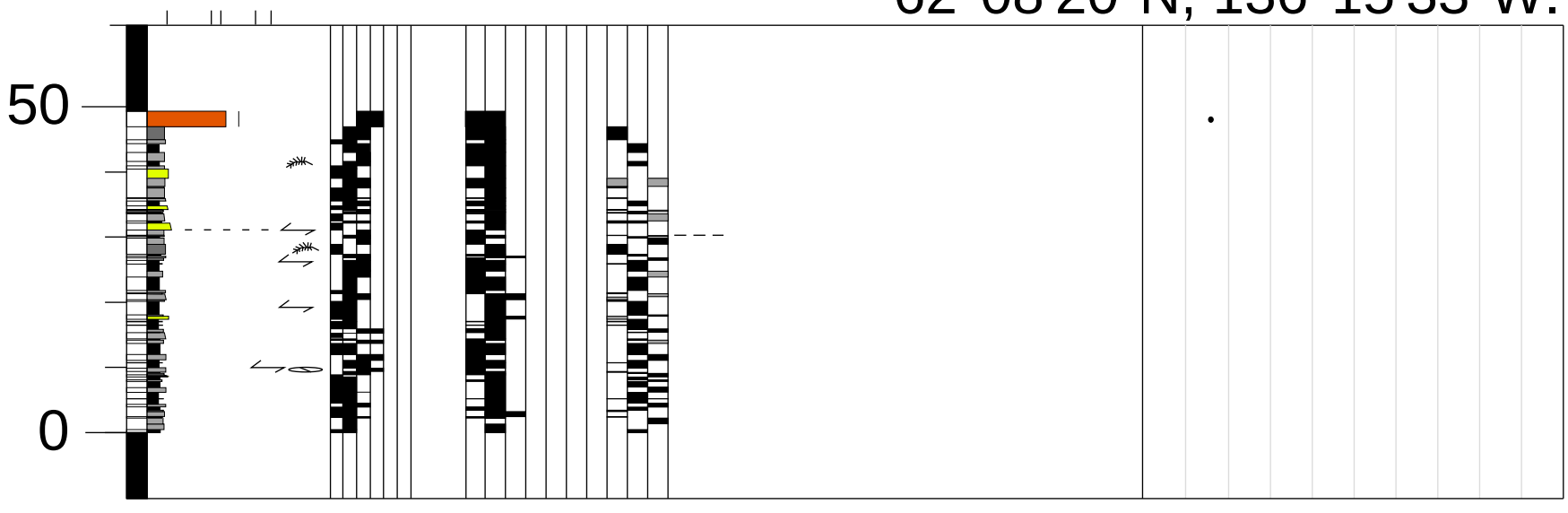

T16 Hootalinqua south

61°35'06"N, 134°50'45"W

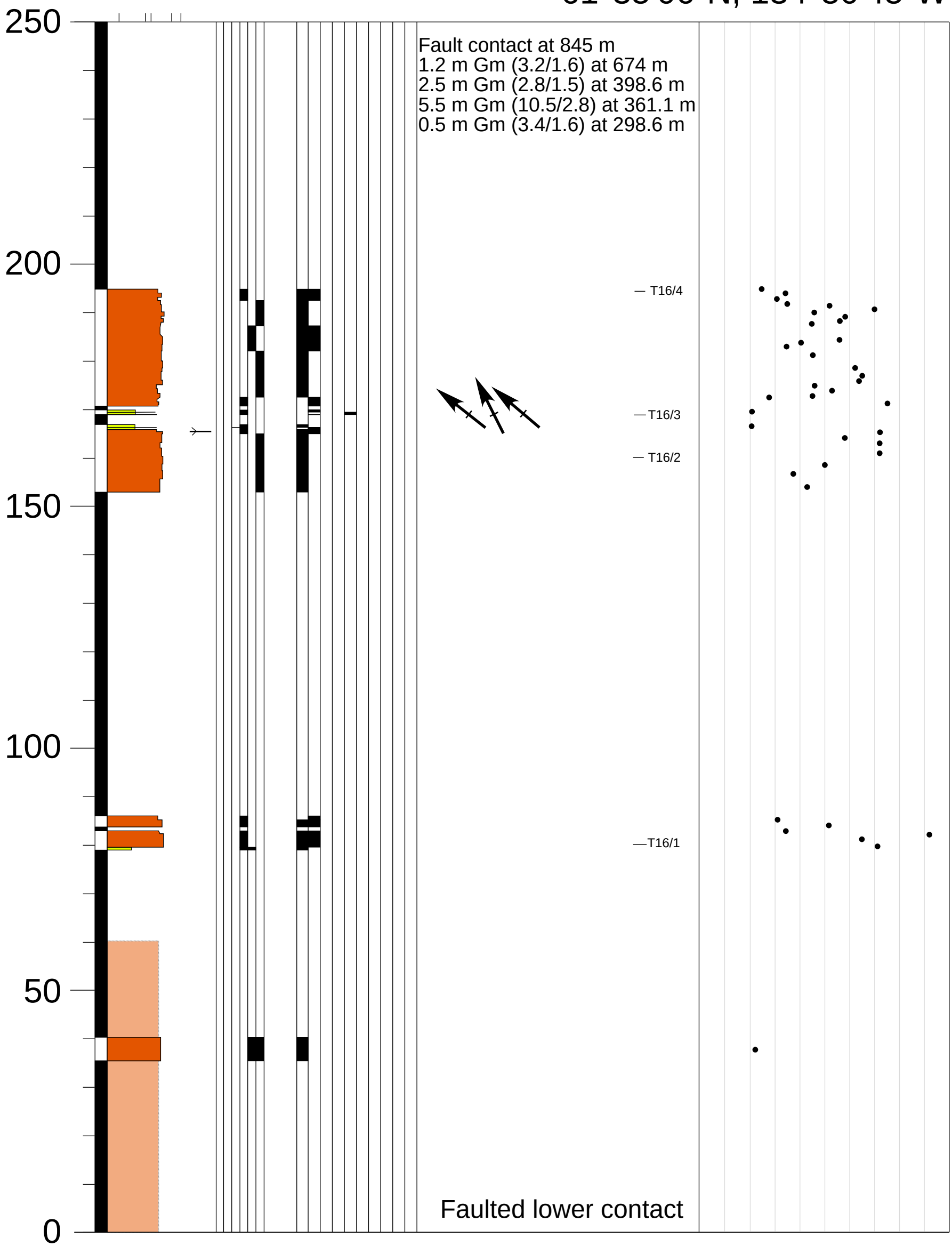

T16 Hootalinqua south

61°35'06"N, 134°50'45"W

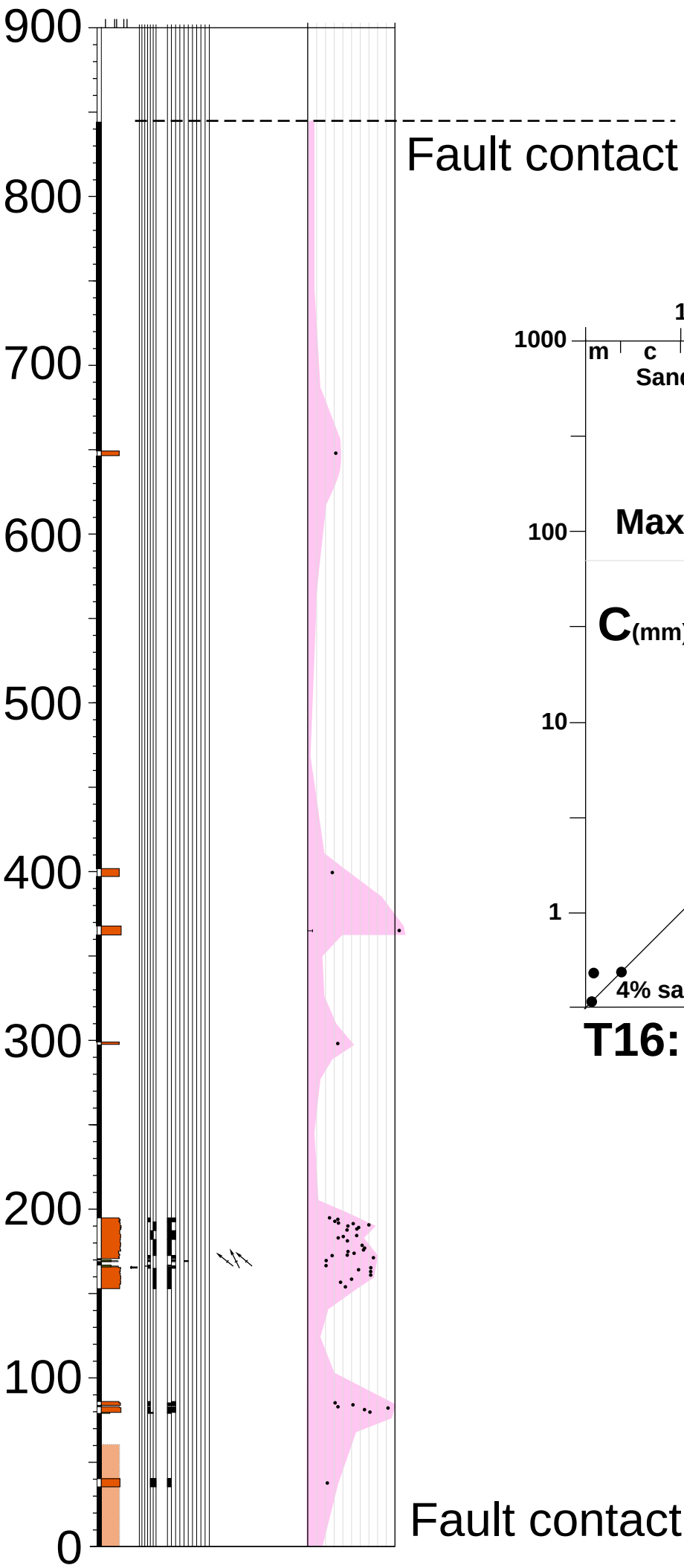

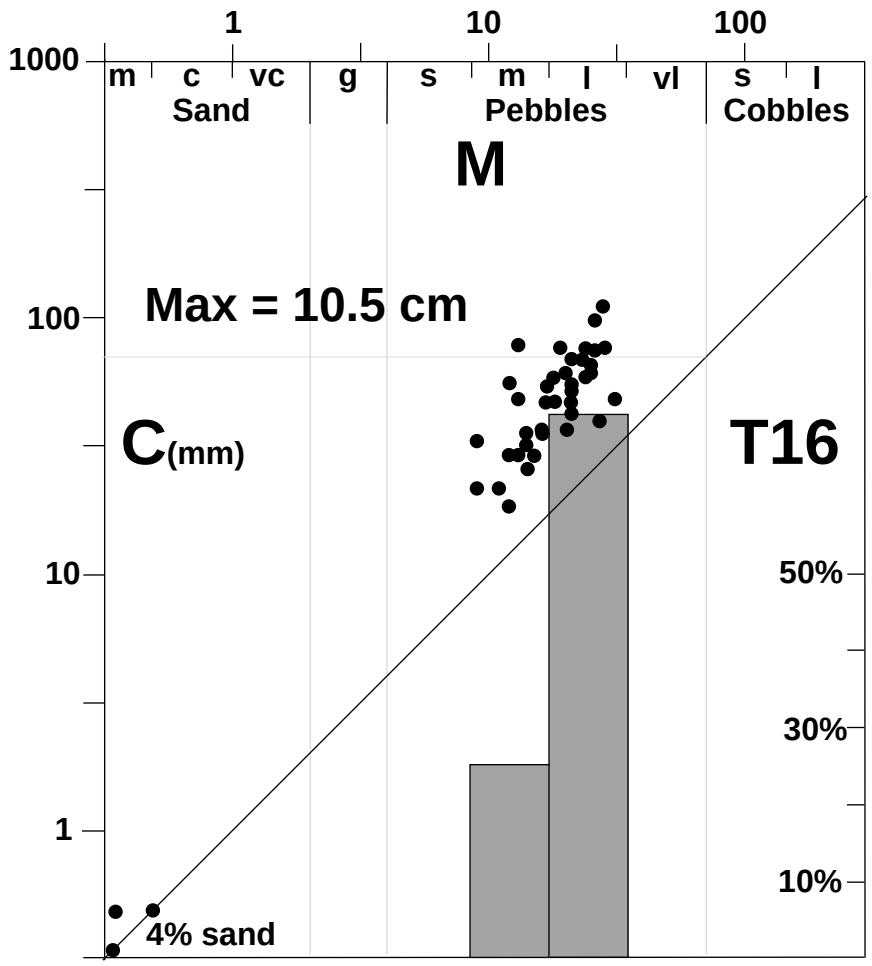

T16: Hootalinqua (South)

T17 Tantalus Butte Mine

62°07'34"N, 136°15'44"W.

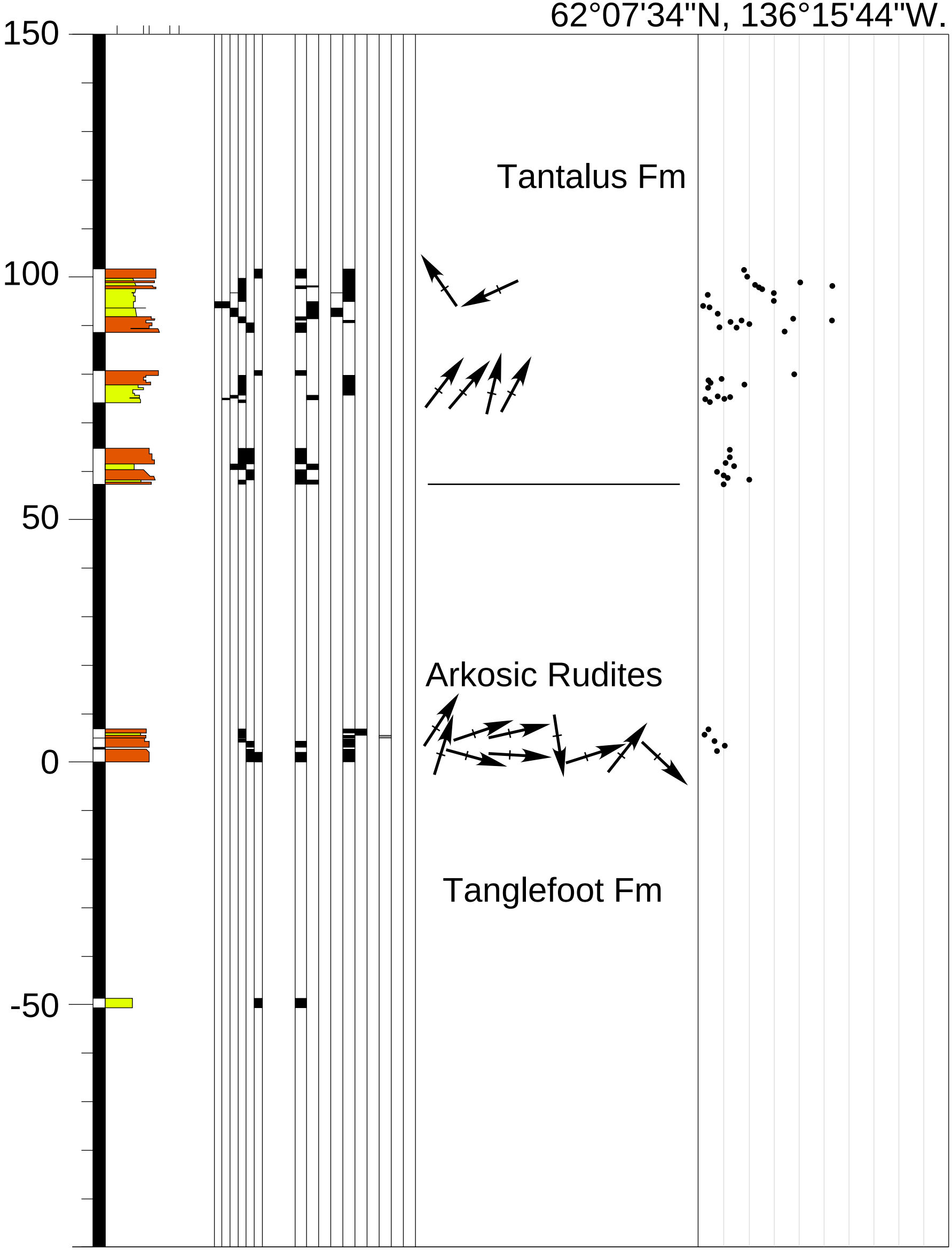

T17 Tantalus Butte Mine

62°07'34"N, 136°15'44"W.

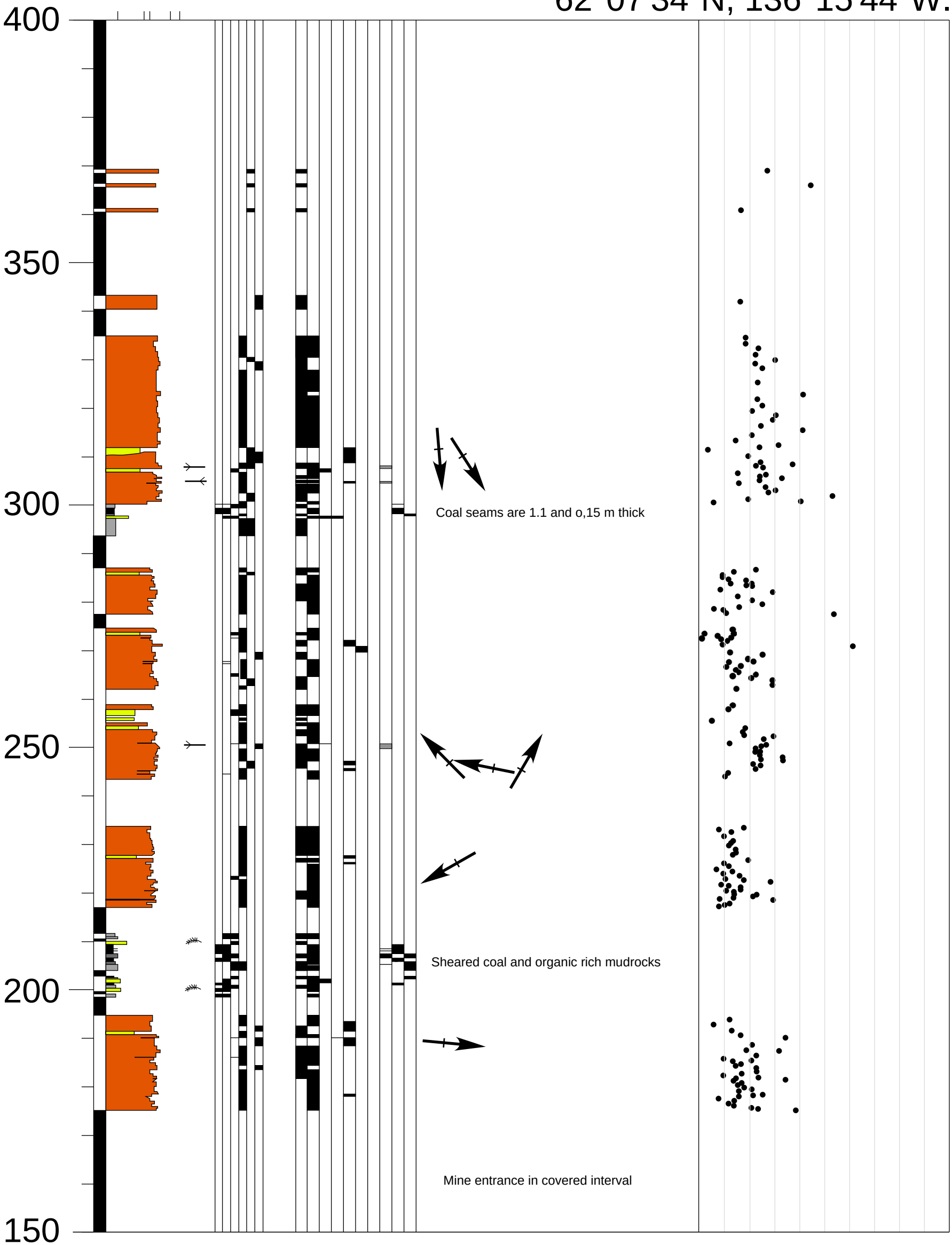

T17 Tantalus Butte Mine

62°07'34"N, 136°15'44"W.

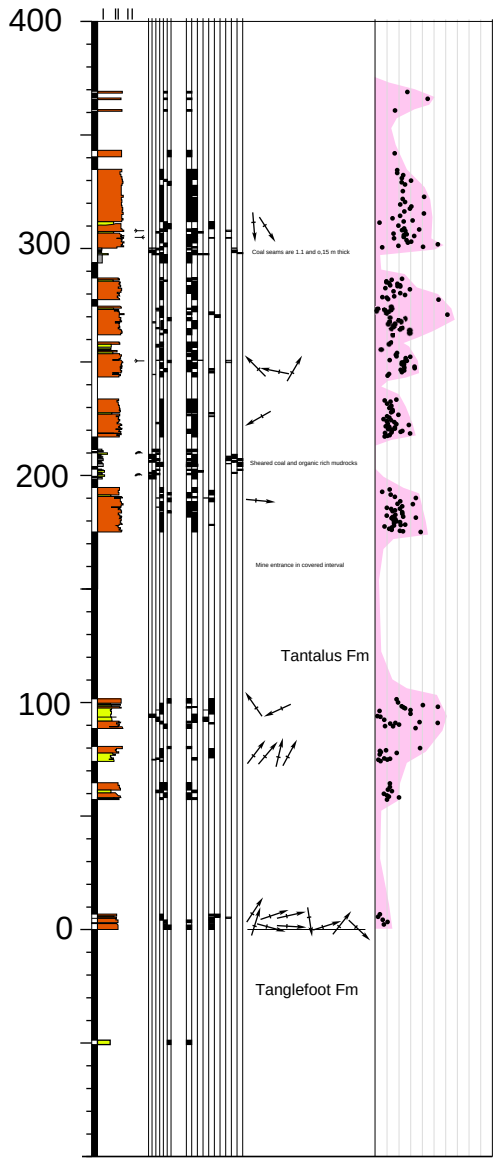

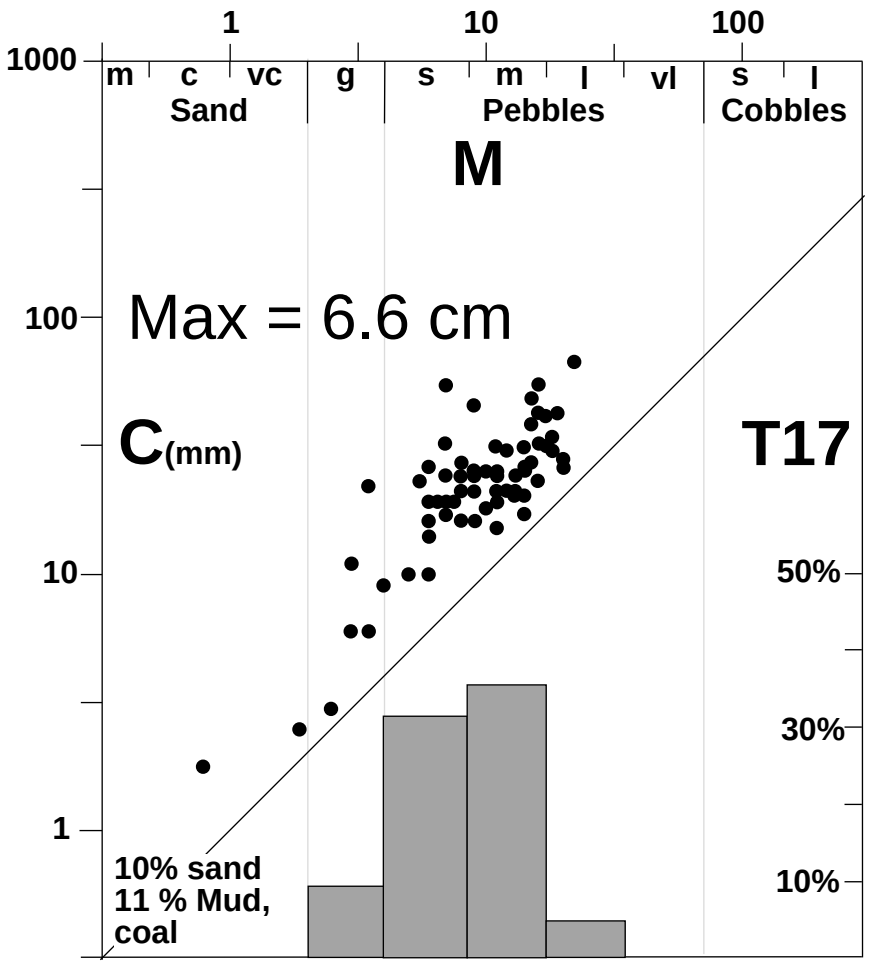

T18 Carmacks Dump

62°04'42"N, 136°15'57"W

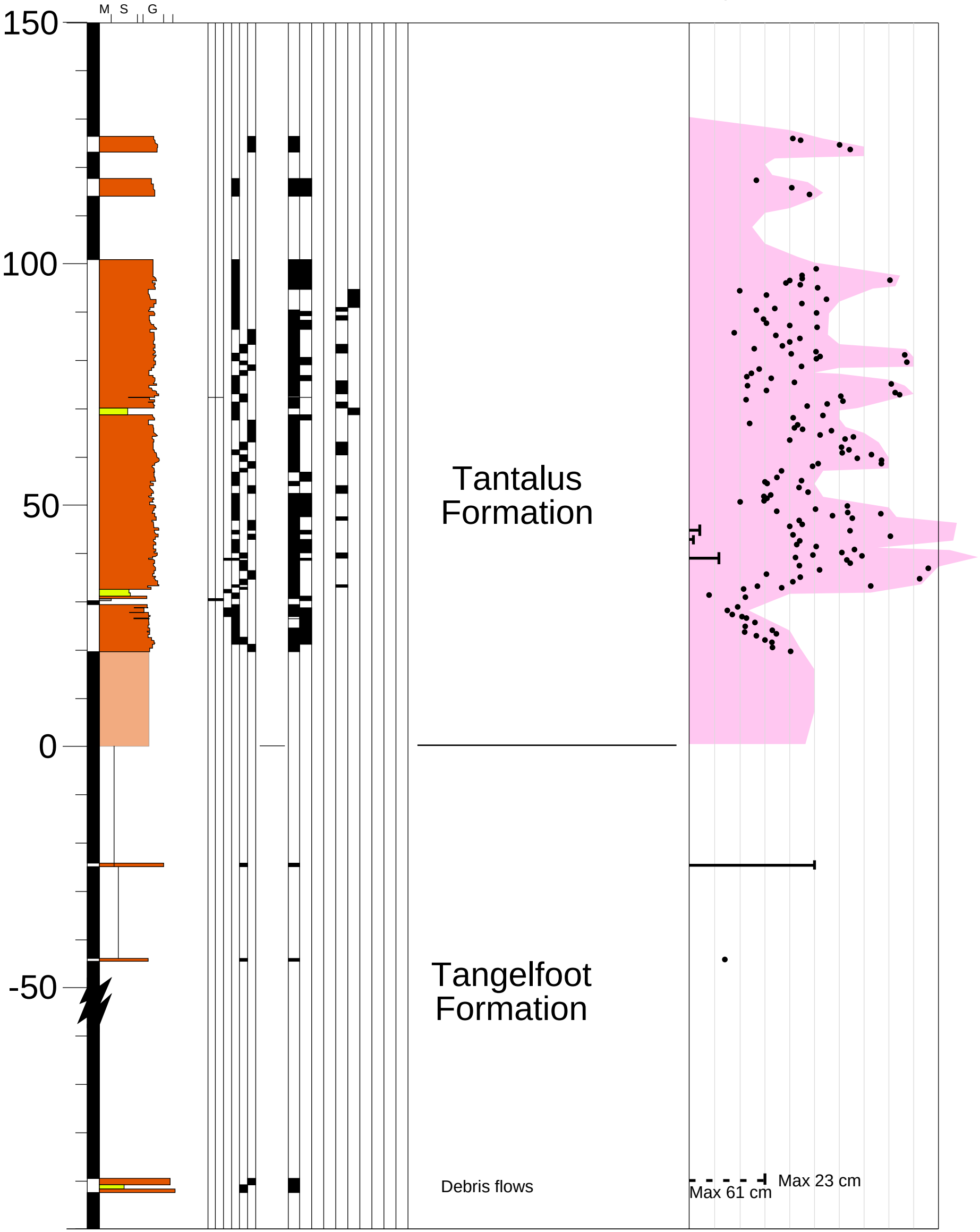

T18 Carmacks Dump
62°04'42"N, 136°15'57"W

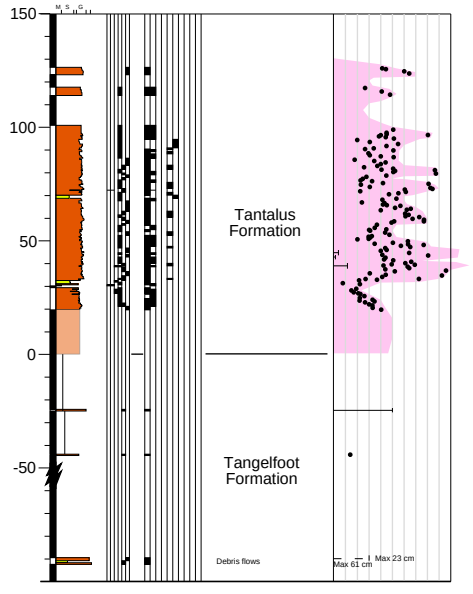

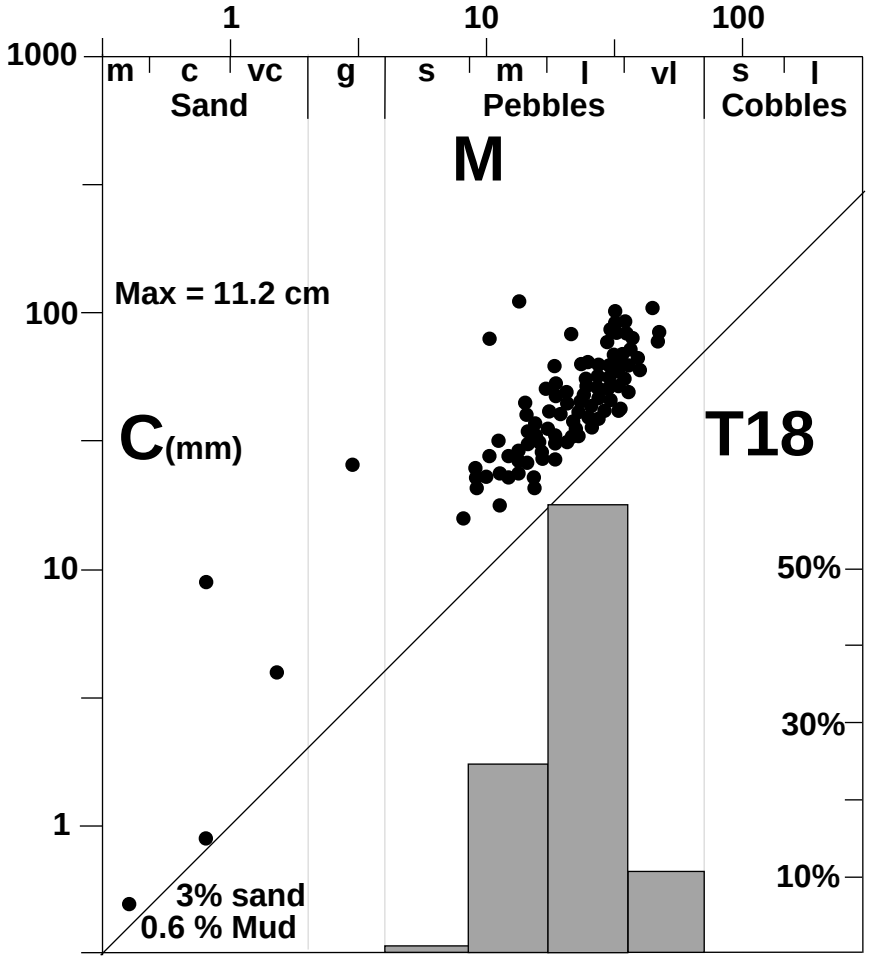

T19 Mt Granger

60°29'54"N, 135°16'42"W

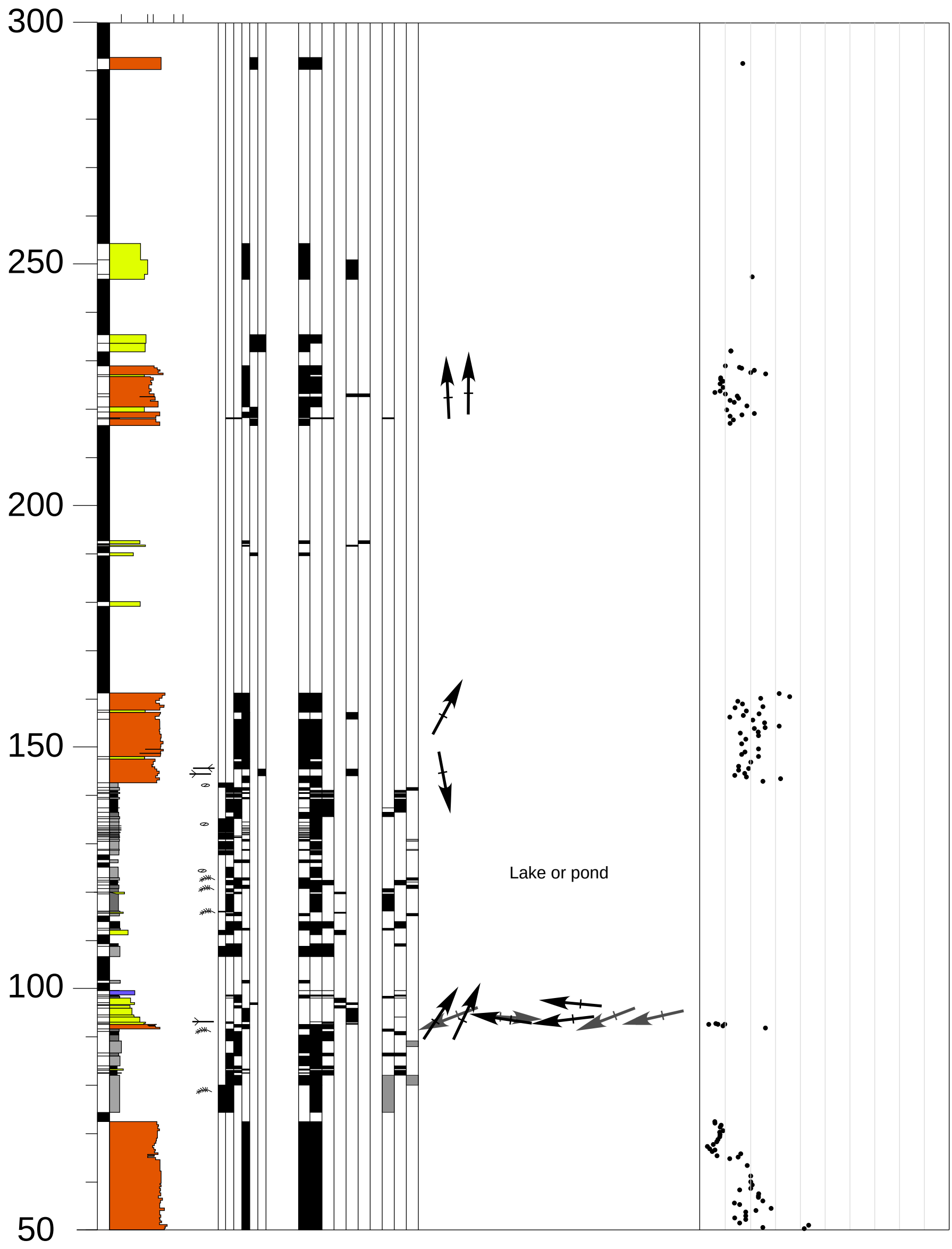

T19 Mt Granger

60°29'54"N, 135°16'42"W

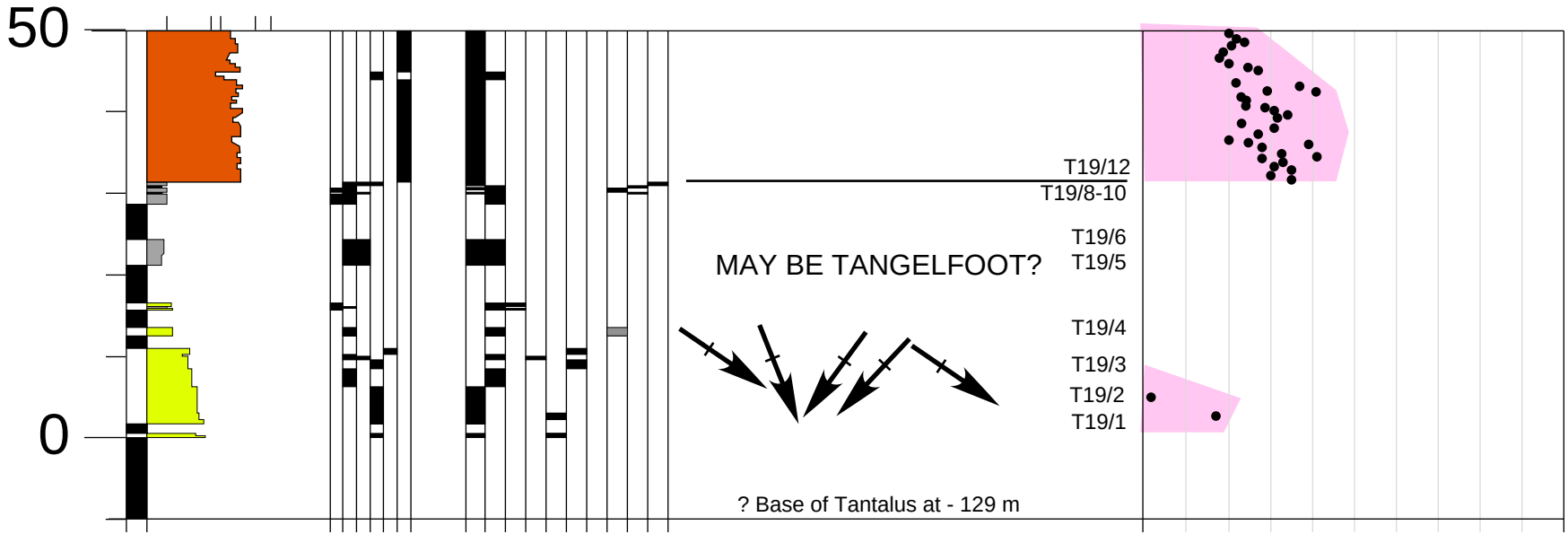

Mt Granger - supplimentary section

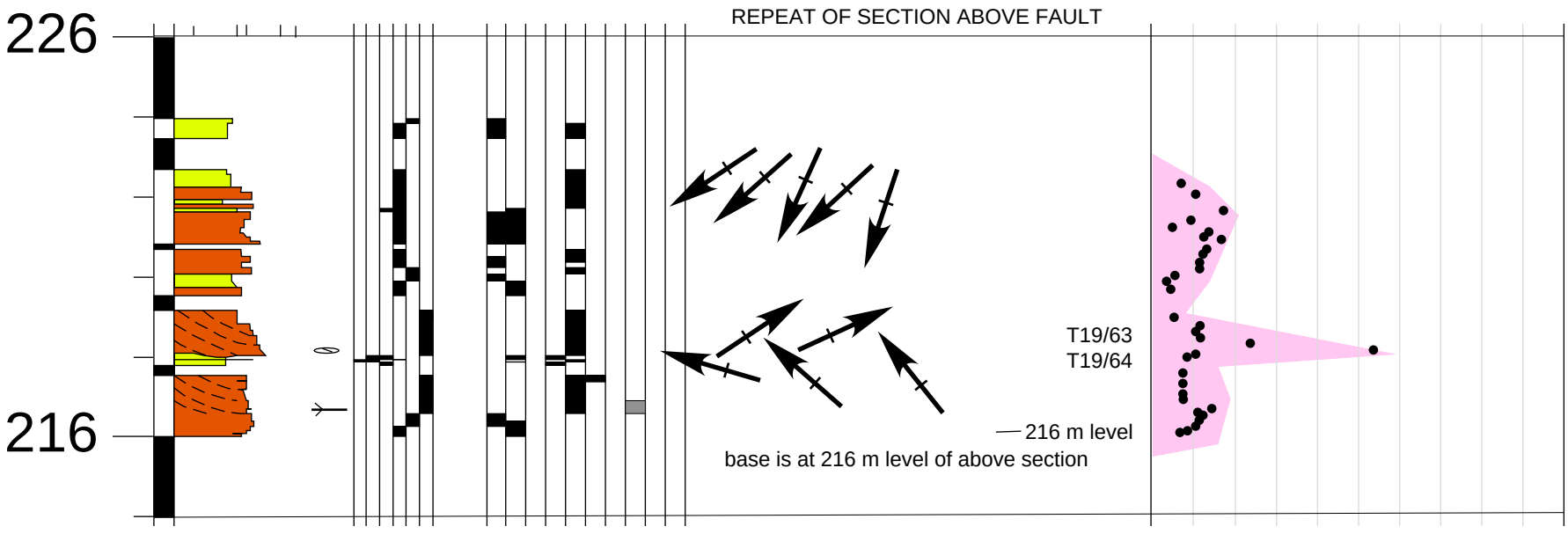

T19 Mt Granger

60°29'54"N, 135°16'42"W

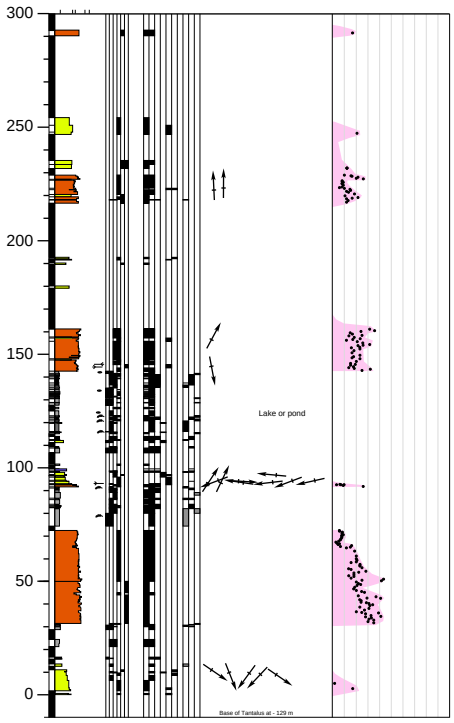

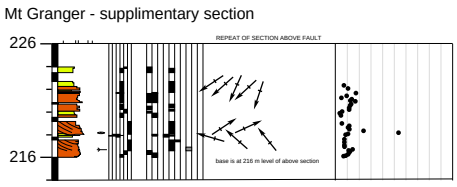

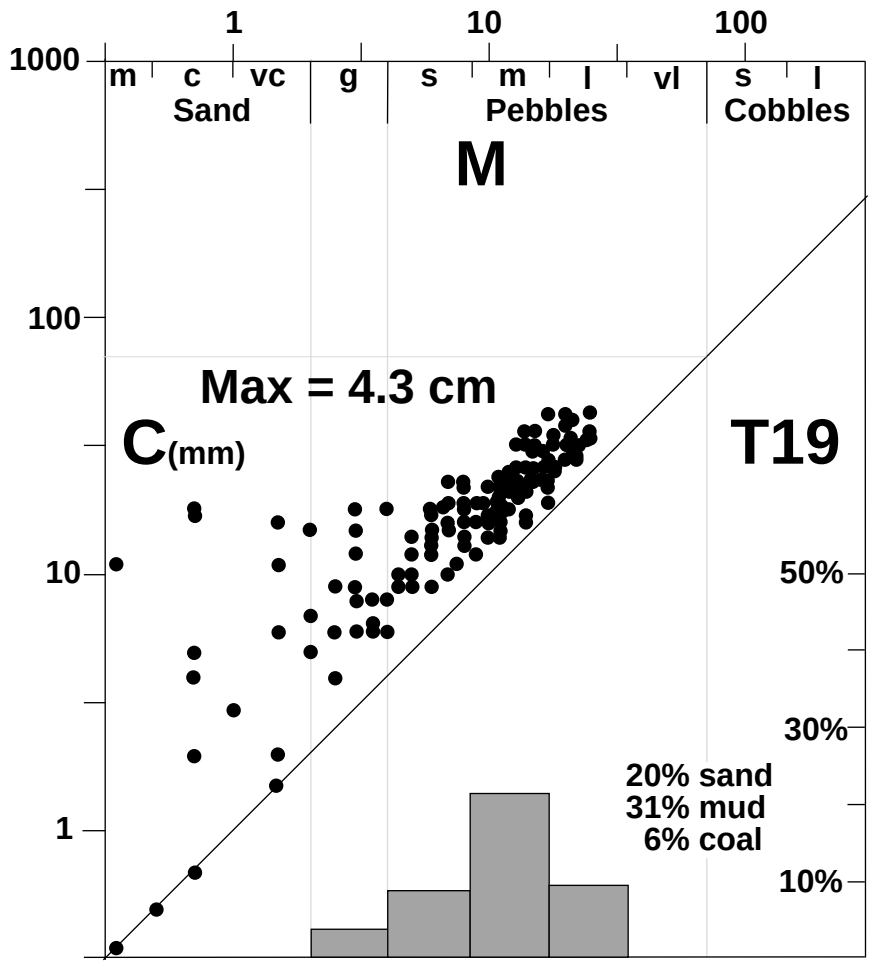

T19: Mt. Granger

T20 Mount Granger

60°29'29"N, 135°15'33"W

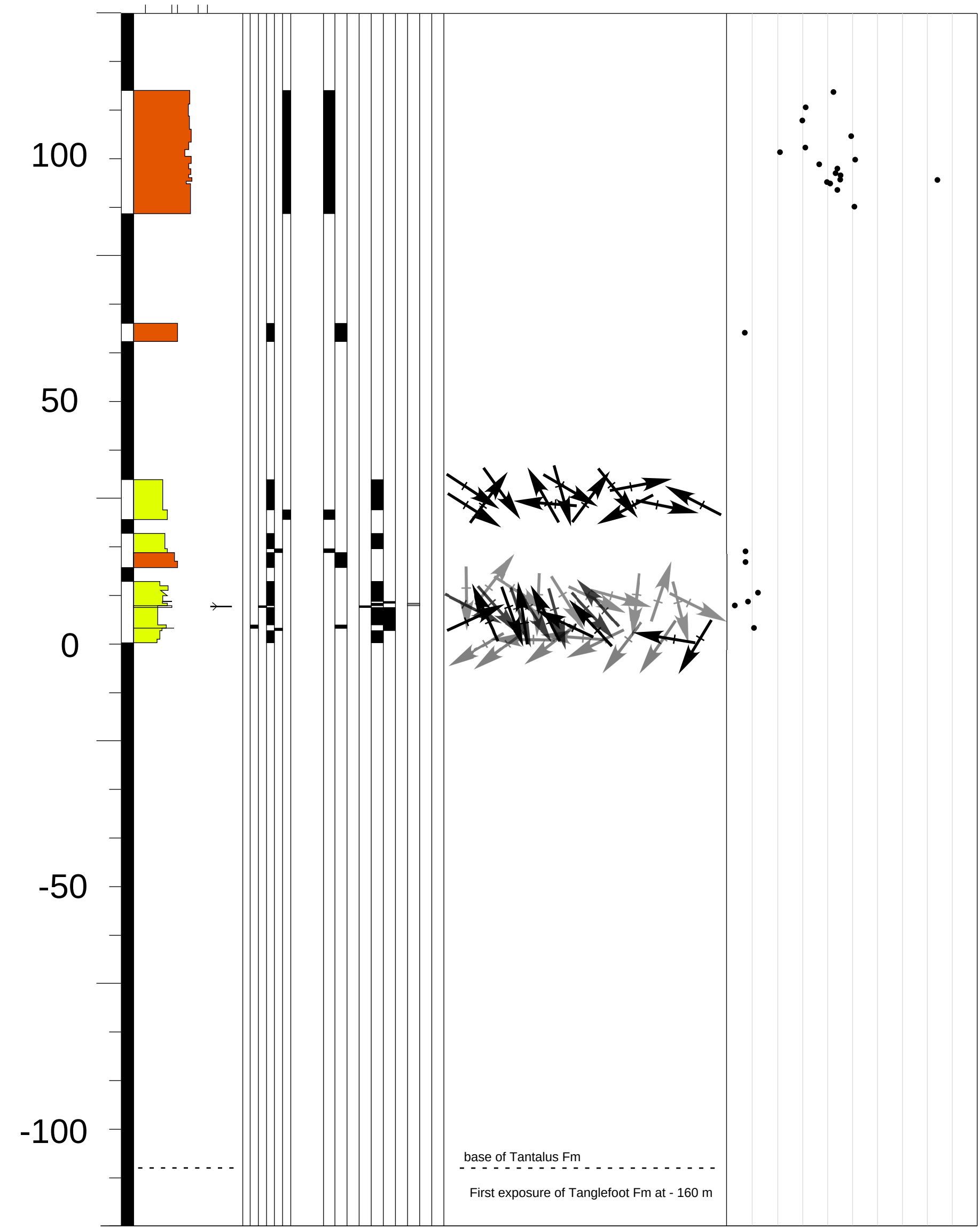

T20 Mount Granger

60°29'29"N,
135°15'33"W

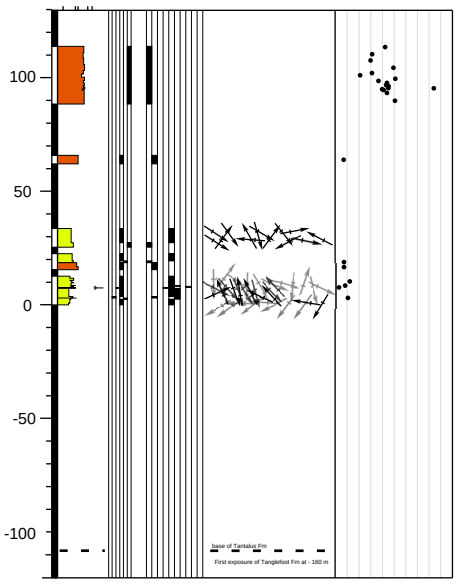

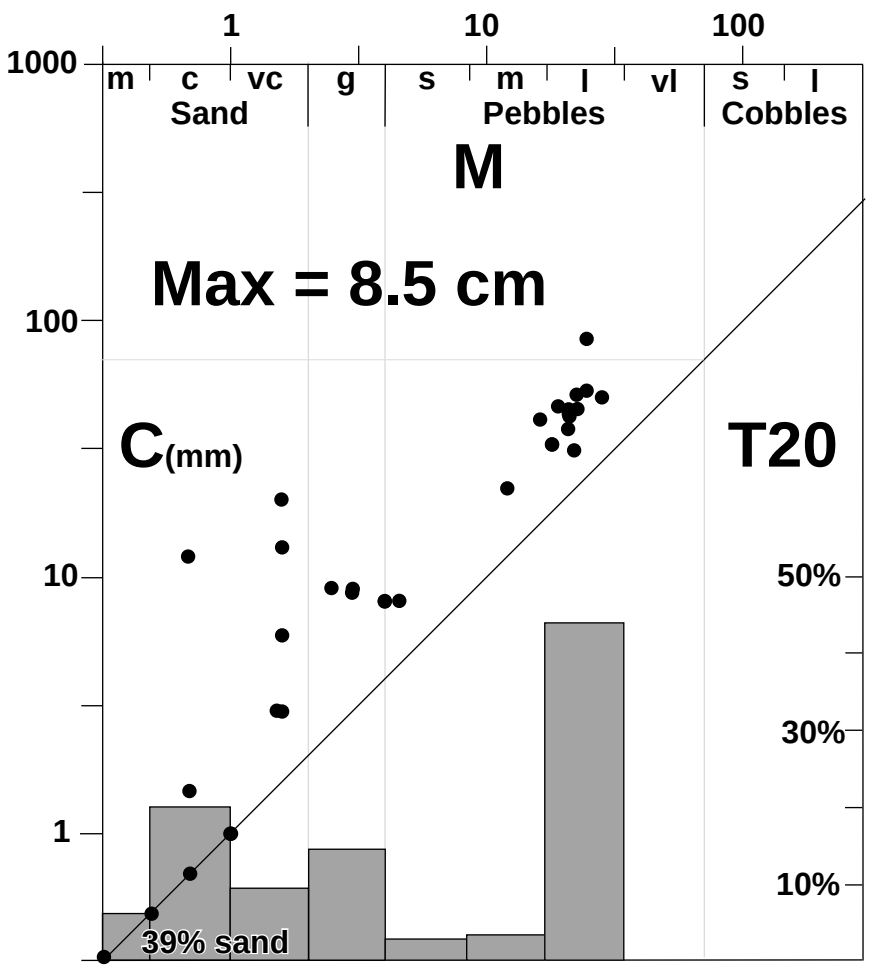

T-21 Ibex Valley

60°37'13"N, 135°26'34"W

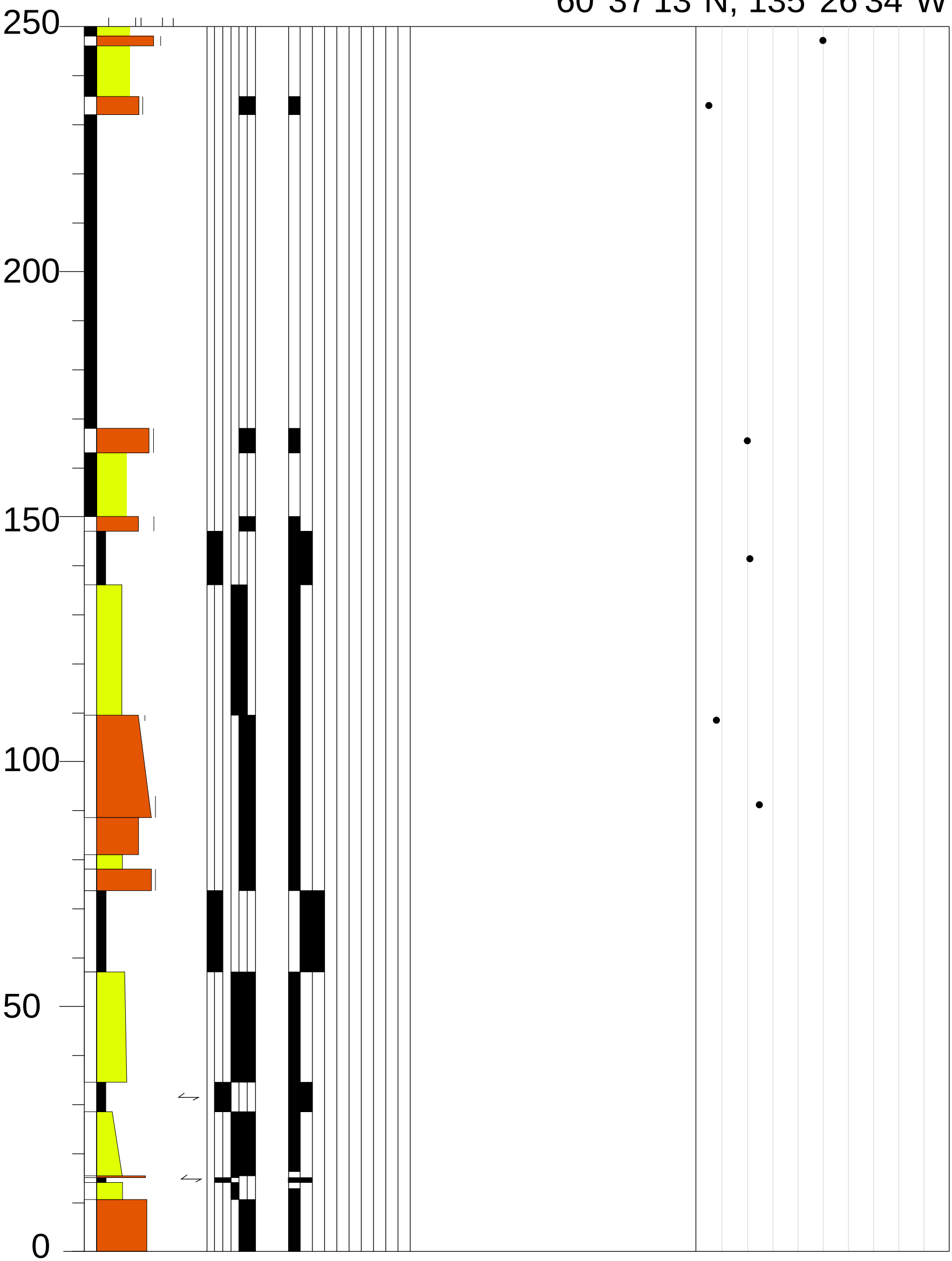

T-21 Ibex Valley

60°37'13"N, 135°26'34"W

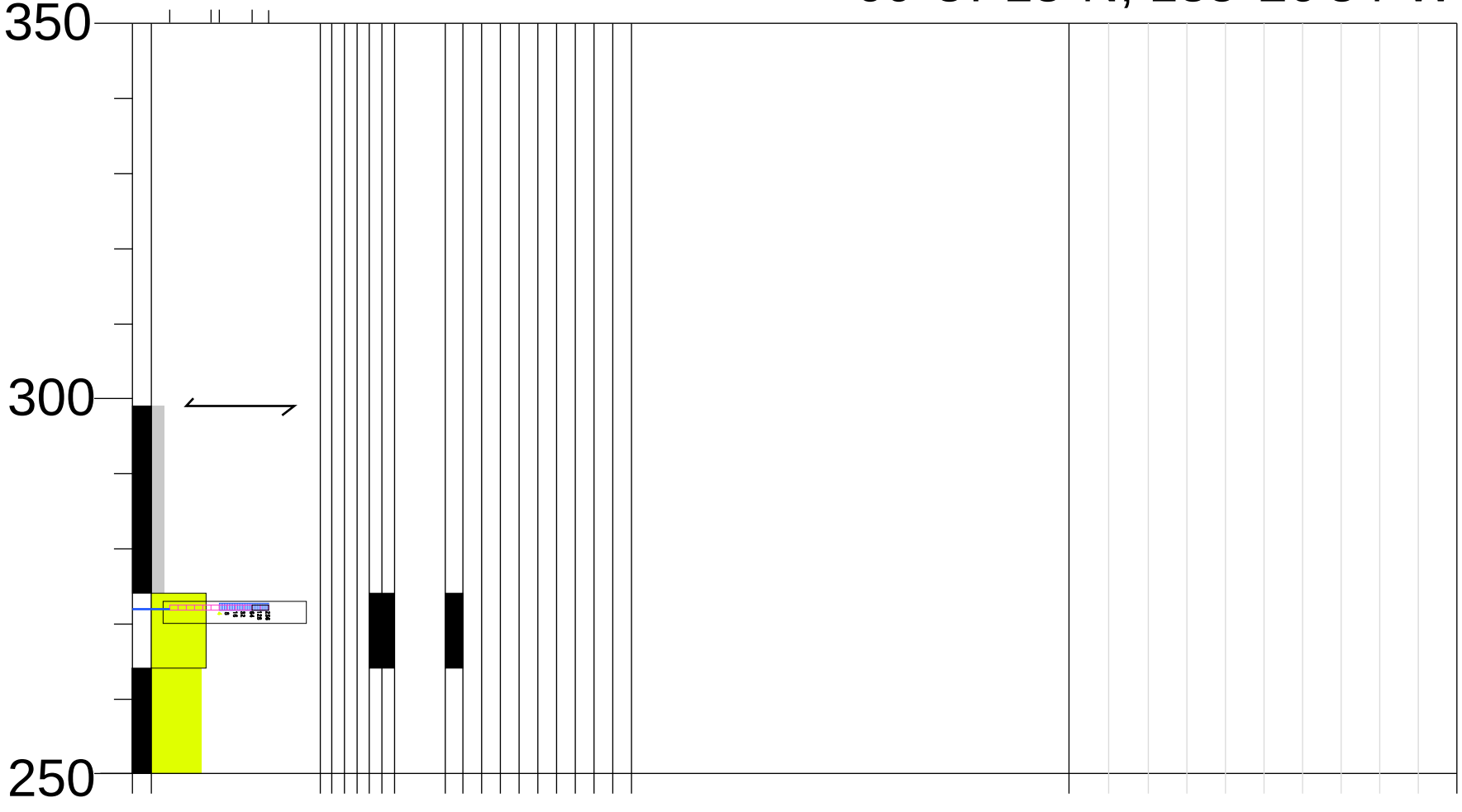

T-21 Ibex Valley

60°37'13"N,
135°26'34"W

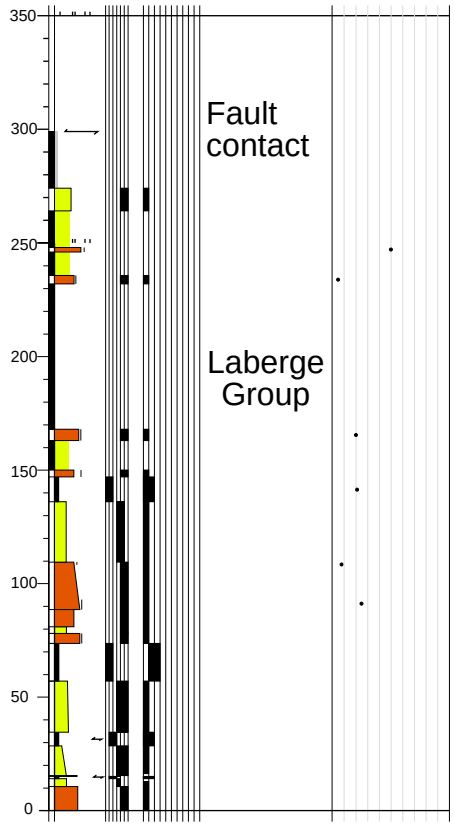

Section 23 Mt Granger

60°29'42"N, 135°17'16"W
60°29’56"N, 135°17’56"W

250
200
150
100
50
0

Large gap, estimated based on 38° dip

4 m wide channel

60°29'42"N, 135°17'16"W

Section 23 Mt Granger

60°29'42"N, 135°17'16"W
60°29’56"N, 135°17’56"W

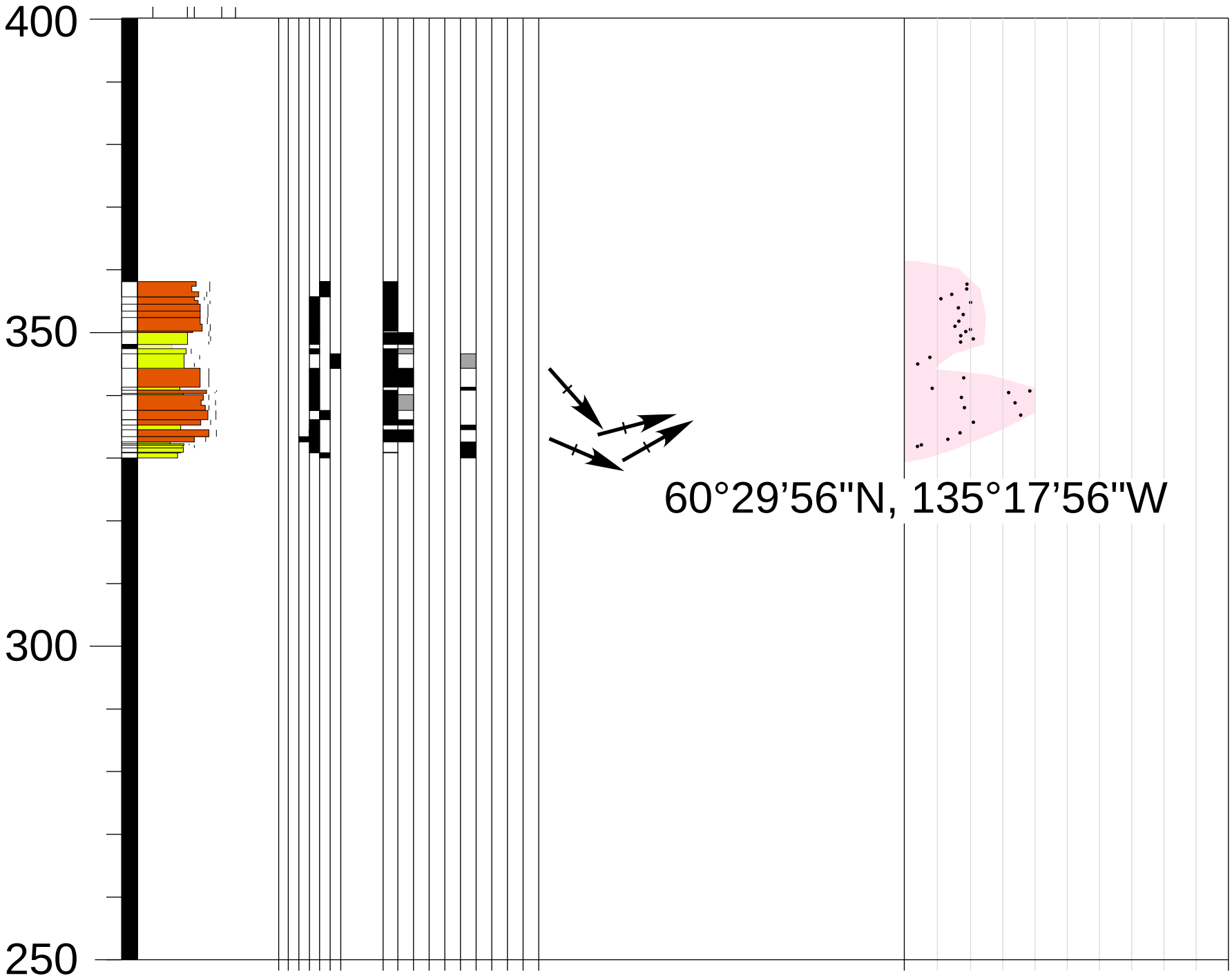

Section 23
Mt Granger

60°29'42"N, 135°17'16"W
60°29’56"N, 135°17’56"W

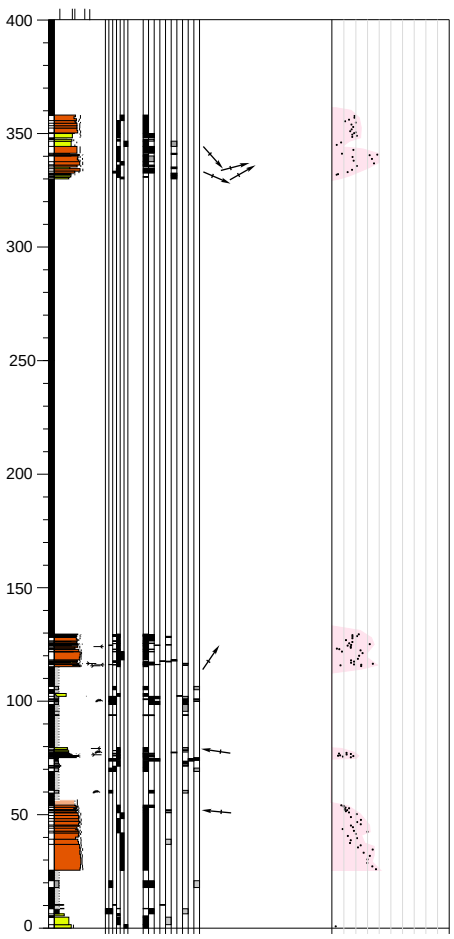

SAME AS T19

L3: Division Mountain, Teslin Creek

61°20'36"N, 136°04'49"W

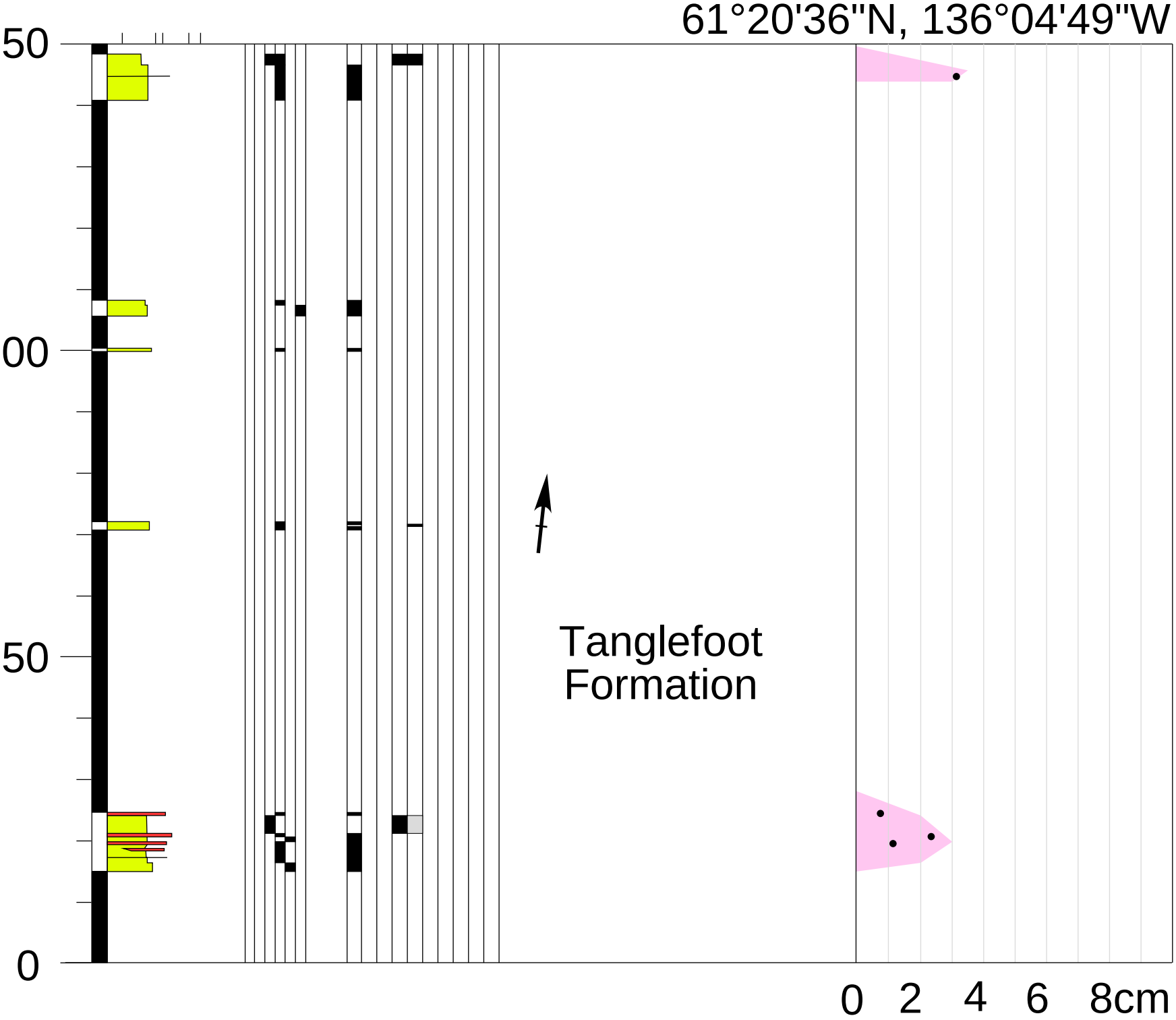

L3: Division Mountain, Teslin Creek

61°20'36"N, 136°04'49"W

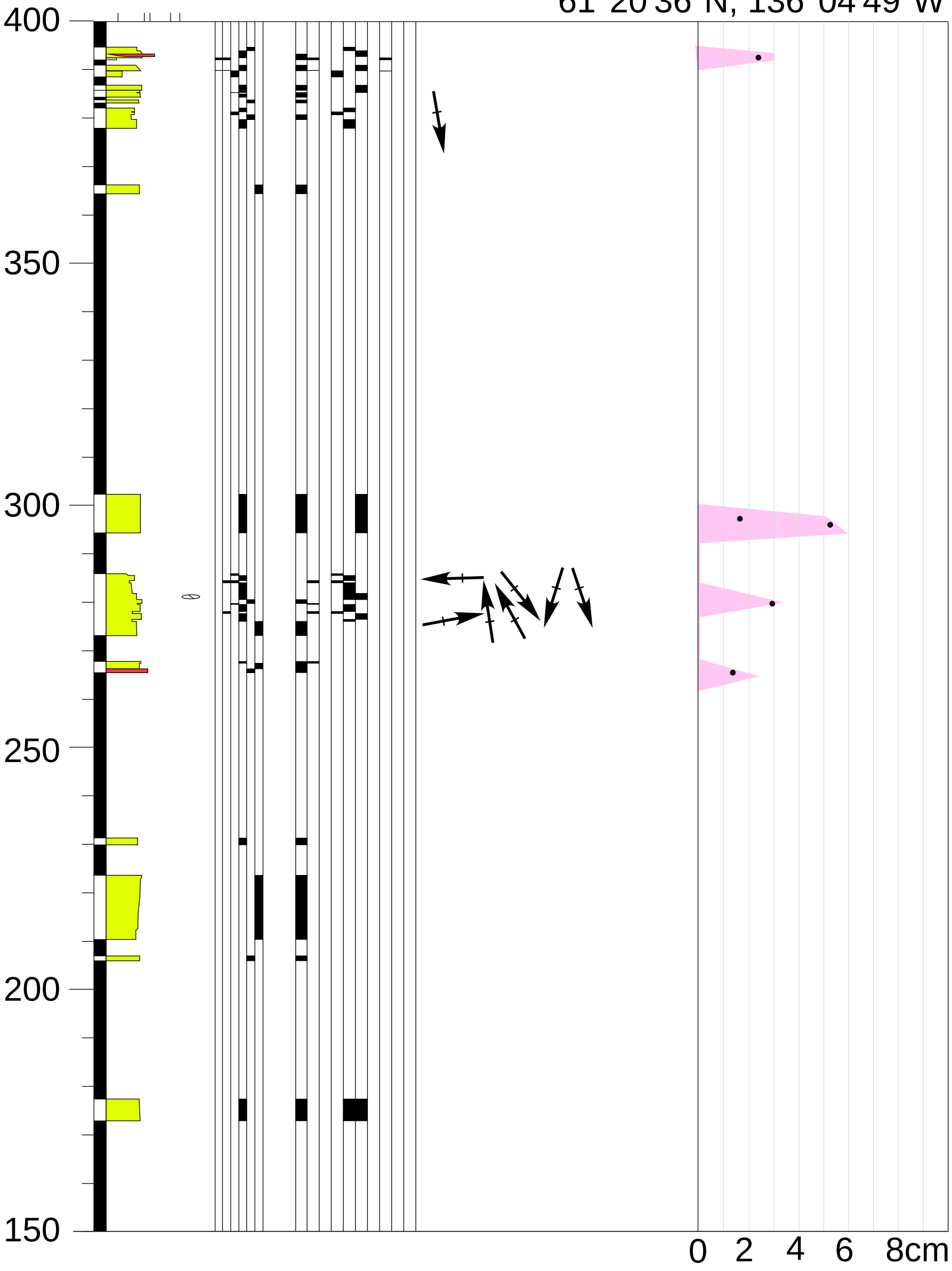

L3: Division Mountain, Teslin Creek

61°20'36"N, 136°04'49"W

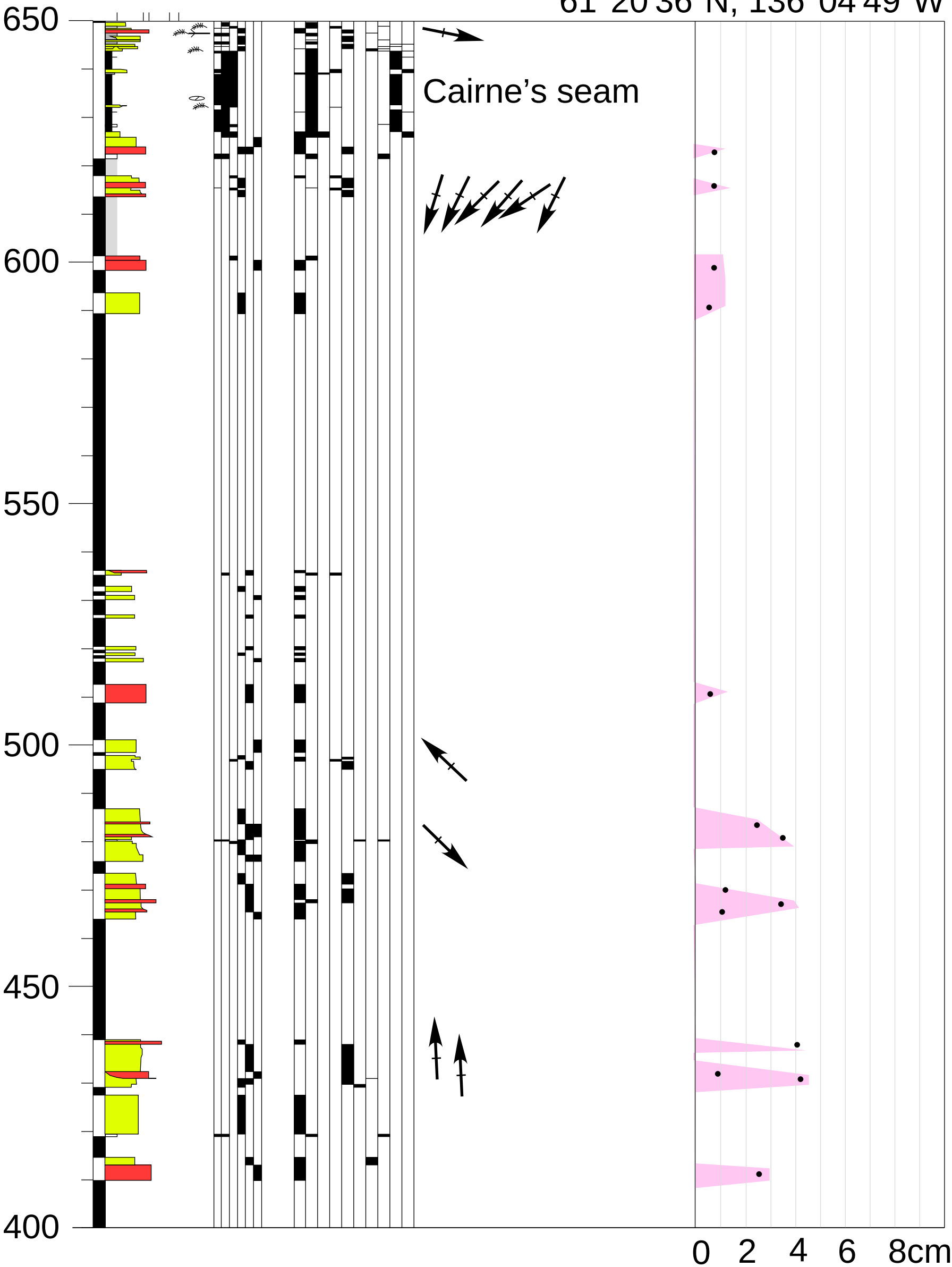

L3: Division Mountain, Teslin Creek

61°20'36"N, 136°04'49"W

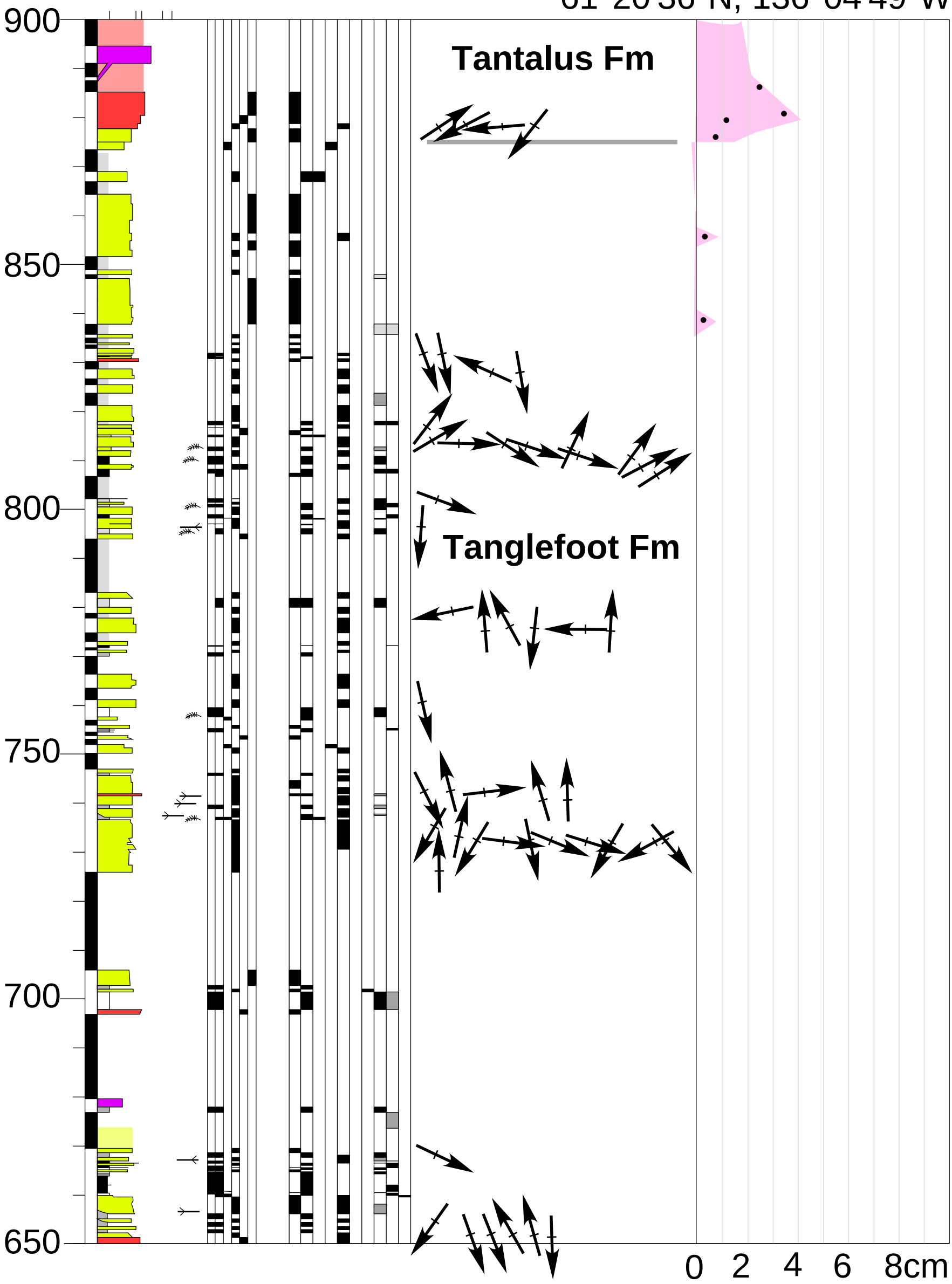

L3: Division Mountain
Teslin Creek

61°20'36"N
136°04'49"W

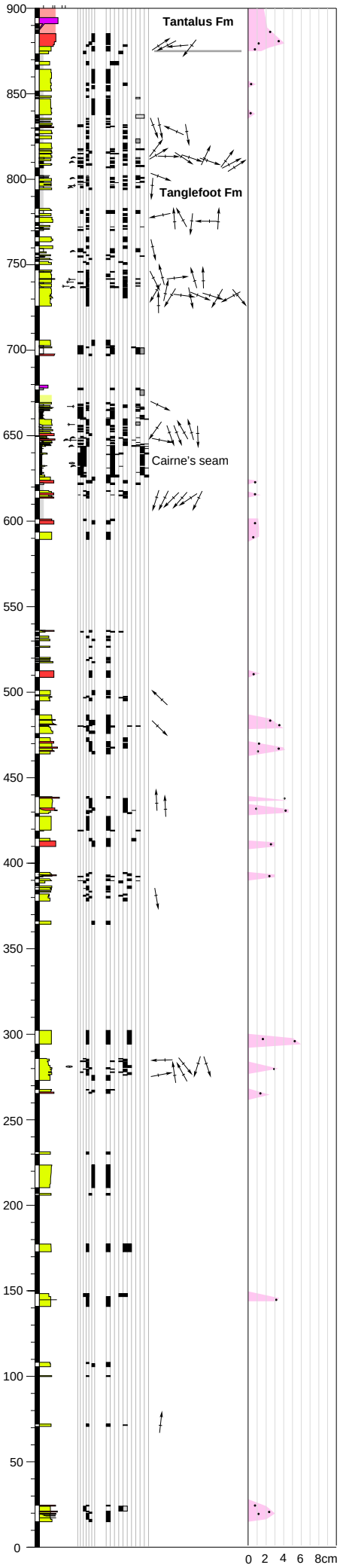

APPENDIX 2 - PETROLOGY

Table 1. Pebble counts
Table 2. Mount Granger
Table 3. Hootalinqua
Table 4. Carmacks
Table 5. Vowel-Braeburn
Table 6. All Tantalus Conglomerate
Table 7. All Tantalus Sandstone
Table 8. All Tanglefoot Conglomerate
Table 9. All Tanglefoot Sandstone

Note: the PDFs of these tables are all oversized; they are also available for download in excel format.

		Clast types (as count)										Calculated percentages						
Location	**Lithology**	**Black**	**Lt Grey**	**Grey-Brown**	**Red**	**Green**	**Qtz**	**Qtz-fedspathic**	**Sandstones**	**SAND (matrix)**	**Total**	***% Gravel***	**% Chert**	**% Qtz**	**% felsic RFs + Sst**	**% Black Chert**	**% Lt Grey Chert**	**%Grey-Brown chert**
Carmacks / Tantalus Butte				T10, 12, 13, 17, 18														
T10-1	sG	139	91	126	0	3	119	2	6	141	627	*77.5*	73.9	24.5	1.6	39.0	25.6	35.4
T10-2	G	253	148	146	2	2	75	25	19	119	789	*84.9*	82.2	11.2	6.6	46.3	27.1	26.7
T10-3b	G	112	108	89	0	0	19	7	3	80	418	*80.9*	91.4	5.6	3.0	36.2	35.0	28.8
T12-1	sG	79	113	30	7	0	45	29	11	24	338	*92.9*	72.9	14.3	12.7	35.6	50.9	13.5
T12-40	G	38	46	37	0	0	13	5	1	172	312	*44.9*	86.4	9.3	4.3	31.4	38.0	30.6
T13-37	G	132	45	215	2	3	66	16	7	46	532	*91.4*	81.7	13.6	4.7	33.7	11.5	54.8
T17-6	G	86	70	13	0	0	25	7	13	25	239	*89.5*	79.0	11.7	9.3	50.9	41.4	7.7
T17-7	sG	62	85	9	0	0	29	6	11	178	380	*53.2*	77.2	14.4	8.4	39.7	54.5	5.8
T17-11	sG	69	39	115	0	0	23	9	3	86	344	*75.0*	86.4	8.9	4.7	30.9	17.5	51.6
T17-12	G	144	71	167	1	0	48	13	11	86	541	*84.1*	84.2	10.5	5.3	37.7	18.6	43.7
T17-13	sG	55	37	51	0	0	26	6	2	63	240	*73.8*	80.8	14.7	4.5	38.5	25.9	35.7
T17-17	G	157	107	153	0	0	15	29	0	20	481	*95.8*	90.5	3.3	6.3	37.6	25.7	36.7
T17-24	sG	149	64	157	2	1	32	10	13	296	724	*59.1*	87.1	7.5	5.4	40.3	17.3	42.4
T17-27	G	154	84	218	4	0	27	10	8	94	599	*84.3*	91.1	5.3	3.6	33.8	18.4	47.8
T17-31	sG	256	107	231	2	0	39	32	17	217	901	*75.9*	87.1	5.7	7.2	43.1	18.0	38.9
Total		*1885*	*1215*	*1757*	*20*	*9*	*601*	*206*	*125*	*1647*	*7456*	*77.9*	*84.1*	*10.3*	*3.5*	*38.8*	*25.0*	*36.2*
Brayeburn/Vowel Mountain				T7, 8, 9														
T1-1	sG	123	178	54	0	0	5	8	0	116	484	*76.0*	96.5	1.4	2.2	34.6	50.1	15.2
T1-11	sG	73	72	193	2	0	25	5	0	98	468	*79.1*	91.9	6.8	1.4	21.6	21.3	57.1
T1-20	G	44	37	61	0	0	34	0	9	31	216	*85.6*	76.8	18.4	4.9	31.0	26.1	43.0
T1-27	G	121	90	65	1	0	48	15	1	60	401	*85.0*	81.2	14.1	4.7	43.8	32.6	23.6
T1-28	sG	70	24	10	0	0	2	13	0	31	150	*79.3*	87.4	1.7	10.9	67.3	23.1	9.6
T1-29	G	50	34	37	0	0	10	11	0	31	173	*82.1*	85.2	7.0	7.7	41.3	28.1	30.6
T6-3	sG	74	63	19	1	1	27	3	3	103	293	*64.8*	83.2	14.2	3.2	47.4	40.4	12.2
T6	sG	50	64	5	0	0	23	5	14	91	252	*63.9*	73.9	14.3	11.8	42.0	53.8	4.2
T7-6	sG	80	52	35	0	1	68	0	1	66	302	*78.1*	71.2	28.8	0.4	47.9	31.1	21.0
T7-8	sG	71	38	99	1	2	55	0	3	133	400	*66.8*	79.0	20.6	1.1	34.1	18.3	47.6
T7-14	sG	96	72	17	0	0	55	0	1	95	336	*71.7*	76.8	22.8	0.4	51.9	38.9	9.2
T7-16	sG	88	81	40	1	0	54	0	5	100	369	*72.9*	78.1	20.1	1.9	42.1	38.8	19.1
T8-5	sG	101	60	77	0	4	17	10	2	85	352	*75.9*	90.6	6.4	4.5	42.4	25.2	32.4
T9-13	sG	83	70	107	5	0	30	15	3	131	444	*70.5*	84.7	9.6	5.8	31.9	26.9	41.2
T9-14	sG	17	36	37	1	3	14	6	0	71	182	*61.0*	84.7	12.6	5.4	18.9	40.0	41.1
T9-20	sG	50	26	95	1	0	20	3	0	55	250	*78.0*	88.2	10.3	1.5	29.2	15.2	55.6
T9-33	G	121	52	98	0	0	20	12	12	69	384	*82.0*	86.0	6.3	7.6	44.6	19.2	36.2
Total		*1312*	*1049*	*1049*	*13*	*11*	*507*	*106*	*54*	*1366*	*5456*	*75.0*	*84.0*	*12.4*	*3.9*	*38.5*	*30.8*	*30.8*
Hootalinqua / Claire Creek				T6, 15, 16, 11														
T6-3	G	74	63	19	1	1	27	3	3	103	293	*64.8*	83.2	14.2	3.2	47.4	40.4	12.2
T6	sG	50	64	5	0	0	23	5	14	91	252	*63.9*	73.9	14.3	11.8	42.0	53.8	4.2
T11-10	sG	99	125	65	0	1	71	1	0	119	480	*75.2*	80.3	19.7	0.3	34.3	43.3	22.5
T11-12	G	49	80	24	0	0	19	6	0	43	221	*80.5*	86.0	10.7	3.4	32.0	52.3	15.7
T15-1	G	125	265	49	2	0	16	46	34	78	615	*87.3*	82.1	3.0	14.9	28.5	60.4	11.2
T16-1	sG	35	28	22	0	0	12	2	12	79	190	*58.4*	76.6	10.8	12.6	41.2	32.9	25.9
T16-3	G	69	27	40	0	1	60	2	15	51	264	*80.7*	64.3	28.2	8.0	50.7	19.9	29.4
T16-4	sG	89	39	91	0	21	26	6	22	196	469	*58.2*	87.9	9.5	10.3	40.6	17.8	41.6
T16-5	sG	31	61	12	0	0	28	3	64	93	292	*68.2*	52.3	14.1	33.7	29.8	58.7	11.5
T16-6	sG	175	159	118	4	3	126	31	111	321	1045	*69.3*	63.4	17.4	19.6	38.7	35.2	26.1
Total		*796*	*911*	*445*	*7*	*27*	*408*	*105*	*275*	*1174*	*4121*	*71.5*	*74.2*	*13.8*	*12.9*	*37.0*	*42.3*	*20.7*
Mt Granger /outliers																		
T2-3	G	19	59	192	0	1	66	3	0	62	401	*84.5*	79.9	19.5	0.9	7.0	21.9	71.1
05W-50	sG	52	24	17	0	0	27	0	0	175	295	*40.7*	77.5	22.5	0.0	55.9	25.8	18.3
05W-69	sG	56	47	13	0	0	14	8	3	63	204	*69.1*	82.3	9.9	5.7	48.3	40.5	11.2
05W-81	sG	71	91	14	0	0	69	10	0	134	389	*65.6*	69.0	27.1	3.9	40.3	51.7	8.0
05W-82	sG	23	43	20	0	0	11	1	0	115	213	*46.0*	87.8	11.2	1.0	26.7	50.0	23.3
T19-7	G	107	182	108	0	5	45	29	5	76	552	*86.2*	84.5	9.5	6.1	27.0	45.8	27.2
T19-13	G	167	237	61	0	0	80	15	3	103	666	*84.5*	82.6	14.2	2.7	35.9	51.0	13.1
T19-23	G	104	123	15	0	1	41	8	7	43	341	*87.4*	81.5	13.8	2.7	43.0	50.8	6.2
T19-27	G	57	101	50	0	0	26	1	0	60	295	*79.7*	88.5	11.1	0.4	27.4	48.6	24.0
T19-29	G	103	181	17	0	0	39	0	3	11	354	*96.9*	87.8	11.4	0.0	34.2	60.1	5.6
T19-59	G	377	319	35	0	0	46	22	6	34	839	*95.9*	90.8	5.7	2.7	51.6	43.6	4.8
T22-11	G	108	229	58	0	0	24	4	2	13	438	*97.0*	92.9	5.6	0.9	27.3	58.0	14.7
Total		*1244*	*1636*	*600*	*0*	*7*	*488*	*101*	*29*	*889*	*4987*	*82.2*	*85.1*	*11.9*	*2.5*	*35.7*	*47.0*	*17.2*
ALL SAMPLES		**5237**	**4811**	**3851**	**40**	**54**	**2004**	**518**	**483**	**5076**	**22020**	**76.9**	**82.6**	**11.8**	**3.1**	**37.7**	**34.6**	**27.7**

Location		Stratigraphic Unit			Point counts (number of observations)												Cements				n	Derived		
Mt Granger, WH Coal		Lithology			Framework grains											n fwk								
Tantalus Fm Conglomerate				detailed	Qm	Qp	Qs	Chert	Srf	Mrf	Fig	Fk	Fp	Fm	Fe	fwk	Voids	Hem	carb	Qtz		%Q	%F	%L
T2-3		G			14	4	14	473	0	0	0	0	0	0	0	505	0	2	0	0	507	6.3	0.0	93.7
T3-1a	0.00	G			7	5	9	482	0	0	0	0	0	0	0	503	0	0	0	22	525	4.2	0.0	95.8
T19-14	70.00	Gm	Tantalus		27	24	172	230	0	0	23	11	0	0	13	500	1	5	33	1	540	44.60	4.80	50.60
T19-23	91.60	Gh	Tantalus		0	0	51	393	31	0	10	0	0	0	15	500	0	3	5	0	508	10.20	3.00	86.80
T19-29	92.40	Gh	Tantalus		0	18	25	347	81	21	0	0	0	0	8	500	0	6	0	0	506	8.60	1.60	89.80
T19-59	217.00	Gm	Tantalus		4	0	50	409	0	0	24	0	0	0	13	500	0	2	0	0	502	10.80	2.60	86.60
T19-60	224.00	SGh	Tantalus		18	16	176	150	3	4	38	33	8	0	54	500	5	1	0	1	507	42.00	19.00	39.00
05W-62		gG			15	18	140	232	0	6	35	0	0	0	54	500	1	38	0	0	539	34.60	10.80	54.60
05W-69		gG			9	1	33	387	1	38	0	0	0	0	31	500	0	11	0	9	520	8.60	6.20	85.20
05W-80		gG			10	11	186	226	7	2	24	2	2	0	42	512	0	0	0	3	515	40.43	8.98	50.59
05W-81		gG			2	2	130	308	6	7	8	13	4	0	22	502	0	11	0	0	513	26.69	7.77	65.54
05W-82		gG			29	1	205	148	0	0	16	42	3	0	56	500	1	55	0	3	559	47.00	20.20	32.80
Sum Cong					**135**	**100**	**1191**	**3785**	**129**	**78**	**178**	**101**	**17**	**0**	**308**	**6022**	**8**	**134**	**38**	**39**	**AVE**	**23.67**	**7.08**	**69.25**
Fwk %					*2.2*	*1.7*	*19.8*	*62.9*	*2.1*	*1.3*	*3.0*	*1.7*	*0.3*	*0.0*	*5.1*	*100.0*	*0.1*	*2.1*	*0.6*	*0.6*	Max	*47.00*	*20.20*	*95.83*
																					MIN	*4.17*	*0.00*	*32.80*
																Fwk = 96.49			Total		6241	17.08	6.78	22.88
Tantalus Fm Sandstone																								
T19-30	93.82	cSt	Tantalus		17	19	238	120	0	2	12	18	2	0	72	500	0	10	0	0	510	54.80	18.40	26.80
T19-31	95.90	f,mSr	Tantalus		19	15	235	106	0	1	12	41	4	0	67	500	0	1	0	2	503	53.80	22.40	23.80
T19-58	188.00	mSm	Tantalus		32	6	76	204	7	2	37	66	7	0	63	500	10	220	81	0	811	22.80	27.20	50.00
T19-61	248.00	g,c-vcSm	Tantalus		30	13	155	169	0	1	11	41	5	0	75	500	0	13	0	0	513	39.60	24.20	36.20
05W-50		g,vcS	Tantalus?		22	9	157	215	7	0	29	20	1	0	40	500	0	17	0	1	518	37.60	12.20	50.20
05W-51		mS	Tantalus?		38	5	94	85	2	11	57	136	32	1	39	500	0	43	7	9	559	27.40	41.60	31.00
05W-61		vcS			10	7	109	247	2	1	18	1	0	0	105	500	2	46	0	3	551	25.20	21.20	53.60
Sum Cong					**168**	**74**	**1064**	**1146**	**18**	**18**	**176**	**323**	**51**	**1**	**461**	**3500**	**12**	**350**	**88**	**15**	**AVE**	**37.3**	**23.9**	**38.8**
Fwk %					*4.8*	*2.1*	*30.4*	*32.7*	*0.5*	*0.5*	*5.0*	*9.2*	*1.5*	*0.0*	*13.2*	*100.0*	*0.3*	*8.8*	*2.2*	*0.4*	Max	*54.8*	*41.6*	*53.6*
																					MIN	*22.8*	*12.2*	*23.8*
																Fwk = 88.27			Total		3965	13.16	9.14	12.32
Tangelfoot Fm Conglomerate																								
T21-12	92.00	Gm	Tangelfoot	44 matrix	17	3	44	338	0	0	77	15	6	0	0	500	0	2	0	0	502	12.80	4.20	83.00
T21-11	106.00	SGm	Tangelfoot	18 matrix	42	18	139	132	0	0	94	59	9	2	5	500	0	10	0	0	510	39.80	15.00	45.20
T21-6	234.00	Gm	Tangelfoot		21	13	219	89	6	6	69	41	8	0	28	500	0	44	0	0	544	50.60	15.40	34.00
Sum Cong					**80**	**34**	**402**	**559**	**6**	**6**	**240**	**115**	**23**	**2**	**33**	**1500**	**0**	**56**	**0**	**0**	**AVE**	**34.4**	**11.5**	**54.1**
Fwk %		Matrix %			*5.3*	*2.3*	*26.8*	*37.3*	*0.4*	*0.4*	*16.0*	*7.7*	*1.5*	*0.1*	*2.2*	*100.0*	*0.0*	*3.5*	*0.0*	*0.0*	Max	*50.6*	*15.4*	*83.0*
		3.8																			MIN	*12.8*	*4.2*	*34.0*
																Fwk = 92.71			Total		1618	19.47	6.35	25.68
Tangelfoot Fm Sandstone																								
T21-14	26.00	vcSm	Tangelfoot	16 matrix	27	4	51	0	4	4	271	45	3	0	91	500	0	22	0	0	522	16.40	27.80	55.80
T21-13	80.00	mfSm	Tangelfoot	6 matrix	52	10	66	0	0	4	207	148	13	0	0	500	0	0	0	0	500	25.60	32.20	42.20
T19-1	0.40	cSt	Lbg	Ab Ig RFs	17	8	190	166	6	1	44	55	10	0	3	500	0	28	18	24	570	43.00	13.60	43.40
T19-2	4.50	g,cSm	Lbg	Ab Ig RFs	28	8	132	119	1	0	38	96	20	2	56	500	0	12	6	13	531	33.60	34.80	31.60
T19-3	9.90	fSr	Lbg	10 x chlori	42	9	69	115	0	0	27	181	22	0	35	500	0	40	20	9	569	24.00	47.60	28.40
T21-8	156.00	mSm	Tangelfoot	32	48	9	142	114	1	3	29	1	0	0	153	500	0	2	0	1	503	39.80	30.80	29.40
Sum Cong					**214**	**48**	**650**	**514**	**12**	**12**	**616**	**526**	**68**	**2**	**338**	**3000**	**0**	**104**	**44**	**47**	**AVE**	**30.4**	**31.1**	**38.5**
Fwk %		Matrix %			*7.1*	*1.6*	*21.7*	*17.1*	*0.4*	*0.4*	*20.5*	*17.5*	*2.3*	*0.1*	*11.3*	*100.0*	*0.0*	*3.2*	*1.4*	*1.5*	Max	*43.0*	*47.6*	*55.8*
		1.0																			MIN	*16.4*	*13.6*	*28.4*
																Fwk = 93.0			Total		3227	10.17	10.99	10.67

Chert types See Appendix 3 for explanation

Sample	A Wht	A Yel	A Gry	A Blk	A grn (rd)	B Wht	B Yel	B Gry	B Blk	B grn (rd)	C Wht	C Yel	C Gry	C Blk	D Wht	D Yel	D Gry	D Blk	E Wht	E Yel	E Gry	E Blk	F Wht	F Yel	F Gry	F Blk	G Wht	G Yel	G Gry	G Blk
Tantalus Fm Conglomerate																														
T2-3	221	8	0	0	0	176	10	0	0	0	0	0	0	0	0	0	0	0	0	0	0	0	0	0	0	0	0	0	0	0
T3-1a	85	25	0	0	0	202	22	0	0	0	0	0	0	0	0	0	0	0	0	0	0	0	0	0	0	0	0	0	0	0
T19-14	10	9	11	8	0	30	1	1	1	0	0	0	0	0	0	0	0	0	0	0	0	0	0	0	0	0	0	0	0	0
T19-23	11	1	0	14	0	50	0	0	0	0	0	0	0	0	0	0	0	0	0	0	0	0	0	0	0	0	0	0	0	0
T19-29	17	0	0	0	0	0	0	0	0	0	0	0	0	0	0	0	0	0	0	0	0	0	0	0	0	0	0	0	0	0
T19-59	13	8	0	1	0	6	0	0	0	0	0	0	0	0	0	0	0	0	0	0	0	0	0	0	0	0	0	0	0	0
T19-60	22	21	9	10	0	10	5	5	0	2	0	0	0	0	0	0	0	0	0	0	0	0	0	0	0	0	0	0	0	0
05W-62	32	45	7	4	0	19	4	12	0	2	0	0	0	0	0	0	0	0	0	0	0	0	0	0	0	0	0	0	0	0
05W-69	18	8	5	6	0	80	0	0	0	0	0	0	0	0	0	0	0	0	0	0	0	0	0	0	0	0	0	0	0	0
05W-80	36	16	7	6	0	8	6	12	3	0	0	0	0	0	0	0	0	0	0	0	0	0	0	0	0	0	0	0	0	0
05W-81	18	24	6	4	0	20	0	0	3	0	0	0	0	0	0	0	0	0	0	0	0	0	0	0	0	0	0	0	0	0
05W-82	25	9	2	2	0	37	3	0	0	0	0	0	0	0	0	0	0	0	0	0	0	0	0	0	0	0	0	0	0	0
Sum Cong	**508**	**174**	**47**	**55**	**0**	**638**	**51**	**30**	**7**	**4**	**0**	**0**	**0**	**0**	**0**	**0**	**0**	**0**	**0**	**0**	**0**	**0**	**0**	**0**	**0**	**0**	**0**	**0**	**0**	**0**
Fwk %	13.4	4.6	1.2	1.5	0.0	16.9	1.3	0.8	0.2	0.1	0.0	0.0	0.0	0.0	0.0	0.0	0.0	0.0	0.0	0.0	0.0	0.0	0.0	0.0	0.0	0.0	0.0	0.0	0.0	0.0
					20.7					19.3				0.0				0.0				0.0				0.0				0.0
	SDEV																													
Tantalus Fm Sandstone																														
T19-30	7	16	13	13	0	15	2	4	0	0	0	0	0	0	0	0	0	0	0	0	0	0	0	0	0	0	0	0	0	0
T19-31	20	13	5	7	0	16	1	3	2	0	0	0	0	0	0	0	0	0	0	0	0	0	0	0	0	0	0	0	0	0
T19-58	31	18	8	20	0	33	0	0	0	0	0	0	0	0	0	0	0	0	0	0	0	0	0	0	0	0	0	0	0	0
T19-61	24	30	11	1	0	16	7	0	0	0	0	0	0	0	0	0	0	0	0	0	0	0	0	0	0	0	0	0	0	0
05W-50	25	2	6	25	0	57	0	3	0	0	0	0	0	0	0	0	0	0	0	0	0	0	0	0	0	0	0	0	0	0
05W-51	6	22	9	15	0	10	0	0	0	0	0	0	0	0	0	0	0	0	0	0	0	0	0	0	0	0	0	0	0	0
05W-61	22	27	3	5	0	34	4	0	1	0	0	0	0	0	0	0	0	0	0	0	0	0	0	0	0	0	0	0	0	0
Sum Cong	**135**	**128**	**55**	**86**	**0**	**181**	**14**	**10**	**3**	**0**	**0**	**0**	**0**	**0**	**0**	**0**	**0**	**0**	**0**	**0**	**0**	**0**	**0**	**0**	**0**	**0**	**0**	**0**	**0**	**0**
Fwk %	11.8	11.2	4.8	7.5	0.0	15.8	1.2	0.9	0.3	0.0	0.0	0.0	0.0	0.0	0.0	0.0	0.0	0.0	0.0	0.0	0.0	0.0	0.0	0.0	0.0	0.0	0.0	0.0	0.0	0.0
					35.3					18.2				0.0				0.0				0.0				0.0				0.0
	SDEV																													
Tangelfoot Fm Conglomerate																														
T21-12	2	0	0	0	0	288	0	0	0	0	0	0	0	0	0	0	0	0	0	0	0	0	0	0	0	0	0	0	0	0
T21-11	4	0	2	3	0	3	0	0	1	0	0	0	0	0	0	0	0	0	0	0	0	0	0	0	0	0	0	0	0	0
T21-6	22	0	1	2	0	20	0	0	0	0	0	0	0	0	0	0	0	0	0	0	0	0	0	0	0	0	0	0	0	0
Sum Cong	**28**	**0**	**3**	**5**	**0**	**311**	**0**	**0**	**1**	**0**	**0**	**0**	**0**	**0**	**0**	**0**	**0**	**0**	**0**	**0**	**0**	**0**	**0**	**0**	**0**	**0**	**0**	**0**	**0**	**0**
Fwk %	5.0	0.0	0.5	0.9	0.0	55.6	0.0	0.0	0.2	0.0	0.0	0.0	0.0	0.0	0.0	0.0	0.0	0.0	0.0	0.0	0.0	0.0	0.0	0.0	0.0	0.0	0.0	0.0	0.0	0.0
					6.4					55.8				0.0				0.0				0.0				0.0				0.0
	SDEV																													
Tangelfoot Fm Sandstone																														
T21-14	0	0	0	0	0	0	0	0	0	0	0	0	0	0	0	0	0	0	0	0	0	0	0	0	0	0	0	0	0	0
T21-13	0	0	0	0	0	0	0	0	0	0	0	0	0	0	0	0	0	0	0	0	0	0	0	0	0	0	0	0	0	0
T19-1	18	25	10	35	0	16	2	7	2	0	0	0	0	0	0	0	0	0	0	0	0	0	0	0	0	0	0	0	0	0
T19-2	12	27	13	18	0	16	2	3	2	0	0	0	0	0	0	0	0	0	0	0	0	0	0	0	0	0	0	0	0	0
T19-3	11	14	11	9	0	43	5	0	0	0	0	0	0	0	0	0	0	0	0	0	0	0	0	0	0	0	0	0	0	0
T21-8	20	6	5	4	0	16	0	2	0	0	0	0	0	0	0	0	0	0	0	0	0	0	0	0	0	0	0	0	0	0
Sum Cong	**61**	**72**	**39**	**66**	**0**	**91**	**9**	**12**	**4**	**0**	**0**	**0**	**0**	**0**	**0**	**0**	**0**	**0**	**0**	**0**	**0**	**0**	**0**	**0**	**0**	**0**	**0**	**0**	**0**	**0**
Fwk %	11.9	14.0	7.6	12.8	0.0	17.7	1.8	2.3	0.8	0.0	0.0	0.0	0.0	0.0	0.0	0.0	0.0	0.0	0.0	0.0	0.0	0.0	0.0	0.0	0.0	0.0	0.0	0.0	0.0	0.0
					46.3					22.6				0.0				0.0				0.0				0.0				0.0
	SDEV																													

Sample	H Wht	H Yel	H Gry	H Blk	I Wht	I Yel	I Gry	I Blk	J Wht	J Yel	J Gry	J Blk	K Wht	K Yel	K Gry	K Blk	L Wht	L Yel	L Gry	L Blk	M Wht	M Yel	M Gry	M Blk	N Wht	N Yel	N Gry	N Blk	O Wht	O Yel	O Gry	O Blk	P Wht	P Yel	P Gry	P Blk
Tantalus Fm Conglomerate																																				
T2-3	0	0	0	0	0	0	0	0	0	0	0	0	0	0	0	0	0	0	0	0	21	0	0	0	0	0	0	0	0	0	0	0	0	0	0	0
T3-1a	0	0	0	0	0	0	0	0	0	0	0	0	0	0	0	0	0	0	0	0	38	0	0	0	0	0	0	0	0	0	0	0	0	0	0	0
T19-14	0	0	0	0	0	0	0	0	2	0	5	0	0	0	0	0	0	0	0	0	11	22	0	2	0	0	0	0	0	0	0	0	0	0	0	0
T19-23	0	0	0	0	0	0	0	0	47	0	0	0	0	0	0	0	0	0	0	0	0	0	0	10	0	0	0	0	0	0	0	0	0	0	0	0
T19-29	0	0	0	0	0	0	0	0	22	0	3	0	0	0	0	0	0	0	0	0	0	0	0	4	0	0	0	0	0	0	0	0	0	0	0	0
T19-59	6	0	0	0	0	0	0	0	0	0	0	0	0	0	0	0	0	0	0	0	15	10	0	0	0	0	0	0	0	0	0	0	0	81	0	0
T19-60	0	0	0	0	0	0	0	0	0	3	0	0	0	0	0	0	0	0	0	0	4	0	0	1	0	0	0	0	0	0	0	0	0	0	0	0
05W-62	0	0	0	0	0	0	0	0	0	0	0	0	0	0	0	0	3	0	0	0	5	5	0	0	0	0	0	0	0	0	0	0	0	0	0	0
05W-69	0	0	0	0	0	0	0	0	5	0	0	4	0	0	0	0	0	0	0	0	26	11	0	9	0	0	0	0	0	0	0	0	0	0	0	0
05W-80	0	0	0	0	0	2	0	0	1	1	0	0	0	0	0	0	0	0	0	0	7	5	0	2	0	0	0	0	0	0	0	0	0	0	0	0
05W-81	0	0	0	0	0	0	0	0	7	0	0	0	0	0	0	0	0	0	0	0	12	5	0	0	0	0	0	0	0	0	0	0	4	0	0	0
05W-82	0	0	0	0	0	0	0	0	3	0	0	0	0	0	0	0	0	0	0	0	4	0	0	2	0	0	0	0	0	0	0	0	0	0	0	0
Sum Cong	**6**	**0**	**0**	**0**	**0**	**2**	**0**	**0**	**87**	**4**	**8**	**4**	**0**	**0**	**0**	**0**	**3**	**0**	**0**	**0**	**143**	**58**	**0**	**30**	**0**	**0**	**0**	**0**	**0**	**0**	**0**	**0**	**4**	**81**	**0**	**0**
Fwk %	0.2	0.0	0.0	0.0	0.0	0.1	0.0	0.0	2.3	0.1	0.2	0.1	0.0	0.0	0.0	0.0	0.1	0.0	0.0	0.0	3.8	1.5	0.0	0.8	0.0	0.0	0.0	0.0	0.0	0.0	0.0	0.0	0.1	2.1	0.0	0.0
				0.2				0.1				2.7				0.0				0.1				6.1				0.0				0.0				2.2
Tantalus Fm Sandstone																																				
T19-30	0	0	0	0	1	0	0	0	7	0	0	0	0	0	0	0	0	0	0	0	1	0	0	1	0	0	0	0	0	0	0	0	0	2	0	0
T19-31	0	0	0	0	0	0	0	0	3	0	0	0	0	0	0	0	0	0	0	0	3	3	0	0	0	0	0	0	0	0	0	0	0	0	0	0
T19-58	0	0	0	0	0	0	0	0	9	0	0	0	0	0	0	0	0	0	0	0	4	0	0	0	0	0	0	0	0	0	0	0	0	0	0	0
T19-61	0	0	0	0	0	0	0	0	3	0	1	2	0	0	0	0	0	0	0	0	14	0	1	1	0	0	0	0	0	0	0	0	0	2	0	0
05W-50	0	0	0	0	2	0	0	0	4	0	1	0	0	0	0	0	0	0	0	0	10	12	0	0	0	0	0	0	0	0	0	0	0	0	0	0
05W-51	0	0	0	0	0	0	0	0	0	0	0	0	0	0	0	0	0	0	0	0	0	0	0	0	0	0	0	0	0	0	0	0	0	0	0	0
05W-61	0	0	0	0	0	0	0	0	7	0	0	0	0	0	0	0	1	0	0	0	0	0	0	0	0	0	0	0	0	0	0	0	11	0	0	0
Sum Cong	**0**	**0**	**0**	**0**	**3**	**0**	**0**	**0**	**33**	**0**	**2**	**2**	**0**	**0**	**0**	**0**	**1**	**0**	**0**	**0**	**32**	**15**	**1**	**2**	**0**	**0**	**0**	**0**	**0**	**0**	**0**	**0**	**11**	**4**	**0**	**0**
Fwk %	0.0	0.0	0.0	0.0	0.3	0.0	0.0	0.0	2.9	0.0	0.2	0.2	0.0	0.0	0.0	0.0	0.1	0.0	0.0	0.0	2.8	1.3	0.1	0.2	0.0	0.0	0.0	0.0	0.0	0.0	0.0	0.0	1.0	0.3	0.0	0.0
				0.0				0.3				3.2				0.0				0.1				4.4				0.0				0.0				1.3
Tangelfoot Fm Conglomerate																																				
T21-12	0	0	0	0	0	0	0	0	18	0	0	0	0	0	0	0	0	0	0	0	0	0	0	0	0	0	0	0	0	0	0	0	18	0	0	0
T21-11	0	0	0	0	2	0	0	0	2	0	0	0	0	0	0	0	0	0	0	0	7	0	3	2	0	0	0	0	0	0	0	0	0	0	0	0
T21-6	0	0	0	0	2	0	0	0	4	0	0	0	0	0	0	0	0	0	0	0	11	0	0	2	0	0	0	0	0	0	0	0	0	0	0	0
Sum Cong	**0**	**0**	**0**	**0**	**4**	**0**	**0**	**0**	**24**	**0**	**0**	**0**	**0**	**0**	**0**	**0**	**0**	**0**	**0**	**0**	**18**	**0**	**3**	**4**	**0**	**0**	**0**	**0**	**0**	**0**	**0**	**0**	**18**	**0**	**0**	**0**
Fwk %	0.0	0.0	0.0	0.0	0.7	0.0	0.0	0.0	4.3	0.0	0.0	0.0	0.0	0.0	0.0	0.0	0.0	0.0	0.0	0.0	3.2	0.0	0.5	0.7	0.0	0.0	0.0	0.0	0.0	0.0	0.0	0.0	3.2	0.0	0.0	0.0
				0.0				0.7				4.3				0.0				0.0				4.5				0.0				0.0				3.2
Tangelfoot Fm Sandstone																																				
T21-14	0	0	0	0	0	0	0	0	0	0	0	0	0	0	0	0	0	0	0	0	0	0	0	0	0	0	0	0	0	0	0	0	0	0	0	0
T21-13	0	0	0	0	0	0	0	0	0	0	0	0	0	0	0	0	0	0	0	0	0	0	0	0	0	0	0	0	0	0	0	0	0	0	0	0
T19-1	0	0	0	0	0	0	0	0	6	0	1	1	0	0	0	0	0	0	0	0	3	1	2	0	0	0	0	0	0	0	0	0	0	0	0	0
T19-2	0	0	0	0	0	0	0	0	0	0	0	0	0	0	0	0	0	0	0	0	1	0	0	0	0	0	0	0	0	0	0	0	0	0	0	0
T19-3	0	0	0	0	0	0	0	0	2	1	0	0	0	0	0	0	0	0	0	0	2	0	0	0	0	0	0	0	0	0	0	0	0	0	0	0
T21-8	0	0	0	0	0	0	0	0	0	0	3	0	0	0	0	0	0	0	0	0	0	0	0	2	0	0	0	0	0	0	0	0	0	0	0	0
Sum Cong	**0**	**0**	**0**	**0**	**0**	**0**	**0**	**0**	**8**	**1**	**4**	**1**	**0**	**0**	**0**	**0**	**0**	**0**	**0**	**0**	**6**	**1**	**2**	**2**	**0**	**0**	**0**	**0**	**0**	**0**	**0**	**0**	**0**	**0**	**0**	**0**
Fwk %	0.0	0.0	0.0	0.0	0.0	0.0	0.0	0.0	1.6	0.2	0.8	0.2	0.0	0.0	0.0	0.0	0.0	0.0	0.0	0.0	1.2	0.2	0.4	0.4	0.0	0.0	0.0	0.0	0.0	0.0	0.0	0.0	0.0	0.0	0.0	0.0
				0.0				0.0				2.7				0.0				0.0				2.1				0.0				0.0				0.0

Sample	Q Wht	Q Yel	Q Gry	Q Blk	R Wht	R Yel	R Gry	R Blk	S Wht	S Yel	S Gry	S Blk	T Wht	T Yel	T Gry	T Blk	U Wht	U Yel	U Gry	U Blk	V Wht	V Yel	V Gry	V Blk
Tantalus Fm Conglomerate																								
T2-3	0	0	0	0	0	0	0	0	0	0	0	0	0	0	0	0	17	0	0	0	18	0	0	0
T3-1a	0	0	0	0	0	0	0	0	0	0	0	0	0	0	0	0	0	0	0	0	55	28	0	0
T19-14	0	2	2	3	0	0	0	0	2	0	0	0	0	0	0	0	0	4	0	21	0	38	5	1
T19-23	143	34	0	0	0	0	0	0	0	0	0	0	0	0	0	0	0	10	0	0	8	28	0	0
T19-29	0	0	19	21	0	0	0	14	0	0	0	0	0	0	0	0	0	0	0	0	51	5	0	5
T19-59	0	38	0	0	0	0	0	0	13	5	0	0	0	0	0	0	0	0	5	0	6	0	0	26
T19-60	0	0	0	1	0	0	0	0	1	2	0	0	0	3	0	0	0	0	3	26	1	6	0	1
05W-62	0	8	2	3	0	0	0	0	3	6	0	3	0	0	0	0	5	1	0	1	4	21	3	1
05W-69	0	18	0	19	0	0	0	0	6	8	0	2	0	0	0	0	7	4	0	0	18	10	0	0
05W-80	0	7	0	8	0	0	0	0	0	0	0	12	0	0	0	0	0	0	0	4	7	17	0	11
05W-81	11	21	0	0	0	0	0	2	4	10	6	4	0	0	0	0	0	19	0	0	18	38	0	0
05W-82	4	0	0	0	0	0	0	0	0	0	0	1	1	0	0	0	2	0	2	3	14	7	0	0
Sum Cong	**158**	**128**	**23**	**55**	**0**	**0**	**0**	**16**	**29**	**31**	**6**	**22**	**1**	**3**	**0**	**0**	**31**	**38**	**10**	**55**	**200**	**198**	**8**	**45**
Fwk %	4.2	3.4	0.6	1.5	0.0	0.0	0.0	0.4	0.8	0.8	0.2	0.6	0.0	0.1	0.0	0.0	0.8	1.0	0.3	1.5	5.3	5.2	0.2	1.2
				9.6				0.4				2.3				0.1				3.5				11.9
Tantalus Fm Sandstone																								
T19-30	0	1	0	0	0	0	0	0	0	2	0	1	1	0	0	0	0	1	0	3	9	5	0	1
T19-31	0	0	2	1	0	0	0	0	0	0	0	0	0	0	0	0	0	1	0	3	4	3	1	4
T19-58	0	0	0	0	0	0	0	0	0	0	0	2	5	0	0	0	0	3	1	6	34	9	3	1
T19-61	0	1	0	0	0	0	0	0	5	0	0	1	1	0	0	0	0	3	0	11	4	8	5	4
05W-50	0	1	0	6	0	0	0	0	0	0	0	4	0	0	0	0	0	8	0	7	24	0	1	0
05W-51	0	0	0	0	0	0	0	0	0	0	0	0	1	0	0	0	0	0	0	0	5	4	3	1
05W-61	0	7	0	0	2	0	0	0	0	0	4	3	1	0	0	0	0	9	6	11	17	15	0	1
Sum Cong	**0**	**10**	**2**	**7**	**2**	**0**	**0**	**0**	**5**	**2**	**4**	**11**	**9**	**0**	**0**	**0**	**0**	**25**	**7**	**41**	**97**	**44**	**13**	**12**
Fwk %	0.0	0.9	0.2	0.6	0.2	0.0	0.0	0.0	0.4	0.2	0.3	1.0	0.8	0.0	0.0	0.0	0.0	2.2	0.6	3.6	8.5	3.8	1.1	1.0
				1.7				0.2				1.9				0.8				6.4				14.5
Tangelfoot Fm Conglomerate																								
T21-12	0	0	0	0	0	0	0	9	0	0	0	0	0	0	0	0	0	0	0	0	0	0	0	0
T21-11	6	0	0	0	0	0	0	1	2	0	0	6	0	0	0	0	0	0	0	0	43	0	4	4
T21-6	7	0	0	0	0	0	0	0	0	0	0	0	0	0	0	0	0	0	2	8	0	0	0	0
Sum Cong	**13**	**0**	**0**	**0**	**0**	**0**	**0**	**10**	**2**	**0**	**0**	**6**	**0**	**0**	**0**	**0**	**0**	**0**	**2**	**8**	**43**	**0**	**4**	**4**
Fwk %	2.3	0.0	0.0	0.0	0.0	0.0	0.0	1.8	0.4	0.0	0.0	1.1	0.0	0.0	0.0	0.0	0.0	0.0	0.4	1.4	7.7	0.0	0.7	0.7
				2.3				1.8				1.4				0.0				1.8				9.1
Tangelfoot Fm Sandstone																								
T21-14	0	0	0	0	0	0	0	0	0	0	0	0	0	0	0	0	0	0	0	0	0	0	0	0
T21-13	0	0	0	0	0	0	0	0	0	0	0	0	0	0	0	0	0	0	0	0	0	0	0	0
T19-1	1	0	0	0	0	0	0	0	0	2	0	0	0	0	0	2	0	1	0	11	2	4	0	3
T19-2	0	3	0	1	0	0	0	0	0	0	0	0	5	0	0	0	0	0	0	2	1	0	2	2
T19-3	0	0	0	0	0	0	0	0	0	0	0	0	1	0	0	0	0	0	0	1	0	7	2	1
T21-8	0	0	0	4	0	0	0	2	0	0	0	1	0	0	0	0	2	0	1	7	6	2	4	6
Sum Cong	**1**	**3**	**0**	**5**	**0**	**0**	**0**	**2**	**0**	**2**	**0**	**1**	**6**	**0**	**0**	**2**	**2**	**1**	**1**	**21**	**9**	**13**	**8**	**12**
Fwk %	0.2	0.6	0.0	1.0	0.0	0.0	0.0	0.4	0.0	0.4	0.0	0.2	1.2	0.0	0.0	0.4	0.4	0.2	0.2	4.1	1.8	2.5	1.6	2.3
				1.8				0.4				0.6				1.6				4.9				8.2

Sample	W Wht	W Yel	W Gry	W Blk	X Wht	X Yel	X Gry	X Blk	Z Wht	Z Yel	Z Gry	Z Blk	A' Wht	A' Yel	A' Gry	A' Blk	B' Wht	B' Yel	B' Gry	B' Blk
Tantalus Fm Conglomerate																				
T2-3	0	0	0	0	0	0	0	0	0	0	0	0	0	0	0	0	2	0	0	0
T3-1a	27	0	0	0	0	0	0	0	0	0	0	0	0	0	0	0	0	0	0	0
T19-14	20	12	1	2	0	0	0	0	4	0	0	0	0	0	0	0	0	0	0	0
T19-23	0	37	0	0	0	0	0	0	0	0	0	0	0	0	0	0	0	0	0	0
T19-29	57	77	0	34	0	0	0	0	0	6	5	7	0	0	0	0	0	0	0	0
T19-59	0	0	0	0	0	0	0	0	85	88	0	0	0	0	0	0	0	0	0	0
T19-60	3	6	0	0	0	0	0	0	4	4	0	0	0	0	0	0	0	0	0	0
05W-62	17	16	0	0	0	0	0	0	0	0	0	0	0	0	0	0	0	0	0	0
05W-69	85	12	0	0	0	0	0	0	0	26	0	0	0	0	0	0	0	0	0	0
05W-80	19	5	0	0	0	0	0	0	13	9	0	0	0	0	0	0	0	0	0	0
05W-81	52	14	4	4	0	0	0	0	0	0	0	0	0	0	0	0	0	0	0	0
05W-82	17	4	2	0	0	0	0	0	0	0	4	0	0	0	0	0	0	0	0	0
Sum Cong	**297**	**183**	**7**	**40**	**0**	**0**	**0**	**0**	**106**	**133**	**9**	**7**	**0**	**0**	**0**	**0**	**2**	**0**	**0**	**0**
Fwk %	7.8	4.8	0.2	1.1	0.0	0.0	0.0	0.0	2.8	3.5	0.2	0.2	0.0	0.0	0.0	0.0	0.1	0.0	0.0	0.0
				13.9				0.0				6.7				0.0				0.1
Tantalus Fm Sandstone																				
T19-30	7	2	5	0	0	0	0	0	0	0	0	0	0	0	0	0	0	0	0	0
T19-31	4	5	1	0	0	0	0	0	1	0	0	0	0	0	0	0	0	0	0	0
T19-58	13	1	0	2	0	0	0	0	1	0	0	0	0	0	0	0	0	0	0	0
T19-61	5	8	0	0	0	0	0	0	0	0	0	0	0	0	0	0	0	0	0	0
05W-50	13	4	0	0	0	0	0	0	0	0	0	0	0	0	0	0	0	0	0	0
05W-51	6	3	0	0	0	0	0	0	0	0	0	0	0	0	0	0	0	0	0	0
05W-61	50	5	0	1	0	0	0	0	0	0	0	0	0	0	0	0	0	0	0	0
Sum Cong	**98**	**28**	**6**	**3**	**0**	**0**	**0**	**0**	**2**	**0**	**0**	**0**	**0**	**0**	**0**	**0**	**0**	**0**	**0**	**0**
Fwk %	8.6	2.4	0.5	0.3	0.0	0.0	0.0	0.0	0.2	0.0	0.0	0.0	0.0	0.0	0.0	0.0	0.0	0.0	0.0	0.0
				11.8				0.0				0.2				0.0				0.0
Tangelfoot Fm Conglomerate																				
T21-12	3	0	0	0	0	0	0	0	0	0	0	0	0	0	0	0	0	0	0	0
T21-11	25	0	10	2	0	0	0	0	0	0	0	0	0	0	0	0	0	0	0	0
T21-6	8	0	0	0	0	0	0	0	0	0	0	0	0	0	0	0	0	0	0	0
Sum Cong	**36**	**0**	**10**	**2**	**0**	**0**	**0**	**0**	**0**	**0**	**0**	**0**	**0**	**0**	**0**	**0**	**0**	**0**	**0**	**0**
Fwk %	6.4	0.0	1.8	0.4	0.0	0.0	0.0	0.0	0.0	0.0	0.0	0.0	0.0	0.0	0.0	0.0	0.0	0.0	0.0	0.0
				8.6				0.0				0.0				0.0				0.0
Tangelfoot Fm Sandstone																				
T21-14	0	0	0	0	0	0	0	0	0	0	0	0	0	0	0	0	0	0	0	0
T21-13	0	0	0	0	0	0	0	0	0	0	0	0	0	0	0	0	0	0	0	0
T19-1	9	1	1	0	0	0	0	0	0	0	0	0	0	0	0	0	0	0	0	0
T19-2	5	3	1	0	0	0	0	0	0	0	0	0	0	0	0	0	0	0	0	0
T19-3	4	1	0	0	0	0	0	0	0	0	0	0	0	0	0	0	0	0	0	0
T21-8	6	5	7	3	0	0	0	0	0	0	0	0	0	0	0	0	0	0	0	0
Sum Cong	**24**	**10**	**9**	**3**	**0**	**0**	**0**	**0**	**0**	**0**	**0**	**0**	**0**	**0**	**0**	**0**	**0**	**0**	**0**	**0**
Fwk %	4.7	1.9	1.8	0.6	0.0	0.0	0.0	0.0	0.0	0.0	0.0	0.0	0.0	0.0	0.0	0.0	0.0	0.0	0.0	0.0
				8.9				0.0				0.0				0.0				0.0

Totals					Chert by colour					Qm	Qp	Qs		Chert Groups			sub			
	W	Y	G	B+R+	White	Yellow	Grey	Black		%	%	%		A to K	L to T +Z	U to W	total	%Mas	%Brec	%spher
					%	%	%	%						MASSIVE	BRECCIATED	SPHERES				
473	455	18	0	0	96.2	3.8	0.0	0.0		43.75	12.50	43.75	T2-3	415	21	35	471	88.1	4.5	7.4
482	407	75	0	0	84.4	15.6	0.0	0.0		33.33	23.81	42.86	T3-1a	334	38	110	482	69.3	7.9	22.8
230	79	88	25	38	34.3	38.3	10.9	16.5	230	12.11	10.76	77.13	T19-14	78	48	104	230	33.9	20.9	45.2
393	259	110	0	24	65.9	28.0	0.0	6.1	393	0.00	0.00	100.00	T19-23	123	187	83	393	31.3	47.6	21.1
347	147	88	27	85	42.4	25.4	7.8	24.5	347	0.00	41.86	58.14	T19-29	42	76	229	347	12.1	21.9	66.0
409	144	233	5	27	35.2	57.0	1.2	6.6	409	7.41	0.00	92.59	T19-59	34	338	37	409	8.3	82.6	9.0
150	45	47	17	41	30.0	31.3	11.3	27.3	150	8.57	7.62	83.81	T19-60	87	17	46	150	58.0	11.3	30.7
232	88	106	24	14	37.9	45.7	10.3	6.0	232	8.67	10.40	80.92	05W-62	125	38	69	232	53.9	16.4	29.7
387	245	97	5	40	63.3	25.1	1.3	10.3	387	20.93	2.33	76.74	05W-69	126	125	136	387	32.6	32.3	35.1
226	91	68	19	48	40.3	30.1	8.4	21.2	226	4.83	5.31	89.86	05W-80	98	65	63	226	43.4	28.8	27.9
308	146	131	16	15	47.4	42.5	5.2	4.9	308	1.49	1.49	97.01	05W-81	82	77	149	308	26.6	25.0	48.4
148	107	23	10	8	72.3	15.5	6.8	5.4	148	12.34	0.43	87.23	05W-82	81	16	51	148	54.7	10.8	34.5
				AVE	**54.1**	**29.8**	**5.3**	**10.7**	**AVE**	**12.8**	**9.7**	**77.5**					**AVE**	**42.7**	**25.8**	**31.5**
				MAX	96.2	57.0	11.3	27.3	MAX	43.8	41.9	100.0					MAX	88.1	82.6	66.0
				MIN	30.0	3.8	0.0	0.0	MIN	0.0	0.0	42.9					MIN	8.3	4.5	7.4
				SDEV	21.8	14.6	4.6	9.4	SDEV	13.6	12.3	19.4					SDEV	23.3	21.5	16.4
120	48	31	22	19	40.0	25.8	18.3	15.8	120	6.20	6.93	86.86	T19-30	78	9	33	120	65.0	7.5	27.5
106	51	26	12	17	48.1	24.5	11.3	16.0	106	7.06	5.58	87.36	T19-31	70	10	26	106	66.0	9.4	24.5
204	130	31	12	31	63.7	15.2	5.9	15.2	204	28.07	5.26	66.67	T19-58	119	12	73	204	58.3	5.9	35.8
169	72	59	18	20	42.6	34.9	10.7	11.8	169	15.15	6.57	78.28	T19-61	95	26	48	169	56.2	15.4	28.4
215	135	27	11	42	62.8	12.6	5.1	19.5	215	11.70	4.79	83.51	05W-50	125	33	57	215	58.1	15.3	26.5
85	28	29	12	16	32.9	34.1	14.1	18.8	85	27.74	3.65	68.61	05W-51	62	1	22	85	72.9	1.2	25.9
247	145	67	13	22	58.7	27.1	5.3	8.9	247	7.94	5.56	86.51	05W-61	103	29	115	247	41.7	11.7	46.6
				AVE	**49.8**	**24.9**	**10.1**	**15.2**	**AVE**	**14.8**	**5.5**	**79.7**					**AVE**	**59.8**	**9.5**	**30.7**
				MAX	63.7	34.9	18.3	19.5	MAX	28.1	6.9	87.4					MAX	72.9	15.4	46.6
				MIN	32.9	12.6	5.1	8.9	MIN	6.2	3.6	66.7					MIN	41.7	1.2	24.5
				SDEV	12.1	8.5	5.0	3.7	SDEV	9.4	1.1	8.8					SDEV	9.9	5.2	7.9
338	329	0	0	9	97.3	0.0	0.0	2.7	338	26.56	4.69	68.75	T21-12	308	27	3	338	91.1	8.0	0.9
132	94	0	19	19	71.2	0.0	14.4	14.4	132	21.11	9.05	69.85	T21-11	17	27	88	132	12.9	20.5	66.7
89	74	0	3	12	83.1	0.0	3.4	13.5	89	8.30	5.14	86.56	T21-6	51	20	18	89	57.3	22.5	20.2
				AVE	**83.9**	**0.0**	**5.9**	**10.2**	**AVE**	**18.7**	**6.3**	**75.1**					**AVE**	**53.8**	**17.0**	**29.3**
				MAX	97.3	0.0	14.4	14.4	MAX	26.6	9.0	86.6					MAX	91.1	22.5	66.7
				MIN	71.2	0.0	0.0	2.7	MIN	8.3	4.7	68.8					MIN	12.9	8.0	0.9
				SDEV	13.1	0.0	7.5	6.5	SDEV	9.4	2.4	10.0					SDEV	39.2	7.8	33.8
0	0	0	0	0	na	na	na	na	0	32.93	4.88	62.20	T21-14	0	0	0	0	na	na	na
0	0	0	0	0	na	na	na	na	0	40.63	7.81	51.56	T21-13	0	0	0	0	na	na	na
166	55	36	21	54	33.1	21.7	12.7	32.5	166	7.91	3.72	88.37	T19-1	123	11	32	166	74.1	6.6	19.3
119	40	35	19	25	33.6	29.4	16.0	21.0	119	16.67	4.76	78.57	T19-2	93	10	16	119	78.2	8.4	13.4
115	63	28	13	11	54.8	24.3	11.3	9.6	115	35.00	7.50	57.50	T19-3	96	3	16	115	83.5	2.6	13.9
114	50	13	22	29	43.9	11.4	19.3	25.4	114	24.12	4.52	71.36	T21-8	56	9	49	114	49.1	7.9	43.0
				AVE	**41.3**	**21.7**	**14.8**	**22.1**	**AVE**	**20.9**	**5.1**	**74.0**					**AVE**	**71.2**	**6.4**	**22.4**
				MAX	54.8	29.4	19.3	32.5	MAX	35.0	7.5	88.4					MAX	83.5	8.4	43.0
				MIN	33.1	11.4	11.3	9.6	MIN	7.9	3.7	57.5					MIN	49.1	2.6	13.4
				SDEV	10.2	7.6	3.6	9.6	SDEV	11.5	1.6	13.0					SDEV	15.2	2.6	14.0

Qm = monocrystalline unstrained quartz
Qp = poltcrystalline quartz
Qs = Strained quartz
Srf = sedimentary rock fragments
Mrf = Metamorphic rock fragments
Mi = Igneous rock fragments

Fk = Potasium feldspar
Fp = plagioclase feldspar
Fm = Microcline
Fe = Epimatrix (feldspar replaced by clays)
Fwk = framework
See Appendix 3 for chert types

SDEV = standard deviation

Location: Hootalinqua/Masons Landing

Location			Stratigraphic Unit		Qm	Qp	Qs	Chert	Srf	Mrf	Fig	Fk	Fp	Fm	Fe	fwk (n1)
Tantalus Sandstones				detailed												
T6-4	99.50	cSt	Tantalus		10	25	92	368	7	5	0	0	0	0	0	507
T11-5	18.00	S	Tantalus		41	29	143	257	1	0	4	0	0	0	25	500
T11-6	28.00	S	Tantalus		37	25	148	241	1	1	5	0	0	0	42	500
T11-9	74.00	mSr	Tantalus		22	14	84	356	3	3	9	0	0	0	9	500
SUM SST					***110***	***93***	***467***	***1222***	***12***	***9***	***18***	***0***	***0***	***0***	***76***	***2007***
Fwk %					5.5	4.6	23.3	60.9	0.6	0.4	0.9	0.0	0.0	0.0	3.8	100.0
					Sum Q=		33.4	Sum RF=		62.8		Sum F=		3.8		
Tantalus Conglomerates																
T6-1	231.00	Gm	Tantalus		11	16	71	321	76	0	11	0	0	0	0	506
T6-3	97.00	Gm	Tantalus		8	13	16	401	56	0	6	0	0	0	0	500
T11-10	92.00	Gm	Tantalus		2	17	67	358	55	0	0	0	0	0	1	500
T11-11	157.00	Gm	Tantalus		1	4	21	429	13	3	34	0	0	0	10	515
T11-12	240.00	Gm	Tantalus		2	3	56	385	31	9	0	0	0	0	14	500
T11-14/40		Gm	Tantalus		6	3	158	297	28	2	0	0	0	0	6	500
T15-1		Gm 18.6/3	Tantalus		0	3	59	316	0	0	168	0	0	0	0	546
T16-1	79.00	Sm	Tantalus		4	11	56	430	0	0	5	0	0	0	3	509
T16-2	166.30	Gm	Tantalus		9	11	73	373	0	26	0	0	0	0	10	502
T16-3	164.00	Gm	Tantalus		0	2	15	467	15	0	0	0	0	0	1	500
T16-4	192.50	Gm-Gh	Tantalus		3	5	32	415	39	0	0	0	0	0	6	500
T16-5	361.10	Gm	Tantalus		0	3	19	348	59	0	571	0	0	0	0	1000
T16-8		Gm	Tantalus		0	1	7	134	0	3	352	0	0	0	3	500
SUM CONG					***46***	***92***	***650***	***4674***	***372***	***43***	***1147***	***0***	***0***	***0***	***54***	***7078***
Fwk %					0.6	1.3	9.2	66.0	5.3	0.6	16.2	0.0	0.0	0.0	0.8	100
					Sum Q=		11.1	Sum RF=		88.1		Sum F=		0.8		
Laberge Sandstones																
T11-2		(g)vcS	Tanglefoot?		69	19	179	43	3	0	3	57	0	2	125	500

Sample	Voids (Cements)	Hem	carb	Qtz	n	Q (Derived)	F	L
Tantalus Sandstones								
T6-4	404	2	0	0	913	25.05	0.00	74.95
T11-5	0	27	95	0	622	42.60	5.00	52.40
T11-6	1	17	36	0	554	42.00	8.40	49.60
T11-9	2	11	0	1	514	24.00	1.80	74.20
SUM SST	***407***	***57***	***131***	***1***	***AVE***	***33.41***	***3.80***	***62.79***
Fwk %	15.6	2.2	5.0	0.0	MAX	42.6	8.4	75.0
	%	%	%	%	MIN	24.00	0.00	49.60
	%Fwk =		77.1		2603			
Tantalus Conglomerates						Q	F	L
T6-1	0	5	0	1	512	19.37	0.00	78.46
T6-3	0	5	0	0	505	7.40	0.00	91.40
T11-10	10	12	0	0	522	17.20	0.20	82.60
T11-11	50	25	25	0	615	5.05	1.94	93.01
T11-12	7	3	36	0	546	12.20	2.80	85.00
T11-14/40	25	18	0	0	543	33.40	1.20	65.40
T15-1	1	6	0	2	555	11.36	0.00	88.64
T16-1	5	5	3	0	522	13.95	0.59	85.46
T16-2	4	15	0	3	524	18.53	1.99	79.48
T16-3	2	6	0	1	509	3.40	0.20	96.40
T16-4	9	10	0	1	520	8.00	1.20	90.80
T16-5	1	7	0	0	1008	2.20	0.00	97.80
T16-8	1	0	0	0	501	1.60	0.60	97.80
SUM CONG	***115***	***117***	***64***	***8***	***AVE***	***11.82***	***0.82***	***87.10***
Fwk %	1.6	1.6	0.87	0.11	MAX	33.40	2.80	97.80
	%	%	%	%	MIN	1.60	0.00	65.40
	% Fwk =		95.9		7382			
Laberge Sandstones						Q	F	L
T11-2	0	21	0	0	521	53.40	####	9.80

Chert types

Sample	A Wht	A Yel	A Gry	A Blk	A grn (rd)	B Wht	B Yel	B Gry	B Blk	B grn (rd)
Tantalus Sandstones										
T6-4	74	56	16	46	0	47	37	14	2	0
T11-5	57	29	18	19	0	59	19	5	11	0
T11-6	55	40	7	24	0	63	7	1	0	0
T11-9	100	49	18	24	0	72	12	8	7	0
SUM SST	***286***	***174***	***59***	***113***	***0***	***241***	***75***	***28***	***20***	***0***
Fwk %	23.4	14.2	4.8	9.2	0.0	19.7	6.1	2.3	1.6	0.0
					51.7					29.8
Tantalus Conglomerates										
T6-1	38	43	4	11	0	53	46	9	2	0
T6-3	35	14	4	4	0	19	5	0	0	0
T11-10	131	0	0	0	0	19	1	0	0	0
T11-11	23	10	2	3	0	9	1	1	0	0
T11-12	32	24	11	6	0	32	2	20	0	0
T11-14/40	23	60	0	8	0	37	14	4	6	0
T15-1	14	3	1	8	0	10	2	0	0	0
T16-1	76	32	2	6	0	22	1	0	0	0
T16-2	50	28	10	22	0	25	3	1	0	0
T16-3	11	6	4	0	0	0	2	0	0	0
T16-4	47	50	9	14	0	27	1	0	0	0
T16-5	50	168	15	11	0	20	0	0	0	0
T16-8	34	51	3	6	0	16	0	3	0	0
SUM CONG	***564***	***489***	***65***	***99***	***0***	***289***	***78***	***38***	***8***	***0***
Fwk %	12.1	10.5	1.4	2.1	0.0	6.2	1.7	0.8	0.2	0.0
					26.0					8.8
Laberge Sandstones										
T11-2	7	0	0	0	0	12	0	0	0	0

Sample	C Wht	C Yel	C Gry	C Blk	D Wht	D Yel	D Gry	D Blk	E Wht	E Yel	E Gry	E Blk	F Wht	F Yel	F Gry	F Blk	G Wht	G Yel	G Gry	G Blk	H Wht	H Yel	H Gry	H Blk
Tantalus Sandstones																								
T6-4	0	0	0	0	0	0	0	0	0	0	0	0	0	0	0	0	0	0	0	0	0	0	0	0
T11-5	0	0	0	0	0	0	0	0	1	0	0	0	0	0	0	0	0	0	0	0	0	0	0	0
T11-6	0	0	0	0	0	0	0	0	0	0	0	0	0	0	0	0	0	0	0	0	0	0	0	0
T11-9	0	0	0	0	0	0	0	0	2	0	0	0	0	0	0	0	0	0	0	0	0	0	0	0
SUM SST	***0***	***0***	***0***	***0***	***0***	***0***	***0***	***0***	***3***	***0***	***0***	***0***	***0***	***0***	***0***	***0***	***0***	***0***	***0***	***0***	***0***	***0***	***0***	***0***
Fwk %	0.0	0.0	0.0	0.0	0.0	0.0	0.0	0.0	0.2	0.0	0.0	0.0	0.0	0.0	0.0	0.0	0.0	0.0	0.0	0.0	0.0	0.0	0.0	0.0
				0.0				0.0				0.2				0.0				0.0				0.0
Tantalus Conglomerates																								
T6-1	0	0	0	0	0	0	0	0	0	0	0	0	0	0	0	0	5	0	4	0	0	0	0	0
T6-3	0	0	0	0	0	0	0	0	1	0	0	0	0	0	0	0	0	0	0	0	0	0	0	0
T11-10	0	0	0	0	0	0	0	0	0	0	0	0	0	0	0	0	0	0	0	0	0	0	0	0
T11-11	0	0	0	0	0	0	0	0	0	0	0	0	0	0	0	0	0	0	0	0	0	0	0	0
T11-12	0	0	0	0	0	0	0	0	0	0	0	0	0	0	0	0	0	0	0	0	0	0	0	0
T11-14/40	0	0	0	0	0	0	0	0	0	0	0	0	0	0	0	0	0	0	0	0	0	0	0	0
T15-1	0	0	0	0	0	0	0	0	0	0	0	0	0	0	0	0	0	0	0	0	0	0	0	0
T16-1	0	0	0	0	0	0	0	0	0	0	0	0	0	0	0	0	0	0	0	0	0	0	0	0
T16-2	0	0	0	0	0	0	0	0	0	0	0	0	0	0	0	0	0	0	0	0	0	0	0	0
T16-3	0	0	0	0	0	0	0	0	0	0	0	0	0	0	0	0	0	0	0	0	0	0	0	0
T16-4	0	0	0	0	0	0	0	0	0	0	0	0	0	0	0	0	0	0	0	0	0	0	0	0
T16-5	0	0	0	0	0	0	0	0	0	0	0	0	0	0	0	0	0	0	0	0	0	0	0	0
T16-8	0	0	0	0	0	0	0	0	0	0	0	0	0	0	0	0	0	0	0	0	0	0	0	0
SUM CONG	***0***	***0***	***0***	***0***	***0***	***0***	***0***	***0***	***1***	***0***	***0***	***0***	***0***	***0***	***0***	***0***	***5***	***0***	***4***	***0***	***0***	***0***	***0***	***0***
Fwk %	0.0	0.0	0.0	0.0	0.0	0.0	0.0	0.0	0.0	0.0	0.0	0.0	0.0	0.0	0.0	0.0	0.1	0.0	0.1	0.0	0.0	0.0	0.0	0.0
				0.0				0.0				0.0				0.0				0.2				0.0
Laberge Sandstones																								
T11-2	0	0	0	0	0	0	0	0	0	0	0	0	0	0	0	0	0	0	0	0	0	0	0	0

Sample	I Wht	I Yel	I Gry	I Blk	J Wht	J Yel	J Gry	J Blk	K Wht	K Yel	K Gry	K Blk	L Wht	L Yel	L Gry	L Blk	M Wht	M Yel	M Gry	M Blk	N Wht	N Yel	N Gry	N Blk
Tantalus Sandstones																								
T6-4	0	0	0	0	0	4	0	0	0	0	0	0	0	0	0	0	7	0	0	2	0	3	0	0
T11-5	0	0	0	0	0	0	0	0	0	0	0	0	0	0	0	0	5	2	0	0	0	0	0	0
T11-6	0	0	0	0	0	0	0	0	0	0	0	0	0	0	0	0	0	0	0	0	1	0	0	0
T11-9	0	0	0	0	0	0	0	0	0	0	0	0	0	0	0	0	7	0	2	0	0	0	0	0
SUM SST	***0***	***0***	***0***	***0***	***0***	***4***	***0***	***0***	***0***	***0***	***0***	***0***	***0***	***0***	***0***	***0***	***19***	***2***	***2***	***2***	***1***	***3***	***0***	***0***
Fwk %	0.0	0.0	0.0	0.0	0.0	0.3	0.0	0.0	0.0	0.0	0.0	0.0	0.0	0.0	0.0	0.0	1.6	0.2	0.2	0.2	0.1	0.2	0.0	0.0
				0.0				0.3				0.0				0.0				2.0				0.3
Tantalus Conglomerates																								
T6-1	0	2	2	0	0	0	0	0	0	0	0	0	0	0	0	0	0	20	0	0	0	2	3	0
T6-3	0	0	0	0	0	0	0	0	0	0	0	0	0	2	0	0	4	24	0	0	0	0	0	0
T11-10	0	0	0	0	0	0	0	0	0	0	0	0	0	0	0	0	111	0	0	0	12	0	0	0
T11-11	0	0	0	0	0	0	0	0	0	0	0	0	0	0	0	0	8	1	0	0	0	0	0	0
T11-12	0	0	0	0	0	0	0	0	0	0	0	0	0	0	0	0	20	2	8	0	7	0	0	0
T11-14/40	0	0	0	0	0	0	0	0	0	0	0	0	0	0	0	0	0	2	0	0	0	0	0	0
T15-1	0	0	0	0	0	0	0	0	0	0	0	0	0	0	0	0	0	186	8	0	0	0	0	0
T16-1	0	0	0	0	0	0	0	0	0	0	0	0	0	0	0	0	3	0	0	0	0	0	0	0
T16-2	0	0	0	0	0	0	0	0	0	0	0	0	0	0	0	0	16	0	1	0	0	0	0	0
T16-3	0	0	0	0	0	0	0	0	0	0	0	0	0	0	0	0	0	0	0	0	0	0	0	0
T16-4	0	0	0	0	11	0	0	0	2	0	0	0	0	0	0	0	2	0	0	0	0	0	0	0
T16-5	0	0	0	0	0	0	0	0	0	0	0	0	0	0	0	0	0	0	4	0	0	0	0	0
T16-8	0	0	0	0	0	0	0	0	0	0	0	0	0	0	0	0	7	0	0	0	0	0	0	0
SUM CONG	***0***	***2***	***2***	***0***	***11***	***0***	***0***	***0***	***2***	***0***	***0***	***0***	***0***	***2***	***0***	***0***	***171***	***235***	***21***	***0***	***19***	***2***	***3***	***0***
Fwk %	0.0	0.0	0.0	0.0	0.2	0.0	0.0	0.0	0.0	0.0	0.0	0.0	0.0	0.0	0.0	0.0	3.7	5.0	0.4	0.0	0.4	0.0	0.1	0.0
				0.1				0.2				0.0				0.0				9.1				0.5
Laberge Sandstones																								
T11-2	0	0	0	0	0	0	0	0	0	0	0	0	0	0	0	0	0	0	0	0	0	0	0	0

Sample	O Wht	O Yel	O Gry	O Blk	P Wht	P Yel	P Gry	P Blk	Q Wht	Q Yel	Q Gry	Q Blk	R Wht	R Yel	R Gry	R Blk	S Wht	S Yel	S Gry	S Blk	T Wht	T Yel	T Gry	T Blk
Tantalus Sandstones																								
T6-4	0	0	3	0	0	0	0	0	0	0	4	9	0	0	0	0	5	0	2	0	0	0	0	0
T11-5	0	0	0	0	0	0	0	0	0	0	0	3	0	0	0	0	0	1	0	0	0	0	0	0
T11-6	0	1	0	0	0	0	0	0	0	0	3	0	0	0	0	0	0	0	0	0	5	0	0	0
T11-9	0	0	0	0	0	0	0	0	0	2	0	1	0	0	0	1	6	6	1	0	3	0	0	0
SUM SST	***0***	***1***	***3***	***0***	***0***	***0***	***0***	***0***	***0***	***2***	***7***	***13***	***0***	***0***	***0***	***1***	***11***	***7***	***3***	***0***	***8***	***0***	***0***	***0***
Fwk %	0.0	0.1	0.2	0.0	0.0	0.0	0.0	0.0	0.0	0.2	0.6	1.1	0.0	0.0	0.0	0.1	0.9	0.6	0.2	0.0	0.7	0.0	0.0	0.0
				0.3				0.0				1.8				0.1				1.7				0.7
Tantalus Conglomerates																								
T6-1	0	0	0	0	0	0	0	0	0	0	0	3	0	0	0	0	0	0	0	0	2	0	0	0
T6-3	0	0	0	0	0	0	0	0	0	0	0	0	0	0	0	0	0	2	0	0	0	0	0	0
T11-10	0	0	0	0	0	0	0	0	0	0	0	0	0	0	0	0	0	0	0	0	0	0	0	0
T11-11	0	0	0	0	0	0	0	0	0	0	0	0	0	0	0	0	0	0	0	0	0	0	0	0
T11-12	4	0	0	0	0	0	0	0	13	0	0	0	0	0	0	11	3	0	0	17	0	0	0	0
T11-14/40	0	0	0	0	0	0	0	0	3	5	0	0	0	0	0	0	4	0	0	0	0	0	0	0
T15-1	0	0	0	0	0	0	0	0	0	0	0	0	0	0	0	0	0	0	0	16	0	0	0	0
T16-1	0	0	0	0	0	0	0	0	64	0	0	0	0	0	0	0	18	5	0	0	0	0	0	0
T16-2	0	0	0	0	0	0	0	0	13	0	0	5	0	0	0	0	10	1	10	1	1	0	0	0
T16-3	0	0	0	0	0	0	0	0	0	234	0	0	0	0	0	0	208	0	0	0	0	0	0	0
T16-4	0	0	0	0	138	0	0	0	42	0	0	0	0	0	0	0	0	5	2	0	0	0	0	0
T16-5	0	0	0	0	0	0	0	0	0	0	0	4	0	0	0	0	3	0	2	2	0	0	0	0
T16-8	0	0	0	0	0	0	0	0	0	0	0	0	0	0	0	0	5	0	0	0	0	0	0	0
SUM CONG	***4***	***0***	***0***	***0***	***138***	***0***	***0***	***0***	***135***	***239***	***0***	***12***	***0***	***0***	***0***	***11***	***251***	***13***	***14***	***36***	***3***	***0***	***0***	***0***
Fwk %	0.1	0.0	0.0	0.0	3.0	0.0	0.0	0.0	2.9	5.1	0.0	0.3	0.0	0.0	0.0	0.2	5.4	0.3	0.3	0.8	0.1	0.0	0.0	0.0
				0.1				3.0				8.3				0.2				6.7				0.1
Laberge Sandstones																								
T11-2	0	0	0	0	0	0	0	0	0	0	0	0	0	0	0	0	0	0	0	0	24	0	0	0

Sample	U Wht	U Yel	U Gry	U Blk	V Wht	V Yel	V Gry	V Blk	W Wht	W Yel	W Gry	W Blk	X Wht	X Yel	X Gry	X Blk
Tantalus Sandstones																
T6-4	0	2	0	7	1	1	6	7	7	2	0	4	0	0	0	0
T11-5	0	0	1	4	6	9	1	4	2	1	0	0	0	0	0	0
T11-6	0	0	0	0	4	14	0	0	8	4	4	0	0	0	0	0
T11-9	1	0	2	0	15	6	0	4	3	2	1	0	0	0	0	0
SUM SST	***1***	***2***	***3***	***11***	***26***	***30***	***7***	***15***	***20***	***9***	***5***	***4***	***0***	***0***	***0***	***0***
Fwk %	0.1	0.2	0.2	0.9	2.1	2.5	0.6	1.2	1.6	0.7	0.4	0.3	0.0	0.0	0.0	0.0
				1.4				6.4				3.1				0.0
Tantalus Conglomerates																
T6-1	0	0	0	5	3	31	8	15	0	0	0	0	0	0	0	0
T6-3	0	0	0	5	0	245	5	32	0	0	0	0	0	0	0	0
T11-10	1	0	0	0	51	0	0	0	32	0	0	0	0	0	0	0
T11-11	0	0	0	0	1	93	0	2	151	0	0	124	0	0	0	0
T11-12	0	24	0	0	35	14	5	35	11	31	0	3	0	0	0	0
T11-14/40	1	8	0	37	1	51	0	0	0	25	0	8	0	0	0	0
T15-1	0	0	0	7	7	27	0	0	6	17	0	4	0	0	0	0
T16-1	0	0	0	10	24	29	15	4	111	7	0	0	0	0	0	0
T16-2	0	49	0	0	11	0	0	45	49	23	0	0	0	0	0	0
T16-3	0	0	0	2	0	0	0	0	0	0	0	0	0	0	0	0
T16-4	0	0	0	0	3	3	0	13	4	42	0	0	0	0	0	0
T16-5	0	0	0	0	2	0	0	0	67	0	0	0	0	0	0	0
T16-8	0	0	0	0	0	1	1	0	2	3	1	1	0	0	0	0
SUM CONG	***2***	***81***	***0***	***66***	***138***	***494***	***34***	***146***	***433***	***148***	***1***	***140***	***0***	***0***	***0***	***0***
Fwk %	0.0	1.7	0.0	1.4	3.0	10.6	0.7	3.1	9.3	3.2	0.0	3.0	0.0	0.0	0.0	0.0
				3.2				17.4				15.4				0.0
Laberge Sandstones																
T11-2	0	0	0	0	0	0	0	0	0	0	0	0	0	0	0	0

Sample	Z Wht	Z Yel	Z Gry	Z Blk	A' Wht	A' Yel	A' Gry	A' Blk	B' Wht	B' Yel	B' Gry	B' Blk	Totals	W	Y	G	B+R+Gr
Tantalus Sandstones																	
T6-4	0	0	0	0	0	0	0	0	0	0	0	0	368	141	105	45	77
T11-5	0	0	0	0	0	0	0	0	0	0	0	0	257	130	61	25	41
T11-6	0	0	0	0	0	0	0	0	0	0	0	0	241	136	66	15	24
T11-9	1	0	0	0	0	0	0	0	0	0	0	0	356	210	77	32	37
SUM SST	***1***	***0***	***0***	***0***	***0***	***0***	***0***	***0***	***0***	***0***	***0***	***0***	***1222***	***617***	***309***	***117***	***179***
Fwk %	0.1	0.0	0.0	0.0	0.0	0.0	0.0	0.0	0.0	0.0	0.0	0.0	100.0	50.5	25.3	9.6	14.6
				0.1				0.0				0.0					
Tantalus Conglomerates																	
T6-1	0	6	0	0	0	0	4	0	0	0	0	0	321	101	150	34	36
T6-3	0	0	0	0	0	0	0	0	0	0	0	0	401	59	292	9	41
T11-10	0	0	0	0	0	0	0	0	0	0	0	0	358	357	1	0	0
T11-11	0	0	0	0	0	0	0	0	0	0	0	0	429	192	105	3	129
T11-12	5	4	0	6	0	0	0	0	0	0	0	0	385	162	101	44	78
T11-14/40	0	0	0	0	0	0	0	0	0	0	0	0	297	69	165	4	59
T15-1	0	0	0	0	0	0	0	0	0	0	0	0	316	37	235	9	35
T16-1	0	0	0	0	0	0	0	0	0	0	0	0	430	319	74	17	20
T16-2	0	0	0	0	0	0	0	0	0	0	0	0	373	174	104	22	73
T16-3	0	0	0	0	0	0	0	0	0	0	0	0	467	219	242	4	2
T16-4	0	0	0	0	0	0	0	0	0	0	0	0	415	276	101	11	27
T16-5	0	0	0	0	0	0	0	0	0	0	0	0	348	142	168	21	17
T16-8	0	0	0	0	0	0	0	0	0	0	0	0	134	64	55	8	7
SUM CONG	***5***	***10***	***0***	***6***	***0***	***0***	***4***	***0***	***0***	***0***	***0***	***0***	***4674***	***2171***	***1793***	***186***	***524***
Fwk %	0.1	0.2	0.0	0.1	0.0	0.0	0.1	0.0	0.0	0.0	0.0	0.0	100.0	46.4	38.4	4.0	11.2
				0.4				0.1				0.0					
Laberge Sandstones																	
T11-2	0	0	0	0	0	0	0	0	0	0	0	0	43	43	0	0	0

Sample		Chert by colour: White	Yellow	Grey	Black			Qm	Qp	Qs		Chert Groups: A to K	L to T +Z	U to W	sub total			
Tantalus Sandstones		%	%	%	%			%	%	%		MASSIVE	BRECCIATED	SPHERES		%Mas	%Brec	%spher
T6-4		38.3	28.5	12.2	20.9	368		7.9	19.7	72.4	T6-4	296	35	37	368	80.4	9.5	10.1
T11-5		50.6	23.7	9.7	16.0	257		19.2	13.6	67.1	T11-5	218	11	28	257	84.8	4.3	10.9
T11-6		56.4	27.4	6.2	10.0	241		17.6	11.9	70.5	T11-6	197	10	34	241	81.7	4.1	14.1
T11-9		59.0	21.6	9.0	10.4	356		18.3	11.7	70.0	T11-9	292	30	34	356	82.0	8.4	9.6
SUM SST	***AVE***	***51.1***	***25.3***	***9.3***	***14.3***	***AVE***		***15.8***	***14.2***	***70.0***					***AVE***	***82.3***	***6.6***	***11.2***
Fwk %	MAX	59.0	28.5	12.2	20.9	MAX		19.2	19.7	72.4					MAX	84.8	9.5	14.1
	MIN	38.3	21.6	6.2	10.0	MIN		7.9	11.7	67.1					MIN	80.4	4.1	9.6
	SD	9.2	3.2	2.5	5.2	SD		5.3	3.7	2.2					SD	1.8	2.8	2.0
Tantalus Conglomerates		White	Yellow	Grey	Black			Qm	Qp	Qs						%Mas	%Brec	%spher
T6-1		31.5	46.7	10.6	11.2	321		11.2	16.3	72.4	T6-1	219	36	62	317	69.1	11.4	19.6
T6-3		14.7	72.8	2.2	10.2	401		21.6	35.1	43.2	T6-3	82	32	287	401	20.4	8.0	71.6
T11-10		99.7	0.3	0.0	0.0	358		2.3	19.8	77.9	T11-10	151	123	84	358	42.2	34.4	23.5
T11-11		44.8	24.5	0.7	30.1	429		3.8	15.4	80.8	T11-11	49	9	371	429	11.4	2.1	86.5
T11-12		42.1	26.2	11.4	20.3	385		3.3	4.9	91.8	T11-12	127	100	158	385	33.0	26.0	41.0
T11-14/40		23.2	55.6	1.3	19.9	297		3.6	1.8	94.6	T11-14/40	152	14	131	297	51.2	4.7	44.1
T15-1		11.7	74.4	2.8	11.1	316		0.0	4.8	95.2	T15-1	38	210	68	316	12.0	66.5	21.5
T16-1		74.2	17.2	4.0	4.7	430		5.6	15.5	78.9	T16-1	139	91	200	430	32.3	21.2	46.5
T16-2		46.6	27.9	5.9	19.6	373		9.7	11.8	78.5	T16-2	139	57	177	373	37.3	15.3	47.5
T16-3		46.9	51.8	0.9	0.4	467		0.0	11.8	88.2	T16-3	23	442	2	467	4.9	94.6	0.4
T16-4		66.5	24.3	2.7	6.5	415		7.5	12.5	80.0	T16-4	161	189	65	415	38.8	45.5	15.7
T16-5		40.8	48.3	6.0	4.9	348		0.0	13.6	86.4	T16-5	264	15	69	348	75.9	4.3	19.8
T16-8		47.8	41.0	6.0	5.2	134		0.0	12.5	87.5	T16-8	113	12	9	134	84.3	9.0	6.7
SUM CONG	***AVE***	***45.4***	***39.3***	***4.2***	***11.1***	***AVE***		***5.3***	***13.5***	***81.2***					***AVE***	***39.4***	***26.4***	***34.2***
Fwk %	MAX	99.7	74.4	11.4	30.1	MAX		21.6	35.1	95.2					MAX	84.3	94.6	86.5
	MIN	11.7	0.3	0.0	0.0	MIN		0.0	1.8	43.2					MIN	4.9	2.1	0.4
	SD	24.2	21.7	3.6	9.0			6.2	8.2	13.4					SD	24.5	28.6	25.8
Laberge Sandstones		White	Yellow	Grey	Black			Qm	Qp	Qs						%Mas	%Brec	%spher
T11-2		100.0	0.0	0.0	0.0	43		25.8	7.1	67.0	T11-2	19	24	0	43	44.2	55.8	0.0

Qm = monocrystalline unstrained quartz
Qp = poltcrystalline quartz
Qs = Strained quartz
Srf = sedimentary rock fragments
Mrf = Metamorphic rock fragments
Mi = Igneous rock fragments

Fk = Potasium feldspar
Fp = plagioclase feldspar
Fm = Microcline
Fe = Epimatrix (feldspar replaced by clays)
Fwk = framework
See Appendix 3 for chert types

SDEV = standard deviation

Location			Stratigraphic Unit		Point counts (number of observations)																			
					Framework Grains											n1	Cements				n	Derived		
Carmacks area																								
Tantalus Conglomerates				detailed	Qm	Qp	Qs	Chert	Srf	Mrf	Fig	Fk	Fp	Fm	Fe	fwk	Voids	Hem	carb	Qtz		Q	F	L
T10-2	0.70	Gm-Gh	Tantalus		1	4	4	356	33	6	26	0	0	0	70	500	0	6	2	0	508	1.8	14.0	84.2
T10-4	97.50	Gm			15	14	82	273	0	6	63	0	0	0	47	500	4	20	32	0	556	22.2	9.4	68.4
T13-33	87.50	Gm			2	16	24	411	46	0	0	0	0	0	1	500	0	1	0	0	501	8.4	0.2	91.4
T13-37		gGm			1	33	89	360	0	17	0	0	0	0	0	500	5	0	0	0	505	24.6	0.0	75.4
T14-24	47.50	Gm			9	2	72	408	0	0	13	0	0	2	4	510	0	14	0	1	525	16.3	1.2	82.5
T17-6	58.00	Gm	Tantalus		1	0	28	446	14	0	0	0	0	0	11	500	3	14	0	0	517	5.8	2.2	92.0
T17-7	59.00	Gm	Tantalus		4	5	119	360	5	5	1	0	0	0	1	500	0	7	18	0	525	25.6	0.2	74.2
T17-8	74.10	vcSm	Tantalus		7	2	153	313	0	0	13	10	0	0	2	500	0	15	1	0	516	32.4	2.4	65.2
T17-11	90.00	Gm	Tantalus		2	0	39	459	0	0	0	0	0	0	0	500	0	8	19	0	527	8.2	0.0	91.8
T17-12	181.50	Gh	Tantalus		1	2	52	434	5	6	0	0	0	0	0	500	4	4	0	0	508	11.0	0.0	89.0
T17-13	194.00	Gh,t	Tantalus		6	1	157	336	0	1	0	0	0	0	6	507	1	1	0	0	509	32.3	1.2	66.5
T17-24	217.00	gSGh	Tantalus		1	1	48	390	22	34	4	0	0	0	0	500	1	1	0	0	502	10.0	0.0	90.0
T17-27	252.00	Gm,h	Tantalus	tr mylonite	1	1	81	324	92	0	0	0	0	0	1	500	0	2	0	0	502	16.6	0.2	83.2
T17-31	308.00	Gmh	Tantalus		2	0	117	375	0	6	0	0	0	0	0	500	0	1	0	0	501	23.8	0.0	76.2
T17-37	321.00	Gh,m	Tantalus		5	2	17	470	3	1	0	0	0	0	2	500	0	6	0	0	506	4.8	0.4	94.8
T17-38	334.00	Gm,h	Tantalus		0	3	58	385	0	0	50	0	0	0	4	500	0	1	0	1	502	12.2	0.8	87.0
T17-39		Gm,h	Tantalus		0	1	23	473	0	0	0	0	0	0	3	500	1	14	0	0	515	4.8	0.6	94.6
T18-5	24.00	Gmh	Tantalus		5	10	61	317	15	14	59	0	0	0	19	500	0	11	0	0	511	15.2	3.8	81.0
T18-7	37.00	Gm	Tantalus		3	0	15	477	0	1	7	0	0	0	3	506	0	6	0	2	514	3.6	0.6	95.8
T18-9	58.00	Gm	Tantalus		0	0	12	488	0	0	0	0	0	0	0	500	0	2	0	0	502	2.4	0.0	97.6
T18-13	126.00	Gm	Tantalus		11	0	184	261	0	0	8	0	0	0	36	500	0	10	0	0	510	39.0	7.2	53.8
Sum G					***77***	***97***	***1435***	***8116***	***235***	***97***	***244***	***10***	***0***	***2***	***210***	***10523***	***19***	***144***	***72***	***4***	***AVE***	***15.3***	***2.1***	***82.6***
%					*0.7*	*0.9*	*13.6*	*77.1*	*2.2*	*0.9*	*2.3*	*0.1*	*0.0*	*0.0*	*2.0*	*100*	*0.2*	*1.3*	*0.7*	*0.0*	Max	39.0	14.0	97.6
					Sum Q=		15.3	Sum RF=		82.6		Sum F=		2.1			%	%	%	%	Min	1.8	0.0	53.8
																	%Fwk =		97.8	n	10762			
Tantalus Sandstones																								
T17-10	75.30	g,vcS	Tantalus		12	2	170	308	0	0	1	6	0	0	1	500	3	21	1	1	526	36.8	1.4	61.8
T17-23	215.00	mcSh	Tantalus		18	8	161	280	2	3	2	20	0	1	5	500	2	37	0	0	539	37.4	5.2	57.4
T17-30	307.00	c-vcSh,w	Tantalus		15	6	123	339	1	3	4	5	0	0	4	500	0	0	0	0	500	28.8	1.8	69.4
T18-6	32.00	cSm	Tantalus		21	2	99	335	7	1	6	2	0	0	27	500	1	22	0	9	532	24.4	5.8	69.8
T18-10	69.00	mcSp	Tantalus	tr chlorite cement	14	3	102	361	10	1	5	0	0	0	4	500	0	27	0	22	549	23.8	0.8	75.4
Sum S					***80***	***21***	***655***	***1623***	***20***	***8***	***18***	***33***	***0***	***1***	***41***	***2500***	***6***	***107***	***1***	***32***	***AVE***	***30.2***	***3.0***	***66.8***
%					*3.2*	*0.8*	*26.2*	*64.9*	*0.8*	*0.3*	*0.7*	*1.3*	*0.0*	*0.0*	*1.6*	*100*	*0.2*	*4.0*	*0.0*	*1.2*	Max	37.4	5.8	75.4
					Sum Q=		30.2	Sum RF=		66.8		Sum F=		3			%	%	%	%	Min	23.8	0.8	57.4
																	%Fwk =		94.5	n =	2646			
Tangelfoot Conglomerate																								
T17-1	0.00	Gm	Tangelfoot	volcLithRudite	14	2	18	0	1	0	373	59	33	0	0	500	1	10	0	0	511	6.8	18.4	74.8
T17-2b	5.00	Gt	Tangelfoot		132	6	182	0	0	0	0	103	0	0	77	500	0	222	0	0	722	64.0	36.0	0.0
T17-3	5.60	Gt	Tangelfoot		26	0	305	0	0	0	32	134	0	0	3	500	0	40	98	0	638	66.2	27.4	6.4
T17-4	1.50	Gm,t	Tangelfoot		14	14	69	0	28	0	58	275	0	0	42	500	0	8	0	0	508	19.4	63.4	17.2
T18-4	>-200	Gm	Tangelfoot		0	1	59	400	23	17	0	0	0	0	0	500	3	8	0	0	511	12.0	0.0	88.0
Sum G					***186***	***23***	***633***	***400***	***52***	***17***	***463***	***571***	***33***	***0***	***122***	***2500***	***4***	***288***	***98***	***0***	***AVE***	***33.7***	***29.0***	***37.3***
%					*7.4*	*0.9*	*25.3*	*16.0*	*2.1*	*0.7*	*18.5*	*22.8*	*1.3*	*0.0*	*4.9*	100.0	0.1	10.0	3.4	0.0	Max	66.2	63.4	88.0
																	%	%	%	%	Min	6.8	0.0	0.0
																	%Fwk =		86.5	n =	2890			
Tangelfoot Fm Sandstone																								
T18-1	-20.00	vcSm	Tangelfoot		55	6	249	0	105	0	2	50	2	0	31	500	0	48	0	0	548	62.0	16.6	21.4
T18-3	>-200	g,vcSm	Tangelfoot		50	11	228	1	0	0	28	161	11	0	10	500	1	29	0	0	530	57.8	36.4	5.8
Sum S					***105***	***17***	***477***	***1***	***105***	***0***	***30***	***211***	***13***	***0***	***41***	***1000***	***1***	***77***	***0***	***0***	***AVE***	***59.9***	***26.5***	***13.6***
%					*10.5*	*1.7*	*47.7*	*0.1*	*10.5*	*0.0*	*3.0*	*21.1*	*1.3*	*0.0*	*4.1*	100.0	0.1	7.1	0.0	0.0	Max	62.0	36.4	21.4
																					Min	57.8	16.6	5.8
																	%Fwk =		92.8	n =	1078			

Chert types

Sample	A				rd	B				rd	C				D				E				F			
	Wht	Yel	Gry	Blk	grn	Wht	Yel	Gry	Blk	grn	Wht	Yel	Gry	Blk	Wht	Yel	Gry	Blk	Wht	Yel	Gry	Blk	Wht	Yel	Gry	Blk
Tantalus Conglomerates																										
T10-2	8	7	5	0	74	0	0	0	0	0	0	0	0	0	0	0	0	0	0	0	0	0	0	0	0	0
T10-4	21	50	6	5	0	24	7	0	0	0	0	0	0	0	1	0	0	0	0	0	0	0	0	0	0	0
T13-33	67	92	13	36	1	8	9	6	0	0	0	0	0	0	0	0	0	0	0	0	0	0	0	0	0	0
T13-37	21	30	6	0	0	20	60	3	0	0	0	0	0	0	0	0	0	0	0	0	0	0	0	0	0	0
T14-24	20	55	27	34	0	58	33	6	3	0	0	0	0	0	0	0	0	0	0	0	0	0	0	0	0	0
T17-6	0	1	0	29	0	156	6	0	0	0	0	0	0	0	0	0	0	0	0	0	0	0	0	0	0	0
T17-7	32	28	0	0	0	65	6	1	0	0	0	0	0	0	0	0	0	0	0	0	0	0	0	0	0	0
T17-8	45	63	9	14	0	57	11	6	0	0	0	0	0	0	0	0	0	0	0	0	0	0	0	0	0	0
T17-11	4	52	0	0	0	45	2	0	0	0	0	0	0	0	0	0	0	0	0	0	0	0	0	0	0	0
T17-12	7	54	0	0	0	10	3	5	7	0	0	0	0	0	0	0	0	0	3	0	0	0	0	7	0	0
T17-13	13	87	8	10	0	12	9	0	0	0	0	0	0	0	0	0	0	0	0	4	0	0	0	0	0	0
T17-24	12	35	17	6	0	11	21	0	0	0	0	0	0	0	0	0	0	0	0	0	0	0	0	0	0	0
T17-27	2	9	2	1	0	19	7	0	2	0	0	0	0	0	0	0	0	0	0	0	0	0	0	0	0	0
T17-31	8	5	5	6	0	8	0	0	0	0	0	0	0	0	0	0	0	0	0	0	0	0	0	0	0	0
T17-37	22	20	1	0	0	10	2	0	0	0	0	0	0	0	0	0	0	0	0	0	0	0	0	0	0	0
T17-38	17	24	1	5	0	107	3	0	0	0	0	0	0	0	0	0	0	0	0	0	0	0	0	0	0	0
T17-39	27	77	7	8	0	23	0	0	0	0	0	0	0	0	0	0	0	0	0	0	0	0	0	0	0	0
T18-5	18	24	4	19	0	13	1	3	0	0	0	0	0	0	0	0	0	0	0	0	0	0	0	0	0	0
T18-7	23	29	9	7	0	26	2	0	0	0	0	0	0	0	0	0	0	0	0	0	0	0	0	0	0	0
T18-9	15	8	4	4	0	4	0	0	0	0	0	0	0	0	0	0	0	0	0	0	0	0	0	0	0	0
T18-13	80	28	24	8	0	34	2	3	0	0	0	0	0	0	0	0	0	0	0	0	0	0	0	0	0	0
Sum G	***462***	***778***	***148***	***192***	***75***	***710***	***184***	***33***	***12***	***0***	***0***	***0***	***0***	***0***	***1***	***0***	***0***	***0***	***3***	***4***	***0***	***0***	***0***	***7***	***0***	***0***
%	5.7	9.6	1.8	2.4	0.9	8.7	2.3	0.4	0.1	0.0	0.0	0.0	0.0	0.0	0.0	0.0	0.0	0.0	0.0	0.0	0.0	0.0	0.0	0.1	0.0	0.0
					20.4					11.6				0.0				0.0				0.1				0.1
Tantalus Sandstones																										
T17-10	51	80	4	27	0	51	15	7	2	0	0	0	0	0	0	0	0	0	0	0	0	0	0	0	0	0
T17-23	83	58	23	12	0	26	9	13	0	0	0	0	0	0	0	0	0	0	0	0	0	0	0	0	0	0
T17-30	65	54	28	17	0	22	8	3	0	2	1	0	0	0	0	0	0	0	0	0	0	0	0	0	0	0
T18-6	79	50	24	15	0	30	13	1	0	0	0	0	0	0	0	0	0	0	0	0	0	0	0	0	0	0
T18-10	115	48	21	9	0	76	6	3	0	0	0	0	0	0	0	0	0	0	0	0	0	0	0	0	0	0
Sum S	***393***	***290***	***100***	***80***	***0***	***205***	***51***	***27***	***2***	***2***	***1***	***0***	***0***	***0***	***0***	***0***	***0***	***0***	***0***	***0***	***0***	***0***	***0***	***0***	***0***	***0***
%	24.2	17.9	6.2	4.9	0.0	12.6	3.1	1.7	0.1	0.1	0.1	0.0	0.0	0.0	0.0	0.0	0.0	0.0	0.0	0.0	0.0	0.0	0.0	0.0	0.0	0.0
					53.2					17.7				0.1				0.0				0.0				0.0
Tangelfoot Conglomerate																										
T17-1	0	0	0	0	0	0	0	0	0	0	0	0	0	0	0	0	0	0	0	0	0	0	0	0	0	0
T17-2b	0	0	0	0	0	0	0	0	0	0	0	0	0	0	0	0	0	0	0	0	0	0	0	0	0	0
T17-3	0	0	0	0	0	0	0	0	0	0	0	0	0	0	0	0	0	0	0	0	0	0	0	0	0	0
T17-4	0	0	0	0	0	0	0	0	0	0	0	0	0	0	0	0	0	0	0	0	0	0	0	0	0	0
T18-4	20	0	0	6	0	4	0	0	0	0	0	0	0	0	0	0	0	0	0	0	0	0	0	0	0	0
Sum G	***20***	***0***	***0***	***6***	***0***	***4***	***0***	***0***	***0***	***0***	***0***	***0***	***0***	***0***	***0***	***0***	***0***	***0***	***0***	***0***	***0***	***0***	***0***	***0***	***0***	***0***
%	5.0	0.0	0.0	1.5	0.0	1.0	0.0	0.0	0.0	0.0	0.0	0.0	0.0	0.0	0.0	0.0	0.0	0.0	0.0	0.0	0.0	0.0	0.0	0.0	0.0	0.0
					6.5					1.0				0.0				0.0				0.0				0.0
Tangelfoot Fm Sandstone																										
T18-1	0	0	0	0	0	0	0	0	0	0	0	0	0	0	0	0	0	0	0	0	0	0	0	0	0	0
T18-3	0	0	0	0	0	1	0	0	0	0	0	0	0	0	0	0	0	0	0	0	0	0	0	0	0	0

Sample	G				H				I				J				K				L			
	Wht	Yel	Gry	Blk	Wht	Yel	Gry	Blk	Wht	Yel	Gry	Blk	Wht	Yel	Gry	Blk	Wht	Yel	Gry	Blk	Wht	Yel	Gry	Blk
Tantalus Conglomerates																								
T10-2	0	0	0	0	0	0	0	0	0	0	0	0	0	0	0	0	0	0	0	0	0	0	0	0
T10-4	0	0	0	0	0	0	0	0	0	0	0	0	0	0	5	0	0	0	0	0	0	0	0	0
T13-33	0	0	0	0	0	0	0	0	0	0	0	0	0	0	0	0	0	0	0	0	0	0	0	0
T13-37	0	0	0	0	0	0	0	0	0	0	0	0	0	0	0	0	0	0	0	0	0	0	0	0
T14-24	0	0	0	0	0	0	0	0	0	0	0	0	0	0	0	0	0	0	0	0	0	0	0	0
T17-6	0	0	0	0	0	0	0	0	0	0	0	0	0	0	0	0	0	0	0	0	0	0	0	0
T17-7	0	0	0	0	0	0	0	0	4	0	0	0	0	0	0	0	0	0	0	0	0	0	0	0
T17-8	0	0	0	0	0	0	0	0	0	0	0	0	0	0	0	0	0	0	0	0	0	0	0	0
T17-11	0	0	0	0	0	0	0	0	0	0	0	0	0	0	0	0	0	0	0	0	0	0	0	0
T17-12	0	0	0	0	0	0	0	0	0	0	0	0	7	0	0	0	0	0	0	0	0	0	0	0
T17-13	0	0	0	0	0	0	0	0	0	0	0	0	0	0	0	0	0	0	0	0	0	0	0	0
T17-24	0	0	0	0	0	0	0	0	0	0	0	0	0	0	0	0	0	0	0	0	0	0	0	0
T17-27	0	0	0	0	0	0	0	0	0	0	0	0	0	0	0	0	0	0	0	0	0	0	0	0
T17-31	0	0	0	0	0	0	0	0	0	0	0	0	0	0	0	0	0	0	0	0	0	0	0	0
T17-37	0	0	0	0	4	0	0	0	0	0	0	0	0	0	0	0	0	0	0	0	0	0	0	0
T17-38	0	0	0	0	0	0	0	0	0	0	0	0	3	0	0	0	0	0	0	0	0	0	0	0
T17-39	0	0	0	0	0	0	0	0	0	0	0	0	9	0	0	0	0	0	0	0	0	0	0	0
T18-5	0	0	0	0	0	0	0	0	0	0	0	0	0	0	0	0	1	0	0	0	0	0	0	0
T18-7	0	0	0	0	0	0	0	0	0	0	0	0	0	0	0	0	0	0	0	0	0	0	0	0
T18-9	0	0	0	0	0	0	0	0	0	0	0	0	2	0	0	0	0	0	0	0	0	0	0	0
T18-13	0	0	0	0	0	0	0	0	0	0	0	0	3	0	1	0	0	0	0	0	0	0	0	0
Sum G	***0***	***0***	***0***	***0***	***4***	***0***	***0***	***0***	***4***	***0***	***0***	***0***	***24***	***0***	***6***	***0***	***1***	***0***	***0***	***0***	***0***	***0***	***0***	***0***
%	0.0	0.0	0.0	0.0	0.0	0.0	0.0	0.0	0.0	0.0	0.0	0.0	0.3	0.0	0.1	0.0	0.0	0.0	0.0	0.0	0.0	0.0	0.0	0.0
				0.0				0.0				0.0				0.4				0.0				0.0
Tantalus Sandstones																								
T17-10	0	0	0	0	1	0	0	0	0	0	0	0	0	0	0	0	0	2	0	0	0	0	0	0
T17-23	1	0	0	0	0	0	0	0	0	0	0	0	0	0	0	0	0	0	0	0	0	0	0	0
T17-30	0	0	0	0	0	0	0	0	1	0	0	0	0	0	0	0	0	0	0	0	2	6	1	0
T18-6	0	0	0	0	0	0	0	0	0	0	0	0	2	2	0	0	1	0	0	0	0	0	0	0
T18-10	0	0	0	0	0	0	0	0	0	0	0	0	4	1	0	0	0	0	0	0	0	0	0	0
Sum S	***1***	***0***	***0***	***0***	***1***	***0***	***0***	***0***	***1***	***0***	***0***	***0***	***6***	***3***	***0***	***0***	***1***	***2***	***0***	***0***	***2***	***6***	***1***	***0***
%	0.1	0.0	0.0	0.0	0.1	0.0	0.0	0.0	0.1	0.0	0.0	0.0	0.4	0.2	0.0	0.0	0.1	0.1	0.0	0.0	0.1	0.4	0.1	0.0
				0.1				0.1				0.1				0.6				0.2				0.6
Tangelfoot Conglomerate																								
T17-1	0	0	0	0	0	0	0	0	0	0	0	0	0	0	0	0	0	0	0	0	0	0	0	0
T17-2b	0	0	0	0	0	0	0	0	0	0	0	0	0	0	0	0	0	0	0	0	0	0	0	0
T17-3	0	0	0	0	0	0	0	0	0	0	0	0	0	0	0	0	0	0	0	0	0	0	0	0
T17-4	0	0	0	0	0	0	0	0	0	0	0	0	0	0	0	0	0	0	0	0	0	0	0	0
T18-4	0	0	0	0	0	0	0	0	0	0	0	0	0	0	0	0	0	0	0	0	0	0	0	0
Sum G	***0***	***0***	***0***	***0***	***0***	***0***	***0***	***0***	***0***	***0***	***0***	***0***	***0***	***0***	***0***	***0***	***0***	***0***	***0***	***0***	***0***	***0***	***0***	***0***
%	0.0	0.0	0.0	0.0	0.0	0.0	0.0	0.0	0.0	0.0	0.0	0.0	0.0	0.0	0.0	0.0	0.0	0.0	0.0	0.0	0.0	0.0	0.0	0.0
				0.0				0.0				0.0				0.0				0.0				0.0
Tangelfoot Fm Sandstone																								
T18-1	0	0	0	0	0	0	0	0	0	0	0	0	0	0	0	0	0	0	0	0	0	0	0	0
T18-3	0	0	0	0	0	0	0	0	0	0	0	0	0	0	0	0	0	0	0	0	0	0	0	0

Sample	M				N				O				P				Q				R			
	Wht	Yel	Gry	Blk	Wht	Yel	Gry	Blk	Wht	Yel	Gry	Blk	Wht	Yel	Gry	Blk	Wht	Yel	Gry	Blk	Wht	Yel	Gry	Blk
Tantalus Conglomerates																								
T10-2	10	0	0	16	0	0	0	0	0	0	0	0	0	0	0	0	0	0	0	0	0	0	0	26
T10-4	8	0	0	0	0	0	0	0	0	0	0	0	0	0	0	0	0	18	0	30	1	0	0	0
T13-33	0	0	0	0	0	0	0	0	0	0	0	0	0	0	0	0	0	0	0	0	0	0	0	0
T13-37	0	14	0	0	0	0	0	0	0	0	0	0	0	0	0	0	21	12	0	19	0	0	0	0
T14-24	6	3	6	5	5	0	0	0	0	0	0	0	0	0	0	0	17	2	0	0	0	0	0	0
T17-6	0	0	0	0	0	0	0	14	0	0	0	0	0	0	0	0	0	23	0	0	0	0	0	0
T17-7	3	0	0	0	0	0	0	0	0	0	0	0	0	0	0	0	11	5	0	6	0	0	0	0
T17-8	5	14	9	3	3	2	0	0	0	0	0	0	0	0	0	0	0	0	0	2	0	0	0	0
T17-11	29	5	0	0	0	0	0	0	0	0	0	0	0	0	0	0	10	16	0	5	0	0	0	0
T17-12	9	4	16	0	0	10	0	0	0	0	0	0	0	0	0	0	0	105	0	0	0	0	0	0
T17-13	1	4	0	0	0	0	0	0	0	0	0	0	0	0	0	0	0	35	0	0	0	0	0	0
T17-24	6	2	0	0	0	0	0	0	0	0	0	0	0	0	0	0	0	52	2	0	0	0	0	0
T17-27	0	5	0	0	0	0	0	0	0	0	0	0	23	22	0	0	5	76	0	0	0	0	0	85
T17-31	0	0	0	0	0	0	0	0	0	0	0	0	0	0	0	0	0	0	0	0	0	0	0	0
T17-37	0	0	0	0	0	0	0	0	0	0	0	0	0	0	0	0	16	0	0	0	0	0	0	0
T17-38	5	10	0	0	0	0	0	0	0	0	0	0	0	0	0	0	0	12	0	0	0	0	0	0
T17-39	5	0	0	0	0	0	0	0	0	0	0	0	0	0	0	0	0	0	4	0	0	0	0	0
T18-5	107	12	2	0	0	0	0	0	0	0	0	0	0	0	0	0	3	46	0	6	0	0	0	0
T18-7	6	111	0	0	0	0	0	0	0	0	0	0	0	0	0	0	5	61	0	0	0	0	0	0
T18-9	1	0	0	0	0	0	0	0	0	0	0	0	0	0	0	0	266	0	0	0	0	0	0	0
T18-13	4	3	1	1	0	0	0	0	0	0	0	0	0	0	0	0	1	36	0	1	0	0	0	0
Sum G	***205***	***187***	***34***	***25***	***8***	***12***	***0***	***14***	***0***	***0***	***0***	***0***	***23***	***22***	***0***	***0***	***355***	***499***	***6***	***69***	***1***	***0***	***0***	***111***
%	2.5	2.3	0.4	0.3	0.1	0.1	0.0	0.2	0.0	0.0	0.0	0.0	0.3	0.3	0.0	0.0	4.4	6.1	0.1	0.9	0.0	0.0	0.0	1.4
				5.6				0.4				0.0				0.6				11.4				1.4
Tantalus Sandstones																								
T17-10	3	12	0	0	0	0	0	0	0	0	0	0	0	0	0	0	0	4	0	5	0	0	0	0
T17-23	0	3	1	1	0	0	0	0	0	0	0	0	0	0	0	0	0	0	0	0	0	0	0	2
T17-30	0	4	5	0	0	0	0	0	1	0	0	0	0	0	0	0	0	3	0	5	3	0	1	1
T18-6	7	55	1	1	0	0	0	0	0	0	0	0	0	0	0	0	0	0	0	0	0	0	0	0
T18-10	3	5	0	2	0	0	0	0	1	0	0	0	0	0	0	0	2	2	1	0	1	0	0	0
Sum S	***13***	***79***	***7***	***4***	***0***	***0***	***0***	***0***	***2***	***0***	***0***	***0***	***0***	***0***	***0***	***0***	***2***	***9***	***1***	***10***	***4***	***0***	***1***	***3***
%	0.8	4.9	0.4	0.2	0.0	0.0	0.0	0.0	0.1	0.0	0.0	0.0	0.0	0.0	0.0	0.0	0.1	0.6	0.1	0.6	0.2	0.0	0.1	0.2
				6.3				0.0				0.1				0.0				1.4				0.5
Tangelfoot Conglomerate																								
T17-1	0	0	0	0	0	0	0	0	0	0	0	0	0	0	0	0	0	0	0	0	0	0	0	0
T17-2b	0	0	0	0	0	0	0	0	0	0	0	0	0	0	0	0	0	0	0	0	0	0	0	0
T17-3	0	0	0	0	0	0	0	0	0	0	0	0	0	0	0	0	0	0	0	0	0	0	0	0
T17-4	0	0	0	0	0	0	0	0	0	0	0	0	0	0	0	0	0	0	0	0	0	0	0	0
T18-4	31	79	0	0	0	0	0	0	45	0	0	0	0	0	0	0	14	12	0	0	0	0	0	0
Sum G	***31***	***79***	***0***	***0***	***0***	***0***	***0***	***0***	***45***	***0***	***0***	***0***	***0***	***0***	***0***	***0***	***14***	***12***	***0***	***0***	***0***	***0***	***0***	***0***
%	7.8	19.8	0.0	0.0	0.0	0.0	0.0	0.0	11.3	0.0	0.0	0.0	0.0	0.0	0.0	0.0	3.5	3.0	0.0	0.0	0.0	0.0	0.0	0.0
				27.5				0.0				11.3				0.0				6.5				0.0
Tangelfoot Fm Sandstone																								
T18-1	0	0	0	0	0	0	0	0	0	0	0	0	0	0	0	0	0	0	0	0	0	0	0	0
T18-3	0	0	0	0	0	0	0	0	0	0	0	0	0	0	0	0	0	0	0	0	0	0	0	0

Sample	S				T				U				V				W				X			
	Wht	Yel	Gry	Blk	Wht	Yel	Gry	Blk	Wht	Yel	Gry	Blk	Wht	Yel	Gry	Blk	Wht	Yel	Gry	Blk	Wht	Yel	Gry	Blk
Tantalus Conglomerates																								
T10-2	0	0	0	1	0	0	0	0	0	0	0	0	65	121	0	16	7	0	0	0	0	0	0	0
T10-4	4	12	0	0	0	4	0	0	1	0	0	17	18	26	5	1	7	2	0	0	0	0	0	0
T13-33	3	0	100	17	0	0	0	0	0	8	0	0	11	4	11	0	0	25	0	0	0	0	0	0
T13-37	0	0	0	0	14	0	0	0	0	17	0	0	25	8	0	6	3	81	0	0	0	0	0	0
T14-24	22	10	4	0	2	0	0	0	2	2	6	0	2	35	8	6	6	16	7	0	0	0	0	0
T17-6	16	0	0	9	6	0	0	0	0	0	0	94	18	0	0	0	4	70	0	0	0	0	0	0
T17-7	11	3	0	0	0	0	0	0	0	0	0	39	46	60	0	0	8	32	0	0	0	0	0	0
T17-8	4	2	17	5	0	0	0	0	0	0	8	12	0	9	0	0	2	8	0	3	0	0	0	0
T17-11	111	9	0	0	0	0	0	0	0	0	0	4	17	48	0	0	25	77	0	0	0	0	0	0
T17-12	26	0	0	0	0	0	0	0	0	3	0	6	12	74	0	0	26	40	0	0	0	0	0	0
T17-13	26	4	0	0	0	0	0	0	0	0	0	5	5	96	0	0	1	11	0	0	0	0	0	0
T17-24	0	0	0	0	0	0	0	0	0	7	0	2	19	102	4	4	51	25	0	0	0	0	0	0
T17-27	0	6	0	0	1	0	0	0	0	23	0	0	3	16	0	0	10	7	0	0	0	0	0	0
T17-31	64	191	0	0	0	0	0	0	0	0	0	0	3	4	0	1	0	80	0	0	0	0	0	0
T17-37	1	126	0	17	0	0	0	0	0	17	0	34	0	160	0	2	11	27	0	0	0	0	0	0
T17-38	0	0	0	0	5	0	0	0	0	20	3	2	8	72	0	0	34	47	7	0	0	0	0	0
T17-39	7	0	3	0	0	0	0	0	0	10	2	1	88	19	14	0	63	17	7	46	0	0	0	0
T18-5	8	0	3	0	0	0	0	0	0	10	0	0	10	9	0	0	10	2	2	0	0	0	0	0
T18-7	2	23	0	0	0	0	0	0	0	12	0	0	3	138	0	0	19	1	0	0	0	0	0	0
T18-9	0	0	0	0	0	0	0	0	0	1	0	0	168	0	0	0	1	14	0	0	0	0	0	0
T18-13	0	2	0	0	0	0	0	0	0	0	0	0	7	8	2	2	7	2	1	0	0	0	0	0
Sum G	***305***	***388***	***127***	***49***	***28***	***4***	***0***	***0***	***3***	***130***	***19***	***216***	***528***	***1009***	***44***	***38***	***295***	***584***	***24***	***49***	***0***	***0***	***0***	***0***
%	3.8	4.8	1.6	0.6	0.3	0.0	0.0	0.0	0.0	1.6	0.2	2.7	6.5	12.4	0.5	0.5	3.6	7.2	0.3	0.6	0.0	0.0	0.0	0.0
				10.7				0.4				4.5				19.9				11.7				0.0
Tantalus Sandstones																								
T17-10	3	5	0	0	2	0	0	0	0	4	0	2	4	5	0	0	9	7	0	2	0	0	0	0
T17-23	4	0	0	0	0	0	0	0	0	0	0	0	4	12	1	2	6	8	9	2	0	0	0	0
T17-30	2	10	0	8	0	0	0	0	0	3	0	2	3	19	2	9	17	19	1	4	0	0	0	0
T18-6	1	4	0	0	1	0	0	0	0	0	0	5	5	3	1	8	24	2	0	0	0	0	0	0
T18-10	0	3	1	0	2	0	0	0	1	2	0	0	14	12	1	1	19	4	1	0	0	0	0	0
Sum S	***10***	***22***	***1***	***8***	***5***	***0***	***0***	***0***	***1***	***9***	***0***	***9***	***30***	***51***	***5***	***20***	***75***	***40***	***11***	***8***	***0***	***0***	***0***	***0***
%	0.6	1.4	0.1	0.5	0.3	0.0	0.0	0.0	0.1	0.6	0.0	0.6	1.8	3.1	0.3	1.2	4.6	2.5	0.7	0.5	0.0	0.0	0.0	0.0
				2.5				0.3				1.2				6.5				8.3				0.0
Tangelfoot Conglomerate																								
T17-1	0	0	0	0	0	0	0	0	0	0	0	0	0	0	0	0	0	0	0	0	0	0	0	0
T17-2b	0	0	0	0	0	0	0	0	0	0	0	0	0	0	0	0	0	0	0	0	0	0	0	0
T17-3	0	0	0	0	0	0	0	0	0	0	0	0	0	0	0	0	0	0	0	0	0	0	0	0
T17-4	0	0	0	0	0	0	0	0	0	0	0	0	0	0	0	0	0	0	0	0	0	0	0	0
T18-4	67	0	0	0	0	0	0	0	0	0	0	12	6	0	0	0	0	4	0	0	0	0	0	0
Sum G	***67***	***0***	***0***	***0***	***0***	***0***	***0***	***0***	***0***	***0***	***0***	***12***	***6***	***0***	***0***	***0***	***0***	***4***	***0***	***0***	***0***	***0***	***0***	***0***
%	16.8	0.0	0.0	0.0	0.0	0.0	0.0	0.0	0.0	0.0	0.0	3.0	1.5	0.0	0.0	0.0	0.0	1.0	0.0	0.0	0.0	0.0	0.0	0.0
				16.8				0.0				3.0				1.5				1.0				0.0
Tangelfoot Fm Sandstone																								
T18-1	0	0	0	0	0	0	0	0	0	0	0	0	0	0	0	0	0	0	0	0	0	0	0	0
T18-3	0	0	0	0	0	0	0	0	0	0	0	0	0	0	0	0	0	0	0	0	0	0	0	0

Sample	Z				A'				B'			
	Wht	Yel	Gry	Blk	Wht	Yel	Gry	Blk	Wht	Yel	Gry	Blk
Tantalus Conglomerates												
T10-2	0	0	0	0	0	0	0	0	0	0	0	0
T10-4	0	0	0	0	0	0	0	0	0	0	0	0
T13-33	0	0	0	0	0	0	0	0	0	0	0	0
T13-37	0	0	0	0	0	0	0	0	0	0	0	0
T14-24	0	0	0	0	0	0	0	0	0	0	0	0
T17-6	0	0	0	0	0	0	0	0	0	0	0	0
T17-7	0	0	0	0	0	0	0	0	0	0	0	0
T17-8	0	0	0	0	0	0	0	0	0	0	0	0
T17-11	0	0	0	0	0	0	0	0	0	0	0	0
T17-12	0	0	0	0	0	0	0	0	0	0	0	0
T17-13	0	5	0	0	0	0	0	0	0	0	0	0
T17-24	12	0	0	0	0	0	0	0	0	0	0	0
T17-27	0	0	0	0	0	0	0	0	0	0	0	0
T17-31	0	0	0	0	0	0	0	0	0	0	0	0
T17-37	0	0	0	0	0	0	0	0	0	0	0	0
T17-38	0	0	0	0	0	0	0	0	0	0	0	0
T17-39	0	36	0	0	0	0	0	0	0	0	0	0
T18-5	0	4	0	0	0	0	0	0	0	0	0	0
T18-7	0	0	0	0	0	0	0	0	0	0	0	0
T18-9	0	0	0	0	0	0	0	0	0	0	0	0
T18-13	0	0	0	0	0	0	0	0	0	0	0	0
Sum G	***12***	***45***	***0***	***0***	***0***	***0***	***0***	***0***	***0***	***0***	***0***	***0***
%	0.1	0.6	0.0	0.0	0.0	0.0	0.0	0.0	0.0	0.0	0.0	0.0
				0.7				0.0				0.0
Tantalus Sandstones												
T17-10	0	1	0	0	0	0	0	0	0	0	0	0
T17-23	0	0	0	0	0	0	0	0	0	0	0	0
T17-30	7	0	0	0	0	0	0	0	0	0	0	0
T18-6	0	0	0	0	0	0	0	0	0	0	0	0
T18-10	0	0	0	0	0	0	0	0	0	0	0	0
Sum S	***7***	***1***	***0***	***0***	***0***	***0***	***0***	***0***	***0***	***0***	***0***	***0***
%	0.4	0.1	0.0	0.0	0.0	0.0	0.0	0.0	0.0	0.0	0.0	0.0
				0.5				0.0				0.0
Tangelfoot Conglomerate												
T17-1	0	0	0	0	0	0	0	0	0	0	0	0
T17-2b	0	0	0	0	0	0	0	0	0	0	0	0
T17-3	0	0	0	0	0	0	0	0	0	0	0	0
T17-4	0	0	0	0	0	0	0	0	0	0	0	0
T18-4	100	0	0	0	0	0	0	0	0	0	0	0
Sum G	***100***	***0***	***0***	***0***	***0***	***0***	***0***	***0***	***0***	***0***	***0***	***0***
%	25.0	0.0	0.0	0.0	0.0	0.0	0.0	0.0	0.0	0.0	0.0	0.0
				25.0				0.0				0.0
Tangelfoot Fm Sandstone												
T18-1	0	0	0	0	0	0	0	0	0	0	0	0
T18-3	0	0	0	0	0	0	0	0	0	0	0	0

Sample	Totals						Chert by colour					Qm	Qp	Qs		Chert Groups			sub			
		W	Y	G	B+R+G		White	Yellov	Grey	Black		%	%	%		A to K	L to T +Z	U to W	total	%Mas	%Brec	%spher
Tantalus Conglomerates							%	%	%	%					Section T1	MASSIVE	BRECCIATED	SPHERES				
T10-2	356	90	128	5	133		31.9	45.4	1.8	20.9	356	11.11	44.44	44.44	T10-2	94	53	209	356	26.4	14.9	58.7
T10-4	273	85	119	16	53		31.1	43.6	5.9	19.4	273	13.51	12.61	73.87	T10-4	119	77	77	273	43.6	28.2	28.2
T13-33	411	89	138	130	54		21.7	33.7	31.7	12.9	411	4.76	38.10	57.14	T13-33	232	120	59	411	56.4	29.2	14.4
T13-37	360	104	222	9	25		28.9	61.7	2.5	6.9	360	0.81	26.83	72.36	T13-37	140	80	140	360	38.9	22.2	38.9
T14-24	408	140	156	64	48		34.3	38.2	15.7	11.8	408	10.84	2.41	86.75	T14-24	236	82	90	408	57.8	20.1	22.1
T17-6	446	200	100	0	146		44.8	22.4	0.0	32.7	446	3.45	0.00	96.55	T17-6	192	68	186	446	43.0	15.2	41.7
T17-7	360	180	134	1	45		50.0	37.2	0.3	12.5	360	3.13	3.91	92.97	T17-7	136	39	185	360	37.8	10.8	51.4
T17-8	313	116	109	49	39		37.1	34.8	15.7	12.5	313	4.32	1.23	94.44	T17-9	205	66	42	313	65.5	21.1	13.4
T17-11	459	241	209	0	9		52.5	45.5	0.0	2.0	459	4.88	0.00	95.12	T17-11	103	185	171	459	22.4	40.3	37.3
T17-12	434	100	300	21	13		23.0	69.1	4.8	3.0	434	1.82	3.64	94.55	T17-12	103	170	161	434	23.7	39.2	37.1
T17-13	336	58	255	8	15		17.3	75.9	2.4	4.5	336	3.66	0.61	95.73	T17-13	143	75	118	336	42.6	22.3	35.1
T17-24	390	111	244	23	12		28.5	62.6	5.9	3.1	390	2.00	2.00	96.00	T17-24	102	74	214	390	26.2	19.0	54.9
T17-27	324	63	171	2	88		19.4	52.8	0.6	27.2	324	1.20	1.20	97.59	T17-27	42	223	59	324	13.0	68.8	18.2
T17-31	375	83	280	5	7		22.1	74.7	1.3	1.9	375	1.68	0.00	98.32	T17-31	32	255	88	375	8.5	68.0	23.5
T17-37	470	64	352	1	53		13.6	74.9	0.2	11.3	470	20.83	8.33	70.83	T17-37	59	160	251	470	12.6	34.0	53.4
T17-38	385	179	188	11	7		46.5	48.8	2.9	1.8	385	0.00	4.92	95.08	T17-38	160	32	193	385	41.6	8.3	50.1
T17-39	473	222	159	37	55		46.9	33.6	7.8	11.6	473	0.00	4.17	95.83	T17-39	151	55	267	473	31.9	11.6	56.4
T18-5	317	170	108	14	25		53.6	34.1	4.4	7.9	317	6.58	13.16	80.26	T18-5	83	191	43	317	26.2	60.3	13.6
T18-7	477	84	377	9	7		17.6	79.0	1.9	1.5	477	16.67	0.00	83.33	T18-7	96	208	173	477	20.1	43.6	36.3
T18-9	488	457	23	4	4		93.6	4.7	0.8	0.8	488	0.00	0.00	100.00	T18-9	37	267	184	488	7.6	54.7	37.7
T18-13	261	136	81	32	12		52.1	31.0	12.3	4.6	261	5.64	0.00	94.36	T18-13	183	49	29	261	70.1	18.8	11.1
Sum G	***8116***					***AVE***	***36.5***	***47.8***	***5.7***	***10.0***	***AVE***	***5.6***	***8.0***	***86.5***					***AVE***	***34.1***	***31.0***	***34.9***
%	100.0					MAX	93.6	79.0	31.7	32.7	MAX	20.8	44.4	100.0					MAX	70.1	68.8	58.7
						MIN	13.6	4.7	0.0	0.8	MIN	0.0	0.0	44.4					MIN	7.6	8.3	11.1
						SDEV	18.5	19.9	7.7	8.9	SDEV	5.8	12.8	15.0					SDEV	18.1	18.7	15.6
Tantalus Sandstones																						
T17-10	308	124	135	11	38		40.3	43.8	3.6	12.3	308	6.52	1.09	92.39	T17-10	240	35	33	308	77.9	11.4	10.7
T17-23	280	124	90	47	19		44.3	32.1	16.8	6.8	280	9.63	4.28	86.10	T17-23	225	11	44	280	80.4	3.9	15.7
T17-30	339	124	126	41	48		36.6	37.2	12.1	14.2	339	10.42	4.17	85.42	T17-30	201	59	79	339	59.3	17.4	23.3
T18-6	335	150	129	27	29		44.8	38.5	8.1	8.7	335	17.21	1.64	81.15	T18-6	217	70	48	335	64.8	20.9	14.3
T18-10	361	238	83	28	12		65.9	23.0	7.8	3.3	361	11.76	2.52	85.71	T18-10	283	23	55	361	78.4	6.4	15.2
Sum S	***1623***					***AVE***	***46.4***	***34.9***	***9.7***	***9.1***	***AVE***	***11.1***	***2.7***	***86.2***					***AVE***	***72.1***	***12.0***	***15.9***
%	100.0					MAX	65.9	43.8	16.8	14.2	MAX	17.2	4.3	92.4					MAX	80.4	20.9	23.3
						MIN	36.6	23.0	3.6	3.3	MIN	6.5	1.1	81.1					MIN	59.3	3.9	10.7
						SDEV	11.4	7.9	5.0	4.3	SDEV	3.9	1.4	4.0					SDEV	9.5	7.2	4.6
Tangelfoot Conglomerate																						
T17-1	0	0	0	0	0		na	na	na	na	0	41.18	5.88	52.94	T17-1	0	0	0	0	na	na	na
T17-2b	0	0	0	0	0		na	na	na	na	0	41.25	1.88	56.88	T17-2b	0	0	0	0	na	na	na
T17-3	0	0	0	0	0		na	na	na	na	0	7.85	0.00	92.15	T17-3	0	0	0	0	na	na	na
T17-4	0	0	0	0	0		na	na	na	na	0	14.43	14.43	71.13	T17-4	0	0	0	0	na	na	na
T18-4	400	287	95	0	18		71.8	23.8	0.0	4.5	400	0.00	1.67	98.33	T18-4	30	348	22	400	7.5	87.0	5.5
Sum G						***AVE***	***71.8***	***23.8***	***0.0***	***4.5***	***AVE***	***20.9***	***4.8***	***74.3***					***AVE***	***7.5***	***87.0***	***5.5***
%						MAX	71.8	23.8	0.0	4.5	MAX	41.3	14.4	98.3					MAX	7.5	87.0	5.5
						MIN	0.0	0.0	0.0	0.0	MIN	0.0	0.0	52.9					MIN	0	0	0
						SDEV	na	na	na	na	SDEV	19.2	5.8	20.4					SDEV	na	na	na
Tangelfoot Fm Sandstone																						
T18-1	0	0	0	0	0		na	na	na	na	0	17.74	1.94	80.32	T18-1	0	0	0	0	na	na	na
T18-3	1	1	0	0	0		100.0	0.0	0.0	0.0	1	17.30	3.81	78.89	T18-3	1	0	0	1	100.0	0.0	0.0

Qm = monocrystalline unstrained quartz
Qp = poltcrystalline quartz
Qs = Strained quartz
Srf = sedimentary rock fragments
Mrf = Metamorphic rock fragments
Mi = Igneous rock fragments

Fk = Potasium feldspar
Fp = plagioclase feldspar
Fm = Microcline
Fe = Epimatrix (feldspar replaced by clays)
Fwk = framework
See Appendix 3 for chert types

SDEV = standard deviation

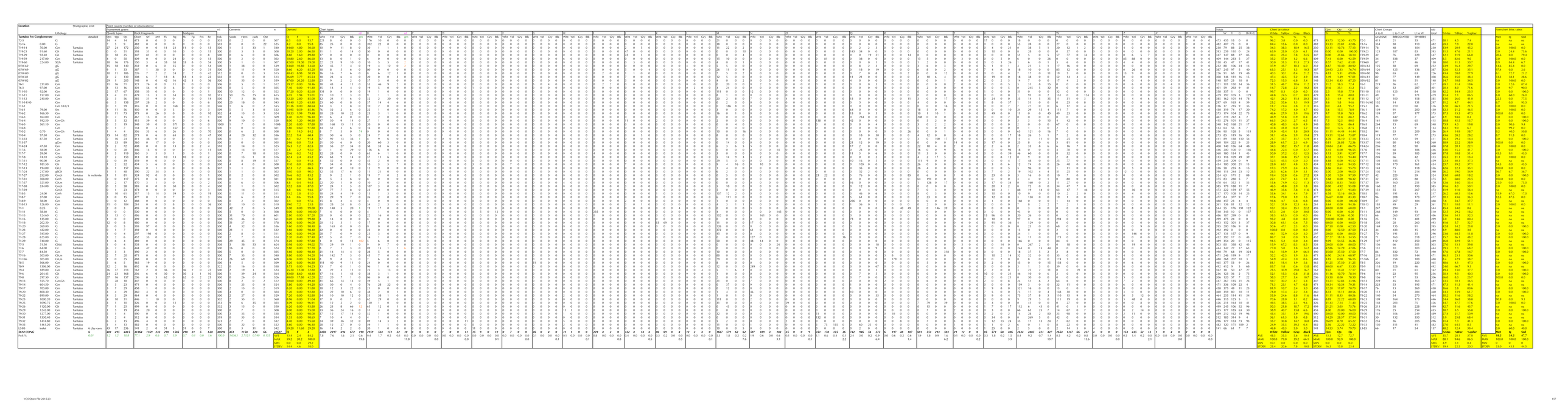

Location		Lithology	Stratigraphic Unit	detrital clay	detailed	Qm	Qp	Qs	Chert	Srf	Mrf	Fig	Fk	Fp	Fm	Fe	n1 fwk	Voids	Hem	carb	Qtz	n		Derived Q	F	L
Tangelfoot Fm Conglomerates						Quartz types			Rock Fragments				Feldspars					Cements								
T21-12	92.00	Gm	Tangelfoot	44	44 matrix	17	3	44	338	0	0	77	15	6	0	0	500	0	2	0	0	502		12.80	4.20	83.00
T21-11	106.00	SGm	Tangelfoot	18	18 matrix	42	18	139	132	0	0	94	59	9	2	5	500	0	10	0	0	510		39.80	15.00	45.20
T21-6	234.00	Gm	Tangelfoot	0		21	13	219	89	6	6	69	41	8	0	28	500	0	44	0	0	544		50.60	15.40	34.00
T17-1	0.00	Gm	Tangelfoot	0	volcLithRudite	14	2	18	0	1	0	373	59	33	0	0	500	1	10	0	0	511		6.8	18.4	74.8
T17-2b	5.00	Gt	Tangelfoot	0		132	6	182	0	0	0	0	103	0	0	77	500	0	222	0	0	722		64.0	36.0	0.0
T17-3	5.60	Gt	Tangelfoot	0		26	0	305	0	0	0	32	134	0	0	3	500	0	40	98	0	638		66.2	27.4	6.4
T17-4	1.50	Gm,t	Tangelfoot	0		14	14	69	0	28	0	58	275	0	0	42	500	0	8	0	0	508		19.4	63.4	17.2
T18-4	>-200	Gm	Tangelfoot	0		0	1	59	400	23	17	0	0	0	0	0	500	3	8	0	0	511		12.0	0.0	88.0
L3-40	4.80	Gm	Tangelfoot	0		63	16	129	0	0	6	90	173	16	0	7	500	2	96	3	0	601		41.60	39.20	19.20
L3-2	599.00	gGm	Tangelfoot	7	7 clay cem.	29	7	331	0	0	0	0	127	0	0	8	502	0	89	121	1	720		73.11	26.89	0.00
L3-61	635.50	Gt	Tangelfoot	87	87 clay matrix	69	5	268	0	0	3	6	128	0	0	21	500	3	13	2	0	605		68.40	29.80	1.80
L3-71	681.00	Gm	Tangelfoot	30	51 org C 30 clay	18	8	340	0	0	0	5	84	0	3	42	500	0	0	0	0	500		73.20	25.80	1.00
Sum Cong				**186**		**445**	**93**	**2103**	**959**	**58**	**32**	**804**	**1198**	**72**	**5**	**233**	**6002**	**9**	**542**	**224**	**1**		AVE	44.0	25.1	30.9
			Matrix/clays =	*2.7*	*Fwk% =*	*7.4*	*1.5*	*35.0*	*16.0*	*1.0*	*0.5*	*13.4*	*20.0*	*1.2*	*0.1*	*3.9*	*100.0*	*0.1*	*7.8*	*3.2*	*0.0*		MAX	73.2	63.4	88.0
																							MIN	6.8	0.0	0.0
																							STDV	25.7	16.9	34.0

Chert types

Location	A Wht	A Yel	A Gry	A Blk	A rd grn	B Wht	B Yel	B Gry	B Blk	B rd grn
T21-12	2	0	0	0	0	288	0	0	0	0
T21-11	4	0	2	3	0	3	0	0	1	0
T21-6	22	0	1	2	0	20	0	0	0	0
T17-1	0	0	0	0	0	0	0	0	0	0
T17-2b	0	0	0	0	0	0	0	0	0	0
T17-3	0	0	0	0	0	0	0	0	0	0
T17-4	0	0	0	0	0	0	0	0	0	0
T18-4	20	0	0	6	0	4	0	0	0	0
L3-40	0	0	0	0	0	0	0	0	0	0
L3-2	0	0	0	0	0	0	0	0	0	0
L3-61	0	0	0	0	0	0	0	0	0	0
L3-71	0	0	0	0	0	0	0	0	0	0
Sum Cong	**48**	**0**	**3**	**11**	**0**	**315**	**0**	**0**	**1**	**0**
	5.0	*0.0*	*0.3*	*1.1*	*0.0*	*32.8*	*0.0*	*0.0*	*0.1*	*0.0*
					6.5					33.0

Location	C Wht	C Yel	C Gry	C Blk	D Wht	D Yel	D Gry	D Blk	E Wht	E Yel	E Gry	E Blk	F Wht	F Yel	F Gry	F Blk	G Wht	G Yel	G Gry	G Blk	H Wht	H Yel	H Gry	H Blk
T21-12	0	0	0	0	0	0	0	0	0	0	0	0	0	0	0	0	0	0	0	0	0	0	0	0
T21-11	0	0	0	0	0	0	0	0	0	0	0	0	0	0	0	0	0	0	0	0	0	0	0	0
T21-6	0	0	0	0	0	0	0	0	0	0	0	0	0	0	0	0	0	0	0	0	0	0	0	0
T17-1	0	0	0	0	0	0	0	0	0	0	0	0	0	0	0	0	0	0	0	0	0	0	0	0
T17-2b	0	0	0	0	0	0	0	0	0	0	0	0	0	0	0	0	0	0	0	0	0	0	0	0
T17-3	0	0	0	0	0	0	0	0	0	0	0	0	0	0	0	0	0	0	0	0	0	0	0	0
T17-4	0	0	0	0	0	0	0	0	0	0	0	0	0	0	0	0	0	0	0	0	0	0	0	0
T18-4	0	0	0	0	0	0	0	0	0	0	0	0	0	0	0	0	0	0	0	0	0	0	0	0
L3-40	0	0	0	0	0	0	0	0	0	0	0	0	0	0	0	0	0	0	0	0	0	0	0	0
L3-2	0	0	0	0	0	0	0	0	0	0	0	0	0	0	0	0	0	0	0	0	0	0	0	0
L3-61	0	0	0	0	0	0	0	0	0	0	0	0	0	0	0	0	0	0	0	0	0	0	0	0
L3-71	0	0	0	0	0	0	0	0	0	0	0	0	0	0	0	0	0	0	0	0	0	0	0	0
Sum Cong	**0**	**0**	**0**	**0**	**0**	**0**	**0**	**0**	**0**	**0**	**0**	**0**	**0**	**0**	**0**	**0**	**0**	**0**	**0**	**0**	**0**	**0**	**0**	**0**
	0.0	*0.0*	*0.0*	*0.0*	*0.0*	*0.0*	*0.0*	*0.0*	*0.0*	*0.0*	*0.0*	*0.0*	*0.0*	*0.0*	*0.0*	*0.0*	*0.0*	*0.0*	*0.0*	*0.0*	*0.0*	*0.0*	*0.0*	*0.0*
				0.0				0.0				0.0				0.0				0.0				0.0

Location	I Wht	I Yel	I Gry	I Blk	J Wht	J Yel	J Gry	J Blk	K Wht	K Yel	K Gry	K Blk	L Wht	L Yel	L Gry	L Blk	M Wht	M Yel	M Gry	M Blk	N Wht	N Yel	N Gry	N Blk
T21-12	0	0	0	0	18	0	0	0	0	0	0	0	0	0	0	0	0	0	0	0	0	0	0	0
T21-11	2	0	0	0	2	0	0	0	0	0	0	0	0	0	0	0	7	0	3	2	0	0	0	0
T21-6	2	0	0	0	4	0	0	0	0	0	0	0	0	0	0	0	11	0	0	2	0	0	0	0
T17-1	0	0	0	0	0	0	0	0	0	0	0	0	0	0	0	0	0	0	0	0	0	0	0	0
T17-2b	0	0	0	0	0	0	0	0	0	0	0	0	0	0	0	0	0	0	0	0	0	0	0	0
T17-3	0	0	0	0	0	0	0	0	0	0	0	0	0	0	0	0	0	0	0	0	0	0	0	0
T17-4	0	0	0	0	0	0	0	0	0	0	0	0	0	0	0	0	0	0	0	0	0	0	0	0
T18-4	0	0	0	0	0	0	0	0	0	0	0	0	0	0	0	0	31	79	0	0	0	0	0	0
L3-40	0	0	0	0	0	0	0	0	0	0	0	0	0	0	0	0	0	0	0	0	0	0	0	0
L3-2	0	0	0	0	0	0	0	0	0	0	0	0	0	0	0	0	0	0	0	0	0	0	0	0
L3-61	0	0	0	0	0	0	0	0	0	0	0	0	0	0	0	0	0	0	0	0	0	0	0	0
L3-71	0	0	0	0	0	0	0	0	0	0	0	0	0	0	0	0	0	0	0	0	0	0	0	0
Sum Cong	**4**	**0**	**0**	**0**	**24**	**0**	**0**	**0**	**0**	**0**	**0**	**0**	**0**	**0**	**0**	**0**	**49**	**79**	**3**	**4**	**0**	**0**	**0**	**0**
	0.4	*0.0*	*0.0*	*0.0*	*2.5*	*0.0*	*0.0*	*0.0*	*0.0*	*0.0*	*0.0*	*0.0*	*0.0*	*0.0*	*0.0*	*0.0*	*5.1*	*8.2*	*0.3*	*0.4*	*0.0*	*0.0*	*0.0*	*0.0*
				0.4				2.5				0.0				0.0				14.1				0.0

Location	O Wht	O Yel	O Gry	O Blk	P Wht	P Yel	P Gry	P Blk	Q Wht	Q Yel	Q Gry	Q Blk	R Wht	R Yel	R Gry	R Blk	S Wht	S Yel	S Gry	S Blk	T Wht	T Yel	T Gry	T Blk
T21-12	0	0	0	0	18	0	0	0	0	0	0	0	0	0	0	9	0	0	0	0	0	0	0	0
T21-11	0	0	0	0	0	0	0	0	6	0	0	0	0	0	0	1	2	0	0	6	0	0	0	0
T21-6	0	0	0	0	0	0	0	0	7	0	0	0	0	0	0	0	0	0	0	0	0	0	0	0
T17-1	0	0	0	0	0	0	0	0	0	0	0	0	0	0	0	0	0	0	0	0	0	0	0	0
T17-2b	0	0	0	0	0	0	0	0	0	0	0	0	0	0	0	0	0	0	0	0	0	0	0	0
T17-3	0	0	0	0	0	0	0	0	0	0	0	0	0	0	0	0	0	0	0	0	0	0	0	0
T17-4	0	0	0	0	0	0	0	0	0	0	0	0	0	0	0	0	0	0	0	0	0	0	0	0
T18-4	45	0	0	0	0	0	0	0	14	12	0	0	0	0	0	0	67	0	0	0	0	0	0	0
L3-40	0	0	0	0	0	0	0	0	0	0	0	0	0	0	0	0	0	0	0	0	0	0	0	0
L3-2	0	0	0	0	0	0	0	0	0	0	0	0	0	0	0	0	0	0	0	0	0	0	0	0
L3-61	0	0	0	0	0	0	0	0	0	0	0	0	0	0	0	0	0	0	0	0	0	0	0	0
L3-71	0	0	0	0	0	0	0	0	0	0	0	0	0	0	0	0	0	0	0	0	0	0	0	0
Sum Cong	**45**	**0**	**0**	**0**	**18**	**0**	**0**	**0**	**27**	**12**	**0**	**0**	**0**	**0**	**0**	**10**	**69**	**0**	**0**	**6**	**0**	**0**	**0**	**0**
	4.7	*0.0*	*0.0*	*0.0*	*1.9*	*0.0*	*0.0*	*0.0*	*2.8*	*1.3*	*0.0*	*0.0*	*0.0*	*0.0*	*0.0*	*1.0*	*7.2*	*0.0*	*0.0*	*0.6*	*0.0*	*0.0*	*0.0*	*0.0*
				4.7				1.9				4.1				1.0				7.8				0.0

Location	U Wht	U Yel	U Gry	U Blk	V Wht	V Yel	V Gry	V Blk	W Wht	W Yel	W Gry	W Blk	X Wht	X Yel	X Gry	X Blk	Z Wht	Z Yel	Z Gry	Z Blk	A' Wht	A' Yel	A' Gry	A' Blk	B' Wht	B' Yel	B' Gry	B' Blk
T21-12	0	0	0	0	0	0	0	0	3	0	0	0	0	0	0	0	0	0	0	0	0	0	0	0	0	0	0	0
T21-11	0	0	0	0	43	0	4	4	25	0	10	2	0	0	0	0	0	0	0	0	0	0	0	0	0	0	0	0
T21-6	0	0	2	8	0	0	0	0	8	0	0	0	0	0	0	0	0	0	0	0	0	0	0	0	0	0	0	0
T17-1	0	0	0	0	0	0	0	0	0	0	0	0	0	0	0	0	0	0	0	0	0	0	0	0	0	0	0	0
T17-2b	0	0	0	0	0	0	0	0	0	0	0	0	0	0	0	0	0	0	0	0	0	0	0	0	0	0	0	0
T17-3	0	0	0	0	0	0	0	0	0	0	0	0	0	0	0	0	0	0	0	0	0	0	0	0	0	0	0	0
T17-4	0	0	0	0	0	0	0	0	0	0	0	0	0	0	0	0	0	0	0	0	0	0	0	0	0	0	0	0
T18-4	0	0	0	12	6	0	0	0	0	4	0	0	0	0	0	0	100	0	0	0	0	0	0	0	0	0	0	0
L3-40	0	0	0	0	0	0	0	0	0	0	0	0	0	0	0	0	0	0	0	0	0	0	0	0	0	0	0	0
L3-2	0	0	0	0	0	0	0	0	0	0	0	0	0	0	0	0	0	0	0	0	0	0	0	0	0	0	0	0
L3-61	0	0	0	0	0	0	0	0	0	0	0	0	0	0	0	0	0	0	0	0	0	0	0	0	0	0	0	0
L3-71	0	0	0	0	0	0	0	0	0	0	0	0	0	0	0	0	0	0	0	0	0	0	0	0	0	0	0	0
Sum Cong	**0**	**0**	**2**	**20**	**49**	**0**	**4**	**4**	**36**	**4**	**10**	**2**	**0**	**0**	**0**	**0**	**100**	**0**	**0**	**0**	**0**	**0**	**0**	**0**	**0**	**0**	**0**	**0**
	0.0	*0.0*	*0.2*	*2.1*	*5.1*	*0.0*	*0.4*	*0.4*	*3.8*	*0.4*	*1.0*	*0.2*	*0.0*	*0.0*	*0.0*	*0.0*	*10.4*	*0.0*	*0.0*	*0.0*	*0.0*	*0.0*	*0.0*	*0.0*	*0.0*	*0.0*	*0.0*	*0.0*
				2.3				5.9				5.4				0.0				10.4				0.0				0.0

Location	Totals n	W	Y	G	B+R+G		Chert by colour White %	Yellow %	Grey %	Black %		Qm %	Qp %	Qs %		Chert Groups A to K MASSIVE	L to T +Z BRECCIATED	U to W SPHERES		%Mas	%Brec	%spher		Non-chert lithic ratios Met	Ig	Sed
T21-12	338	329	0	0	9		97.3	0.0	0.0	2.7		26.56	4.69	68.75	T21-12	308	27	3		91.1	8.0	0.9		0.0	100.0	0.0
T21-11	132	94	0	19	19		71.2	0.0	14.4	14.4		21.11	9.05	69.85	T21-11	17	27	88		12.9	20.5	66.7		0.0	100.0	0.0
T21-6	89	74	0	3	12		83.1	0.0	3.4	13.5		8.30	5.14	86.56	T21-6	51	20	18		57.3	22.5	20.2		7.4	85.2	7.4
T17-1	0	0	0	0	0		na	na	na	na		41.18	5.88	52.94	T17-1	0	0	0		na	na	na		0.0	99.7	0.3
T17-2b	0	0	0	0	0		na	na	na	na		41.25	1.88	56.88	T17-2b	0	0	0		na	na	na		na	na	na
T17-3	0	0	0	0	0		na	na	na	na		7.85	0.00	92.15	T17-3	0	0	0		na	na	na		0.0	100.0	0.0
T17-4	0	0	0	0	0		na	na	na	na		14.43	14.43	71.13	T17-4	0	0	0		na	na	na		0.0	67.4	32.6
T18-4	400	287	95	0	18		71.8	23.8	0.0	4.5		0.00	1.67	98.33	T18-4	30	348	22		7.5	87.0	5.5		42.5	0.0	57.5
L3-40	0	0	0	0	0		na	na	na	na		30.29	7.69	62.02	L3-40	0	0	0		na	na	na		6.3	93.8	0.0
L3-2	0	0	0	0	0		na	na	na	na		7.90	1.91	90.19	L3-2	0	0	0		na	na	na		na	na	na
L3-61	0	0	0	0	0		na	na	na	na		20.18	1.46	78.36	L3-61	0	0	0		na	na	na		33.3	66.7	0.0
L3-71	0	0	0	0	0		na	na	na	na		4.92	2.19	92.90	L3-71	0	0	0		na	na	na		0.0	100.0	0.0
						Ave	**80.9**	**5.9**	**4.4**	**8.8**	**Ave**	**18.7**	**4.7**	**76.7**					**Ave**	**42.2**	**34.5**	**23.3**	**Ave**	**9.9**	**79.2**	**10.9**
						Max	97.3	23.8	14.4	14.4	Max	41.3	14.4	98.3					Max	91.1	87.0	66.7	Max	42.5	100.0	57.5
						Min	71.2	0.0	0.0	4.5	Min	0.0	0.0	52.9					Min	7.5	8.0	5.5	Min	0.0	0.0	0.0
						STDV	12.285	11.875	6.8228	6.038	STDV	13.876	4.134	15.27					STDV	39.52	35.6	30.052	STDV	15.7	31.5	19.6

Location		Lithology	Stratigraphic Unit	detrital clay	detailed	Qm	Qp	Qs	Chert	Srf	Mrf	Fig	Fk	Fp	Fm	Fe	n1 fwk	Voids	Hem	carb	Qtz	n	Q	F	L
						Point counts (number of observations): Framework grains – Quartz types			Rock Fragments				Feldspars					Cements					Derived		
Tangelfoot Fm Sandstones																									
T21-14	26.00	vcSm	Tangelfoot	16	16 matrix	27	4	51	0	4	4	271	45	3	0	91	500	0	22	0	0	522	16.40	27.80	55.80
T21-13	80.00	mfSm	Tangelfoot	6	6 matrix	52	10	66	0	0	4	207	148	13	0	0	500	0	0	0	0	500	25.60	32.20	42.20
T18-1	-20.00	vcSm	Tangelfoot	0		55	6	249	0	105	0	2	50	2	0	31	500	0	48	0	0	548	62.0	16.6	21.4
L3-42	56.50	c-vcSt	Tangelfoot	0		85	17	161	0	0	3	16	187	26	0	5	500	4	31	2	0	537	52.60	43.60	3.80
L3-45	208.00	vcSm	Tangelfoot	0		67	12	183	0	3	8	13	169	14	0	31	500	0	40	16	1	557	52.40	42.80	4.80
L3-48	350.00	c-vcSm	Tangelfoot	15	15 clay cem.	68	7	170	0	1	13	14	181	22	6	20	502	0	10	12	0	539	48.80	45.62	5.58
L3-54	471.00	vcSm	Tangelfoot	2	2 clay cem.	68	10	136	0	0	5	22	190	57	4	10	502	0	11	0	3	518	42.63	51.99	5.38
L3-55	502.00	g-vcSm	Tangelfoot	19	19 clay cem	89	11	143	0	0	3	37	178	28	2	9	500	0	4	1	0	524	48.60	43.40	8.00
L3-56	575.00	g-vcSm	Tangelfoot	18	18 clay cem.	87	9	159	0	0	2	19	181	28	8	9	502	1	26	16	0	563	50.80	45.02	4.18
L3-75	812.50	g-vcSt	Tangelfoot	65	65 clay cem/epi	44	11	324	0	0	0	0	96	0	4	23	502	0	3	0	0	570	75.50	24.50	0.00
L3-77	836.00	g-vcGSt	Tangelfoot	0		54	11	370	0	2	0	0	57	0	0	8	502	1	72	91	0	666	86.65	12.95	0.40
T19-1	0.40	cSt	Lbg	0	Ab Ig RFs	17	8	190	166	6	1	44	55	10	0	3	500	0	28	18	24	570	43.00	13.60	43.40
T19-2	4.50	g,cSm	Lbg	0	Ab Ig RFs	28	8	132	119	1	0	38	96	20	2	56	500	0	12	6	13	531	33.60	34.80	31.60
T19-3	9.90	fSr	Lbg	10	10 x chlorite	42	9	69	115	0	0	27	181	22	0	35	500	0	40	20	9	569	24.00	47.60	28.40
T21-8	156.00	mSm	Tangelfoot	32	32	48	9	142	114	1	3	29	1	0	0	153	500	0	2	0	1	503	39.80	30.80	29.40
T11-2		(g)vcS	? Tanglefoot?	0		69	19	179	43	3	0	3	57	0	2	125	500	0	21	0	0	521	53.40	36.80	9.80
T18-3	>-200	g,vcSm	Tangelfoot	0		50	11	228	1	0	0	28	161	11	0	10	500	1	29	0	0	530	57.8	36.4	5.8
T9-1	30.25	vc-cSm	Tanglefoot	0		40	29	287	23	15	0	0	85	1	3	17	500	5	8	19	3	535	71.20	21.20	7.60
T9-2	120.00	(g)vcSt	Tanglefoot	0		89	10	229	7	44	0	0	66	2	1	52	500	16	1	7	0	524	65.60	24.20	10.20
L3-39	0.00	cSm,r	Tangelfoot	0		54	5	205	1	3	1	32	171	23	2	3	500	7	46	0	10	563	52.80	39.80	7.40
L3-51	411.00	c-vcSm	Tangelfoot	17	17 clay cem.	70	9	172	1	1	4	21	179	32	3	10	502	7	20	3	0	545	50.00	44.62	5.38
L3-80	859.00	mcSr	Tangelfoot	77	77 clay	129	14	189	16	0	1	1	65	0	0	17	432	0	158	160	0	827	76.85	18.98	4.17
Sum Sst				***277***		***1332***	***239***	***4034***	***606***	***189***	***52***	***824***	***2599***	***314***	***37***	***718***	***10944***	***42***	***632***	***371***	***64***	***Ave***	***51.4***	***33.4***	***15.2***
				2.2		*12.2*	*2.2*	*36.9*	*5.5*	*1.7*	*0.5*	*7.5*	*23.7*	*2.9*	*0.3*	*6.6*	*100.0*	*0.3*	*5.1*	*3.0*	*0.5*	Max	86.65	51.99	55.80
																						Min	16.40	12.95	0.00
																						STDV	17.57	11.88	16.01

Chert types

Location	A Wht	A Yel	A Gry	A Blk	A rd grn	B Wht	B Yel	B Gry	B Blk	B rd grn
T21-14	0	0	0	0	0	0	0	0	0	0
T21-13	0	0	0	0	0	0	0	0	0	0
T18-1	0	0	0	0	0	0	0	0	0	0
L3-42	0	0	0	0	0	0	0	0	0	0
L3-45	0	0	0	0	0	0	0	0	0	0
L3-48	0	0	0	0	0	0	0	0	0	0
L3-54	0	0	0	0	0	0	0	0	0	0
L3-55	0	0	0	0	0	0	0	0	0	0
L3-56	0	0	0	0	0	0	0	0	0	0
L3-75	0	0	0	0	0	0	0	0	0	0
L3-77	0	0	0	0	0	0	0	0	0	0
T19-1	18	25	10	35	0	16	2	7	2	0
T19-2	12	27	13	18	0	16	2	3	2	0
T19-3	11	14	11	9	0	43	5	0	0	0
T21-8	20	6	5	4	0	16	0	2	0	0
T11-2	7	0	0	0	0	12	0	0	0	0
T18-3	0	0	0	0	0	1	0	0	0	0
T9-1	11	2	0	0	0	0	0	0	0	0
T9-2	0	0	0	0	0	2	0	0	0	0
L3-39	0	0	0	0	0	0	0	0	0	0
L3-51	0	0	0	0	0	1	0	0	0	0
L3-80	3	1	0	1	0	7	0	0	1	0
Sum Sst	***82***	***75***	***39***	***67***	***0***	***114***	***9***	***12***	***5***	***0***
	13.5	*12.4*	*6.4*	*11.1*	*0.0*	*18.8*	*1.5*	*2.0*	*0.8*	*0.0*
					43.4					23.1

Location	C Wht	C Yel	C Gry	C Blk	D Wht	D Yel	D Gry	D Blk	E Wht	E Yel	E Gry	E Blk	F Wht	F Yel	F Gry	F Blk	G Wht	G Yel	G Gry	G Blk	H Wht	H Yel	H Gry	H Blk	I Wht	I Yel	I Gry	I Blk
T21-14	0	0	0	0	0	0	0	0	0	0	0	0	0	0	0	0	0	0	0	0	0	0	0	0	0	0	0	0
T21-13	0	0	0	0	0	0	0	0	0	0	0	0	0	0	0	0	0	0	0	0	0	0	0	0	0	0	0	0
T18-1	0	0	0	0	0	0	0	0	0	0	0	0	0	0	0	0	0	0	0	0	0	0	0	0	0	0	0	0
L3-42	0	0	0	0	0	0	0	0	0	0	0	0	0	0	0	0	0	0	0	0	0	0	0	0	0	0	0	0
L3-45	0	0	0	0	0	0	0	0	0	0	0	0	0	0	0	0	0	0	0	0	0	0	0	0	0	0	0	0
L3-48	0	0	0	0	0	0	0	0	0	0	0	0	0	0	0	0	0	0	0	0	0	0	0	0	0	0	0	0
L3-54	0	0	0	0	0	0	0	0	0	0	0	0	0	0	0	0	0	0	0	0	0	0	0	0	0	0	0	0
L3-55	0	0	0	0	0	0	0	0	0	0	0	0	0	0	0	0	0	0	0	0	0	0	0	0	0	0	0	0
L3-56	0	0	0	0	0	0	0	0	0	0	0	0	0	0	0	0	0	0	0	0	0	0	0	0	0	0	0	0
L3-75	0	0	0	0	0	0	0	0	0	0	0	0	0	0	0	0	0	0	0	0	0	0	0	0	0	0	0	0
L3-77	0	0	0	0	0	0	0	0	0	0	0	0	0	0	0	0	0	0	0	0	0	0	0	0	0	0	0	0
T19-1	0	0	0	0	0	0	0	0	0	0	0	0	0	0	0	0	0	0	0	0	0	0	0	0	0	0	0	0
T19-2	0	0	0	0	0	0	0	0	0	0	0	0	0	0	0	0	0	0	0	0	0	0	0	0	0	0	0	0
T19-3	0	0	0	0	0	0	0	0	0	0	0	0	0	0	0	0	0	0	0	0	0	0	0	0	0	0	0	0
T21-8	0	0	0	0	0	0	0	0	0	0	0	0	0	0	0	0	0	0	0	0	0	0	0	0	0	0	0	0
T11-2	0	0	0	0	0	0	0	0	0	0	0	0	0	0	0	0	0	0	0	0	0	0	0	0	0	0	0	0
T18-3	0	0	0	0	0	0	0	0	0	0	0	0	0	0	0	0	0	0	0	0	0	0	0	0	0	0	0	0
T9-1	0	0	0	0	0	0	0	0	0	0	0	0	0	0	0	0	0	0	0	0	0	0	0	0	0	0	0	0
T9-2	0	0	0	0	0	0	0	0	0	0	0	0	0	0	0	0	0	0	0	0	0	0	0	0	0	0	0	0
L3-39	0	0	0	0	0	0	0	0	0	0	0	0	0	0	0	0	0	0	0	0	0	0	0	0	0	0	0	0
L3-51	0	0	0	0	0	0	0	0	0	0	0	0	0	0	0	0	0	0	0	0	0	0	0	0	0	0	0	0
L3-80	0	0	0	0	0	0	0	0	0	0	0	0	0	0	0	0	0	0	0	0	0	0	0	0	0	0	0	0
Sum Sst	***0***	***0***	***0***	***0***	***0***	***0***	***0***	***0***	***0***	***0***	***0***	***0***	***0***	***0***	***0***	***0***	***0***	***0***	***0***	***0***	***0***	***0***	***0***	***0***	***0***	***0***	***0***	***0***
	0.0	*0.0*	*0.0*	*0.0*	*0.0*	*0.0*	*0.0*	*0.0*	*0.0*	*0.0*	*0.0*	*0.0*	*0.0*	*0.0*	*0.0*	*0.0*	*0.0*	*0.0*	*0.0*	*0.0*	*0.0*	*0.0*	*0.0*	*0.0*	*0.0*	*0.0*	*0.0*	*0.0*
				0.0				0.0				0.0				0.0				0.0				0.0				0.0

Location	J Wht	J Yel	J Gry	J Blk	K Wht	K Yel	K Gry	K Blk	L Wht	L Yel	L Gry	L Blk	M Wht	M Yel	M Gry	M Blk	N Wht	N Yel	N Gry	N Blk	O Wht	O Yel	O Gry	O Blk	P Wht	P Yel	P Gry	P Blk
T21-14	0	0	0	0	0	0	0	0	0	0	0	0	0	0	0	0	0	0	0	0	0	0	0	0	0	0	0	0
T21-13	0	0	0	0	0	0	0	0	0	0	0	0	0	0	0	0	0	0	0	0	0	0	0	0	0	0	0	0
T18-1	0	0	0	0	0	0	0	0	0	0	0	0	0	0	0	0	0	0	0	0	0	0	0	0	0	0	0	0
L3-42	0	0	0	0	0	0	0	0	0	0	0	0	0	0	0	0	0	0	0	0	0	0	0	0	0	0	0	0
L3-45	0	0	0	0	0	0	0	0	0	0	0	0	0	0	0	0	0	0	0	0	0	0	0	0	0	0	0	0
L3-48	0	0	0	0	0	0	0	0	0	0	0	0	0	0	0	0	0	0	0	0	0	0	0	0	0	0	0	0
L3-54	0	0	0	0	0	0	0	0	0	0	0	0	0	0	0	0	0	0	0	0	0	0	0	0	0	0	0	0
L3-55	0	0	0	0	0	0	0	0	0	0	0	0	0	0	0	0	0	0	0	0	0	0	0	0	0	0	0	0
L3-56	0	0	0	0	0	0	0	0	0	0	0	0	0	0	0	0	0	0	0	0	0	0	0	0	0	0	0	0
L3-75	0	0	0	0	0	0	0	0	0	0	0	0	0	0	0	0	0	0	0	0	0	0	0	0	0	0	0	0
L3-77	0	0	0	0	0	0	0	0	0	0	0	0	0	0	0	0	0	0	0	0	0	0	0	0	0	0	0	0
T19-1	6	0	1	1	0	0	0	0	0	0	0	0	3	1	2	0	0	0	0	0	0	0	0	0	0	0	0	0
T19-2	0	0	0	0	0	0	0	0	0	0	0	0	1	0	0	0	0	0	0	0	0	0	0	0	0	0	0	0
T19-3	2	1	0	0	0	0	0	0	0	0	0	0	2	0	0	0	0	0	0	0	0	0	0	0	0	0	0	0
T21-8	0	0	3	0	0	0	0	0	0	0	0	0	0	0	0	2	0	0	0	0	0	0	0	0	0	0	0	0
T11-2	0	0	0	0	0	0	0	0	0	0	0	0	0	0	0	0	0	0	0	0	0	0	0	0	0	0	0	0
T18-3	0	0	0	0	0	0	0	0	0	0	0	0	0	0	0	0	0	0	0	0	0	0	0	0	0	0	0	0
T9-1	4	0	0	0	0	0	0	0	0	0	0	0	0	6	0	0	0	0	0	0	0	0	0	0	0	0	0	0
T9-2	0	0	0	0	0	0	0	0	0	0	0	0	0	0	0	0	0	0	0	0	0	0	0	0	0	0	0	0
L3-39	0	0	0	0	0	0	0	0	0	0	0	0	0	0	0	0	0	0	0	0	0	0	0	0	0	0	0	0
L3-51	0	0	0	0	0	0	0	0	0	0	0	0	0	0	0	0	0	0	0	0	0	0	0	0	0	0	0	0
L3-80	0	0	0	0	0	0	0	0	0	0	0	0	0	0	0	0	0	0	0	0	0	0	0	0	0	0	0	0
Sum Sst	***12***	***1***	***4***	***1***	***0***	***0***	***0***	***0***	***0***	***0***	***0***	***0***	***6***	***7***	***2***	***2***	***0***	***0***	***0***	***0***	***0***	***0***	***0***	***0***	***0***	***0***	***0***	***0***
	2.0	*0.2*	*0.7*	*0.2*	*0.0*	*0.0*	*0.0*	*0.0*	*0.0*	*0.0*	*0.0*	*0.0*	*1.0*	*1.2*	*0.3*	*0.3*	*0.0*	*0.0*	*0.0*	*0.0*	*0.0*	*0.0*	*0.0*	*0.0*	*0.0*	*0.0*	*0.0*	*0.0*
				3.0				0.0				0.0				2.8				0.0				0.0				0.0

Location	Q Wht	Q Yel	Q Gry	Q Blk	R Wht	R Yel	R Gry	R Blk	S Wht	S Yel	S Gry	S Blk	T Wht	T Yel	T Gry	T Blk	U Wht	U Yel	U Gry	U Blk	V Wht	V Yel	V Gry	V Blk	W Wht	W Yel	W Gry	W Blk
T21-14	0	0	0	0	0	0	0	0	0	0	0	0	0	0	0	0	0	0	0	0	0	0	0	0	0	0	0	0
T21-13	0	0	0	0	0	0	0	0	0	0	0	0	0	0	0	0	0	0	0	0	0	0	0	0	0	0	0	0
T18-1	0	0	0	0	0	0	0	0	0	0	0	0	0	0	0	0	0	0	0	0	0	0	0	0	0	0	0	0
L3-42	0	0	0	0	0	0	0	0	0	0	0	0	0	0	0	0	0	0	0	0	0	0	0	0	0	0	0	0
L3-45	0	0	0	0	0	0	0	0	0	0	0	0	0	0	0	0	0	0	0	0	0	0	0	0	0	0	0	0
L3-48	0	0	0	0	0	0	0	0	0	0	0	0	0	0	0	0	0	0	0	0	0	0	0	0	0	0	0	0
L3-54	0	0	0	0	0	0	0	0	0	0	0	0	0	0	0	0	0	0	0	0	0	0	0	0	0	0	0	0
L3-55	0	0	0	0	0	0	0	0	0	0	0	0	0	0	0	0	0	0	0	0	0	0	0	0	0	0	0	0
L3-56	0	0	0	0	0	0	0	0	0	0	0	0	0	0	0	0	0	0	0	0	0	0	0	0	0	0	0	0
L3-75	0	0	0	0	0	0	0	0	0	0	0	0	0	0	0	0	0	0	0	0	0	0	0	0	0	0	0	0
L3-77	0	0	0	0	0	0	0	0	0	0	0	0	0	0	0	0	0	0	0	0	0	0	0	0	0	0	0	0
T19-1	1	0	0	0	0	0	0	0	0	2	0	0	0	0	0	2	0	1	0	11	2	4	0	3	9	1	1	0
T19-2	0	3	0	1	0	0	0	0	0	0	0	0	5	0	0	0	0	0	0	2	1	0	2	2	5	3	1	0
T19-3	0	0	0	0	0	0	0	0	0	0	0	0	1	0	0	0	0	0	0	1	0	7	2	1	4	1	0	0
T21-8	0	0	0	4	0	0	0	2	0	0	0	1	0	0	0	0	2	0	1	7	6	2	4	6	6	5	7	3
T11-2	0	0	0	0	0	0	0	0	0	0	0	0	24	0	0	0	0	0	0	0	0	0	0	0	0	0	0	0
T18-3	0	0	0	0	0	0	0	0	0	0	0	0	0	0	0	0	0	0	0	0	0	0	0	0	0	0	0	0
T9-1	0	0	0	0	0	0	0	0	0	0	0	0	0	0	0	0	0	0	0	0	0	0	0	0	0	0	0	0
T9-2	0	0	0	0	0	0	0	0	0	0	0	0	0	0	0	0	0	0	0	0	5	0	0	0	0	0	0	0
L3-39	0	0	0	0	0	0	0	0	0	0	0	0	1	0	0	0	0	0	0	0	0	0	0	0	0	0	0	0
L3-51	0	0	0	0	0	0	0	0	0	0	0	0	0	0	0	0	0	0	0	0	0	0	0	0	0	0	0	0
L3-80	0	0	0	0	0	0	0	0	2	0	0	0	0	0	0	0	0	0	0	0	1	0	0	0	0	0	0	0
Sum Sst	***1***	***3***	***0***	***5***	***0***	***0***	***0***	***2***	***2***	***2***	***0***	***1***	***31***	***0***	***0***	***2***	***2***	***1***	***1***	***21***	***15***	***13***	***8***	***12***	***24***	***10***	***9***	***3***
	0.2	*0.5*	*0.0*	*0.8*	*0.0*	*0.0*	*0.0*	*0.3*	*0.3*	*0.3*	*0.0*	*0.2*	*5.1*	*0.0*	*0.0*	*0.3*	*0.3*	*0.2*	*0.2*	*3.5*	*2.5*	*2.1*	*1.3*	*2.0*	*4.0*	*1.7*	*1.5*	*0.5*
				1.5				0.3				0.8				5.4				4.1				7.9				7.6

Location	X Wht	X Yel	X Gry	X Blk	Z Wht	Z Yel	Z Gry	Z Blk	A' Wht	A' Yel	A' Gry	A' Blk	B' Wht	B' Yel	B' Gry	B' Blk
T21-14	0	0	0	0	0	0	0	0	0	0	0	0	0	0	0	0
T21-13	0	0	0	0	0	0	0	0	0	0	0	0	0	0	0	0
T18-1	0	0	0	0	0	0	0	0	0	0	0	0	0	0	0	0
L3-42	0	0	0	0	0	0	0	0	0	0	0	0	0	0	0	0
L3-45	0	0	0	0	0	0	0	0	0	0	0	0	0	0	0	0
L3-48	0	0	0	0	0	0	0	0	0	0	0	0	0	0	0	0
L3-54	0	0	0	0	0	0	0	0	0	0	0	0	0	0	0	0
L3-55	0	0	0	0	0	0	0	0	0	0	0	0	0	0	0	0
L3-56	0	0	0	0	0	0	0	0	0	0	0	0	0	0	0	0
L3-75	0	0	0	0	0	0	0	0	0	0	0	0	0	0	0	0
L3-77	0	0	0	0	0	0	0	0	0	0	0	0	0	0	0	0
T19-1	0	0	0	0	0	0	0	0	0	0	0	0	0	0	0	0
T19-2	0	0	0	0	0	0	0	0	0	0	0	0	0	0	0	0
T19-3	0	0	0	0	0	0	0	0	0	0	0	0	0	0	0	0
T21-8	0	0	0	0	0	0	0	0	0	0	0	0	0	0	0	0
T11-2	0	0	0	0	0	0	0	0	0	0	0	0	0	0	0	0
T18-3	0	0	0	0	0	0	0	0	0	0	0	0	0	0	0	0
T9-1	0	0	0	0	0	0	0	0	0	0	0	0	0	0	0	0
T9-2	0	0	0	0	0	0	0	0	0	0	0	0	0	0	0	0
L3-39	0	0	0	0	0	0	0	0	0	0	0	0	0	0	0	0
L3-51	0	0	0	0	0	0	0	0	0	0	0	0	0	0	0	0
L3-80	0	0	0	0	0	0	0	0	0	0	0	0	0	0	0	0
Sum Sst	***0***	***0***	***0***	***0***	***0***	***0***	***0***	***0***	***0***	***0***	***0***	***0***	***0***	***0***	***0***	***0***
	0.0	*0.0*	*0.0*	*0.0*	*0.0*	*0.0*	*0.0*	*0.0*	*0.0*	*0.0*	*0.0*	*0.0*	*0.0*	*0.0*	*0.0*	*0.0*
				0.0				0.0				0.0				0.0

Location	Totals n	W	Y	G	B+R+G		Chert by colour White %	Yellow %	Grey %	Black %		Qm %	Qp %	Qs %
T21-14	0	0	0	0	0		na	na	na	na		32.93	4.88	62.20
T21-13	0	0	0	0	0		na	na	na	na		40.63	7.81	51.56
T18-1	0	0	0	0	0		na	na	na	na		17.74	1.94	80.32
L3-42	0	0	0	0	0		na	na	na	na		32.32	6.46	61.22
L3-45	0	0	0	0	0		na	na	na	na		25.57	4.58	69.85
L3-48	0	0	0	0	0		na	na	na	na		27.76	2.86	69.39
L3-54	0	0	0	0	0		na	na	na	na		31.78	4.67	63.55
L3-55	0	0	0	0	0		na	na	na	na		36.63	4.53	58.85
L3-56	0	0	0	0	0		na	na	na	na		34.12	3.53	62.35
L3-75	0	0	0	0	0		na	na	na	na		11.61	2.90	85.49
L3-77	0	0	0	0	0		na	na	na	na		12.41	2.53	85.06
T19-1	166	55	36	21	54		33.1	21.7	12.7	32.5		7.91	3.72	88.37
T19-2	119	40	35	19	25		33.6	29.4	16.0	21.0		16.67	4.76	78.57
T19-3	115	63	28	13	11		54.8	24.3	11.3	9.6		35.00	7.50	57.50
T21-8	114	50	13	22	29		43.9	11.4	19.3	25.4		24.12	4.52	71.36
T11-2	43	43	0	0	0		100.0	0.0	0.0	0.0		25.8	7.1	67.0
T18-3	1	1	0	0	0		100.0	0.0	0.0	0.0		17.30	3.81	78.89
T9-1	23	15	8	0	0		65.2	34.8	0.0	0.0		11.24	8.15	80.62
T9-2	7	7	0	0	0		100.0	0.0	0.0	0.0		27.13	3.05	69.82
L3-39	1	1	0	0	0		100.0	0.0	0.0	0.0		20.45	1.89	77.65
L3-51	1	1	0	0	0		100.0	0.0	0.0	0.0		27.89	3.59	68.53
L3-80	16	13	1	0	2		81.3	6.3	0.0	12.5		38.86	4.22	56.93
						Ave	***73.8***	***11.6***	***5.4***	***9.2***	***Ave***	***25.3***	***4.5***	***70.2***
						Max	100.0	34.8	19.3	32.5	Max	40.63	8.15	88.37
						Min	33.1	0.0	0.0	0.0	Min	7.91	1.89	51.56
						Stdv	28.4399	13.4922	7.722	12.109	Stdv	9.439	1.9846	9.712

	Chert Groups A to K MASSIVE	L to T +Z BRECCIATED	U to W SPHERES		%Mas	%Brec	%spher		Non-chert lithic ratios Met	Ig	Sed
T21-14	0	0	0		na	na	na		1.4	97.1	1.4
T21-13	0	0	0		na	na	na		1.9	98.1	0.0
T18-1	0	0	0		na	na	na		0.0	1.9	98.1
L3-42	0	0	0		na	na	na		15.8	84.2	0.0
L3-45	0	0	0		na	na	na		33.3	54.2	12.5
L3-48	0	0	0		na	na	na		46.4	50.0	3.6
L3-54	0	0	0		na	na	na		18.5	81.5	0.0
L3-55	0	0	0		na	na	na		7.5	92.5	0.0
L3-56	0	0	0		na	na	na		9.5	90.5	0.0
L3-75	0	0	0		na	na	na		na	na	na
L3-77	0	0	0		na	na	na		0.0	0.0	100.0
T19-1	123	11	32		74.1	6.6	19.3		2.0	86.3	11.8
T19-2	93	10	16		78.2	8.4	13.4		0.0	97.4	2.6
T19-3	96	3	16		83.5	2.6	13.9		0.0	100.0	0.0
T21-8	56	9	49		49.1	7.9	43.0		9.1	87.9	3.0
T11-2	19	24	0		44.2	55.8	0.0		0.0	50.0	50.0
T18-3	1	0	0		100.0	0.0	0.0		0.0	100.0	0.0
T9-1	17	6	0		73.9	26.1	0.0		0.0	0.0	100.0
T9-2	2	0	5		28.6	0.0	71.4		0.0	0.0	100.0
L3-39	0	1	0		0.0	100.0	0.0		2.8	88.9	8.3
L3-51	1	0	0		100.0	0.0	0.0		15.4	80.8	3.8
L3-80	13	2	1		81.3	12.5	6.3		50.0	50.0	0.0
				Ave	***64.8***	***20.0***	***15.2***	***Ave***	***7.2***	***67.4***	***25.4***
				Max	100.0	100.0	71.4	Max	50.0	100.0	100.0
				Min	0.0	0.0	0.0	Min	0.0	0.0	0.0
				Stdv	31.028	31.2062	22.78196	Stdv	15.0	37.6	39.5

APPENDIX 3 - CHERT TYPES (by texture)

Colour determined in plain polarized light

Each pair of photograph shows chert types in plain polarized light (ppl), adjacent to a view in cross polarized light (with "x" after primary letter designation).

Massive chert (A-M)

A. Predominantly massive, uniform, microcrystalline chert, with minor clusters of mesocrystalline quartz (>20 μm). Ax: viewed in xpl.

B. Massive microcrystalline chert, with textures suggesting replacement of a carbonate grainstone (note dark rims). Bx: viewed in xpl.

C. Massive, micro and meso crystalline chert, possibly reflecting porphyroid neomorphic recrystallization, with secondary fractures. Cx: viewed in xpl.

D. Massive, micro and meso crystalline chert. Dx: viewed in xpl.

E. Patchy, massive micro and mesocrystalline quartz, with minor dark bands. Dx: viewed in xpl.

F. Banded microcrystalline quartz. Fx: viewed in xpl.

G. Massive microcrystalline quartz, with clusters of mesocrystalline quartz with diffuse boundaries (possibly indicating porphyroid neomorphic recrystallization). Gx: viewed in xpl.

H. Massive microcrystalline quartz, with larger clusters of mesocrystalline quartz with diffuse boundaries (possibly indicating porphyroid neomorphic recrystallization). Hx: viewed in xpl.

I. Massive microcrystalline quartz, with clusters of mesocrystalline quartz, producing a clotted texture. Ix: viewed in xpl.

J. Massive chert with hint of clotted texture (microcrystalline quartz, surrounded by mesocrystalline quartz - possibly reflecting replacement of void fill around pelloids in carbonate protolith). Jx: viewed in xpl.

K. Massive microcrystalline chert, with poorly defined zones of mesocrystalline quartz (possibly reflecting replacement of void fill around pelloids or intraclasts in carbonate protolith). Kx: viewed in xpl.

A'. Massive micro to mesocrystalline chert (similar to E). A'x: viewed in xpl.

B'. Grain similar to type E, adjacent to grain consisting entirely of chalcedony. B'x: viewed in xpl.

Brecciated chert (L to T + Z)

L. Predominantly massive microcrystalline quartz, with poorly defined re-healed fractures (best seen in ppl). Lx: viewed in xpl.

M. Microcrystalline chert cut by two generations of mesocrystalline quartz: dark area reflects later precipitation of iron sesquioxides in late fracture. Mx: viewed in xpl.

N. Similar to M. Mx: viewed in xpl.

O. Microcrystalline chert, with minor clusters of mesocrystalline quartz, with bands of mesocrystalline quartz along bedding planes, cut by quartz filled fractures (with uniform extinction of individual crystals) indicative of druzy infill of later fractures. Ox: viewed in xpl.

P. Microcrystalline quartz, with iron sesquioxide filled fractures. Px: viewed in xpl.

Q. Microcrystalline chert, with abundant clusters of mesocrystalline chert, cut by fracture fill quartz. Qx: viewed in xpl.

R. Microcrystalline chert with multiple fractures filled with equant quartz. Rx: viewed in xpl.

S. Highly brecciated chert, with dispersed remnants of microcrystalline chert. Sx: viewed in xpl,

T. Brecciated microcrystalline chert with late fracture fill chalcedony. Tx: viewed in xpl.

Z. Chertified microcrystalline breccia. Zx: viewed in xpl.

Chert with spheres (U to W)

U. Microcrystalline chert, with abundant, well defined spheres of mesocrystalline chert (possibly replacement of radiolarians). Ux: viewed in xpl.

V. Microcrystalline quartz with abundant spherical to sub-spherical clusters of mesocrystalline chert, with diffuse margins (possibly replacement of radiolarians). Vx: viewed in xpl.

W. Diffuse clusters of mesocrystalline quartz in microcrystalline matrix. Wx viewed in xpl.

Other quartz-rich grains

Y. Moderately poorly sorted siltstone (Quartz-lutite). Note sutured contacts between grains. Yx" viewed in xpl.

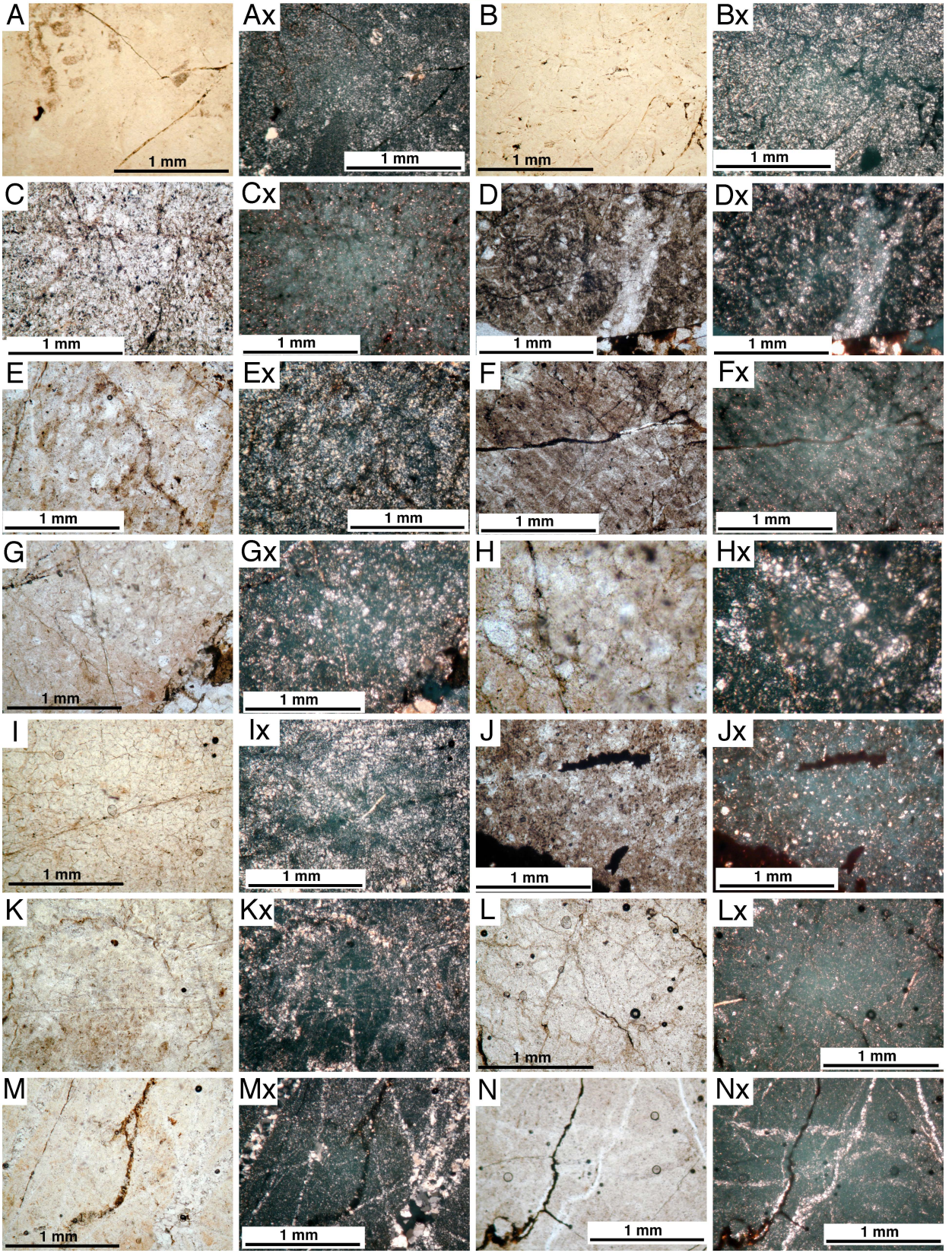
A
1 mm
Ax
1 mm
B
1 mm
Bx
1 mm
C
1 mm
Cx
1 mm
D
1 mm
Dx
1 mm
E
1 mm
Ex
1 mm
F
1 mm
Fx
1 mm
G
1 mm
Gx
1 mm
H
Hx
I
1 mm
Ix
1 mm
J
1 mm
Jx
1 mm
K
Kx
L
1 mm
Lx
1 mm
M
1 mm
Mx
1 mm
N
1 mm
Nx
1 mm

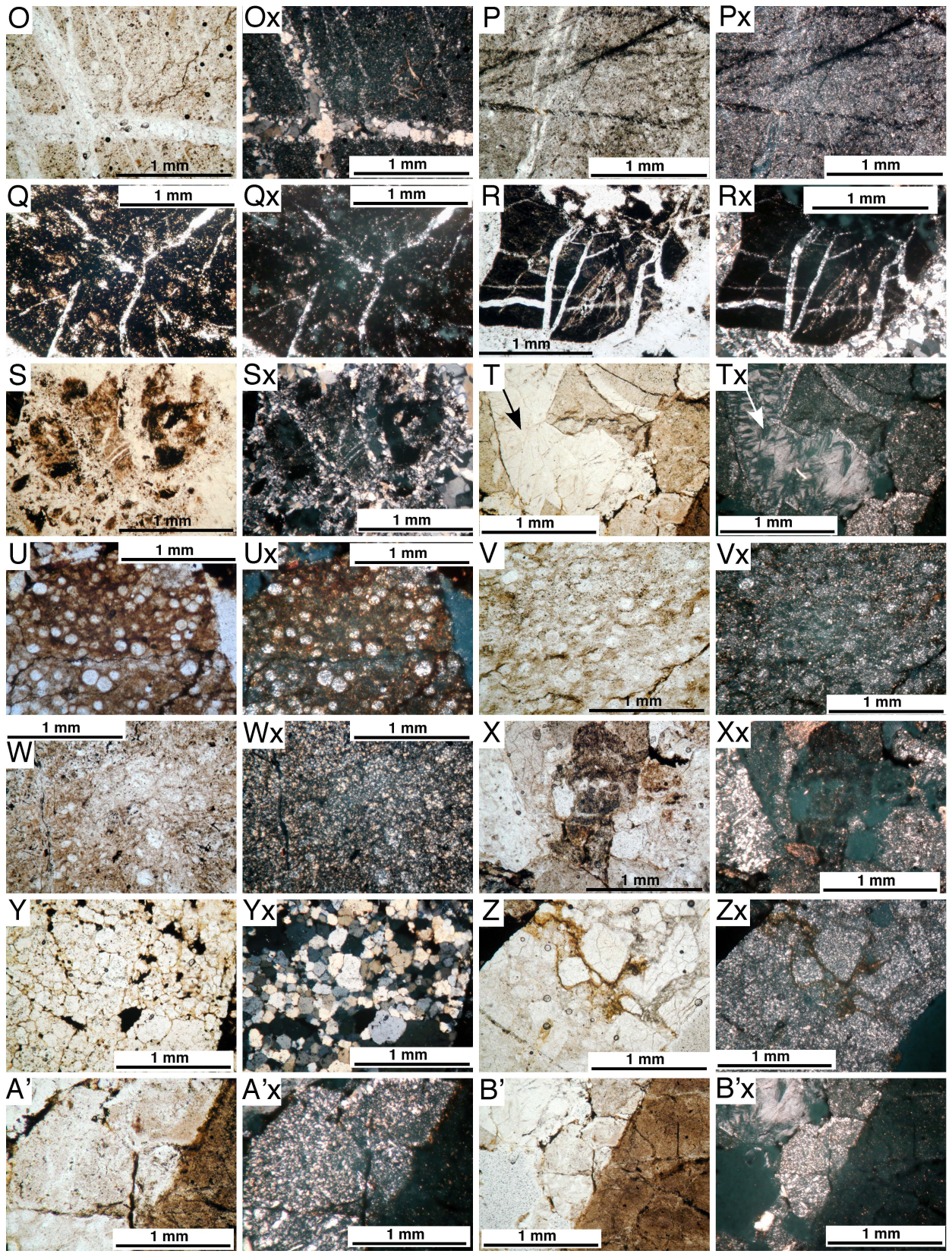
O
1 mm
Ox
1 mm
P
1 mm
Px
1 mm
Q
1 mm
Qx
1 mm
R
1 mm
Rx
1 mm
S
1 mm
Sx
1 mm
T
1 mm
Tx
1 mm
U
1 mm
Ux
1 mm
V
1 mm
Vx
1 mm
1 mm
W
Wx
1 mm
X
1 mm
Xx
1 mm
Y
1 mm
Yx
1 mm
Z
1 mm
Zx
1 mm
A'
1 mm
A'x
1 mm
B'
1 mm
B'x
1 mm

APPENDIX 4 – TANTALUS ZIRCON DATA

Methodology for zircon analysis

U-Pb geochronology of zircons was conducted by laser ablation multicollector inductively coupled plasma mass spectrometry (LA-MC-ICPMS). According to Gehrels (pers. com., 2005), the analyses involved ablation of zircon with a New Wave DUV193 Excimer laser (operating at a wavelength of 193 nm) using a spot diameter of 25 - 50 microns. The ablated material was transported in helium into the plasma source of a Micromass Isoprobe, which was equipped with a flight tube of sufficient width that U, Th, and Pb isotopes were measured simultaneously. All measurements were made in static mode, using Faraday detectors for ^{238}U, ^{232}Th, $^{208-206}Pb$, and an ion-counting channel for ^{204}Pb. Ion yields were 0.5-1.0 mv per ppm. Each analysis consisted of one 20-second integration on peaks with the laser off (for backgrounds), 20 one-second integration with the laser firing, and a 30-second delay to purge the previous sample and prepare for the next analysis. The ablation pit was typically about 15 microns deep.

Gehrels (pers. com., 2005) noted that for each analysis, the errors in determining $^{206}Pb/^{238}U$ and $^{206}Pb/^{204}Pb$ resulted in a measurement error of ~1-2% (at 2-sigma level) in the $^{206}Pb/^{238}U$ age. The errors in measurement of $^{206}Pb/^{207}Pb$ and $^{206}Pb/^{204}Pb$ also resulted in ~1-2% (at 2-sigma level) uncertainty in age for grains that are >1.0 Ga, but are substantially larger for younger grains, due to low intensity of the ^{207}Pb signal. For most analyses, the cross-over in precision of $^{206}Pb/^{238}U$ and $^{206}Pb/^{207}Pb$ ages occurs at 0.8-1.0 Ga.

Common Pb correction was accomplished using the measured ^{204}Pb, and assumed an initial Pb composition from Stacey and Kramers (1975), with uncertainties of 1.0 for $^{206}Pb/^{204}Pb$ and 0.3 for $^{207}Pb/^{204}Pb$. The measurement of ^{204}Pb was unaffected by the presence of ^{204}Hg as backgrounds were measured on peaks (thereby subtracting any background ^{204}Hg and ^{204}Pb), and very little Hg was present in the argon gas.

Gehrels (pers. com. 2005) noted that inter-element fractionation of Pb/U was generally ~20%, whereas fractionation of Pb isotopes was generally ~2%. In-run analysis of fragments of a large zircon crystal (generally every fifth measurement), with a known age of 564 ± 4 Ma (2-sigma error), was used to correct for this fractionation. The uncertainty resulting from the calibration correction was generally 2-3% (2-sigma) for both $^{206}Pb/^{207}Pb$ and $^{206}Pb/^{238}U$ ages.

The analytical data are provided in Appendix 4b. Uncertainties shown in this appendix are at the 1-sigma level, and include only measurement errors. Interpreted ages are based on $^{206}Pb/^{238}U$ for <800 Ma grains and on $^{206}Pb/^{207}Pb$ for >800 Ma grains. This division at 800 Ma results from the increasing uncertainty of $^{206}Pb/^{238}U$ ages and the decreasing uncertainty of $^{206}Pb/^{207}Pb$ ages as a function of age. Analyses that are >30% discordant (by comparison of $^{206}Pb/^{238}U$ and $^{206}Pb/^{207}Pb$ ages) or >5% reverse discordant (in italics in Appendix 4) are not considered further.

REFERENCE

Stacey, J.S. and Kramers, J.D., 1975. Approximation of terrestrial lead isotope evolution by a two stage model. Earth and Planetary Science Letters, vol. 26, p. 207-221.

Appendix 4 U-Pb geochronologic analyses by Laser-Ablation Multicollector ICP Mass Spectrometery

				Isotopic ratios					Apparent ages (Ma)							
sample	U (ppm)	$^{206}Pb/^{204}Pb$	U/Th	$^{207}Pb/^{235}U$	± (%)	$^{206}Pb/^{238}U$	± (%)	error corr.	$^{206}Pb/^{238}U$	± (Ma)	$^{207}Pb/^{235}U$	± (Ma)	$^{206}Pb/^{207}Pb$	± (Ma)	BEST AGE	± (Ma)
TB1-89	691	10790	1.0	0.16494	6.8	0.02419	1.1	0.17	154.1	1.7	155	10	170	156	154	2
TB1-55	344	2654	1.4	0.17591	11.2	0.02468	2.2	0.19	157.2	3.3	165	17	272	252	157	3
TB1-77	651	12119	1.8	0.16772	6.7	0.02485	1.0	0.15	158.2	1.6	157	10	146	154	158	2
TB1-72	980	16321	1.3	0.17488	5.6	0.02510	1.0	0.18	159.8	1.6	164	9	219	128	160	2
TB1-22	912	4605	1.2	0.16511	6.5	0.02554	1.6	0.25	162.6	2.6	155	9	43	150	163	3
TB1-44	708	5664	1.0	0.17449	6.0	0.02577	1.0	0.17	164.0	1.6	163	9	153	139	164	2
TB1-7	323	4245	0.9	0.18915	11.3	0.02630	1.2	0.11	167.4	2.0	176	18	292	258	167	2
TB1-58	225	1482	0.9	0.19545	32.9	0.02640	3.0	0.09	168.0	5.0	181	55	358	758	168	5
TB1-9	586	5969	1.4	0.17862	6.3	0.02737	1.0	0.16	174.0	1.7	167	10	66	148	174	2
TB1-65	897	697	1.5	0.21727	5.5	0.02741	2.9	0.51	174.3	4.9	200	10	510	105	174	5
TB1-70	383	7564	1.3	0.21367	6.9	0.02870	1.9	0.28	182.4	3.4	197	12	371	149	182	3
TB1-53	463	2103	0.9	0.21706	5.8	0.02922	2.6	0.45	185.7	4.8	200	11	366	118	186	5
TB1-31	311	3964	1.3	0.19174	10.5	0.02957	1.0	0.10	187.8	1.9	178	17	51	250	188	2
TB1-81	446	2405	1.5	0.21272	4.9	0.02985	1.4	0.28	189.6	2.6	196	9	271	108	190	3
TB1-74	148	916	0.9	0.21167	17.0	0.02993	3.0	0.17	190.1	5.6	195	30	254	388	190	6
TB1-43	369	4142	1.3	0.21077	8.9	0.02995	1.0	0.11	190.2	1.9	194	16	243	203	190	2
TB1-8	142	1744	1.4	0.23274	16.7	0.03015	1.8	0.11	191.5	3.4	213	32	452	372	192	3
TB1-91	712	12060	2.1	0.21576	3.8	0.03038	1.5	0.39	192.9	2.8	198	7	264	81	193	3
TB1-10	204	3357	1.3	0.19987	15.5	0.03065	2.1	0.13	194.6	3.9	185	26	64	366	195	4
TB1-5	209	1725	1.2	0.21320	11.4	0.03066	1.5	0.13	194.7	2.8	196	20	215	263	195	3
TB1-19	227	2354	1.6	0.19035	12.0	0.03076	2.1	0.18	195.3	4.1	177	19	-62	288	195	4
TB1-98	379	6177	1.7	0.21112	9.5	0.03076	1.0	0.11	195.3	1.9	195	17	185	220	195	2
TB1-73	255	6601	1.9	0.21845	10.3	0.03083	1.5	0.15	195.7	2.9	201	19	259	235	196	3
TB1-25	275	3702	1.3	0.23235	7.8	0.03087	1.1	0.14	196.0	2.2	212	15	395	173	196	2
TB1-23	541	6248	2.5	0.20142	4.8	0.03093	1.6	0.35	196.4	3.2	186	8	61	106	196	3
TB1-60	268	4985	1.7	0.22200	12.6	0.03100	1.1	0.09	196.8	2.1	204	23	283	289	197	2
TB1-11	257	3563	3.3	0.22387	7.9	0.03109	2.4	0.31	197.4	4.7	205	15	295	171	197	5
TB1-47	414	15632	1.7	0.21512	7.6	0.03113	1.3	0.17	197.6	2.5	198	14	201	175	198	3
TB1-100	370	8561	1.5	0.20780	9.0	0.03117	1.0	0.11	197.9	2.0	192	16	116	211	198	2
TB1-52	91	1446	1.4	0.16796	25.2	0.03119	2.2	0.09	198.0	4.2	158	37	-413	664	198	4
TB1-14	140	960	2.0	0.20306	20.9	0.03128	1.3	0.06	198.5	2.5	188	36	54	503	199	3
TB1-29	304	3286	2.6	0.21370	5.9	0.03134	1.5	0.25	198.9	2.9	197	11	169	133	199	3
TB1-3	129	2027	1.2	0.20214	7.9	0.03135	1.9	0.24	199.0	3.7	187	13	37	183	199	4
TB1-1	397	4178	1.6	0.19430	6.8	0.03140	1.6	0.23	199.3	3.1	180	11	-62	161	199	3
TB1-49	649	12859	2.1	0.21277	5.8	0.03149	1.2	0.20	199.9	2.3	196	10	148	134	200	2
TB1-17	184	2342	1.6	0.22368	15.2	0.03152	2.7	0.18	200.0	5.3	205	28	262	346	200	5
TB1-13	257	1834	1.9	0.19549	12.6	0.03155	2.8	0.22	200.2	5.5	181	21	-59	300	200	6

				Isotopic ratios					Apparent ages (Ma)							
sample	U (ppm)	$^{206}Pb/^{204}Pb$	U/Th	$^{207}Pb/^{235}U$	± (%)	$^{206}Pb/^{238}U$	± (%)	error corr.	$^{206}Pb/^{238}U$	± (Ma)	$^{207}Pb/^{235}U$	± (Ma)	$^{206}Pb/^{207}Pb$	± (Ma)	BEST AGE	± (Ma)
TB1-54	289	307	2.1	0.26912	16.1	0.03157	1.6	0.10	200.4	3.2	242	35	668	344	200	3
TB1-68	293	5488	1.9	0.24185	8.7	0.03161	1.3	0.15	200.6	2.5	220	17	432	191	201	3
TB1-15	153	2213	1.3	0.22515	14.1	0.03162	2.3	0.16	200.7	4.5	206	26	269	319	201	5
TB1-39	127	1848	1.1	0.17082	17.7	0.03162	2.3	0.13	200.7	4.5	160	26	-405	460	201	5
TB1-64	239	5450	1.5	0.23024	14.7	0.03167	2.6	0.18	201.0	5.1	210	28	317	330	201	5
TB1-18	287	1594	1.5	0.21746	10.9	0.03176	1.4	0.13	201.6	2.7	200	20	179	253	202	3
TB1-20	275	3095	1.3	0.22322	8.5	0.03196	1.2	0.14	202.8	2.5	205	16	226	195	203	3
TB1-61	447	6444	2.2	0.22218	6.8	0.03199	4.6	0.67	203.0	9.1	204	13	212	118	203	9
TB1-79	125	2101	1.2	0.16510	29.6	0.03199	2.5	0.08	203.0	5.0	155	43	-526	803	203	5
TB1-56	102	2119	1.0	0.24950	28.4	0.03210	2.0	0.07	203.6	4.0	226	58	467	638	204	4
TB1-97	205	5805	1.7	0.22906	14.4	0.03210	1.8	0.12	203.7	3.5	209	27	275	328	204	4
TB1-26	194	4378	1.8	0.24939	13.2	0.03211	2.4	0.18	203.8	4.7	226	27	465	288	204	5
TB1-34	69	1051	1.4	0.26402	24.6	0.03233	2.3	0.09	205.1	4.6	238	52	576	540	205	5
TB1-86	311	7768	2.0	0.22922	10.8	0.03233	1.0	0.09	205.1	2.0	210	21	260	249	205	2
TB1-4	353	5220	1.4	0.21220	6.5	0.03234	1.0	0.15	205.2	2.0	195	12	79	152	205	2
TB1-33	224	2526	1.4	0.22741	10.4	0.03255	1.4	0.13	206.5	2.8	208	20	226	238	207	3
TB1-63	178	2831	1.5	0.17544	22.1	0.03256	1.4	0.06	206.5	2.9	164	34	-411	583	207	3
TB1-90	480	5621	2.6	0.21609	8.5	0.03262	1.7	0.20	207.0	3.5	199	15	101	197	207	4
TB1-41	183	1357	1.8	0.24456	18.4	0.03270	1.5	0.08	207.4	3.1	222	37	381	414	207	3
TB1-32	378	5741	2.4	0.21248	8.3	0.03279	1.0	0.12	208.0	2.1	196	15	49	197	208	2
TB1-94	306	7687	1.6	0.24034	6.7	0.03283	1.0	0.15	208.3	2.1	219	13	333	151	208	2
TB1-38	171	3335	1.3	0.22703	11.5	0.03287	1.8	0.15	208.5	3.6	208	22	199	264	209	4
TB1-99	97	2510	1.6	0.17694	34.8	0.03290	2.5	0.07	208.7	5.1	165	53	-416	930	209	5
TB1-66	208	3060	2.2	0.21173	13.6	0.03296	1.0	0.07	209.0	2.1	195	24	28	327	209	2
TB1-30	280	6551	1.0	0.21127	8.0	0.03301	1.0	0.13	209.4	2.1	195	14	19	191	209	2
TB1-75	83	2854	2.0	0.31448	20.7	0.03355	1.9	0.09	212.7	3.9	278	50	868	431	213	4
TB1-28	247	5352	0.6	0.26036	9.0	0.03367	1.0	0.11	213.5	2.1	235	19	456	200	214	2
TB1-93	100	3001	1.1	0.30681	23.9	0.03369	2.3	0.10	213.6	4.9	272	57	808	504	214	5
TB1-80	116	1992	1.2	0.26607	16.8	0.03408	1.7	0.10	216.0	3.5	240	36	477	372	216	4
TB1-40	225	3541	4.3	0.23202	9.7	0.03440	1.1	0.11	218.0	2.3	212	19	144	226	218	2
TB1-42	79	1932	1.5	0.26102	37.8	0.03446	2.9	0.08	218.4	6.1	236	80	409	871	218	6
TB1-46	47	723	2.2	0.23052	30.8	0.03648	3.6	0.12	231.0	8.2	211	59	-12	753	231	8
TB1-92	331	6599	1.9	0.25110	6.4	0.03662	1.4	0.23	231.9	3.3	228	13	182	144	232	3
TB1-48	37	1823	3.0	0.27949	34.4	0.03748	4.5	0.13	237.2	10.6	250	76	375	788	237	11
TB1-67	148	3977	2.4	0.33655	15.7	0.03915	1.1	0.07	247.5	2.6	295	40	686	336	248	3
TB1-6	552	8872	1.5	0.27654	4.7	0.03950	1.1	0.24	249.7	2.7	248	10	231	104	250	3
TB1-71	360	7912	1.4	0.26878	7.6	0.04007	1.1	0.14	253.3	2.7	242	16	131	177	253	3
TB1-76	272	6048	1.7	0.28902	11.3	0.04042	2.4	0.21	255.5	6.0	258	26	279	254	256	6
TB1-69	526	10641	1.7	0.29095	4.6	0.04164	2.5	0.55	263.0	6.5	259	11	226	88	263	7

		Isotopic ratios							Apparent ages (Ma)							
sample	U (ppm)	$^{206}Pb/^{204}Pb$	U/Th	$^{207}Pb/^{235}U$	± (%)	$^{206}Pb/^{238}U$	± (%)	error corr.	$^{206}Pb/^{238}U$	± (Ma)	$^{207}Pb/^{235}U$	± (Ma)	$^{206}Pb/^{207}Pb$	± (Ma)	BEST AGE	± (Ma)
TB1-16	224	3945	1.6	0.33076	8.0	0.04504	2.9	0.36	284.0	8.0	290	20	340	170	284	8
TB1-27	54	1189	1.2	0.32203	30.6	0.04842	2.4	0.08	304.8	7.2	284	76	111	734	305	7
TB1-2	73	1123	1.0	0.38399	20.4	0.04940	1.9	0.09	310.9	5.6	330	58	467	454	311	6
TB1-45	532	9983	1.7	0.37548	3.1	0.05026	1.0	0.32	316.1	3.1	324	9	378	66	316	3
TB1-59	120	2611	1.0	0.36400	24.7	0.05087	1.0	0.04	319.9	3.2	315	67	281	573	320	3
TB1-21	142	2470	0.8	0.35341	9.2	0.05208	2.8	0.31	327.3	9.0	307	25	158	206	327	9
TB1-83	101	4797	1.0	0.40512	10.7	0.05226	1.4	0.13	328.4	4.6	345	31	461	235	328	5
TB1-36	158	4125	0.8	0.31741	16.1	0.05228	1.0	0.06	328.5	3.2	280	39	-109	396	329	3
TB1-95	261	6431	1.2	0.35796	6.3	0.05246	1.7	0.27	329.6	5.5	311	17	171	142	330	6
TB1-84	350	10068	1.7	0.38834	5.0	0.05275	1.7	0.33	331.4	5.4	333	14	345	107	331	5
TB1-24	278	5904	1.3	0.39162	5.6	0.05311	1.1	0.19	333.6	3.5	336	16	349	124	334	4
TB1-57	59	2640	1.4	0.26509	47.4	0.05312	2.9	0.06	333.7	9.4	239	101	-616	1353	334	9
TB1-51	117	3758	1.3	0.37451	16.0	0.05359	1.9	0.12	336.5	6.1	323	44	226	369	337	6
TB1-50	89	2058	2.0	0.43417	16.3	0.05363	1.5	0.09	336.8	4.9	366	50	556	357	337	5
TB1-88	202	7604	0.7	0.39506	4.4	0.05427	1.6	0.35	340.7	5.2	338	13	320	94	341	5
TB1-82	219	7965	0.7	0.42142	9.8	0.05456	1.0	0.10	342.4	3.3	357	30	453	217	342	3
TB1-96	61	2778	1.1	0.41771	23.3	0.05575	2.3	0.10	349.7	8.0	354	70	385	528	350	8
TB1-85	434	11471	1.1	0.39652	4.0	0.05614	1.2	0.30	352.1	4.1	339	11	251	87	352	4
TB1-37	442	1830	1.6	0.45798	4.7	0.05815	1.0	0.22	364.4	3.6	383	15	496	101	364	4
TB1-62	74	11397	1.0	5.60322	2.3	0.34468	1.9	0.81	1909.1	30.9	1917	20	1925	24	1925	24
TB1-35	95	3455	1.0	7.62905	4.6	0.38767	4.1	0.89	2112.0	73.0	2188	41	2261	36	2261	36
TB2-19	290	2558	1.6	0.17917	27.8	0.02203	3.2	0.12	140.5	4.5	167	43	566	612	141	5
TB2-84	451	6526	0.8	0.17895	17.3	0.02262	1.7	0.10	144.2	2.4	167	27	506	381	144	2
TB2-57	318	3479	1.8	0.16162	22.4	0.02274	1.9	0.08	144.9	2.7	152	32	266	519	145	3
TB2-88	250	10025	2.2	0.13276	36.2	0.02288	1.5	0.04	145.8	2.2	127	43	-221	935	146	2
TB2-15	305	2153	1.8	0.14887	32.7	0.02317	2.1	0.06	147.7	3.0	141	43	29	801	148	3
TB2-69	449	3677	1.4	0.14267	10.6	0.02341	2.5	0.23	149.2	3.6	135	13	-100	254	149	4
TB2-21	248	6681	2.0	0.21576	25.1	0.02370	2.9	0.11	151.0	4.3	198	45	807	529	151	4
TB2-24	220	3093	2.0	0.18699	21.5	0.02424	3.8	0.18	154.4	5.8	174	34	450	474	154	6
TB2-65	256	2786	1.9	0.18872	27.4	0.02445	2.9	0.10	155.7	4.4	176	44	451	614	156	4
TB2-16	253	2608	1.7	0.14676	13.7	0.02454	3.1	0.23	156.3	4.8	139	18	-146	333	156	5
TB2-37	547	8039	1.3	0.21052	6.3	0.02482	1.7	0.28	158.0	2.7	194	11	657	129	158	3
TB2-43	496	5099	1.5	0.18626	10.3	0.02489	1.0	0.10	158.5	1.6	173	16	382	231	159	2
TB2-1	514	2223	1.5	0.16908	18.7	0.02513	6.2	0.33	160.0	9.9	159	28	138	417	160	10
TB2-70	239	3113	2.0	0.19720	23.3	0.02553	2.4	0.10	162.5	3.9	183	39	453	522	163	4
TB2-77	187	3270	2.4	0.24603	25.0	0.02588	3.1	0.12	164.7	5.0	223	50	897	519	165	5
TB2-30	341	3306	1.3	0.21731	20.4	0.02624	1.8	0.09	166.9	2.9	200	37	606	445	167	3
TB2-59	179	1012	2.0	0.19441	32.6	0.02625	3.2	0.10	167.0	5.3	180	54	359	750	167	5

				Isotopic ratios					Apparent ages (Ma)							
sample	U (ppm)	$^{206}Pb/^{204}Pb$	U/Th	$^{207}Pb/^{235}U$	± (%)	$^{206}Pb/^{238}U$	± (%)	error corr.	$^{206}Pb/^{238}U$	± (Ma)	$^{207}Pb/^{235}U$	± (Ma)	$^{206}Pb/^{207}Pb$	± (Ma)	BEST AGE	± (Ma)
TB2-14	133	1445	0.8	0.19984	25.2	0.02822	4.3	0.17	179.4	7.6	185	43	257	578	179	8
TB2-17	331	2578	1.7	0.21518	15.4	0.02861	1.9	0.13	181.8	3.5	198	28	394	345	182	4
TB2-96	416	11419	1.9	0.19968	22.3	0.02872	1.1	0.05	182.6	1.9	185	38	214	522	183	2
TB2-78	620	2151	1.1	0.21123	12.0	0.02879	2.6	0.22	183.0	4.7	195	21	338	266	183	5
TB2-74	428	5249	1.4	0.21556	13.3	0.02893	3.0	0.23	183.9	5.5	198	24	372	292	184	6
TB2-85	95	1044	1.5	0.21701	20.6	0.02910	4.4	0.22	184.9	8.1	199	37	375	457	185	8
TB2-68	582	12051	0.6	0.20030	8.3	0.02912	1.1	0.14	185.0	2.1	185	14	190	193	185	2
TB2-95	264	4486	1.4	0.19714	15.2	0.02914	1.6	0.11	185.2	3.0	183	25	151	356	185	3
TB2-75	426	4387	1.7	0.17959	19.7	0.02936	2.4	0.12	186.5	4.3	168	31	-90	484	187	4
TB2-35	311	4626	1.9	0.22873	11.8	0.02938	1.8	0.15	186.7	3.2	209	22	470	259	187	3
TB2-41	491	8022	1.7	0.20039	11.4	0.02940	2.0	0.17	186.8	3.6	186	19	168	262	187	4
TB2-11	198	2049	2.1	0.27051	16.1	0.02942	2.7	0.17	186.9	5.0	243	35	828	333	187	5
TB2-63	460	8859	1.5	0.21049	16.5	0.02966	1.9	0.12	188.4	3.6	194	29	262	379	188	4
TB2-56	429	7523	1.7	0.18927	11.1	0.02972	1.2	0.11	188.8	2.2	176	18	8	267	189	2
TB2-28	172	1258	1.6	0.22185	29.0	0.03002	2.5	0.09	190.7	4.7	203	54	354	665	191	5
TB2-25	234	2781	1.8	0.20299	26.7	0.03006	2.1	0.08	190.9	3.9	188	46	147	634	191	4
TB2-38	378	3824	2.3	0.21231	13.6	0.03009	1.8	0.13	191.1	3.4	196	24	249	311	191	3
TB2-99	187	3527	2.2	0.23540	22.7	0.03012	2.2	0.10	191.3	4.2	215	44	479	506	191	4
TB2-27	139	1213	1.4	0.27402	60.3	0.03015	2.2	0.04	191.5	4.1	246	133	804	1399	192	4
TB2-73	389	26976	1.6	0.19393	18.2	0.03014	2.6	0.14	191.5	4.8	180	30	32	433	192	5
TB2-51	180	2335	2.3	0.20833	22.3	0.03016	5.5	0.24	191.6	10.3	192	39	199	508	192	10
TB2-66	302	767	1.6	0.17051	32.2	0.03016	3.9	0.12	191.6	7.4	160	48	-288	834	192	7
TB2-58	283	4698	1.7	0.19313	15.1	0.03029	1.9	0.13	192.4	3.6	179	25	10	361	192	4
TB2-64	157	2673	2.4	0.22327	22.2	0.03029	4.3	0.19	192.4	8.1	205	41	348	499	192	8
TB2-79	654	13482	2.0	0.20509	10.6	0.03033	2.0	0.18	192.6	3.7	189	18	150	245	193	4
TB2-10	653	4996	2.1	0.21592	5.7	0.03035	1.0	0.18	192.7	1.9	199	10	268	128	193	2
TB2-90	62	1943	1.7	0.21285	71.6	0.03050	4.7	0.07	193.7	8.9	196	128	223	1917	194	9
TB2-12	413	4246	3.2	0.20952	16.0	0.03062	1.7	0.10	194.4	3.2	193	28	178	372	194	3
TB2-18	249	2615	2.1	0.26628	15.4	0.03091	3.3	0.21	196.3	6.3	240	33	690	322	196	6
TB2-8	169	1460	1.6	0.27667	32.4	0.03093	3.6	0.11	196.4	6.9	248	71	770	694	196	7
TB2-52	154	2172	2.4	0.19642	37.6	0.03093	2.3	0.06	196.4	4.5	182	63	1	932	196	5
TB2-22	116	1669	2.8	0.20300	31.8	0.03094	3.1	0.10	196.5	6.0	188	55	78	769	197	6
TB2-67	332	1271	2.6	0.20951	22.3	0.03096	2.2	0.10	196.5	4.2	193	39	152	526	197	4
TB2-76	170	3000	2.3	0.26001	32.7	0.03096	3.3	0.10	196.6	6.3	235	69	636	719	197	6
TB2-71	474	3547	2.4	0.21938	13.3	0.03098	2.9	0.21	196.7	5.5	201	24	257	300	197	6
TB2-9	109	1009	2.7	0.30151	38.9	0.03105	4.7	0.12	197.1	9.1	268	92	941	822	197	9
TB2-7	442	1667	3.2	0.21396	16.4	0.03123	1.7	0.10	198.3	3.3	197	29	180	381	198	3
TB2-81	304	2624	1.7	0.21270	17.0	0.03137	3.3	0.19	199.1	6.4	196	30	156	392	199	6
TB2-53	358	3699	1.5	0.23584	11.3	0.03155	3.3	0.29	200.2	6.5	215	22	380	244	200	7

				Isotopic ratios					Apparent ages (Ma)							
sample	U (ppm)	$^{206}Pb/^{204}Pb$	U/Th	$^{207}Pb/^{235}U$	± (%)	$^{206}Pb/^{238}U$	± (%)	error corr.	$^{206}Pb/^{238}U$	± (Ma)	$^{207}Pb/^{235}U$	± (Ma)	$^{206}Pb/^{207}Pb$	± (Ma)	BEST AGE	± (Ma)
TB2-45	482	9631	3.3	0.22537	8.7	0.03157	1.1	0.12	200.4	2.1	206	16	275	199	200	2
TB2-39	318	4280	1.8	0.20816	17.6	0.03166	3.2	0.18	200.9	6.4	192	31	83	413	201	6
TB2-23	531	8511	2.2	0.19993	10.4	0.03177	1.6	0.15	201.6	3.1	185	18	-21	249	202	3
TB2-55	258	3036	1.5	0.21580	11.6	0.03179	1.2	0.10	201.7	2.4	198	21	159	269	202	2
TB2-72	387	8490	2.1	0.22922	13.5	0.03203	1.3	0.09	203.3	2.5	210	26	281	309	203	3
TB2-32	186	1678	1.5	0.20366	39.0	0.03218	2.7	0.07	204.2	5.4	188	67	-8	972	204	5
TB2-50	138	1986	2.1	0.20342	49.4	0.03245	5.6	0.11	205.9	11.2	188	85	-31	1261	206	11
TB2-44	214	3398	2.8	0.24063	15.0	0.03261	1.7	0.11	206.9	3.5	219	30	351	339	207	4
TB2-33	221	1997	1.7	0.23473	27.9	0.03278	2.3	0.08	207.9	4.7	214	54	283	646	208	5
TB2-91	145	1830	2.8	0.18976	32.7	0.03278	2.5	0.08	207.9	5.1	176	53	-228	841	208	5
TB2-60	274	4173	2.1	0.24420	16.0	0.03278	3.0	0.19	208.0	6.2	222	32	372	355	208	6
TB2-62	216	5216	1.5	0.21307	37.3	0.03292	2.6	0.07	208.8	5.4	196	67	46	917	209	5
TB2-83	254	1956	1.5	0.18250	23.3	0.03294	2.8	0.12	208.9	5.7	170	37	-339	603	209	6
TB2-5	215	1423	2.9	0.21390	13.9	0.03297	2.3	0.16	209.1	4.7	197	25	52	329	209	5
TB2-47	356	7097	2.6	0.25052	19.3	0.03308	1.4	0.07	209.8	3.0	227	39	409	433	210	3
TB2-3	140	854	2.6	0.21737	22.0	0.03310	3.5	0.16	209.9	7.1	200	40	81	522	210	7
TB2-94	400	6544	1.8	0.23146	18.4	0.03336	1.6	0.09	211.6	3.3	211	35	210	427	212	3
TB2-4	167	1142	1.7	0.32028	22.1	0.03361	2.3	0.10	213.1	4.7	282	54	902	458	213	5
TB2-61	121	1921	1.8	0.29202	29.5	0.03412	3.2	0.11	216.3	6.8	260	68	677	641	216	7
TB2-48	201	2743	1.9	0.27905	18.1	0.03417	1.8	0.10	216.6	3.8	250	40	575	394	217	4
TB2-87	161	6479	2.1	0.24278	18.0	0.03417	3.7	0.20	216.6	7.8	221	36	264	406	217	8
TB2-20	85	900	3.5	0.25813	34.2	0.03482	4.6	0.13	220.6	9.9	233	71	361	784	221	10
TB2-29	328	3785	2.9	0.21172	12.9	0.03507	3.0	0.24	222.2	6.6	195	23	-123	311	222	7
TB2-92	220	3249	2.1	0.26051	14.8	0.03524	6.4	0.44	223.2	14.1	235	31	355	302	223	14
TB2-6	207	1560	4.8	0.22455	31.8	0.03540	4.4	0.14	224.3	9.7	206	59	-2	776	224	10
TB2-13	113	1605	4.0	0.23106	20.5	0.03543	4.2	0.21	224.4	9.3	211	39	64	483	224	9
TB2-97	55	1209	1.4	0.21176	27.8	0.03545	3.9	0.14	224.6	8.6	195	49	-149	695	225	9
TB2-31	89	1840	1.9	0.28202	21.1	0.03896	2.3	0.11	246.4	5.6	252	47	307	482	246	6
TB2-93	230	1495	4.4	0.29355	17.8	0.03959	4.1	0.23	250.3	10.0	261	41	362	394	250	10
TB2-54	833	429	1.1	0.32122	35.6	0.04075	5.6	0.16	257.5	14.2	283	88	498	796	258	14
TB2-36	444	4809	1.9	0.32551	11.7	0.04280	7.1	0.61	270.2	18.8	286	29	418	208	270	19
TB2-100	218	618	1.3	0.26868	26.1	0.04319	4.2	0.16	272.6	11.2	242	56	-49	637	273	11
TB2-80	84	2192	2.1	0.36369	31.3	0.04564	6.3	0.20	287.7	17.8	315	85	522	686	288	18
TB2-49	352	4882	2.8	0.35554	11.3	0.04627	2.6	0.23	291.6	7.5	309	30	442	245	292	8
TB2-82	467	815	1.3	0.38056	13.6	0.04659	1.8	0.13	293.5	5.2	327	38	576	293	294	5
TB2-34	324	5279	1.3	0.33738	8.2	0.04710	2.1	0.26	296.7	6.2	295	21	283	182	297	6
TB2-42	185	2717	1.4	0.34101	17.6	0.04816	1.0	0.06	303.2	3.0	298	46	257	407	303	3
TB2-89	159	5396	1.4	0.40335	20.7	0.04993	1.4	0.07	314.1	4.2	344	61	552	455	314	4
TB2-86	108	2155	1.8	0.36300	26.5	0.05222	2.8	0.11	328.1	8.9	315	72	214	619	328	9

				Isotopic ratios					Apparent ages (Ma)							
sample	U (ppm)	$^{206}Pb/^{204}Pb$	U/Th	$^{207}Pb/^{235}U$	± (%)	$^{206}Pb/^{238}U$	± (%)	error corr.	$^{206}Pb/^{238}U$	± (Ma)	$^{207}Pb/^{235}U$	± (Ma)	$^{206}Pb/^{207}Pb$	± (Ma)	BEST AGE	± (Ma)
TB2-26	102	2069	2.5	0.36271	22.3	0.05319	3.9	0.17	334.1	12.7	314	60	170	519	334	13
TB2-2	88	584	1.5	0.34462	49.7	0.05768	3.5	0.07	361.5	12.2	301	130	-148	1303	362	12
TB2-40	*340*	*19456*	*4.0*	*2.45202*	*4.7*	*0.13869*	*4.4*	*0.92*	*837.2*	*34.2*	*1258*	*34*	*2074*	*33*	*2074*	*33*
TB2-46	390	61053	1.3	5.13062	2.3	0.28911	2.2	0.93	1637.1	31.5	1841	20	2080	15	2080	15
TB3-34	1351	1367	2.1	0.14331	7.0	0.02446	3.4	0.49	155.8	5.2	136	9	-197	152	156	5
TB3-80	126	2472	1.1	0.18203	18.3	0.02449	3.4	0.19	156.0	5.3	170	29	367	407	156	5
TB3-69	588	25707	2.5	0.17740	5.0	0.02468	1.4	0.28	157.2	2.2	166	8	291	110	157	2
TB3-12	266	1657	0.9	0.15094	18.4	0.02479	1.4	0.08	157.8	2.2	143	24	-102	453	158	2
TB3-29	122	1800	1.1	0.14445	21.5	0.02511	2.1	0.10	159.9	3.3	137	28	-243	545	160	3
TB3-90	322	2854	1.0	0.17130	14.0	0.02556	5.2	0.38	162.7	8.4	161	21	129	306	163	8
TB3-13	171	8010	0.7	0.19589	20.0	0.02562	1.3	0.06	163.1	2.0	182	33	431	449	163	2
TB3-100	530	11502	2.5	0.19602	5.9	0.02564	1.0	0.17	163.2	1.6	182	10	431	129	163	2
TB3-48	187	8226	1.6	0.19603	9.3	0.02688	1.4	0.15	171.0	2.4	182	15	324	208	171	2
TB3-14	306	1630	0.2	0.16041	18.9	0.02728	1.5	0.08	173.5	2.5	151	27	-188	476	174	3
TB3-74	237	808	2.1	0.13091	19.9	0.02737	2.5	0.13	174.1	4.3	125	23	-734	556	174	4
TB3-77	248	8008	2.0	0.18882	7.5	0.02810	2.7	0.37	178.7	4.8	176	12	135	164	179	5
TB3-60	196	6547	1.2	0.19176	13.2	0.02823	1.2	0.09	179.5	2.1	178	22	160	309	180	2
TB3-24	166	2405	2.6	0.18236	19.4	0.02854	2.3	0.12	181.4	4.2	170	30	15	466	181	4
TB3-52	279	16156	1.9	0.20135	8.7	0.02876	1.6	0.18	182.8	2.8	186	15	230	197	183	3
TB3-32	166	1539	1.7	0.21746	22.5	0.02909	3.9	0.18	184.9	7.2	200	41	380	504	185	7
TB3-67	150	5603	1.9	0.22219	16.2	0.02981	2.1	0.13	189.4	3.9	204	30	373	362	189	4
TB3-11	307	11421	1.4	0.20254	3.9	0.02985	1.1	0.27	189.6	2.0	187	7	158	87	190	2
TB3-73	233	1604	1.9	0.18278	21.5	0.03007	3.8	0.18	191.0	7.1	170	34	-106	525	191	7
TB3-23	334	4662	1.6	0.21424	6.6	0.03019	1.5	0.23	191.7	2.8	197	12	262	148	192	3
TB3-25	404	3446	4.4	0.19933	9.1	0.03032	1.3	0.14	192.6	2.5	185	15	83	214	193	3
TB3-33	117	1678	1.6	0.16676	22.5	0.03043	2.2	0.10	193.2	4.1	157	33	-367	587	193	4
TB3-5	332	18311	2.1	0.20999	8.7	0.03046	2.4	0.27	193.4	4.6	194	15	195	195	193	5
TB3-28	544	12792	2.7	0.21526	6.2	0.03045	2.3	0.37	193.4	4.4	198	11	253	131	193	4
TB3-1	484	987	4.0	0.23807	12.6	0.03046	3.8	0.30	193.5	7.2	217	25	479	267	194	7
TB3-81	195	1187	1.6	0.16604	26.2	0.03051	3.3	0.13	193.7	6.3	156	38	-385	685	194	6
TB3-62	267	6473	1.9	0.21225	11.2	0.03054	1.0	0.09	193.9	1.9	195	20	214	258	194	2
TB3-22	362	47899	2.5	0.21699	5.5	0.03061	1.0	0.18	194.3	1.9	199	10	260	124	194	2
TB3-10	323	5205	2.2	0.22121	6.8	0.03062	2.0	0.29	194.4	3.7	203	13	303	149	194	4
TB3-76	150	7931	1.4	0.18563	15.8	0.03063	3.0	0.19	194.5	5.8	173	25	-113	385	195	6
TB3-19	505	23663	3.0	0.22933	2.9	0.03075	1.2	0.42	195.2	2.3	210	5	375	59	195	2
TB3-21	85	962	2.5	0.16947	31.8	0.03079	2.2	0.07	195.5	4.2	159	47	-356	838	196	4
TB3-87	105	3058	1.8	0.19128	22.6	0.03080	3.5	0.15	195.5	6.7	178	37	-53	549	196	7
TB3-15	156	2547	1.3	0.25521	17.0	0.03082	1.7	0.10	195.7	3.3	231	35	605	367	196	3

				Isotopic ratios					Apparent ages (Ma)							
sample	U (ppm)	$^{206}Pb/^{204}Pb$	U/Th	$^{207}Pb/^{235}U$	± (%)	$^{206}Pb/^{238}U$	± (%)	error corr.	$^{206}Pb/^{238}U$	± (Ma)	$^{207}Pb/^{235}U$	± (Ma)	$^{206}Pb/^{207}Pb$	± (Ma)	BEST AGE	± (Ma)
TB3-54	226	3803	2.3	0.21628	9.5	0.03083	1.1	0.11	195.7	2.1	199	17	235	219	196	2
TB3-44	396	10032	2.0	0.22887	6.9	0.03086	3.2	0.46	195.9	6.1	209	13	362	139	196	6
TB3-49	386	2471	3.7	0.19768	12.6	0.03086	1.3	0.10	196.0	2.4	183	21	21	303	196	2
TB3-4	383	23429	2.5	0.23129	4.4	0.03097	2.2	0.50	196.6	4.3	211	8	378	85	197	4
TB3-93	286	3358	2.4	0.21541	12.6	0.03097	3.8	0.30	196.6	7.4	198	23	216	279	197	7
TB3-72	242	9620	1.9	0.22543	10.2	0.03106	4.4	0.43	197.2	8.5	206	19	313	211	197	9
TB3-43	188	1876	1.7	0.25726	10.8	0.03108	2.1	0.20	197.3	4.1	233	22	605	229	197	4
TB3-3	234	4659	2.6	0.21534	10.8	0.03109	3.2	0.30	197.4	6.3	198	20	206	240	197	6
TB3-2	204	1562	1.8	0.17612	21.1	0.03115	3.0	0.14	197.7	5.9	165	32	-287	536	198	6
TB3-85	333	4530	1.8	0.22046	8.2	0.03117	2.6	0.31	197.8	5.0	202	15	255	179	198	5
TB3-26	272	9749	2.3	0.23321	6.6	0.03118	1.5	0.22	197.9	2.8	213	13	381	144	198	3
TB3-51	172	921	1.9	0.26643	36.8	0.03125	3.6	0.10	198.4	7.0	240	79	668	809	198	7
TB3-45	144	2882	2.5	0.21774	15.3	0.03128	2.8	0.19	198.6	5.6	200	28	217	350	199	6
TB3-92	196	8833	1.8	0.23462	13.2	0.03136	2.2	0.16	199.0	4.2	214	25	382	293	199	4
TB3-46	108	2205	1.9	0.21377	14.5	0.03137	2.3	0.16	199.1	4.5	197	26	168	335	199	5
TB3-89	134	4929	1.9	0.26487	18.9	0.03136	6.1	0.32	199.1	11.9	239	40	648	386	199	12
TB3-7	419	12057	2.7	0.20761	4.7	0.03146	1.1	0.24	199.7	2.2	192	8	93	108	200	2
TB3-84	185	2183	2.0	0.19610	20.8	0.03151	4.1	0.20	200.0	8.0	182	35	-48	499	200	8
TB3-39	235	9119	3.1	0.20972	13.6	0.03157	3.6	0.26	200.4	7.1	193	24	108	312	200	7
TB3-20	308	3129	1.6	0.20169	11.7	0.03174	1.1	0.10	201.4	2.2	187	20	2	281	201	2
TB3-53	149	6957	1.7	0.20620	13.2	0.03176	2.3	0.17	201.5	4.5	190	23	54	310	202	5
TB3-9	396	2224	0.5	0.19716	14.4	0.03181	1.3	0.09	201.9	2.6	183	24	-58	351	202	3
TB3-55	185	4170	1.3	0.20416	15.9	0.03187	3.0	0.19	202.2	5.9	189	27	22	377	202	6
TB3-64	63	3252	2.1	0.27272	27.0	0.03188	2.1	0.08	202.3	4.2	245	59	676	585	202	4
TB3-50	254	12399	2.4	0.21685	10.4	0.03198	1.0	0.10	202.9	2.0	199	19	156	242	203	2
TB3-91	114	2217	2.1	0.22589	15.8	0.03204	3.3	0.21	203.3	6.5	207	30	247	357	203	7
TB3-17	246	9849	3.5	0.22650	7.1	0.03215	1.2	0.16	204.0	2.4	207	13	245	163	204	2
TB3-78	175	6185	3.2	0.23471	10.9	0.03223	3.2	0.30	204.5	6.5	214	21	321	236	205	7
TB3-36	180	12561	2.9	0.25344	9.8	0.03227	4.7	0.48	204.7	9.5	229	20	490	189	205	10
TB3-63	282	11365	3.3	0.23700	6.5	0.03231	1.0	0.15	205.0	2.0	216	13	337	146	205	2
TB3-83	165	1496	1.2	0.22714	19.0	0.03236	4.5	0.24	205.3	9.1	208	36	236	429	205	9
TB3-70	229	31279	1.1	0.21853	6.9	0.03240	1.2	0.17	205.5	2.4	201	13	144	158	206	2
TB3-59	195	58202	2.4	0.25063	9.4	0.03253	1.0	0.11	206.4	2.0	227	19	448	208	206	2
TB3-57	241	3665	1.6	0.23692	5.0	0.03259	1.0	0.20	206.7	2.1	216	10	317	111	207	2
TB3-95	342	34480	2.2	0.23177	7.4	0.03280	3.2	0.43	208.1	6.5	212	14	252	155	208	7
TB3-98	113	8915	2.4	0.27579	11.7	0.03285	2.8	0.24	208.4	5.8	247	26	635	246	208	6
TB3-65	94	1870	1.6	0.19563	20.3	0.03308	1.9	0.09	209.8	4.0	181	34	-174	508	210	4
TB3-66	283	11556	1.2	0.24463	6.9	0.03313	1.9	0.27	210.1	3.9	222	14	352	151	210	4
TB3-88	275	7883	1.9	0.26926	8.8	0.03372	5.5	0.63	213.8	11.7	242	19	526	150	214	12

				Isotopic ratios					Apparent ages (Ma)							
sample	U (ppm)	$^{206}Pb/^{204}Pb$	U/Th	$^{207}Pb/^{235}U$	± (%)	$^{206}Pb/^{238}U$	± (%)	error corr.	$^{206}Pb/^{238}U$	± (Ma)	$^{207}Pb/^{235}U$	± (Ma)	$^{206}Pb/^{207}Pb$	± (Ma)	BEST AGE	± (Ma)
TB3-79	132	1934	2.6	0.25378	14.2	0.03477	5.4	0.38	220.4	11.7	230	29	326	299	220	12
TB3-99	134	2497	1.9	0.28808	12.7	0.03509	2.9	0.23	222.3	6.3	257	29	587	269	222	6
TB3-56	439	9996	2.7	0.25605	5.7	0.03628	1.5	0.26	229.8	3.3	232	12	249	126	230	3
TB3-75	107	1558	2.5	0.28778	15.4	0.04019	3.5	0.23	254.0	8.8	257	35	283	344	254	9
TB3-82	62	1207	2.5	0.28049	25.9	0.04071	5.4	0.21	257.2	13.7	251	58	194	596	257	14
TB3-68	532	11747	0.8	0.34964	2.7	0.04600	1.1	0.39	289.9	3.0	305	7	417	55	290	3
TB3-97	215	5862	2.3	0.36903	7.1	0.04634	1.4	0.20	292.0	4.0	319	20	520	153	292	4
TB3-58	241	12317	1.3	0.41564	4.9	0.05153	1.0	0.21	323.9	3.2	353	15	549	104	324	3
TB3-6	136	1390	1.3	0.34624	20.1	0.05172	1.6	0.08	325.1	4.9	302	52	126	475	325	5
TB3-42	87	6651	1.7	0.38111	11.9	0.05226	2.8	0.23	328.4	9.0	328	33	324	264	328	9
TB3-41	105	10980	1.7	0.43467	4.4	0.05235	1.3	0.30	329.0	4.1	367	13	611	90	329	4
TB3-94	106	2576	1.8	0.40836	16.3	0.05323	4.9	0.30	334.3	16.0	348	48	438	347	334	16
TB3-16	59	1782	1.2	0.39939	13.6	0.05339	1.6	0.12	335.3	5.3	341	39	382	304	335	5
TB3-47	68	1561	1.9	0.44823	19.1	0.05344	2.9	0.15	335.6	9.6	376	60	633	409	336	10
TB3-30	79	4481	1.3	0.44820	8.7	0.05352	1.4	0.16	336.1	4.5	376	27	630	185	336	5
TB3-96	102	6114	1.3	0.48646	6.3	0.05440	1.5	0.24	341.5	5.0	403	21	769	130	342	5
TB3-8	430	34762	1.8	0.43777	1.8	0.05550	1.0	0.57	348.2	3.4	369	5	499	32	348	3
TB3-31	319	3438	1.7	0.40920	9.5	0.05694	4.2	0.44	357.0	14.5	348	28	291	196	357	15
TB3-18	119	5480	2.3	0.46921	11.2	0.05728	1.0	0.09	359.0	3.5	391	36	582	243	359	4
TB3-38	268	11660	1.5	0.46494	5.1	0.05753	2.9	0.57	360.6	10.0	388	16	553	91	361	10
TB3-35	260	41464	4.7	0.45071	6.1	0.05855	4.2	0.69	366.8	15.0	378	19	446	99	367	15
TB3-27	222	183518	1.5	4.92100	5.8	0.28391	5.7	0.99	1611.0	81.8	1806	49	2039	12	2039	12
TB3-71	169	229982	0.7	6.02818	3.4	0.34386	3.3	0.98	1905.2	54.6	1980	30	2059	13	2059	13
TB3-40	20	3362	2.0	8.13460	4.1	0.40594	2.2	0.55	2196.3	41.6	2246	37	2292	58	2292	58
C1-36	234	4614	2.3	0.19459	13.8	0.02527	1.2	0.08	160.9	1.8	181	23	446	308	161	2
C1-44	182	5822	3.9	0.17725	11.0	0.02553	1.0	0.09	162.5	1.6	166	17	212	255	163	2
C1-96	124	4780	2.9	0.20510	12.9	0.02572	2.1	0.16	163.7	3.3	189	22	524	280	164	3
C1-39	106	4643	4.2	0.17357	22.4	0.02613	1.9	0.08	166.3	3.1	163	34	107	532	166	3
C1-47	203	4669	3.5	0.19261	13.5	0.02614	2.6	0.19	166.4	4.2	179	22	347	301	166	4
C1-58	197	1727	3.7	0.16413	20.8	0.02616	1.4	0.07	166.5	2.3	154	30	-28	507	167	2
C1-84	150	1571	3.3	0.18718	18.4	0.02636	1.6	0.09	167.7	2.7	174	29	263	423	168	3
C1-38	1041	28340	0.9	0.18192	3.0	0.02641	1.1	0.37	168.1	1.9	170	5	193	64	168	2
C1-93	159	4565	2.7	0.20745	12.0	0.02656	1.3	0.11	169.0	2.1	191	21	478	264	169	2
C1-76	213	7873	4.7	0.17425	11.2	0.02660	1.0	0.09	169.2	1.7	163	17	75	266	169	2
C1-17	161	10271	2.3	0.21783	12.6	0.02691	1.4	0.11	171.2	2.4	200	23	556	273	171	2
C1-5	142	4284	1.7	0.16103	22.0	0.02710	1.2	0.05	172.4	2.0	152	31	-162	551	172	2
C1-97	134	5688	2.4	0.24669	12.2	0.02714	1.2	0.10	172.6	2.1	224	24	804	254	173	2
C1-87	110	3389	3.5	0.16523	39.7	0.02731	1.4	0.04	173.7	2.5	155	57	-118	1012	174	3

				Isotopic ratios					Apparent ages (Ma)							
sample	U (ppm)	$^{206}Pb/^{204}Pb$	U/Th	$^{207}Pb/^{235}U$	± (%)	$^{206}Pb/^{238}U$	± (%)	error corr.	$^{206}Pb/^{238}U$	± (Ma)	$^{207}Pb/^{235}U$	± (Ma)	$^{206}Pb/^{207}Pb$	± (Ma)	BEST AGE	± (Ma)
C1-28	269	2582	2.0	0.17771	8.2	0.02758	1.0	0.12	175.4	1.7	166	13	36	195	175	2
C1-64	150	4753	3.0	0.16725	18.9	0.02783	2.3	0.12	176.9	4.0	157	28	-134	468	177	4
C1-69	351	6488	2.9	0.19195	6.8	0.02783	1.1	0.17	177.0	2.0	178	11	196	155	177	2
C1-18	351	11945	2.7	0.19025	6.7	0.02793	1.6	0.24	177.6	2.8	177	11	167	151	178	3
C1-91	128	899	2.8	0.20000	22.3	0.02793	3.2	0.14	177.6	5.5	185	38	282	510	178	6
C1-45	223	14996	2.2	0.21052	11.7	0.02797	1.1	0.09	177.8	2.0	194	21	395	263	178	2
C1-13	159	4675	2.5	0.19387	18.4	0.02799	1.9	0.10	178.0	3.3	180	30	206	427	178	3
C1-66	100	2037	3.6	0.21100	14.9	0.02806	2.0	0.13	178.4	3.5	194	26	393	333	178	4
C1-82	260	10724	2.3	0.20043	7.9	0.02809	1.0	0.13	178.6	1.8	186	13	274	180	179	2
C1-68	205	6270	1.1	0.20141	18.4	0.02825	1.1	0.06	179.6	1.9	186	31	273	423	180	2
C1-4	302	10717	2.2	0.21050	8.8	0.02831	1.0	0.11	180.0	1.8	194	16	368	197	180	2
C1-16	159	3623	4.0	0.17862	15.9	0.02832	3.4	0.21	180.0	6.1	167	25	-16	378	180	6
C1-92	419	23513	1.7	0.19252	6.8	0.02831	1.0	0.15	180.0	1.8	179	11	163	157	180	2
C1-8	83	4814	1.3	0.17212	38.3	0.02838	1.9	0.05	180.4	3.4	161	57	-112	972	180	3
C1-34	425	1579	1.6	0.18986	6.6	0.02841	1.3	0.19	180.6	2.3	177	11	122	153	181	2
C1-73	347	17582	2.3	0.19329	5.9	0.02843	1.0	0.17	180.7	1.8	179	10	162	136	181	2
C1-37	276	11386	2.2	0.19979	9.2	0.02849	1.0	0.11	181.1	1.8	185	16	234	210	181	2
C1-63	336	14013	1.6	0.20780	7.8	0.02857	1.6	0.21	181.6	2.9	192	14	318	174	182	3
C1-33	263	6017	2.2	0.18912	10.5	0.02859	1.5	0.15	181.7	2.8	176	17	98	246	182	3
C1-49	395	879	1.6	0.22390	10.6	0.02867	1.3	0.13	182.2	2.4	205	20	478	233	182	2
C1-27	279	13674	2.5	0.21851	9.0	0.02878	1.3	0.14	182.9	2.3	201	16	415	199	183	2
C1-95	315	12103	1.8	0.21116	7.3	0.02880	1.0	0.14	183.0	1.8	195	13	336	164	183	2
C1-12	331	8218	2.0	0.20258	9.7	0.02882	1.0	0.10	183.2	1.8	187	17	240	223	183	2
C1-1	260	10927	2.0	0.22046	14.8	0.02888	1.0	0.07	183.6	1.8	202	27	427	331	184	2
C1-30	319	4998	1.8	0.21264	9.3	0.02901	1.1	0.12	184.3	2.1	196	17	336	209	184	2
C1-59	257	16733	1.9	0.21050	10.6	0.02914	1.0	0.09	185.1	1.8	194	19	303	241	185	2
C1-31	219	8119	1.5	0.20692	15.4	0.02916	1.0	0.07	185.3	1.8	191	27	262	355	185	2
C1-24	279	10093	2.0	0.19801	8.7	0.02919	1.0	0.12	185.5	1.8	183	15	157	202	186	2
C1-35	360	3569	1.7	0.19771	6.7	0.02924	1.4	0.21	185.8	2.6	183	11	150	153	186	3
C1-32	349	8515	2.5	0.20865	8.0	0.02931	1.0	0.13	186.2	1.8	192	14	269	183	186	2
C1-88	190	4004	1.6	0.20081	14.0	0.02933	1.4	0.10	186.3	2.5	186	24	179	326	186	3
C1-51	277	5594	2.0	0.20641	12.1	0.02936	1.0	0.08	186.5	1.9	191	21	240	278	187	2
C1-20	424	18772	1.9	0.19940	4.9	0.02939	1.0	0.20	186.7	1.8	185	8	158	112	187	2
C1-21	267	6475	2.0	0.18381	10.5	0.02938	1.0	0.10	186.7	1.8	171	17	-35	255	187	2
C1-40	153	7522	1.4	0.20907	12.6	0.02938	1.7	0.14	186.7	3.2	193	22	268	287	187	3
C1-85	399	3050	4.0	0.17940	7.0	0.02938	1.0	0.14	186.7	1.8	168	11	-95	171	187	2
C1-56	267	1728	1.2	0.21058	16.0	0.02940	1.2	0.08	186.8	2.2	194	28	283	367	187	2
C1-65	466	10074	2.8	0.20922	5.8	0.02944	1.0	0.17	187.1	1.8	193	10	265	132	187	2
C1-22	256	8384	2.3	0.22029	11.4	0.02947	1.0	0.09	187.2	1.9	202	21	380	256	187	2

		Isotopic ratios							Apparent ages (Ma)							
sample	U (ppm)	$^{206}Pb/^{204}Pb$	U/Th	$^{207}Pb/^{235}U$	± (%)	$^{206}Pb/^{238}U$	± (%)	error corr.	$^{206}Pb/^{238}U$	± (Ma)	$^{207}Pb/^{235}U$	± (Ma)	$^{206}Pb/^{207}Pb$	± (Ma)	BEST AGE	± (Ma)
C1-9	119	2713	1.6	0.19208	17.1	0.02949	1.4	0.08	187.4	2.6	178	28	61	408	187	3
C1-53	227	6533	1.5	0.19636	18.6	0.02964	1.2	0.06	188.3	2.2	182	31	102	442	188	2
C1-54	266	6574	1.9	0.21758	8.1	0.02974	1.3	0.16	188.9	2.4	200	15	332	181	189	2
C1-11	285	5733	2.0	0.18866	11.2	0.02978	1.1	0.10	189.1	2.1	176	18	-5	269	189	2
C1-23	370	9532	1.9	0.19756	5.6	0.02979	1.0	0.18	189.2	1.9	183	9	104	130	189	2
C1-52	253	10306	1.8	0.18812	8.5	0.02994	1.2	0.15	190.2	2.3	175	14	-25	203	190	2
C1-7	164	5393	1.7	0.20079	18.4	0.03007	1.5	0.08	191.0	2.7	186	31	120	435	191	3
C1-41	462	16208	1.8	0.20253	7.1	0.03017	3.5	0.48	191.6	6.5	187	12	133	147	192	7
C1-10	81	3166	1.5	0.22456	27.2	0.03019	2.7	0.10	191.7	5.1	206	51	369	619	192	5
C1-48	270	4496	3.3	0.20701	8.6	0.03028	1.1	0.12	192.3	2.0	191	15	176	200	192	2
C1-2	174	10263	2.5	0.21730	11.5	0.03034	1.0	0.09	192.7	1.9	200	21	283	264	193	2
C1-74	208	7370	2.1	0.20951	8.5	0.03037	1.2	0.14	192.8	2.3	193	15	197	196	193	2
C1-29	368	5326	2.8	0.22190	5.4	0.03039	1.0	0.19	193.0	1.9	204	10	327	120	193	2
C1-89	289	7550	2.1	0.21335	7.6	0.03054	1.5	0.20	193.9	2.9	196	14	226	173	194	3
C1-42	133	5703	2.6	0.18503	28.3	0.03057	1.2	0.04	194.1	2.2	172	45	-116	708	194	2
C1-6	264	6392	3.5	0.22327	8.0	0.03078	1.3	0.16	195.4	2.4	205	15	312	179	195	2
C1-19	234	3546	2.5	0.21080	16.7	0.03081	1.8	0.11	195.6	3.5	194	30	177	390	196	4
C1-62	163	6109	1.6	0.23208	7.3	0.03088	1.1	0.15	196.1	2.1	212	14	392	161	196	2
C1-81	214	8519	4.0	0.20777	10.9	0.03097	1.0	0.09	196.6	1.9	192	19	131	255	197	2
C1-78	297	17331	2.4	0.22225	8.6	0.03110	1.0	0.12	197.4	1.9	204	16	278	197	197	2
C1-98	231	6644	2.2	0.22119	6.4	0.03109	1.1	0.17	197.4	2.1	203	12	268	145	197	2
C1-94	368	5433	1.6	0.23759	7.1	0.03128	4.0	0.56	198.5	7.8	216	14	416	132	199	8
C1-43	84	1644	3.7	0.21967	27.9	0.03130	1.8	0.06	198.7	3.5	202	51	236	654	199	4
C1-67	227	15415	2.9	0.23447	9.8	0.03132	1.2	0.13	198.8	2.4	214	19	383	218	199	2
C1-25	135	6312	2.5	0.25774	15.5	0.03136	1.8	0.12	199.0	3.6	233	32	590	336	199	4
C1-75	155	5192	2.5	0.19483	14.0	0.03144	1.0	0.07	199.5	2.0	181	23	-58	342	200	2
C1-77	256	7353	1.7	0.22743	10.1	0.03144	1.1	0.10	199.5	2.1	208	19	306	229	200	2
C1-60	294	15153	3.5	0.23244	8.9	0.03149	2.0	0.23	199.8	4.0	212	17	352	195	200	4
C1-79	206	9975	2.4	0.22922	8.9	0.03158	1.0	0.11	200.4	2.0	210	17	313	201	200	2
C1-70	291	9971	2.6	0.21977	8.9	0.03170	1.0	0.11	201.2	2.0	202	16	208	205	201	2
C1-80	210	6275	2.1	0.22742	15.2	0.03179	1.0	0.07	201.8	2.0	208	29	280	349	202	2
C1-72	190	4104	3.0	0.22792	13.2	0.03188	1.6	0.12	202.3	3.3	209	25	279	301	202	3
C1-14	141	484	2.2	0.28583	15.3	0.03198	1.9	0.12	202.9	3.7	255	35	769	321	203	4
C1-46	153	8276	1.9	0.22297	11.2	0.03216	1.6	0.14	204.1	3.2	204	21	208	258	204	3
C1-61	169	5764	3.3	0.22403	16.3	0.03217	1.8	0.11	204.1	3.7	205	30	218	378	204	4
C1-3	389	306	4.9	0.20515	18.9	0.03222	1.9	0.10	204.4	3.7	190	33	7	456	204	4
C1-50	112	5945	2.9	0.21247	18.6	0.03256	1.3	0.07	206.6	2.6	196	33	65	446	207	3
C1-99	218	6386	2.9	0.24170	13.9	0.03328	5.2	0.38	211.0	10.8	220	27	315	293	211	11
C1-71	80	10230	2.9	0.25752	20.3	0.03375	2.5	0.12	214.0	5.3	233	42	426	453	214	5

				Isotopic ratios					Apparent ages (Ma)							
sample	U (ppm)	$^{206}Pb/^{204}Pb$	U/Th	$^{207}Pb/^{235}U$	± (%)	$^{206}Pb/^{238}U$	± (%)	error corr.	$^{206}Pb/^{238}U$	± (Ma)	$^{207}Pb/^{235}U$	± (Ma)	$^{206}Pb/^{207}Pb$	± (Ma)	BEST AGE	± (Ma)
C1-100	82	1859	2.3	0.22587	9.7	0.03455	1.7	0.17	218.9	3.6	207	18	70	229	219	4
C1-15	417	492	3.7	0.31586	9.7	0.03902	1.5	0.15	246.8	3.6	279	24	556	210	247	4
C1-90	283	1492	2.4	0.34051	11.9	0.04508	1.1	0.09	284.2	2.9	298	31	403	267	284	3
C1-57	212	2371	1.6	0.37400	5.9	0.05267	2.1	0.35	330.9	6.8	323	16	263	128	331	7
C1-86	195	7075	2.2	0.42162	9.7	0.05565	1.0	0.11	349.1	3.5	357	29	410	216	349	4
C1-55	380	43196	4.2	0.72103	1.9	0.08998	1.0	0.52	555.4	5.3	551	8	534	36	555	5
C1-26	*194*	*3191*	*7.8*	*3.30126*	*2.6*	*0.21194*	*1.8*	*0.70*	*1239.1*	*20.2*	*1481*	*20*	*1848*	*34*	*1848*	*34*

206Pb/204Pb is measured ratio.
Analyses in red/italics are excluded due to >10% error in critical age, >30% discordance, or >5% reverse discordance.
All errors are at the 1-sigma level, and include only random uncertainties.
Best age = 206Pb/238U ages for analyses younger than 1.0 Ga and 206Pb/207Pb ages for analyses older than 1.0 Ga.
U concentration and U/Th are calibrated by comparison with NBS SRM 610 and have uncertainty of ~25%.
Decay constants: 235U=9.8485x10-10. 238U=1.55125x10-10, 238U/235U=137.88.
Isotope ratios are corrected for Pb/U fractionation by comparison with standard zircon with an age of 564 ± 4 Ma (2-sigma).
Initial Pb composition interpreted from Stacey and Kramers (1975), with uncertainties of 1.0 for 206Pb/204Pb and 0.3 for 207Pb/204Pb.